The biological and clinical characterisation and validation of novel biomarkers in colorectal cancer

Seán Fitzgerald B.Sc., M.Sc.

This thesis is submitted to Dublin City University for the degree of Ph.D.

July 2015

Based on research carried out at
School of Biotechnology,
Dublin City University,
Dublin 9, Ireland.

Supervisors: Professor Richard O'Kennedy
Dr. Gregor Kijanka

External Supervisor: Professor Elaine Kay
Department of Pathology,
RCSI, Beaumont Hospital.

Declaration

I hereby certify that this material, which I now submit for assessment on the programme of study leading to the award of Ph.D. is entirely my own work, that I have exercised reasonable care to ensure that the work is original, and does not to the best of my knowledge breach any law of copyright, and has not been taken from the work of others save and to the extent that such work has been cited and acknowledged within the text of my work.

Signed: _____ ID No.: _____ Date: _____

Acknowledgements

Firstly, I would like to express my sincere gratitude and appreciation to my supervisors Prof. Richard O'Kennedy, Prof. Elaine Kay and Dr. Gregor Kijanka. This thesis would not have been possible without the expert advice and guidance that I received from each of you, both on an academic and personal level. I am especially grateful to Dr. Gregor Kijanka for his endless guidance, wisdom and friendship throughout my PhD.

I would like to thank all the members of the Applied Biochemistry Group and the School of Biotechnology in DCU for their help, support and friendship over the last few years. In addition, I would like to thank all of my colleagues in the Biomedical Diagnostics Institute who funded and supported this work.

I would like to acknowledge and thank Dr. Katherine Sheehan, Dr. Tony O'Grady, Mr. Robert Cummins, Dr. Joanna Fay, Ms. Etáin Daly, Ms. Deirdre Hyland, Ms. Joan Kehoe and all of the staff at the RCSI Histopathology Department of Beaumont Hospital for their help and support with my research.

I would also like to thank Prof. Lance Liotta, Dr. Virginia Espina and all at the Centre for Applied Proteomics and Molecular Medicine, George Mason University, Virginia, USA, for allowing me to visit their laboratory and for their valued contribution in a very successful collaboration.

Finally, I would like to thank my parents, Mike and Olive, my family and friends, and especially my girlfriend Aoife, for their love, support and advice during the course of my 10-year stay in university.

Table of Contents:

Abstract

The biological and clinical characterisation and validation of novel biomarkers in colorectal cancer

Seán Fitzgerald

Colorectal cancer (CRC) is the second deadliest type of cancer in Ireland after lung cancer and therapy resistance is a major problem leading to treatment failure in CRC. There is a need for novel independent prognostic biomarkers in CRC that can accurately predict prognosis and predictive biomarkers capable of predicting a patient's likelihood to respond to a particular therapy. A previous study carried out in this laboratory identified biologically relevant antigens with potential utility as diagnostic, prognostic, predictive and therapeutic biomarkers in CRC, (Kijanka *et al.*, 2010).

The aim of this PhD project is to evaluate the CRC tissue expression patterns of two of these novel cancer-specific antigens (CerS5 & TRIM28) and to further investigate their role in CRC.

Immunohistochemical staining of CerS5 and TRIM28 was evaluated using tissue microarrays constructed from colorectal cancer patient-tissue samples. The effects of both CerS5 and TRIM28 expression on tumourigenic processes were further characterised using reverse-phase protein microarrays constructed from laser capture micro-dissection enriched tumour epithelium and stroma cells.

CerS5 was found to be a novel prognostic biomarker in CRC patients. Proteomic analysis demonstrated a shift from apoptosis-related pathways in CerS5 Low cases to autophagy in CerS5 High cases. CerS5 expression levels can also identify colorectal cancer patients that would potentially benefit from neoadjuvant therapy (CerS5 High). Hence, it could potentially be used as a predictive biomarker in CRC.

A High TRIM28 expression ratio between epithelial and stromal compartments in colorectal cancer tissue was found to be an independent predictor of poor prognosis. The pathophysiological role of TRIM28 in carcinogenesis may be dependent on expression levels and cell type within the tumour microenvironment and thus a combinatorial approach assessing the tumour cells as well as the corresponding stromal cells may prove to be a more comprehensive way of predicting survival in human cancer

List of Abbreviations:

ADP – adenosine diphosphate

AKT – Protein kinase B

APC – adenomatous polyposis coli

APS – ammonium persulphate

ATP – adenosine triphosphate

bFGF – basic fibroblast growth factor

BSA – bovine serum albumin

CAF – cancer associated fibroblast

CBF-A – CarG box-binding factor-A

CDases – ceramidases

CerS – ceramide synthase

CerS1 – ceramide synthase 1

CerS 2 – ceramide synthase 2

CerS 3 – ceramide synthase 3

CerS 4 – ceramide synthase 4

CerS 5 – ceramide synthase 5

CerS 6 – ceramide synthase 6

CK – ceramide kinase

COX2 – cyclooxygenase 2

CRC – colorectal cancer

CSA – catalysed signal amplication

CT – computed tomography

C1P – ceramide-1-phosphate

C1PP – C1P-phosphatase

DAB – 3, 3'-diaminobenzadine

DAG – diacylglycerol

DES – dihydroceramide desaturase

dH_2O – distilled water

DMSO – dimethyl sulfoxide

DNA – deoxyribonucleic acid

ECL – enhanced chemiluminescence

ECM – extracellular matrix

E. coli – *Escherichia coli*

EGFR – epidermal growth factor receptor

EMT – epithelial-mesenchymal transition

eNos – endothelial nitric oxide synthase

ERK – extracellular-signal-regulated kinases

E2F1 – transcription factor E2F1

FAP – familial adenomatous polyposis

FAP – Fibroblast activation protein, alpha

FBS – foetal bovine serum

FB1 – fumonisin B1

FFPE – formalin-fixed paraffin-embedded

FSP1 – fibroblast-specific protein

GCS – glucosylceramide synthase

GI – gastrointestinal

GIST – gastrointestinal stromal tumour

HDACs – histone deacetylases

His – histidine

His-tag – polyhistidine tag

HNPCC – hereditary non-polyposis colon cancer

HP1 – heterochromatin protein 1

hr – hour

H&E – haematoxylin and eosin

IgG – immunoglobulin G

IHC – immunohistochemical

IMAC – immobilized metal ion affinity chromatography

IPTG – isopropyl-β-D-galactopyranoside

IR – infrared

KAP1 – Krüppel-associated protein

kDa – kilodalton

KRAB – Krüppel-associated box

KRAB-ZPFs – Krüppel-associated box zinc finger proteins

LCM – laser capture microdissection

mAb – monoclonal antibody

MAGE – melanoma associated antigen

MAPK – mitogen-activated protein kinases

MDM2 – murine double minute 2

MEM – minimum essential media

MMP-2 – matrix metalloproteinase-2

MMP-9 – matrix metalloproteinase-9

MRI – magnetic resonance imaging

mRNA – messenger RNA

MW – molecular weight

M-Stage – metastasis status

Ni – nickel

N-Stage – nodal status

OCT – optimal cutting temperature compound

pAb – polyclonal antibody

PAF – platelet-activating factor

PAGE – polyacrylamide gel electrophoresis

PBS – phosphate buffered saline

PBS-T – phosphate buffered saline tween

PC – phosphatidylcholine

PCR – polymerase chain reaction

PDGF – platelet-derived growth factor

PHDs – plant homeodomains

PIL – patient information leaflet

PP2A – protein phosphatase 2

P53 – tumour protein 53

RBCC – ring, B-box, coiled coil

RNA – ribonucleic acid

RNase – ribonuclease

RPMI – Roswell Park Memorial Institute medium

RPPA – reverse-phase protein-microarrays

SPT – serine palmitoyl transferase

SDS – sodium dodecyl sulfate

SGPP1 – S-1-P phosphatase

SMase – sphingomyelinase

SMS – sphingomyelin synthase

SPHK1 – Sphingosine kinase 1

SPT – serine palmitoyl transferase

S1P – Sphingosine-1-phosphate

TAM – tumour associated macrophage

TCEP – tris(2-carboxyethyl)phosphine

TEMED – tetramethylethylenediamine

TGF-β – transforming growth factor beta

TIF1β – transcriptional intermediary factor 1β

TM – transmembrane

TMA – tissue microarray

TMB – 3,3′,5,5′-tetramethylbenzidine

T-PER – tissue protein extraction reagent

TRAIL – TNF-related apoptosis-inducing ligand

TRIM – tripartite motif

TRIM28 – tripartite motif-containing 28

T-Stage – tumour stage

UV – ultraviolet

VEGF – vascular endothelial growth factor

VEGFR2 – vascular endothelial growth factor receptor 2

Wnt – Wingless-related integration site

5-FU – fluorouracil

α-SMA – alpha smooth muscle actin

ρ – Rho

Units

dpi	Dots per inch
µg	Micro-gram
µL	Micro-litre
g	Grams
g	Gravity
(k) Da	(Kilo) Dalton
L	Litre
M	Molar
mg	Milligram
mL	Millilitre
mM	Millimolar
ng	Nano-gram
nm	Nano-metre
°C	Degree Celsius
Ppb	Parts per billion
Ppm	Parts per million
RI	Refractive Index
RPM	Revolutions per minute
U	Unit
V	Volt
v/v	Volume per volume
w/v	Weight per volume
pg	Picogram

List of Figures:

Chapter Three: Colorectal Cancer Patient Cohort and Clinicopathological Features of the Patients

Chapter Four: CerS5 and its Role in Colorectal Cancer

Chapter Five: TRIM28 and its Role in Colorectal Cancer

List of Tables:

Publications, Awards, Presentations and Patent applications:

Publications:

Fitzgerald S, Sheehan KM, Espina V, O'Grady A, Cummins R, Kenny D, Liotta LA, O'Kennedy R, Kay EW and Kijanka G. *High CerS5 expression levels associate with reduced patient survival and transition from apoptotic to autophagy signalling pathways in colorectal cancer.* The Journal of Pathology: Clinical Research, 17 Nov 2014.

Fitzgerald S, Sheehan KM, O'Grady A, Kenny D, O'Kennedy R, Kay EW and Kijanka G. *The relationship between epithelial and stromal TRIM28 expression predicts survival in colorectal cancer patients.* Journal of Gastroenterology and Hepatology, 2013. Jun;28(6):967-74.

O'Reilly J-A, Fitzgerald J, **Fitzgerald S**, Kenny D, Kay EW, O'Kennedy R, and Kijanka G (2015). *Diagnostic Potential of Zinc Finger Protein-Specific Autoantibodies and Associated Linear B-Cell Epitopes in Colorectal Cancer*. PLoS ONE 10(4): e0123469.

Fitzgerald S, Sheehan KM, Espina V, Cummins R, O'Grady A, Kenny D, Liotta LA, Kay EW, O'Kennedy R, and Kijanka G. *Molecular characterization of epithelial and stromal crosstalk associated with TRIM28 expression levels in the tumour microenvironment in colorectal cancer.* (Manuscript in preparation).

Awards:

- The Faculty of Science and Health Outstanding Graduate Researcher 2013 Dublin City University
- Pathological Society Visiting Fellowship, 2013, from the Pathological Society of Great Britain and Ireland
- Orla Benson Scholarship for 2012 from the Dublin City University Educational Trust and the School of Biotechnology
- 3rd Prize in the CSET 'Thesis-in-Three' Competition. Awarded oral presentation: 'How TRIM is your Bowel? - Marker protein Expression in Colorectal Cancer'. Thesis in Three Competition, 9th November 2011, Mansion House, Dublin.

Conference Presentations:

Fitzgerald S, Espina V, Sheehan KM, Cummins R, O'Grady A, Kenny D, O'Kennedy R, Liotta LA, Kay EW and Kijanka G. *Molecular characterization of epithelial and stromal crosstalk associated with TRIM28 expression levels in colorectal cancer.* AACR Special Conference on Cellular Heterogeneity in the Tumor Microenvironment; 2014 Feb 26-Mar 1; San Diego, CA. Philadelphia (PA): AACR; Cancer Res 2015;75: Abstract nr B55. doi:10.1158/1538-7445.CHTME14-B55. (Poster presentation).

Fitzgerald S, Sheehan KM, O'Grady A, Kenny D, O'Kennedy R, Kay EW and Kijanka G. *Increased ceramide synthase 5 expression is associated with lymphovascular invasion, metastasis and poor survival in colorectal cancer*. American Association of Cancer Research (AACR), 2013, Washington DC, USA. (Poster presentation).

Fitzgerald S, Sheehan KM, O'Grady A, Kenny D, O'Kennedy R, Kay EW and Kijanka G. *The tumour-specific antigen TRIM28 is an independent prognostic marker in colorectal cancer.* 24th EORTC-NCI-AACR Symposium on 'Molecular Targets and Cancer Therapeutics' 6-9 November 2012, Dublin, Ireland; European Journal of Cancer, Volume 48, Supplement 6, Page 169, November 2012. (Poster presentation).

Fitzgerald S, Kay EW, Cummins R, Sheehan KM, O'Grady A, O'Kennedy R, Kenny D and Kijanka G. *Cancer and humoral immunity; Translational potential for diagnostic and therapeutic targets.* Irish Society of Immunology Annual Meeting, 20-21 September 2012, Dublin, Ireland; Tumour Immunology Session. (Oral presentation).

Fitzgerald S, Sheehan KM, O'Grady A, Kenny D, O'Kennedy R, Kay EW and Kijanka G. *TRIM28 expression in neoplastic epithelial and stromal compartments predicts survival in colorectal cancer.* EACR and IACR joint conference on "The Tumour Microenvironment" to 17th-19th September 2012, Dublin, Ireland. (Poster presentation).

Fitzgerald S, Sheehan KM, O'Grady A, Kenny D, O'Kennedy R, Kay EW and Kijanka G. *Expression of the tumour-specific antigen TRIM28 in neoplastic epithelial and stromal compartments is an independent prognostic marker in colorectal cancer.* NICB conference "Biotechnology In Action: Stem Cells & Tissue Engineering, Biopharmaceutical Production and Cancer Biomarkers" 4th - 6th September 2012, Dublin, Ireland. (Poster presentation).

Patent application:

Fitzgerald S. '*CerS5 as a predictive variable of response to cancer therapy and in particular neoadjuvant cancer therapy***'.** G.B. Patent Application Number GB1322694.9. Application Filed 20th of December, 2013.

Chapter 1

Introduction and Aims of the Research

1.1 The Colon and Rectum

The colon and rectum are parts of the digestive system, also called the gastrointestinal (GI) system. The GI system is responsible for the breakdown and absorption of various foods and liquids needed to sustain life and rids the body of solid waste (faecal matter). The digestion process begins after food is chewed and swallowed. It then travels through the oesophagus to the stomach. In the stomach, food is partially broken down and sent to the small intestine, where digestion continues and most of the nutrients are absorbed. The small intestine then joins the large intestine in the lower right abdomen. The small and large intestines are occasionally referred to as the small and large bowel. The first and longest part of the large intestine is the colon, a muscular tube about 5 feet long. Water and mineral nutrients are absorbed from the food matter in the colon (Devroede and Phillips, 1969).

As previously described (Whalen, 1975) the colon is composed of 5 main parts (as can be seen in Fig. 1.1):

- The first section of the colon is called the caecum and it is found in the lower right side of a person's abdomen, where the small intestine first attaches to the large intestine.
- The second section is called the ascending colon, so-called because it extends upwards on the right side of a person's abdomen. The ascending colon carries faeces from the caecum superiorly along the right side of the abdominal cavity to the transverse colon. In the ascending colon, bacteria digest the transitory faecal matter in order to release vitamins. The intestinal wall absorbs water, nutrients, and vitamins from the faeces and allows absorption of these materials into the bloodstream. The unwanted waste material is moved upwards toward the transverse section of the colon by a process known as peristalsis.

- The third section is called transverse colon, because it crosses the body from the hepatic flexure of the colon on the right side of the abdomen, to the splenic flexure on the left hand side of the abdomen.
- The descending colon continues downward on the left side. The function of the descending colon in the digestive system is to store faeces that will be emptied into the rectum.
- The final segment of the colon is called the sigmoid colon because of its ‘S’ shape. The walls of the sigmoid colon are muscular, and contract to increase the pressure inside the colon, causing the stool to move into the rectum.

The sigmoid colon then joins the rectum, which is the final straight portion of the large intestine and measures about 6 inches in length. The rectum follows the shape of the sacrum and connects to the anus. It acts as a temporary storage site for faeces before passing them to the anus, from where they are excreted from the body. As the rectal walls expand due to the materials filling it from within, stretch receptors from the nervous system located in the rectal walls stimulate the desire to defecate (Jorge and Wexner, 1997).

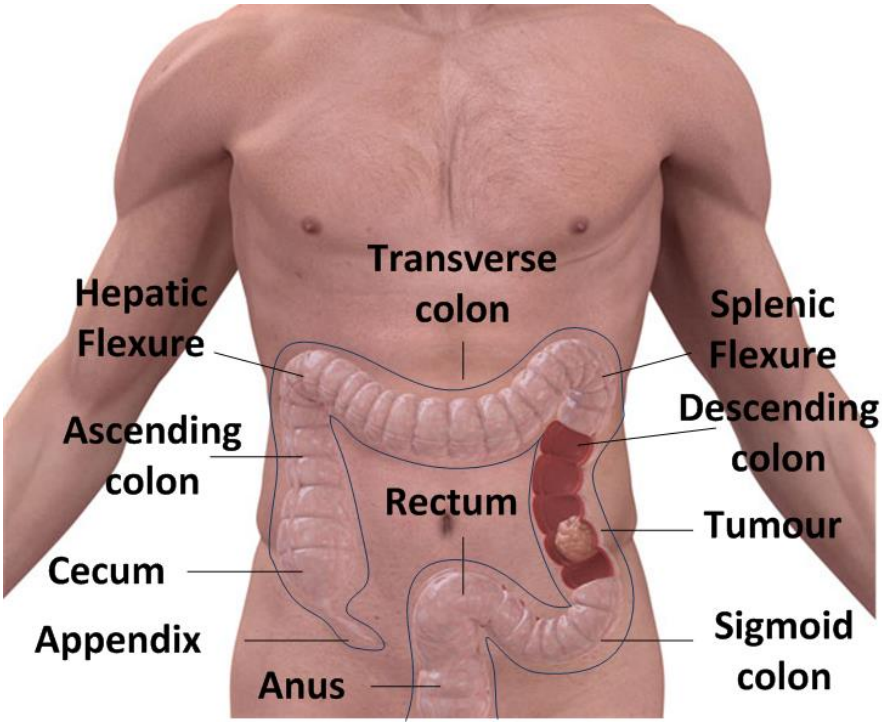

Figure 1.1: The anatomy of the colon and rectum. (Taken and adapted from www.gograph.com).

1.2 Colorectal Cancer

Colorectal cancer (CRC) generally originates from the uncontrolled growth of the epithelial cells in the lining of the colon or rectum of the gastrointestinal tract (Ponz de Leon and Percesepe, 2000). Cell division is the process a cell undergoes to make copies of itself and this process is normally well regulated so that a cell divides only when instructed to do so and when conditions are favourable for division. A cancerous cell, in stark contrast, is an unruly cell that violates this scheme and increases its propensity to proliferate when it would normally rest. This unregulated cell division leads to an accumulation of cells that form a lump or tumour, without an apparent function in the body (Weinberg, 1996).

In the human genome, there are many different types of genes that control cell growth in a very systematic, precise way. When these genes have an error in their DNA code, they may not work properly, and are said to be "altered" or mutated. An accumulation of many mutations in different genes occurring in a specific group of cells over time is required to cause malignancy (Vogelstein and Kinzler, 2004). The different types of genes, that when mutated can lead to the development of cancer include oncogenes, tumour-suppressor genes and DNA-repair genes (Knudson, 2002). What specifically causes mutations to occur in these genes is largely unknown. However, mutations can be caused by carcinogens (factors known to increase the risk of cancer) (Program, 2011) and the development of mutations is also a natural part of the aging process (Tosato *et al.*, 2007).

Benign tumours of the colorectum are referred to as polyps. A polyp is a growth of tissue that develops in the lining of the colon or rectum. Benign polyps can be easily removed during a colonoscopy and are generally not life-threatening. An example of a benign polyp can be seen in figure 1.2 (B). Most polyps remain benign (termed hyperplastic polyps) and the chance of them becoming cancerous is very low. However, other polyps such as adenomatous polyps are termed pre-cancerous polys and if they are not removed, over time they can become malignant (cancerous), (Bond, 2003), and grow into larger, more invasive tumours like those that can be seen in figure 1.2 (C&D).

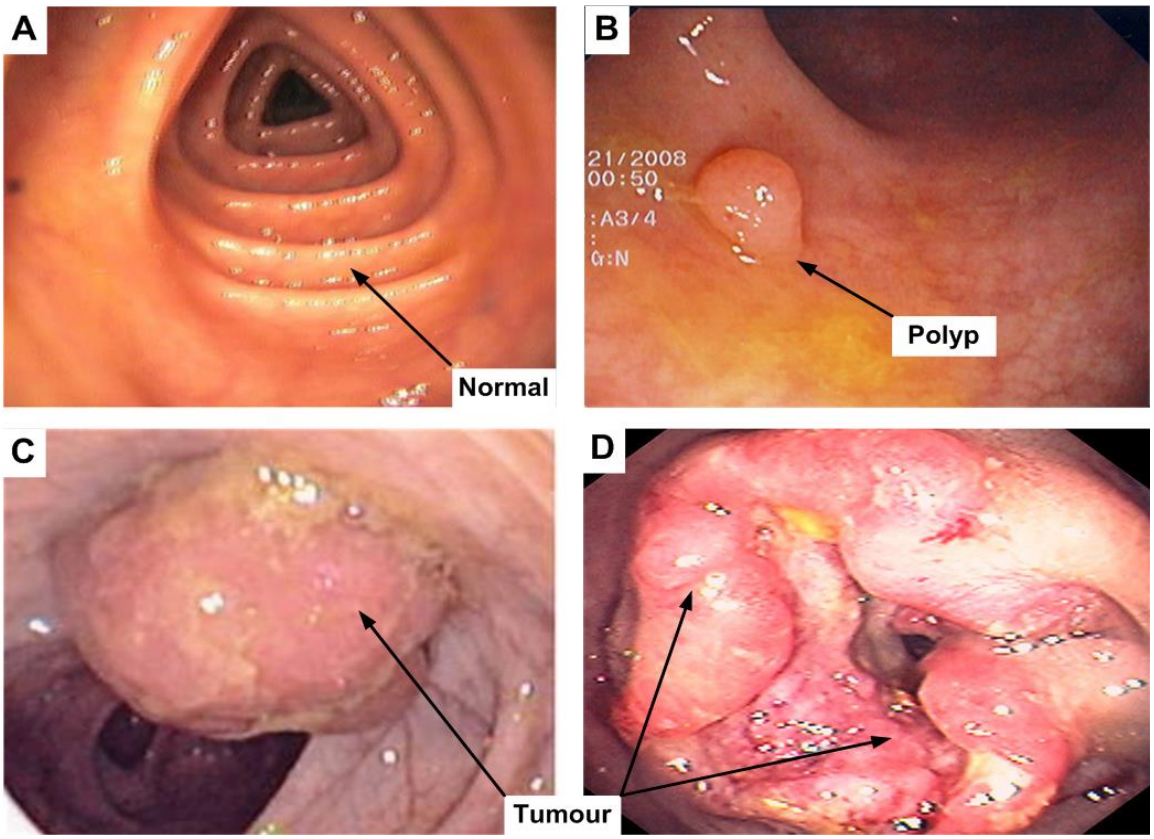

Figure 1.2: Advancing stages of CRC. Composition of photographs taken during colonoscopy procedures on patients with varying stages of CRC. (A) is a picture of normal colonic lumen as seen through a colonoscopy camera. (B) is a picture of a benign polyp. (C) is a picture of a relatively advanced tumour protruding well into the colon. (D) is a picture of a very advanced tumour that is completely occluding the colon. Images taken from: (A); www.portalesmedicos.com, (B); www.medword.com, (C&D); www.gastrointestinalatlas.com

Colorectal cancer usually develops slowly over a period of 10 to 15 years and adenomatous polyps or adenomas are the most likely to become cancerous, though fewer than 10% of adenomas progress to cancer (Sloan *et al.*, 2009). Cancer cells can travel to virtually anywhere in the body via the lymphatic and circulatory systems. The lymphatic system collects fluids, or lymph, lost from blood vessels and returns it to the blood vessels, thus allowing cancer cells to gain access to the bloodstream. Cancer of the colorectum most commonly spreads to the liver and the lungs, where 'secondary'

tumours form (Gutman and Fidler, 1995). The spread of tumours to distant organs is called the metastasis and once metastasis has occurred in CRC, a complete cure of the cancer is unlikely (Kindler and Shulman, 2001).

Mutations in the Wnt-signalling pathway, resulting in increased signalling activity, are thought to be the most frequent cause of CRC. The Wnt-signalling pathway is a network of proteins that passes signals from receptors on the surface of the cell into the nucleus, where it can bind to DNA and alter the expression of genes. It controls cell-cell communication in the embryo and adult (Logan and Nusse, 2004). These mutations can be inherited or acquired and most likely occur in the intestinal crypt stem cells (Cancer, 2006; Mellert *et al.*, 2011). Stem cells are cells found in all multicellular organisms, that can divide (through mitosis) and differentiate into diverse specialized cell types and can self-renew to produce more stem cells. The adenomatous polyposis coli (APC) gene, which produces the APC protein, is the most commonly mutated gene in CRC. The APC protein is responsible for preventing a build-up of the *β*-catenin protein and when a mutation occurs, the levels of active APC protein are diminished. Without APC, *β*-catenin accumulates to high levels and translocates to the nucleus, where it binds to DNA. Once DNA-bound, *β*-catenin activates the transcription of several genes that, when expressed at high levels, can cause cancer (Okamoto *et al.*, 2006).

Colorectal cancer generally occurs more frequently in the left colon than in the right colon, as shown in figure 1.3. The anatomical distribution of colorectal cancer has significant clinical implications for investigating patients with suspected colorectal malignancy. The symptoms can also be different depending on the location of the tumour. For example, right-sided tumours typically present at a more advanced stage (Nawa *et al.*, 2008), and often present with subtle symptoms such as weight loss and anaemia, as opposed to rectal bleeding, change in bowel habit, and tenesmus which are

more evident in left-sided tumours (Lee *et al.*, 2014) and usually caused by growth of the tumour outward into the lumen, obstructing the flow of faeces.

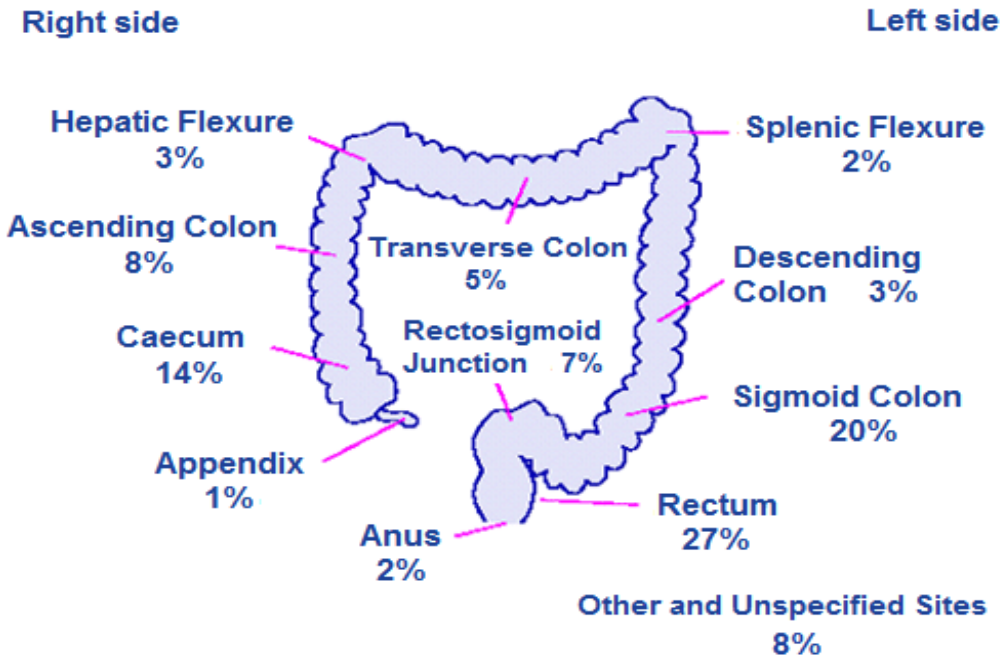

Figure 1.3: Anatomical representation of the most common sites of occurrence of CRC. Taken from www.cancerresearchuk.org

1.2.1 Epidemiology of Colorectal Cancer

Globally, CRC is the third most commonly diagnosed cancer in males and the second in females, with over 1.36 million new cases and 694,000 deaths estimated to have occurred in 2012 (Ferlay *et al.*, 2014). However, the incidences and mortality rates of colorectal cancer vary 10-fold around the world. The highest estimated rates are in Australia/New Zealand (44.8 and 32.2 per 100,000 in men and women, respectively), and the lowest in Western Africa (4.5 and 3.8 per 100,000 in men and women, respectively) (Ferlay *et al.*, 2014). Differences in diet and variable exposure to environmental carcinogens, combined with a background of genetically determined susceptibility, would appear to account for the differences in incidence rates.

In Ireland, colorectal cancer was the second deadliest type of cancer in 2011, after lung cancer, accounting for about 11.7% of all cancer deaths (National Cancer Registry Ireland, 2014). It was also the second most commonly diagnosed cancer in each sex, after prostate cancer in men and breast cancer in women, with approximately 2,436 new cases being diagnosed annually, 1,405 in men and 1,031 in women (National Cancer Registry Ireland, 2014). That corresponds to about one newly diagnosed case every 4 hours in Ireland. Approximately 1,040 people (610 men and 430 women) die from colorectal cancer each year in Ireland (National Cancer Registry Ireland, 2014). Ireland has the ninth highest incidence rate in Europe (Ferlay *et al.*, 2013), as can be seen in figure. 1.4.

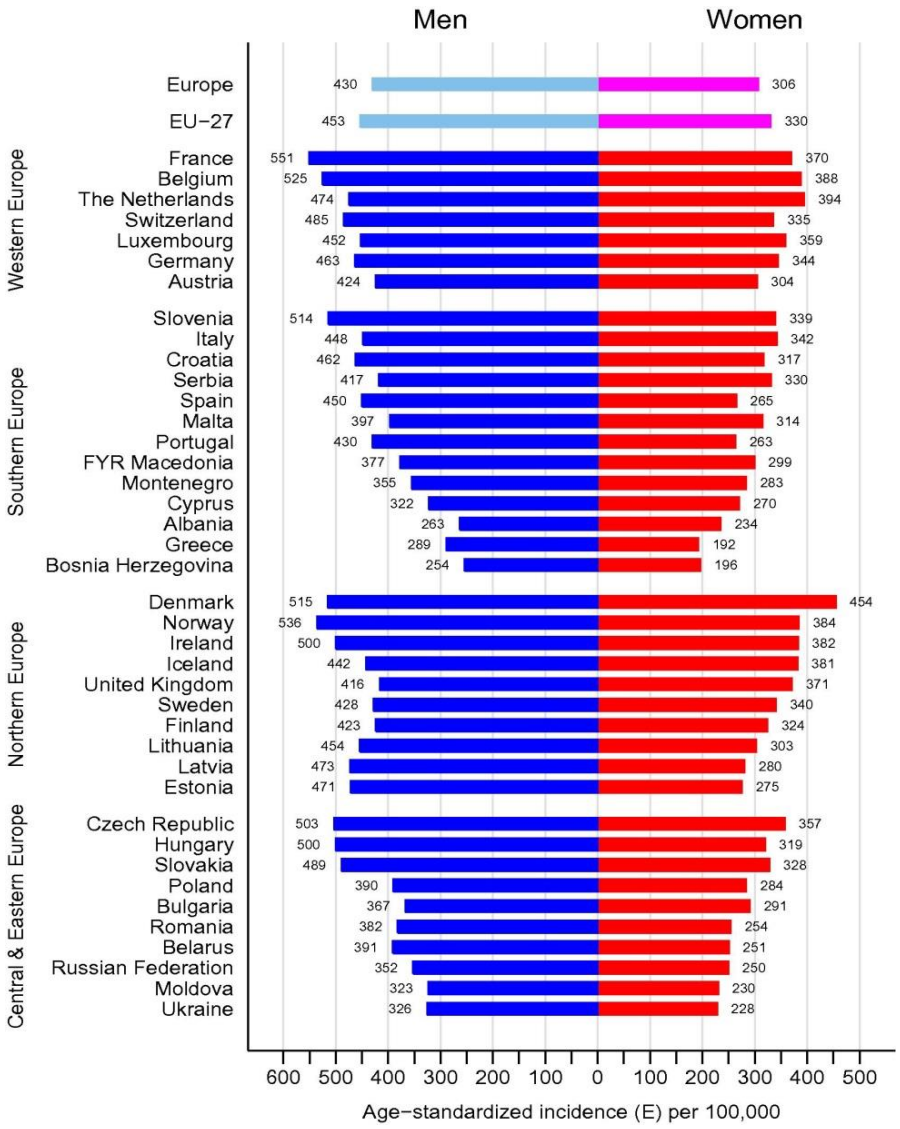

<u>Figure 1.4:</u> Incidences rates of CRC amongst men and women in Europe. (Taken from Ferlay et al., 2013).

The median age at diagnosis for cancer of the colon and rectum is 69 years of age (Howlader, 2012). However, the incidence and death rates for colorectal cancer increase with age, with the incidence rate being more than 15 times higher in adults 50 years and older than in those 20 to 49 years (Howlader, 2012). Screening is effective at decreasing the chance of dying from colorectal cancer and is recommended starting at the age of 50 and continuing until a person is 75 years old.

Anyone can develop colorectal cancer, but overall the incidences and mortality rates of colorectal cancer are about 35% to 40% higher in men than in women (American Cancer Society, 2011). The reasons for this are not completely understood, but are most probably due to the complex interactions between gender-related differences in exposure to hormones and risk factors. Gender differences in risk patterns may also help explain why the proportion of colorectal tumours occurring in the rectum is higher in men (31%) than in women (24%).

Over the last 15 years the number of cases of colorectal cancer has risen by approximately 20% in both sexes. By 2020 the number of new cases of colorectal cancer diagnosed each year in Ireland is projected to increase by 79% in men and 56% in women. This projected growth is attributable to an increasing and ageing population (National Cancer Registry Ireland, 2006).

1.2.2 Causes, symptoms and diagnosis of colorectal cancer

A family history of colorectal cancer; specifically forms such as familial adenomatous polyposis (FAP), Gardner syndrome, and hereditary nonpolyposis colon cancer (HNPCC), can predispose an individual to developing colorectal cancer. Each of these conditions is caused in part by a known genetic mutation. Chronic inflammatory bowel diseases such as Crohn's disease or ulcerative colitis are associated with colorectal cancer (Gillen *et al.*, 1994), as is the presence of a large number of non-cancerous polyps along the wall of the colon or rectum (Shinya and Wolff, 1979). Other risk factors include physical inactivity and a diet high in fats.

Early stage colorectal cancer often has little or no symptoms, therefore presenting symptoms are often indicative of relatively advanced CRC (Nawa *et al.*, 2008), which is why screening and early detection is so important. Because colorectal cancer is a

disease of the GI tract, many of the symptoms are associated with abnormal digestion and elimination. The majority of patients presenting with symptomatic CRC have symptoms such as hematochezia (blood in the stool), abdominal pain, otherwise unexplained iron deficiency anaemia, a change in bowel habits, a new onset of constipation, diarrhoea that lasts for more than a few days or unintentional weight loss (www.cancer.ie). These symptoms accompany a variety of different illnesses, and hence a physician should be consulted to determine their cause and to confirm a diagnosis.

Diagnosis of colon and rectal cancers is made by means of several techniques. During a digital rectal examination, the physician inserts a gloved finger into the rectum and feels its surface for abnormalities. A faecal test may also be used to detect the presence of blood in the stool (Young *et al.*, 2002). In order to examine the rectum more carefully, a physician may use a narrow, flexible tube called a sigmoidoscope to look at the lining of the rectum and the distal colon. Colonoscopy uses a similar device to examine the entire colon. A biopsy may also be performed in which a small piece of tissue is removed using the colonoscope and then examined under a microscope by a pathologist for signs of cancer. New non-invasive imaging techniques may also be used in the diagnosis of CRC and these include magnetic resonance imaging (MRI), computed tomography (CT) scans and Positron emission tomography (PET) scans (Maas *et al.*, 2011). If cancer is discovered, the degree to which it has spread (metastasised) from the colon or rectum is then determined, either by taking biopsies from surrounding tissue/organs, or using one of the previously mentioned imaging techniques.

1.2.3 Histopathology of Colorectal Cancer

The histopathology of a tumour is usually reported from the analysis of tissue taken from a biopsy or surgery. A histopathology report will usually contain a detailed description of all aspects of the tumour. The type of colon tumour describes the cells from which the tumour arises. Adenocarcinoma is the most common type, accounting for 95-98% of colorectal cancers (www.oncolink.org). Two subtypes of adenocarcinoma are signet ring and mucinous adenocarcinoma, which are both named for the way the cells look under the microscope. Sometimes, tumour cells are discohesive and secrete mucus, which invades the interstitium producing large pools of mucus/colloid (mucinous adenocarcinoma). If the mucus remains inside the tumour cell, it pushes the nucleus at the periphery and these are referred to as signet-ring cell tumours (Makino et al., 2006). The other 2-5% of cancers found in the colon, are generally lymphomas, gastrointestinal stromal tumour (GIST), and carcinoid tumours.

Normal colorectal mucosa is a highly organised network of glands composed of epithelial cells. These glands are inter-connected by stromal cells (Fig 1.5). Adenocarcinoma is a malignant epithelial tumour, originating from the glandular epithelium of the colorectal mucosa (Fig 1.6) and glandular formation is the basis for histologic tumour grading in CRC. In well differentiated adenocarcinoma >95% of the tumour is gland forming. Moderately differentiated adenocarcinoma shows 50-95% gland formation while poorly differentiated adenocarcinomas are mostly solid with <50% gland formation. The majority of colorectal adenocarcinomas are diagnosed as moderately differentiated (~70%), with well and poorly differentiated carcinomas account for 10% and 20%, respectively (Fleming *et al.*, 2012).

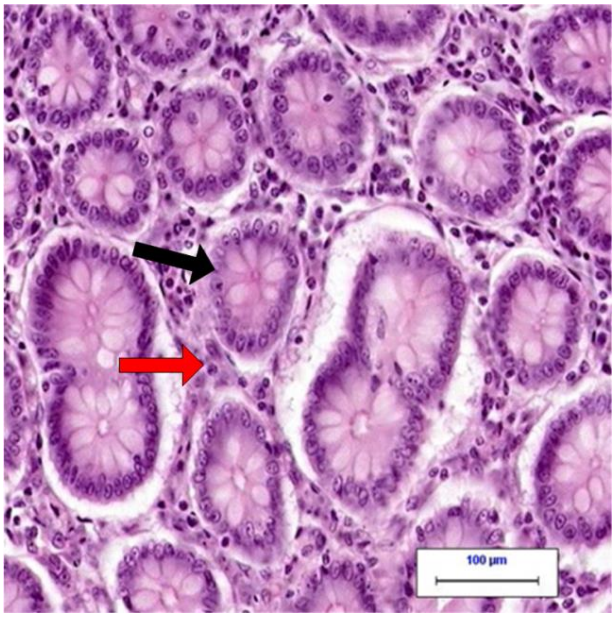

Figure 1.5: Normal Colonic Mucosa. Normal colonic crypts when transected have the appearance of gun barrels (black arrow). There is little lamina propria between the crypts (red arrow). Nuclei are basally placed and uniform. (Taken and adapted from www.MyBiopsy.org).

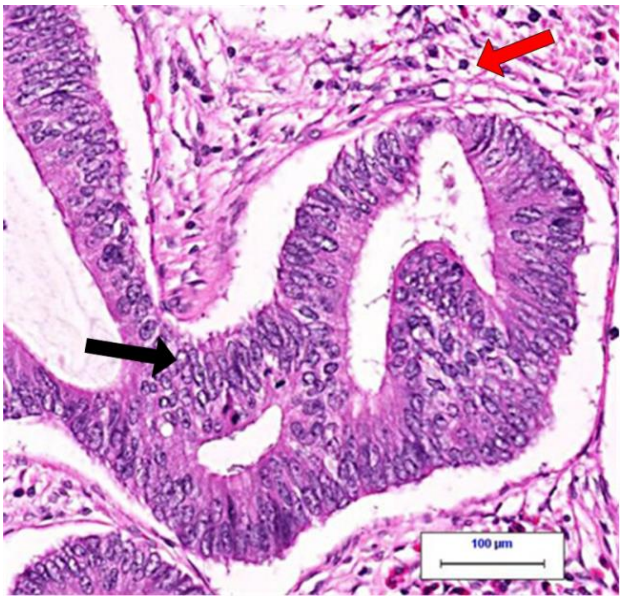

Figure 1.6: Cancerous Colonic tissue. Transverse section of an invasive adenocarcinoma. The cancerous cells are seen in the centre and at the top left of the image (black arrow). The biopsy contains colonic mucosa showing infiltrative glands surrounded by desmoplastic stroma consistent with submucosal invasion (red arrow). (Taken and adapted from www.MyBiopsy.org).

If left untreated the tumour will grow and invade the muscularis mucosae, then the submucosa, thence the muscularis propria and, finally, the serosa. From here the disease will then spread to other organs, as can be seen in figure 1.7.

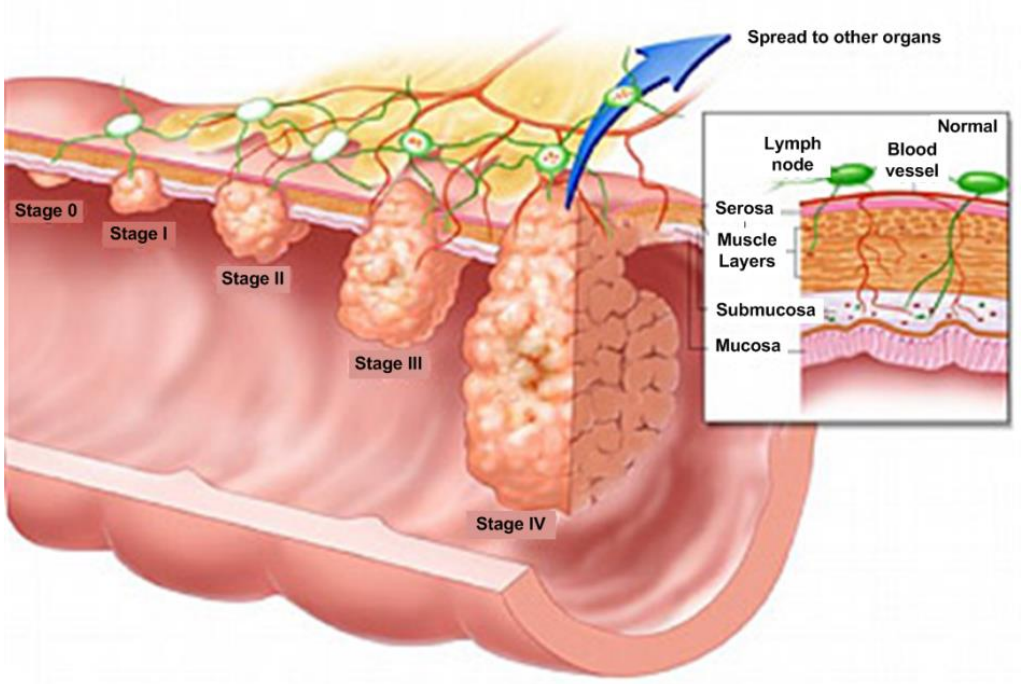

Figure 1.7: Colorectal cancer progression. Stage 0: The tumour has not grown beyond the inner lining of the colon or rectum. Stage I: The tumour has spread through the muscularis mucosae. Stage II: The cancer has grown through the submucosa Stage III: The tumour has grown through the muscularis propria and the serosa and may also spread to local lymph nodes. Stage IV: The tumour has spread from the colon or rectum to distant organs, such as the liver, lungs, or ovaries. The insert shows in more detail the tissue layers within the colorectum. (Taken and adapted from www.digestivehealth.net).

1.2.4 The Dukes and TNM Staging Systems

In 1932 the British pathologist Cuthbert Dukes (1890-1977) devised a classification system for colorectal cancer which was an accurate prognostic indicator and a predictor of mortality (Dukes, 1932). Before the Dukes classification, the main prognostic tool was a histological grading system, based solely on cell differentiation and which had a limited prognostic value. Dukes classification of colorectal cancer initially seemed to be a crude classification based on the level of cancer invasion, but is in fact rather sophisticated and still relevant nearly 80 years after its publication. The system classifies the tumour into stage A, B, C or D based on the following guidelines:

Dukes A: Invasion into but not through the bowel wall (90% 5-year survival).
Dukes B: Invasion through the bowel wall but not involving lymph nodes (70% 5-year survival).
Dukes C: Involvement of lymph nodes (30% 5-year survival)
Dukes D: Widespread metastases (5% 5-year survival).

The Dukes staging system was originally published for rectal cancer only and did not include distant metastases. However, the system was later adapted as follows:

- Adapted by Kirklin in 1949 and later by Astler and Coller in 1953 to include both colon and rectal tumours. (Kirklin *et al.*, 1949; Astler and Coller, 1954)
- Revised by Turnbull in 1967 to include stage for un-resectable tumours and distant metastases. (Turnbull *et al.*, 1967)

Due to its accuracy in predicting prognosis, its reproducibility and its simplicity, the Dukes staging system was used internationally for many years. However, this system has now largely been replaced by the more detailed TNM staging system and is no longer recommended for use in clinical practice (Edge and Compton, 2010).

The TNM-Staging System:

The TNM Classification of Malignant Tumours is a cancer staging system, first devised by Pierre Denoix for use in all solid tumours (Denoix, 1946). This system utilises the extent of the primary tumour (Tis-4), the absence or presence of cancer in the lymph nodes (N0-2), and the existence of metastasis (M0 or 1) to assign a TNM rating, which corresponds to a stage. All of these classifiers are used to determine the stage of the cancer and what treatment is needed. The American Joint Committee on Cancer 5th Edition TNM rating is summarised in table 1.1.

Table 1.1: The American Joint Committee on Cancer 5th Edition TNM Stages

Taken and adapted from the American Joint Committee on Cancer website (https://cancerstaging.org).

	Primary Tumour (T)
TX	Primary tumour cannot be assessed
T0	No evidence of primary tumour
Tis	Carcinoma in situ: intraepithelial or invasion of lamina propria
T1	Tumour invades submucosa
T2	Tumour invades muscularis propria
T3	Tumour invades through the muscularis propria into pericolorectal tissues
T4a	Tumour penetrates to the surface of the visceral peritoneum
T4b	Tumour directly invades or is adherent to other organs or structures
	Regional Lymph Nodes (N)
NX	Regional lymph nodes cannot be assessed
N0	No regional lymph node metastasis
N1	Metastasis in 1–3 regional lymph nodes
N1a	Metastasis in one regional lymph node
N1b	Metastasis in 2–3 regional lymph nodes
N1c	Tumour deposit(s) in the subserosa, mesentery, or nonperitonealized pericolic or perirectal tissues without regional nodal metastasis
N2	Metastasis in 4 or more regional lymph nodes
N2a	Metastasis in 4–6 regional lymph nodes
N2b	Metastasis in 7 or more regional lymph nodes
	Distant Metastasis (M)
M0	No distant metastasis
M1	Distant metastasis
M1a	Metastasis confined to one organ or site (for example, liver, lung, ovary, non-regional node)
M1b	Metastases in more than one organ/site or the peritoneum

These ratings are then combined to form an overall stage for the cancer. For example:

Stage IIA (T3, N0, M0): The cancer has grown into the outermost layers of the colon or rectum but has not gone through them (T3). It has not reached nearby organs. It has not yet spread to the nearby lymph nodes or distant sites.

Stage IIIA (T1 or 2, N1, M0) the cancer has spread through the submucosa or muscle layer and into 1-3 lymph nodes, but has not spread to other areas of the body.

Stage IV (Any T, Any N, M1): the cancer has spread to other areas of the body (i.e. liver, lungs). This is also called Dukes D colorectal cancer.

Lymphovascular invasion refers to the spread of cancer cells to the blood vessels and/or the lymphatics system. The presence of Lymphovascular invasion can be used to identify patients with sporadic primary colorectal cancer with aggressive tumours and as a factor that independently indicates an unfavourable prognosis (Lim *et al.*, 2010).

1.2.5 Prevention, Prognosis and Treatment of Colorectal Cancer

A lifestyle that includes regular exercise and a diet low in fats and high in fibre helps to prevent colorectal cancer. A report published in 2005 that analysed data on the use of the pain-reliever, aspirin, and cancer risk in different study groups over a 20-year period, revealed that consistent use of aspirin lowered the risk for colon cancer by 23 percent (Chan *et al.*, 2005).

Colorectal cancer patients have an excellent five-year survival rate when the disease is detected early, and those patients often go on to live long, healthy lives. Overall, only 39% of colorectal cancer patients diagnosed between 2004 and 2010 had localized-

stage disease, for which the 5-year relative survival rate is 89.9%. Five-year survival rates for patients diagnosed at the regional and distant stage are 70.5% and 12.9%, respectively, (Table 1.2). The 5-year relative survival rate for colorectal cancer has increased from 51% for cases diagnosed in the mid-1970s to 67% for cases diagnosed in 1999-2006. The introduction of 5-fluoroucil-based adjuvant chemotherapy for resectable stage III colon cancer was a significant advance in colorectal cancer treatment as it reduced mortality by up to 30% (Moertel *et al.*, 1990).

Table 1.2: Stage Distribution and 5-year Relative Survival by Stage at Diagnosis for 2004-2010, (all races, both sexes). (Taken and adapted from www.cancer.gov).

Stage Distribution and 5-year Relative Survival by Stage at Diagnosis for 2002-2008, All Races, Both Sexes		
Stage at Diagnosis	**Stage Distribution (%)**	**5-year Relative Survival (%)**
Localized (confined to primary site)	39	89.8
Regional (spread to regional lymph nodes)	36	70.5
Distant (cancer has metastasised)	20	12.9
Unknown (unstaged)	5	33.2

Colorectal cancer is generally treated by surgery, often in combination with chemotherapy, or radiation depending on the site of the cancer and the degree to which it has spread. For cancers localized to the colon or rectum, surgery is usually all that is required. For very early-stage tumours of the colon or rectum, a colonoscope/ laparoscope may be used to remove the cancerous polyps (Green *et al.*, 2013). Other early colonic or rectal tumours require a surgical resection, whereby the portion of the colon or rectum containing the cancerous tissue is removed along with surrounding tissue and nearby lymph nodes, and the remainder of the organ is repaired if possible (Guillem *et al.*, 1997).

For more advanced tumours where cancer has spread to other parts of the body chemotherapy is administered before and/or after surgery and the standard first-line chemotherapy for metastatic colorectal cancer generally consists of one of two regimens: FOLFOX (5-FU (Fluorouracil), leucovorin, and oxaliplatin) or FOLFIRI (5-FU, leucovorin, and irinotecan) (Kelly and Cassidy, 2007). Radiation therapy is often used in combination with chemotherapy in the treatment of rectal cancer (Schmoll *et al.*, 2012), but is not currently used in the treatment of colon cancer due to the sensitivity of the colon to radiation (Martenson *et al.*, 2004). Radiation therapy is generally used either before surgery to help shrink the tumour or following surgery to destroy any remaining cancerous tissue (Glimelius, 2002). Side effects of both radiation and chemotherapy may include vomiting, diarrhoea, and fatigue.

Other novel treatments currently in various stages of development include:

• Target Therapies: Several targeted therapies are already used to treat colorectal cancer, including bevacizumab (Avastin), cetuximab (Erbitux), and panitumumab (Vectibix). Bevacizumab, a monoclonal antibody that helps cut off the nutrient supply to the tumour by suppressing blood vessel growth (anti-angiogenesis), may also help

improve survival when included with standard treatment regimens (Giantonio *et al.*, 2007). Cetuximab and panitumumab, both monoclonal antibodies against the epidermal growth factor receptor (EGFR), have also been shown to improve survival when administered with multi-agent chemotherapy. These antibodies, however, are only effective in patients whose tumours lack RAS mutations (Lièvre *et al.*, 2006; Amado *et al.*, 2008). Doctors continue to study the best way to give these drugs to make them more effective and newer studies are trying to determine if using them with chemotherapy in earlier stage cancers as part of adjuvant therapy may further reduce the risk of recurrence.

• Adoptive Cell Therapy. Unlike vaccines that prevent infectious diseases, these vaccines are meant to boost the patient's immune reaction to fight colorectal cancer more effectively. For example, some vaccines involve removing some of the patient's own immune system cells (called dendritic cells) from the blood, genetically modifying or treating them with chemicals to enhance their activity, and then re-introducing them into the patient with the goal of improving the immune system’s anti-cancer response (Besser *et al.*, 2009). At this time, these types of vaccines are only available in clinical trials; such as U.S. National Institutes of Health phase I/II clinical trial on the use of anti-VEGFR2 gene engineered CD8+ lymphocytes for the treatment of metastatic cancer (Rosenberg, 2010).

• Gene studies to determine optimal, individualized treatment for advanced colorectal cancer based on patient gene profile (Mariadason *et al.*, 2003; De Mattos-Arruda *et al.*, 2011).

1.3 Biomarkers in Colorectal Cancer

The National Institutes of Health Biomarkers Definitions Working Group defined a biomarker as “a characteristic that is objectively measured and evaluated as an indicator of normal biological processes, pathogenic processes, or pharmacologic responses to a therapeutic intervention”, (Biomarkers Definition Working Group, 2001). Understanding and exploiting this relationship between measurable biological processes and clinical outcomes is crucial to disease management. Biomarkers can be used at all stages of disease including screening and detection, diagnosis, prognosis, predicting response to therapy and as therapeutic targets.

An ideal biomarker should have the following characteristics:

- Be safe and easy to measure
- Be cost efficient to follow up
- Be consistent across gender and ethnic groups
- Be modifiable with treatment

The use of biomarkers in clinical practice as well as in research has become commonplace and they are routinely used to predict serious illnesses such as diabetes and cardiovascular disease. A list of commonly used biomarkers in CRC is summarised in Table 1.3.

Table 1.3: Summary of currently used biomarkers in CRC.

Screening / Diagnostic Biomarkers:	Description:	Benefits:	Limitations:
Faecal occult blood test	A fecal occult blood test (FOBT) checks for hidden (occult) blood in the stool (feces)	Cost-Effective	Relatively Low Specificity, Poor Patient-Compliance
Septin 9	Hypermethylation of its promoter region is known to be associated with CRC	Good Specificity (90%)	Poor Senitivity (72%)
CEA	Measurement of the CEA level is commonly used as part of the follow up after curative resection for CRC	Cost-Effective	CRC has already occured
Predictive Biomarkers:	**Description:**	**Benefits:**	**Limitations:**
KRAS	In chemotherapy-refractory metastatic CRC, a KRAS mutation predicts a complete lack of response to anti-EGFR therapy	Identifies Non-responders to anti-EGFR therapy	Only Effective in patients with mutant KRAS
B-RAF	B-RAF mutations may have a predictive role in the response to therapy with antiEGFR in patients with wild-type KRAS	Identifies Non-responders to anti-EGFR therapy	Only Effective in patients with mutant B-RAF
DPD	Involved in the catabolism of uracil and thymine and is the initial rate-limiting enzyme involved in the metabolism of 5-FU in the liver	Predicts patients who are likely to suffer serious 5-FU toxicity	No currently available assays can accurately assess DPD status
Prognostic Biomarkers:	**Description:**	**Benefits:**	**Limitations:**
KRAS	As Above	Independent Predictor of Prognosis	Only accurate for a small percentage of CRC patients
B-RAF	As Above	Independent Predictor of Prognosis	Only accurate for a small percentage of CRC patients
Mismatch Repair Deficiency	DNA damage is not recognized by the deficient mismatch repair system and therefore, apoptosis is not triggered and the cancerous cell survives	Independent Predictor of Prognosis	Only accurate for a small percentage of CRC patients

In a previous study carried out in this laboratory, it was demonstrated that screening high-density protein arrays can distinguish unique antibody profiles that discriminate between symptomatic patients with and without colorectal cancer and can identify biologically relevant antigens with potential utility as diagnostic, prognostic, predictive and therapeutic biomarkers in CRC, as shown previously, (Kijanka *et al.*, 2010). Although many studies have looked at these cancer-specific antibodies, little is known about the corresponding antigens and their relevance in disease.

Eighteen antigens associated with colorectal cancer and 4 antigens associated with the absence of the disease were identified from a training set of sex- and age-matched patients and controls. These markers were confirmed to have corresponding antibodies in sera of a larger cohort of patients (Kijanka *et al.*, 2010). Expression of two of these identified antigens; tripartite motif-containing 28 (TRIM28) and longevity assurance gene homologue 5 (CerS5) was further characterised by quantitative reverse transcription-PCR. Significantly elevated mRNA levels for TRIM28 and CerS5 antigens in colorectal tumours compared with adjacent normal tissue were found (Fig. 1.8).

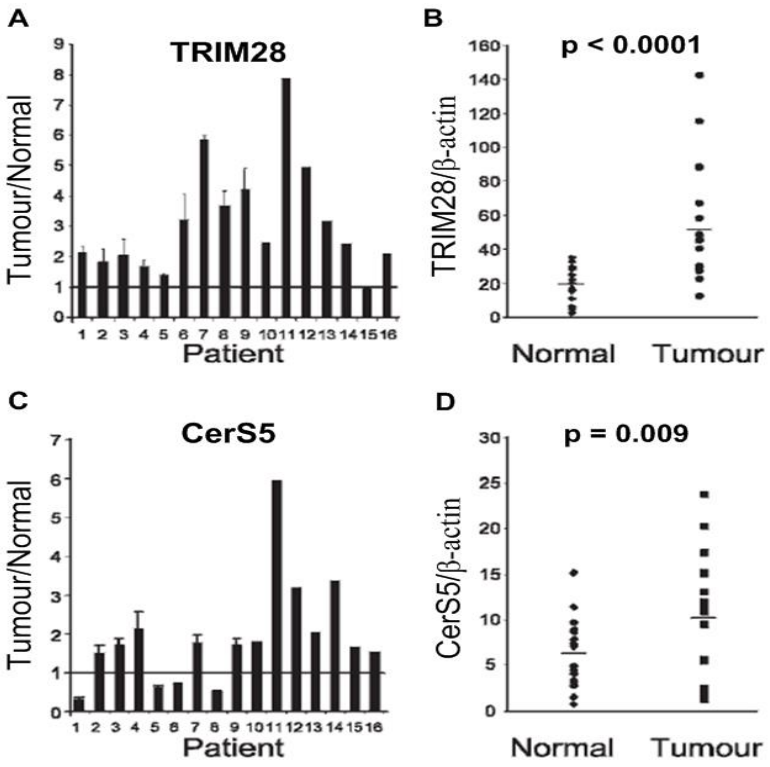

Figure 1.8: mRNA levels of TRIM28 and CerS5 antigens are significantly elevated in colorectal tumours compared with adjacent normal tissue. The graphs represent the ratios between gene expression of TRIM28 (A & B) and CerS5 (C & D) at the mRNA level in tumour compared with adjacent normal tissue in patients with CRC. The line represents the average expression in either tumour or normal tissue. p-values were calculated using the Wilcoxon rank-sum method. (Taken and adapted from Kijanka et al., 2010).

1.4 CerS5, Ceramide Synthases and Sphingolipid Metabolism in CRC

CerS5, also called TRH4, is a 392 amino acid endoplasmic reticulum, multi-pass membrane protein that functions as a bona fide (dihydro) ceramide synthase (Fig. 1.9) and is thought to be a key regulator in the network of specialized and compartmentalized enzymes that regulate sphingolipid metabolism. The bioactive sphinogolipids including, ceramide, Sphingosine, and Sphingosine-1-phosphate (S1P) have important roles to play in several types of signalling and regulation of many cellular processes including cell proliferation, apoptosis, senescence, angiogenesis and transformation. In sphingolipid metabolism, ceramide is regarded as the key intermediate in the pathway of sphingolipid biosynthesis (Merrill, 2002). Sphingolipids are also important bioactive molecules in various aspects of cancer biology, with ceramide being a crucial cell death signalling molecule. Ceramide regulates numerous cell-stress responses including the induction of apoptosis (Mullen and Obeid, 2012) and cell senescence (Venable and Yin, 2009) and S1P plays important roles in cell survival, migration and inflammation (Hait *et al.*, 2006; Van Brocklyn and Williams, 2012). Alterations of ceramide levels and/or increased levels of S1P are increasingly implicated in various stages of cancer pathogenesis, including an anti-apoptotic phenotype, metastasis and escape from senescence. Ceramide is synthesized *de novo* from serine and palmitoyl CoA through the action of serine palmitoyl transferase (SPT) and ceramide synthases.

The CerS (Ceramide Synthase) proteins are a family of proteins that are highly conserved from yeasts to mammals. Six members of this family of proteins have been characterized (CerS1, CerS2, CerS3, CerS4, CerS5 and CerS6). The CerS family subdivide into two distinct groups, with CerS1 in its own category and CerSs 2–6 on a separate branch. This is consistent with the fact that CerS1 is much closer to the yeast proteins than the others (Mizutani *et al.*, 2005). The six human CerS genes are located

on different chromosomes, with the exception of CerS1 and 4, which are located on the same chromosome but at distant locations (Pewzner-Jung *et al.*, 2006). The CerS family of proteins also share similar transmembrane profiles of four to seven predicted transmembrane (TM) domains, although the exact number of TM domains, and their topology, has not been resolved experimentally (Winter and Ponting, 2002; Futerman and Riezman, 2005; Yu *et al.*, 2006). Membrane localization of mammalian CerS1, CerS4, CerS5, and CerS6 (Venkataraman and Futerman, 2002; Riebeling *et al.*, 2003; Mizutani *et al.*, 2005) is established to be in the endoplasmic reticulum.

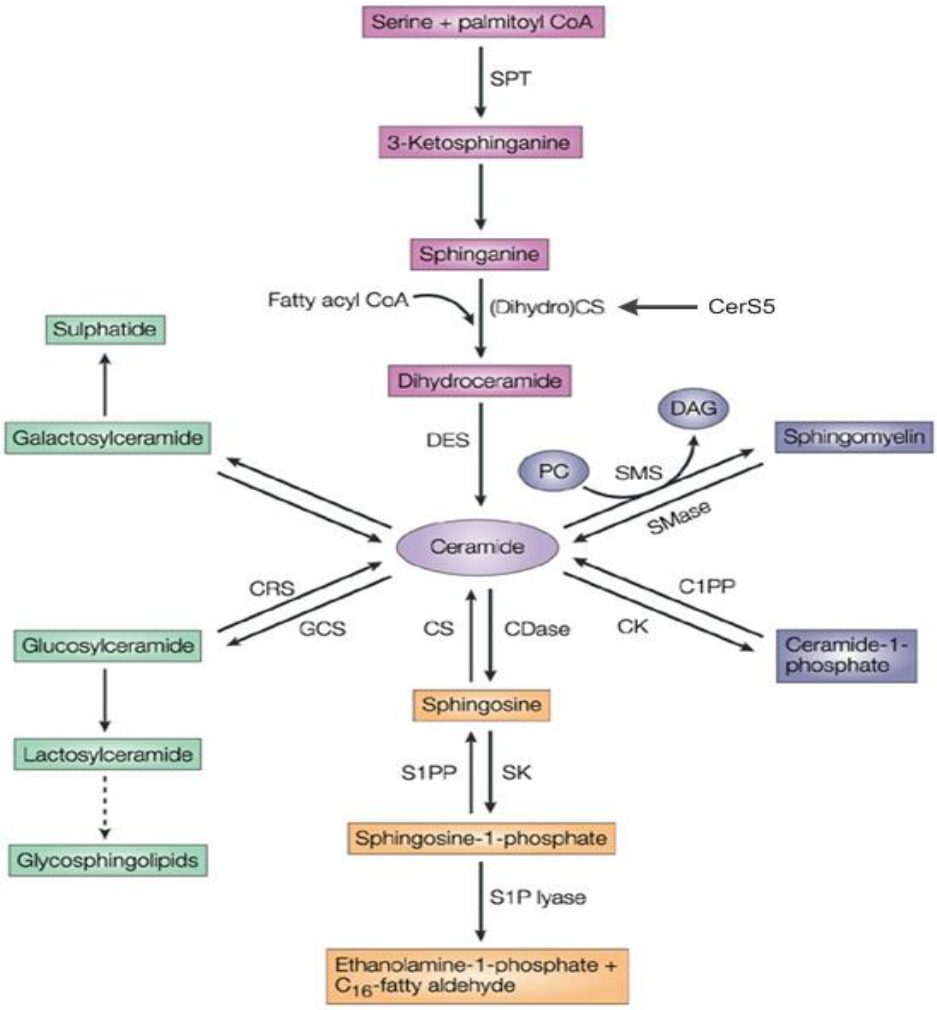

Figure 1.9: Pathways of sphingolipid metabolism. Ceramide can be formed *de novo* (pink) or from hydrolysis of sphingomyelin (blue) or cerebrosides (green). Conversely, ceramide can be phosphorylated by ceramide kinase to yield ceramide-1-phosphate, or can serve as a substrate for the synthesis of sphingomyelin or glycolipids. Ceramide can be metabolized (orange) by ceramidases (CDases) to yield Sphingosine, which in turn is phosphorylated by Sphingosine kinases (SKs) to generate Sphingosine-1-phosphate (S1P). S1P can be cleared by the action of specific phosphatases that regenerate Sphingosine or by the action of a lyase that cleaves S1P into ethanolamine-1-phosphate and a C16-fatty-aldehyde. C1PP, ceramide-1-phosphate phosphatase; CRS, cerebrosidase; CK, ceramide kinase; CS, ceramide synthase; DAG, diacylglycerol; DES, dihydroceramide desaturase; GCS, glucosylceramide synthase; CerS5, longevity assurance homolog 5; PC, phosphatidylcholine; SGPP1, S-1-P phosphatase; SMS, sphingomyelin synthase; SMase, sphingomyelinase; SPT, serine palmitoyl transferase. (Taken and adapted from Ogretmen and Hannun, 2004).

The first evidence for specific functional roles of mammalian CerS genes was obtained upon overexpression of CerS1, which resulted in a selective increase in C_{18}-ceramide in mammalian cells (Venkataraman *et al.*, 2002). CerS4 was subsequently shown to selectively utilize $C_{18/20}$ and C_{16} acyl-CoAs (Riebeling *et al.*, 2003), CerS6 was found to produce shorter acyl chain ceramides (C_{14} and C_{16}) (Mizutani *et al.*, 2005), and CerS3 produced C_{18}- and C_{24}-ceramides (Mizutani *et al.*, 2005; Mizutani *et al.*, 2006). Verification that mammalian CerS proteins are *bona fide* ceramide synthases, rather than regulators of endogenous ceramide synthases, was obtained when purified CerS5 was shown to possess synthase activity (Lahiri and Futerman, 2005). This suggests that CerS proteins are genuine ceramide synthases, with each mammalian CerS family member utilizing a relatively restricted subset of fatty acyl-CoAs.

CerS5 is thought to preferentially generate C_{16}-ceramide and increased generation of C_{16}-ceramide has been shown in response to CerS5 expression (Venkataraman *et al.*, 2002; Riebeling *et al.*, 2003). The generation of C_{16}-ceramide is suggested to be specifically involved in apoptotic signalling. C_{16}-ceramide levels were shown to continually increase in a time-dependent manner in SW480 cells after TRAIL (tumour necrosis factor-related apoptosis-inducing ligand) treatment and this increase was accompanied by decreases in intracellular sphingosine (White-Gilbertson *et al.*, 2009). TRAIL is a death receptor ligand that selectively kills cancer cells without toxicity to normal cells. It was also shown that the ceramide synthase inhibitor fumonisin B1, significantly inhibited the increase in C_{16}-ceramide in SW480 colon cancer cells (White-Gilbertson *et al.*, 2009). This data suggests that ceramide synthases utilize sphingosine as a substrate to generate C_{16}-ceramide in the salvage pathway of sphingolipid synthesis, leading to apoptosis in the cell.

Under normal circumstances sphingolipid metabolism is perfectly balanced between the pro-apoptotic ceramide and Sphingosine and the pro-survival Sphingosine-1-phosphate. However, abnormalities in sphingolipid metabolism disturb the balance between various tumour-promoting and tumour-suppressing sphingolipid species, thereby influencing the overall fate of the cell (Sliva *et al.*, 2000). Ceramide can be metabolized to Sphingosine through the action of ceramidase (Mao *et al.*, 2000) and Sphingosine, in turn, can be phosphorylated by Sphingosine kinase, producing S1P (Olivera *et al.*, 1994). Increasing intracellular ceramide levels through exposure to exogenous ceramide or the ceramidase inhibitor B13, induces apoptosis in cancer cells (Selzner *et al.*, 2001; Renert *et al.*, 2009). Ceramide can directly bind to protein phosphatase 2A (PP2A), thereby enhancing the association of PP2A to pro-apoptotic endothelial nitric oxide synthase (eNos) and reducing the association between eNos and anti-apoptotic AKT, which ultimately promotes apoptosis through dephosphorylation of AKT (Zhang *et al.*, 2012). S1P on the other hand binds to G protein-coupled receptors, increasing motility of cancer cells through coupling to Rac and Rho GTPases, as well as proliferation through the mitogen-activated protein kinases (MAPK) pathway (Pyne and Pyne, 2010). Furthermore, S1P inhibits ceramide-induced apoptosis through the activation of the extracellular signal–regulated protein kinase (ERK), also a MAPK family member (Cuvillier *et al.*, 1996). Consequently, ceramide and S1P have antagonistic cellular effects mediated through different signalling pathways.

Chemotherapy can alter the balance of sphingolipid metabolism and drive the cell towards apoptosis. The molecular mechanisms involved in chemotherapy-induced apoptosis are diverse and depend on cell type and drugs used. However, a common pathway leading to tumour cell death has been shown to implicate the generation of ceramide (Dimanche-Boitrel *et al.*, 2011) through *de novo* ceramide synthesis, activation of sphingomyelinase, and blockage of glucosylceramide formation (Morales *et al.*, 2007).

The resulting ceramide-driven apoptosis is mediated by the activation of various protein kinases, phosphatases and ultimately caspases (Morales *et al.*, 2007). Celecoxib, a selective cyclooxygenase-2 (COX-2) inhibitor that induces apoptosis and inhibits proliferation in cancer cells, also leads to elevated levels of the pro-apoptotic C16-ceramide (Schiffmann *et al.*, 2010). Daunorubicin, an inhibitor of DNA replication, promotes ceramide formation and apoptosis by stimulating ceramide synthase activity, which in turn can be reversed by the ceramide synthase inhibitor Fumonisin B1 (Bose *et al.*, 1995). Camptothecin, a topoisomerase I inhibitor, stimulates *de novo* ceramide synthesis through activation of serine-palmitoyltransferase and ceramide synthase, leading to ceramide-induced growth inhibition via caspase-3 (Chauvier *et al.*, 2002). Ionizing radiation can also induce ceramide formation and initiate apoptosis via the mitochondrial (intrinsic) pathway (Kolesnick and Fuks, 2003).

1.5 TRIM28 and the TRIM Family

TRIM28, also known as KAP1 and TIF1β, is a universal co-repressor, mediating transcriptional control through interaction with Krüppel associated box (KRAB) zinc finger proteins (Friedman *et al.*, 1996; Kim *et al.*, 1996; Moosmann *et al.*, 1996). TRIM28 is an essential partner in several multiple-protein complexes and is involved in a wide range of biological processes (Schultz *et al.*, 2001; Iyengar and Farnham, 2011). It belongs to the Tripartite Motif (TRIM) family of proteins, which have been implicated in many pathological conditions, including developmental disorders, neurodegenerative diseases, viral infections, innate immunity and cancer (Ozato *et al.*, 2008; Hatakeyama, 2011). In humans and mice there are more than 70 known TRIM proteins which are encoded by approximately 71 genes in humans, several of which are clustered together. TRIM family members arose from a common ancestral gene, however, TRIM genes evolved independently, which is highlighted by their scattered presence throughout the genome and their species-specific functions (Hatakeyama, 2011).

The TRIM or RBCC (Ring, B-box, Coiled-Coil) motif defines the superfamily. This is made up of a ring domain, one or two box domains and an associated coiled-coil domain in the amino-terminal region. Importantly, the multi-domain structure of the TRIM protein family infers a host of interactions through ring-finger domains, zinc binding motifs, and coiled-coil regions (Meroni and Diez-Roux, 2005; Hatakeyama, 2011). The presence of a ring domain allows for the conjugation of proteins with ubiquitin which enhances the biological flexibility of TRIM proteins. The RBCC motif is conserved amongst various species, indicating that this is the defining characteristic of the superfamily. In cases where one domain of the RBCC motif is missing, the other domains are conserved in order and spacing (Agricola *et al.*, 2011)**.**

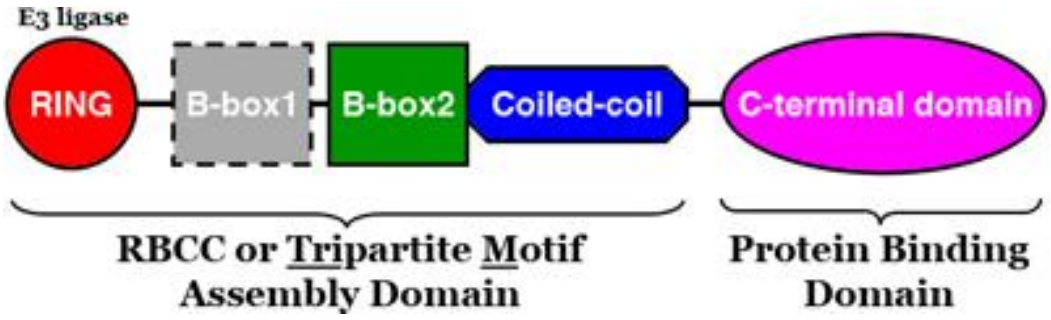

Figure 1.10: The Tripartite Motif. (Taken from University Virginia, 2014).

The ring domain is a zinc binding motif which is found 10-20 amino acids from the first methionine at the N-terminal portion of most of the TRIM proteins. Ring domains modulate ubiquitination events. Ubiquitination is a post-translational modification which regulates cell physiology. The ubiquitin-mediated proteolytic pathway plays an important role in the removal of short- lived regulatory proteins, which includes those that contribute to cell-cycle regulation, DNA repair, transcriptional regulation, cell signalling and protein quality control. When dealing with cancer, oncogene products and tumour suppressors are regulated by post-transcriptional modification (Reymond *et al.*, 2001).

The E3-ubiquitin ligase activity of the ring domain makes TRIM proteins a focus for cancer research, as they are involved in the regulation of oncoproteins and tumour suppressor proteins. E3 ubiquitin ligases act as scaffold proteins, which mediate the interaction between E2 ubiquitin-conjugating enzyme and the substrate (Ciechanover, 1998). Through the formation of homodimers and heterodimers TRIM proteins can have a range of substrate specificities by switching their binding partners. Most TRIM proteins function as E3 ubiquitin ligases and many members are involved in the oncogenic processes. TRIM family genes can also be translocated to other genes and are involved in carcinogenesis and cancer progression (Herquel *et al.*, 2011b).

The B-BOX also contains a zinc binding domain. This domain has a similar structure to that of the RING domain, indicating that they evolved from a common ancestor. The coiled coiled domain follows on from the B-Box domain. This domain mediates homomeric and heteromeric interactions among TRIM family members and other proteins, particularly self-association. Specific subcellular structures are defined by the protein-protein interactions which involve the coiled-coiled domains through the formation of high-molecular mass complexes (Torok & Etkin, 2001). The TRIM superfamily is broken down into families, based on the sequences in the C-terminal region, C-I to C-IX. This system is based on the association of particular domains with specific subcellular localization (Ozato *et al.*, 2008).

TRIM28 is a member of the C-VI family, which also includes TRIM24 and TRIM33. This sub-family is characterized by the presence of the plant homeodomains (PHDs); these are found in nuclear proteins and are believed to have a role in chromatin-mediated transcriptional regulation. PHDs are paired with bromodomains (BROMO); these recognise acetylated lysine residues, which can be found on the N-terminal tails of

histones. Transcriptional repression is mediated by the pairing of these domains (Le Douarin *et al.*, 1998).

A recent study has proposed that through transcriptional regulation of multiple epithelial and mesenchymal markers, TRIM28 may have both tumour suppressing and oncogenic activities, much like the TGF-β signalling pathway is known to play a complex role in tumourigenesis. They found that TRIM28 influences TGF-β-induced EMT in lung cancer (Chen *et al.*, 2014). In normal tissues and early stage cancers, TRIM28 is responsible for cell-cycle regulation through E2F transcription factors and HDACs; therefore, TRIM28 shows an anti-proliferative function and acts as a tumour suppressor. In late stage or metastatic cancers, high levels of TRIM28 contribute to EMT through transcription regulation of epithelial and mesenchymal genes. As a result, cells with high levels of TRIM28 tend to have a more invasive and metastatic nature (Chen *et al.*, 2014).

The up-regulation of the TRIM28 gene has been shown in gastric cancer and is associated with poor prognosis (Yokoe *et al.*, 2010). The tumour-promoting role of TRIM28 is associated with inactivation of p53-dependent apoptosis. The tumour-suppressor p53 has a major impact on carcinogenesis and it accumulates in cells in response to DNA damage, leading to DNA repair, cell cycle arrest or apoptosis (Green and Kroemer, 2009). These tumour-suppressor functions are inactivated by TRIM28, which interrupts the acetylation of key DNA-binding domains within the p53 protein (Mellert *et al.*, 2011). TRIM28 mediates such p53 inactivation through interactions with the oncogenic protein MDM2 (Wang *et al.*, 2005; Okamoto *et al.*, 2006), cancer testis antigens MAGE (Yang *et al.*, 2007) and through the suppression of the transcription factor E2F1 (Wang *et al.*, 2007).

Conversely, other studies suggest a role for TRIM28 as a tumour-suppressor (Herquel *et al.*, 2011a) and inactivation of TRIM28 has been shown to promote the formation of

murine hepatocellular carcinoma (Herquel *et al.*, 2011b). The tumour-suppressor activity of TRIM28 is mediated through its role in DNA repair mechanisms, (Peng *et al.*, 2002; White *et al.*, 2006; Goodarzi *et al.*, 2008; Kepkay *et al.*, 2011) as well as through the silencing of retroviral DNA and epigenetic stability (Rowe *et al.*, 2010; Messerschmidt *et al.*, 2012). DNA is protected from damage by chromatin compaction present in heterochromatin. This compaction restricts the ability of DNA damage response proteins to access the site. Hence, DNA damage in heterochromatin is resistant to repair and the surrounding chromatin structure needs to be de-condensed (Cann and Dellaire, 2010). When double-stranded breaks occur, this involves the inhibition of TRIM28 transcriptional repressor. TRIM28 operates as a co-repressor for the Kruppel-associated box containing zinc-finger proteins (KRAB-ZFP's). These are a large class of eukaryotic transcription factors. The RING-finger B-box coiled domain of TRIM28 can bind to the KRAB-ZFP's which have bound chromatin in a sequence dependent manner (Huntley *et al.*, 2006). TRIM28 then induces transcriptional repression and chromatin condensation by recruiting HP1, the histone methyltransferase SETDB1 and mi-2α. This function of TRIM28 relies on the SUMOylation of 3 lysine residues, where TRIM28 functions as an intermolecular E3 ligase (Schultz *et al.*, 2002). It has been shown that TRIM28 is phosphorylated in a DNA-damage dependent manner and this phosphorylated TRIM28 co-localises with sites of DNA damage. This phosphorylation regulates the SUMOylation of TRIM28 and as a result, its function in transcriptional condensation (Ziv *et al.*, 2006).

Although numerous studies have investigated the tumour-promoting and tumour-suppressor activity of TRIM28 in cancer, little is known about the expression of TRIM28 in the tumour microenvironment. Interestingly, TRIM28 forms part of a ternary complex with the fibroblast-specific protein (FSP1) and CArG box–binding factor–A (CBF-A) which controls the expression of a wide spectrum of epithelial-mesenchymal transition responsive genes, enabling the transformation of epithelial cells into a spindle-shaped

fibroblast morphology (Venkov *et al.*, 2007; Venkov *et al.*, 2011). Therefore, the balance of TRIM28 expression in cancer epithelium and the surrounding stroma may be a critical determinant of the tumour-promoting or tumour-suppressing phenotype of the protein. By dissecting the effects of TRIM28 in stromal fibroblasts and epithelial tumour cells, the aim is to elucidate the complex relationship between stromal and epithelial compartments in colorectal cancer as it has been previously shown that the TRIM28 gene is overexpressed in CRC (Kijanka *et al.*, 2010).

1.6 The Tumour Microenvironment

The interactions between tumour cells and the surrounding stroma play a significant role in the progression of cancer (Liotta and Kohn, 2001). Tumours are not merely masses of neoplastic cells but complex tissues composed of cellular and non-cellular elements, with the main cellular components being fibroblasts, endothelial cells and immune cells. Together these produce a range of factors which make up the non-cellular contributors to the tumour stroma, such as the extracellular matrix (ECM), proteins, proteases, cytokines and growth factors (Weber *et al.*, 2007). Invasive tumour cells interact with the microenvironment and remodel it into a milieu supportive of tumour growth and tumour progression and consequently the focus of many evolving therapies is on the elimination of stromal support by destroying the stromal cells or by inhibiting feedback stimulation of cancer growth. The reciprocal interactions between epithelial and stromal cells play a crucial role in cancer progression. It has been demonstrated that cancer cells which are enclosed in tumour stroma are 10-100 fold more tumourigenic than cancer cells which are in a stroma free environment (Engels *et al.*, 2012).

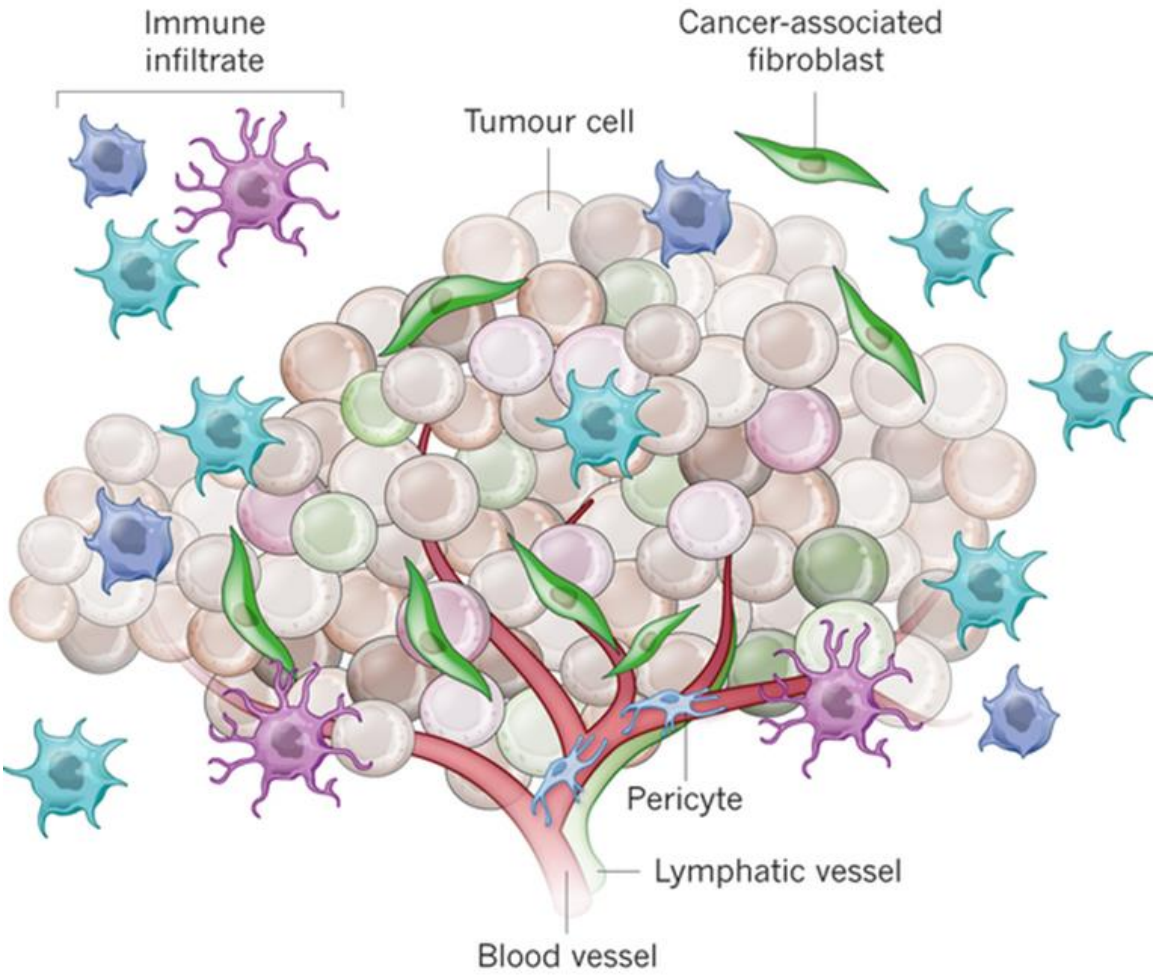

Figure 1.11: The Tumour Microenvironment. This illustration depicts the tumour cells, immune cells, vascular network and the fibroblast cells. (Image taken from Junttila & de Sauvage, 2013).

In the early stages of tumour growth, cancer cells form a neoplastic lesion that is embedded in the microenvironment of a given tissue (usually epithelium) but separated from the surrounding tissue and contained within the boundary of a basement membrane. This is referred to as carcinoma in situ (CIS) (Hanahan and Weinberg, 2000). CIS is associated with a stroma similar to that observed during wound healing, and it is commonly referred to as 'reactive stroma' (Dvorak, 1986). It was suggested that this reactive stroma and cancer cells communicate with each other through the basement membrane barrier. However, this communication is not yet fully understood

(Ronnov-Jessen *et al.*, 1996). Normal stroma contains a small number of fibroblasts in association with a physiological ECM, whereas reactive stroma contains an increased number of fibroblasts and displays enhanced capillary density and type I collagen and fibrin deposition (Ronnov-Jessen *et al.*, 1996). Tumour cells invade this reactive stroma during cancer development from CIS to invasive carcinoma. Invasive carcinoma involves the expansion of tumour stroma and increased deposition of the ECM (Brown *et al.*, 1999).

Stroma promotes tumour growth through the stimulation of vasculature and connective tissue and by supressing the immune response. The vasculature provides oxygenation and nutrients while the ECM and connective tissue are required for adherence, structure and the release of growth factors, cytokines and chemokines which act in a paracrine manner to signal to cancer cells (Teppo *et al.*, 2013). It was demonstrated that T cells which permeate the tumour, along with other leukocytes, release cytokines which activate the stroma and drive tumour expansion (Seung *et al.*, 1995). For cancer cell growth, these cell-stroma interactions are critical. This signalling relationship appears to be dependent on oncogene mutation in cancer cells which triggers them to release molecules, which activate non-malignant stromal cells to produce factors that promote cancer cell growth.

1.6.1 Fibroblasts and Cancer-Associated Fibroblasts

Fibroblast cells are large and flat, with elongated processes protruding from the body of the cell, making the spindle-like appearance of the cell. Fibroblasts are the most common cell type found in the connective tissue and they form the structural framework of tissues through their secretion of ECM components. Fibroblasts produce a collagen subunit, called topcollagen. This is then used to make larger collagenous aggregates. They also generate glycoproteins and polysaccharides which surround collagen fibres of dense connective tissue, making the ECM. This ECM then contributes to the physical properties of the connective tissue. Fibroblasts have a role to play in maintaining the homeostasis of the surrounding epithelia, through the secretion of growth factors. Fibroblasts also have many other functions including regulation of epithelial differentiation, regulation of inflammation and they are also involved in wound healing (Chang *et al.*, 2002).

However, fibroblasts are emerging as key cells in the progression, growth and spread of cancers and are found to be associated with cancer cells at all stages of cancer progression (Kalluri and Zeisberg, 2006). Fibroblasts within the tumour stroma acquire a modified phenotype, similar to fibroblasts associated with wound healing (Ryan *et al.*, 1973; Barsky *et al.*, 1984; Schor *et al.*, 1988). Such 'activated' fibroblasts within the tumour stroma have been termed cancer-associated fibroblasts (CAFs). Evidence suggests that CAFs control cell motility and the metastatic spread of cancer to secondary organs. This is achieved through their ability to invade surrounding tissues through the remodelling of the ECM and this then allows for cancer metastases (Joyce and Pollard, 2009). Signals which are secreted by cancer cells will elicit a stromal response which kick starts a cycle of paracrine signalling, resulting in tumour invasion and the loss of tissue integrity.

The origin of CAFs is still debated, and can differ between different areas of a tumour. Evidence suggests that the CAFs origin can be i) resident ii) mesenchymal stem cell derived (MSC derived) or iii) mutational. Tumour cells secrete the growth factors TGF-β, PDGF and bFGF which can activate stromal cells which include resting fibroblasts. CAFs present in the tumour originate mainly by activation of local fibroblasts. This trans-differentiation is followed by the expression of the CAF-specific genes in fibroblasts, which include α-SMA and FAP (Gallagher *et al.*, 2005). Epithelial cells have also been suggested as a source of CAFs, which can become fibroblasts through the EMT process. They may also originate directly from carcinoma cells through EMT. This enables cancer cells in adopting mesenchymal cell phenotype, demonstrated by an increase in their migratory capacity and invasiveness (Gallagher *et al.*, 2005).

1.7 Project Aims

The aim of this PhD project is to evaluate the tissue expression patterns of two previously identified novel colorectal cancer-specific antigens (CerS5 and TRIM28) and to investigate the potential significance and role of these novel antigens in colorectal cancer. This involves:

- Creating a database containing information on the familial history, medical history, clinical and pathological information, treatment regimen, disease recurrence and patient outcome for all of the patients in our cohort.
- Constructing tissue microarrays (TMAs) from corresponding CRC tissue samples for each of the patients in the cohort.
- Performing immunohistochemical analysis on these TMAs and examining the tissue expression patterns of CerS5 and TRIM28.
- Assessing the associations between CerS5 and TRIM28 expression patterns and the clinicopathological features, disease recurrence and patient outcome information of the cohort.
- Constructing reverse-phase protein microarrays from laser capture micro-dissection enriched tumour epithelium and stroma cells isolated from fresh-frozen CRC tissue sample.
- Further characterising the effects of both CerS5 and TRIM28 expression on tumourigenic processes.

Chapter 2

Materials and Methods

2.1 Introduction

This chapter describes the methodologies employed in this project, accompanied by general background information on each technique. The full description of each technique is restricted to this chapter, with specific deviations from the standard technique being mentioned, where necessary, in later chapters.

2.2 Materials

2.2.1 Equipment List

Table 2.1: List of Equipment

Equipment:	**Supplier:**
Power Pac	Bio-Rad Laboratories, 1000 Alfred Nobel Drive, Hercules, CA 94547, USA.
Mini-PROTEAN® Tetra Cell	
Trans-Blot®SD Semi-Dry Transfer System	
Gel Doc™ EZ Imaging System	
Pierce G2 Fast Blotter	Thermo Fisher Scientific Inc., 81 Wyman Street, Waltham, MA 02451, USA.
LaminAir HB2448K Laminair Flow Hood	
Sigma 2K15 Centrifuge	
Branson Sonifier™ S-450 Digital Sonicator	
GENE GNome Imager	Syngene Europe office, Beacon House, Nuffield Road, Cambridge, CB4 1TF, UK.
Lauda Aqualing AL12 Water Bath	Mason Technologies, 228 South Circular Road, Dublin 8, Ireland.
Nikon DIAPHOT Camera	Nikon Corproration, Chiyoda, Tokyo, Japan.
Hera Cell 150 Incubator	Unitech, Airton Raod, Tallagh, Dublin 24, Ireland.
Optika XDS-2FL Inverted HBO Fluorescence Microscope	OPTIKA SRL, Via Rigla, 30 - 24010 Ponteranica (BG), Italy.
Microplate Shaker	Laboratory Supplies Ltd., John F. Kennedy Drive, Naas Road, Dublin 12, Ireland.
Safire II Microplate Reader	Tecan Group Ltd, Seestrasse 103, 8708 Männedorf, Switzerland.
Aushon 2470 Arrayer	Aushon BioSystems, 43 Manning Rd, Billerica, MA 01821, USA.

Dako Autostainer	Dako Denmark A/S, Produktionsvej 42, DK-2600, Glostrup, Denmark.
NovaRay CCD Imager	Alpha Innotech, San Leonardo, CA, USA.
UMAX 2100XL Flatbed Scanner	Umax Technologies Inc., 3561 Gateway Blvd., Fremont, CA, 945386585, USA.
ArcturusXT™ Laser Capture Microdissection System	Life Technologies, 3175 Staley Road, Grand Island, NY 14072 USA.
Tissue-Arrayer™	Beecher Instruments, Silver Springs, MD, USA.
Leica CM3050 Cyrostat	Leica Microsystems, Newcastle Upon Tyne, NE12 8EW, UK.
Leica Bond-Max™ automated Immunohistochemisty Instrument	
Rotary Microtome	
Nikon Eclipse E400 Microscope	Nikon Instruments Inc., Melville, NY 11747-3064, USA.
Nikon DXM 1200 Digital Camera	
ND-1000 Spectrophotometer (Nanodrop)	NanoDrop Technologies, Inc., 3411 Silverside Rd 100BC, Wilmington, DE19810-4803, USA.
Vapour-line *eco* 25 autoclave	VWR International Ltd., Orion Business Campus, Northwest Business Park, Ballycoolin, Blanchardstown, Dublin 15, Ireland.
Chyo JK-180 Balance	Medical Supply Company Ltd, Damastown, Mulhuddart, Dublin 15, Ireland.
Mettler PJ300 Balance	
Grant Y6 Water Bath	Grant Instruments (Cambridge) Ltd., Shepreth, Royston, Herts., SG8 6Pz, UK.
Eppendorf 5810R Centrifuge	Eppendorf House, Gateway 1000 Whittle Way, Arlington Business Park, Stevenage SG1 2FP, UK.
New Brunswick Excella E25 Shaking Incubator	
Sciolgex D1008 Mini-centrifuge	SCILOGEX, LLC., 1275 Cromwell Avenue, C-6, Rocky Hill, CT 06067, USA.
Sciolgex MX-S Vortex	
Stuart Platform Shaker STR6	Stuart Scientific, Beacon Road, Stone, Staffordshire, ST15 0SA, UK.
Stuart Roller Mixer SRT1	

2.2.2 General Buffers

The constituents of each buffer are dissolved in 900mL distilled and deionised water and adjusted to a final pH of 7.4. The solution is then made up to a final volume of 1L. All components were analytical grade.

Phosphate-buffered saline (PBS) (150 mM, pH 7.4):

8g of NaCl

0.2g of KCl

1.44g of Na_2HPO_4

0.24g of KH_2PO_4

PBS Tween 20 (PBST):

0.5mL of Tween 20 detergent (Sigma) was added to PBS to give a final concentration of 0.05% (v/v).

2.2.3 Buffers for Sodium Dodecyl Sulphate-Polyacrylamide Gel Electrophoresis (SDS-PAGE)

Table 2.2: SDS-PAGE reagents

Solution	12.5% (w/v) Separation Gel (1 gel/6mls)	4.5% (w/v) Stacking Gel (1 gel/2.5mls)
1M TrisHCl, pH 8.8	1.5ml	-
1M TrisHCl, pH 6.8	-	0.300mL
30% (w/v) acrylamide (Acrylagel)	2.5mL	0.375mL
2% (w/v) bisacrylamide (Bis-Acrylagel)	1mL	0.150mL
Distilled H_20	0.934mL	1.740mL
10% (w/v) sodium dodecyl sulphate (SDS)	0.30mL	0.024mL
10% (w/v) ammonium persulfate (APS)	0.030mL	0.024mL
TEMED	.006mL	.0025mL

10X Electrophoresis Buffer Volume (1 L):

196 mM Glycine	144 g
50M Tris (pH 8.3)	30 g
0.1% (w/v) SDS	10 g
dH_20 to 1L	

4X Loading Dye Volume (10mL):

Tris 0.5M (pH 6.8)	2.5mL
Glycerol	2mL
2-mercaptoethanol	0.5mL
20 % (w/v) SDS	2.5mL
Bromophenol blue	20 ppm
dH_20	2.5mL

Coomassie Stain Volume (500mL):

0.2 % (v/v) Coomassie blue R-250	1 g
45 % (v/v) Methanol	225mL
45 % (v/v) Water	225mL
10 % (v/v) Acetic acid	50mL

Coomassie Destain Volume (1 L):

10 % (v/v) Acetic acid	100mL
25 % (v/v) Methanol	250mL
65 % Water	650mL

2.2.4 Buffers for Western Blotting

Transfer Buffer Volume (1 L)

Tris	3.03 g
Glycine	14.4 g
Methanol	200mL

Adjust to 1L with dH_20

2.2.5 Buffers for protein purification under denaturing conditions:

Lysis buffers

Buffer A (1 litre):

100 mM NaH_2PO_4	13.8 g (MW 137.99 g/mol)
10 mM TrisHCl	1.2 g (MW 121.1 g/mol)
6 M GuHCl	573 g guanidine hydrochloride

Adjust pH to 8.0 using 1M NaOH.

Buffer B (1 litre):

100 mM NaH_2PO_4	13.8 g (MW 137.99 g/mol)
10 mM TrisHCl	1.2 g (MW 121.1 g/mol)
8 M Urea	480.5 g (MW 60.06 g/mol)

Adjust pH to 8.0 using 1M NaOH.

Wash buffer

Buffer C (1 litre):

100 mM NaH_2PO_4	13.8 g (MW 137.99 g/mol)
10 mM TrisHCl	1.2 g (MW 121.1 g/mol)
8 M Urea	480.5 g (MW 60.06 g/mol)

Adjust pH to 6.3 using 12M HCl.

Elution buffers

Buffer D (1 litre):

100 mM NaH_2PO_4	13.8 g (MW 137.99 g/mol)
10 mM TrisHCl	1.2 g (MW 121.1 g/mol)
8 M Urea	480.5 g (MW 60.06 g/mol)

Adjust pH to 5.9 using 12M HCl.

Buffer E (1 litre):

100 mM NaH_2PO_4	13.8 g (MW 137.99 g/mol)
10 mM TrisHCl	1.2 g (MW 121.1 g/mol)
8 M Urea	480.5 g (MW 60.06 g/mol)

Adjust pH to 4.5 using 12M HCl.

2.2.6 Cell Lysis Buffer

Tris-HCl	0.0757g
10% SDS	2mL
Glycerol	1mL
dH_20	10mL

2.2.7 General Reagents

Table 2.3: List of Commonly Used Reagents**:**

Reagent:	Supplier:
PageRuler™ Plus Prestained Protein Ladder	AGB Scientific Limited - A VWR International Company, Orion Business Campus, Northwest Business Park, Ballycoolin, Dublin 15, Ireland.
InstantBlue Single Step Coomassie Based Gel Stain	Expedeon Ltd., Unit 12 Buckingway Business Park, Anderson Road, Swavesey, Cambridge CB24 4AE, United Kingdom.
MycoAlert® Mycoplasma Detection Kit	Lonza Ltd. , Muechensteinstrasse 38 4002 Basel, Switzerland.
Enhanced chemiluminescence (ECL) Western Blotting Substrate TCEP (Tris(2-carboxyethyl)phosphine) T-PER (Tissue Protein Extraction Reagent) TMB (3,3',5,5'-tetramethylbenzidin) Blotting Substrate Solution NiNTA Resin	Thermo Fisher Scientific Inc., 81 Wyman Street, Waltham, MA 02451, USA.
1X Trypsin EDTA Solution	Sigma Aldrich Ireland Limited, Vale Rd, Arklow, Co. Wicklow, Ireland

2.2.8 Commercial Antibodies

Table 2.4: List of primary antibodies used to probe RPPA slides

Antibody	Source	Species	Dilution	Phospho or Total Protein
Acid Ceramidase	LS	Mouse	1 : 20	Total
Acetyl-coA Ser73	CS	Rabbit	1 : 100	Phospho
AKT Thr 308	CS	Rabbit	1 :100	Phospho
AMPKβ1 s108	CS	Rabbit	1 : 50	Phospho
Bax	CS	Rabbit	1 : 500	Total
Bcl-2 Ser70	CS	Rabbit	1 : 500	Phospho
Beclin 1	CS	Rabbit	1 : 100	Total
β-Actin	CS	Rabbit	1 : 500	Total
Ceramide	LS	Mouse	1 : 20	Total
CerS1	LS	Goat	1 : 50	Total
CerS2	LS	Rabbit	1 : 1000	Total
CerS3	LS	Rabbit	1 : 100	Total
CerS4	LS	Rabbit	1 : 100	Total
CerS5	LS	Rabbit	1 : 200	Total
CerS6	LS	Mouse	1 : 200	Total
Cleaved Caspase 3	CS	Rabbit	1 : 50	Phospho
Cleaved Caspase 7	CS	Rabbit	1 : 100	Phospho
Cox2	BD	Mouse	1 : 500	Total
E-Cadherin	CS	Rabbit	1 : 100	Total
EGFR y1045	CS	Rabbit	1 : 100	Phospho
EGFR y1148	BS	Rabbit	1 : 500	Phospho
eNos s1177	CS	Rabbit	1 : 200	Phospho
JNK S183/185	CS	Rabbit	1 : 500	Phospho
LC3B	CS	Rabbit	1 : 100	Total
LCK y505	In	Rabbit	1 : 200	Phospho
MDM2	CS	Rabbit	1 : 500	Phospho
MMP9	CS	Rabbit	1 : 1000	Total
mTor S2481	CS	Rabbit	1 : 100	Phospho
p53 Ser15	CS	Rabbit	1 : 1000	Phospho
PI3K	BD	Mouse	1 : 100	Total
PP2A	CS	Rabbit	1 : 1000	Total
RAGE	CS	Rabbit	1 : 250	Total
Ras GFR s91	CS	Rabbit	1 : 250	Phospho
RUNX1	Ab	Rabbit	1 : 5000	Total
SGPP1	LS	Rabbit	1 : 200	Total
SPHK1	CS	Rabbit	1 : 100	Total
Survivin	CS	Rabbit	1 : 1000	Total
TNFR1	CS	Rabbit	1 : 50	Total
VEGFR y117	CS	Rabbit	1 : 250	Phospho

Abbreviations: Ab, Abcam (Cambridge, UK); BD BD Biosciences (San Jose, CA,USA); BS, Biosource Int. (Camarillo, CA, USA); CS, Cell Signalling Technology (Beverly, MA, USA); In, Invitrogen Corporation (Camarillo, CA, USA) LS, LifeSpan BioSciences, Inc. (Seattle, WA, USA)

Table 2.5: List of additional antibodies used in IHC, RPPA and Western Blot analysis

Primary Antibodies:	**Supplier:**
Rabbit anti-TRIM28 mAb	Cell Signalling Technology Inc, Danvers, MA, USA.
Mouse anti-p53 mAb	Dako Denmark A/S, Produktionsvej 42, DK-2600, Glostrup, Denmark.
Rabbit anti-β-Actin pAb	Sigma Aldrich, 3050 Spruce Street, St. Louis, MO 63103, USA.
Secondary Antibodies:	**Supplier:**
Goat anti-rabbit IgG, peroxidase conjugated pAb Rabbit anti-goat IgG, peroxidase conjugated pAb Goat anti-mouse IgG, peroxidase conjugated pAb	Sigma Aldrich, 3050 Spruce Street, St. Louis, MO 63103, USA.
Biotinylated rabbit anti-goat IgG antibody Biotinylated goat anti-rabbit IgG antibody	VECTOR LABORATORIES, INC. 30 Ingold Road, Burlingame, CA 94010, USA.
Biotinylated goat anti-mouse IgG antibody	Dako Denmark A/S, Produktionsvej 42, DK-2600, Glostrup, Denmark.

2.2.9 *E. coli* Protein Purification

Product:	**Source:**
***E. coli* Clones:**	
TRIM28 Clone: IMGSp800C11583 Size: 835 AA (1-835)	imaGenes GmbH, 10 Robert-Rössle-Str., 13125 Berlin, Germany.
CerS5 Clone: IMGSp800M17513 Size: 326 AA (67-392)	imaGenes GmbH, 10 Robert-Rössle-Str., 13125 Berlin, Germany.
Vector:	
pQE30NST	Qiagen Ltd., Skelton House, Lloyd Street North, Manchester M15 6SH, UK.
***E.coli* Strain:**	
SCS1	Agilent Technologies (Stratagene), 5301 Stevens Creek Blvd, Santa Clara, CA 95051, USA.

2.3 TRIM28 and CerS5 Protein Expression and Antibody Validation Methods

2.3.1 Protein Expression

Protein expression systems are very widely used in the life sciences, biotechnology and medicine. Expression of a recombinant protein can be approached in general by constructing a plasmid that encodes for the desired protein, introducing the plasmid into the required host cell, growing the host cells and inducing protein expression. Cells expressing the protein are then lysed, which releases the protein of interest, which can then be purified and finally SDS-PAGE analysis can be performed to verify the presence of the protein. *E. coli* is one of the most widely used expression hosts, and DNA is normally introduced in a plasmid expression vector (Hunt, 2005; Graslund *et al.*, 2008). The techniques for overexpression of proteins in *E. coli* are well developed and work by increasing the number of copies of the gene or increasing the binding strength of the promoter region so assisting transcription.

2.3.2 Protocol for Expression of TRIM28 and CerS5

On day one, two 1L conical flasks and two 100mL flasks were autoclaved and 1L of Terrific Media was prepared as follows:

800mL distilled H_2O
12g Tryptone
24g Yeast extract
4mL Glycerol
The volume was adjusted to 900mL with distilled H_2O and the mixture was sterilized by autoclaving. The mixture was then allowed to cool to room temperature and the volume was adjusted to 1000mL with 100mL of a filter sterilized solution of 0.17M KH_2PO_4 and 0.72M K_2HPO_4.
Antibiotics: 100µg/mL ampicillin; 15µg/mL kanamycin.

Terrific media (200mL) was then added to each of the 1L flasks and placed in a 37ºC incubator overnight. Terrific media (50mL) was added to each of the 100mL flasks for inoculation. One of the 100mL flasks was then inoculated with the TRIM28 expressing *E.coli* clone using an inoculation stick, while the other was inoculated with the CerS5 expressing *E.coli* clone. The inoculated cultures were grown overnight at 37ºC in a shaking incubator.

On day two, 1mL of the overnight culture containing the TRIM28 clone was added to one of the 1L flasks containing 200mL pre-warmed media and 1mL of the overnight culture containing the CerS5 clone was added to the 1L flask containing 200mL pre-warmed media. A 1mL sample of each (TRIM28 and CerS5) was then taken immediately before induction. This was the non-induced control and the cells were pelleted and dissolved in 4x SDS-PAGE loading and frozen until required. Expression was then induced by adding IPTG to a final concentration of 1mM (200µL IPTG to 200mL culture medium) to each of the 1L flasks. The cultures were then incubated at 30ºC overnight. Another 1mL sample of each (TRIM28 and CerS5) was then taken. This was the induced control and again

the cells were pelleted and dissolved in 4x SDS-PAGE loading buffer and frozen until required. The 200mL over-night culture was then harvested by centrifugation at 10,000 x g for 20 min. Finally, the supernatant was discarded and the cell pellet was snap frozen in liquid nitrogen and stored at -80ºC until purification.

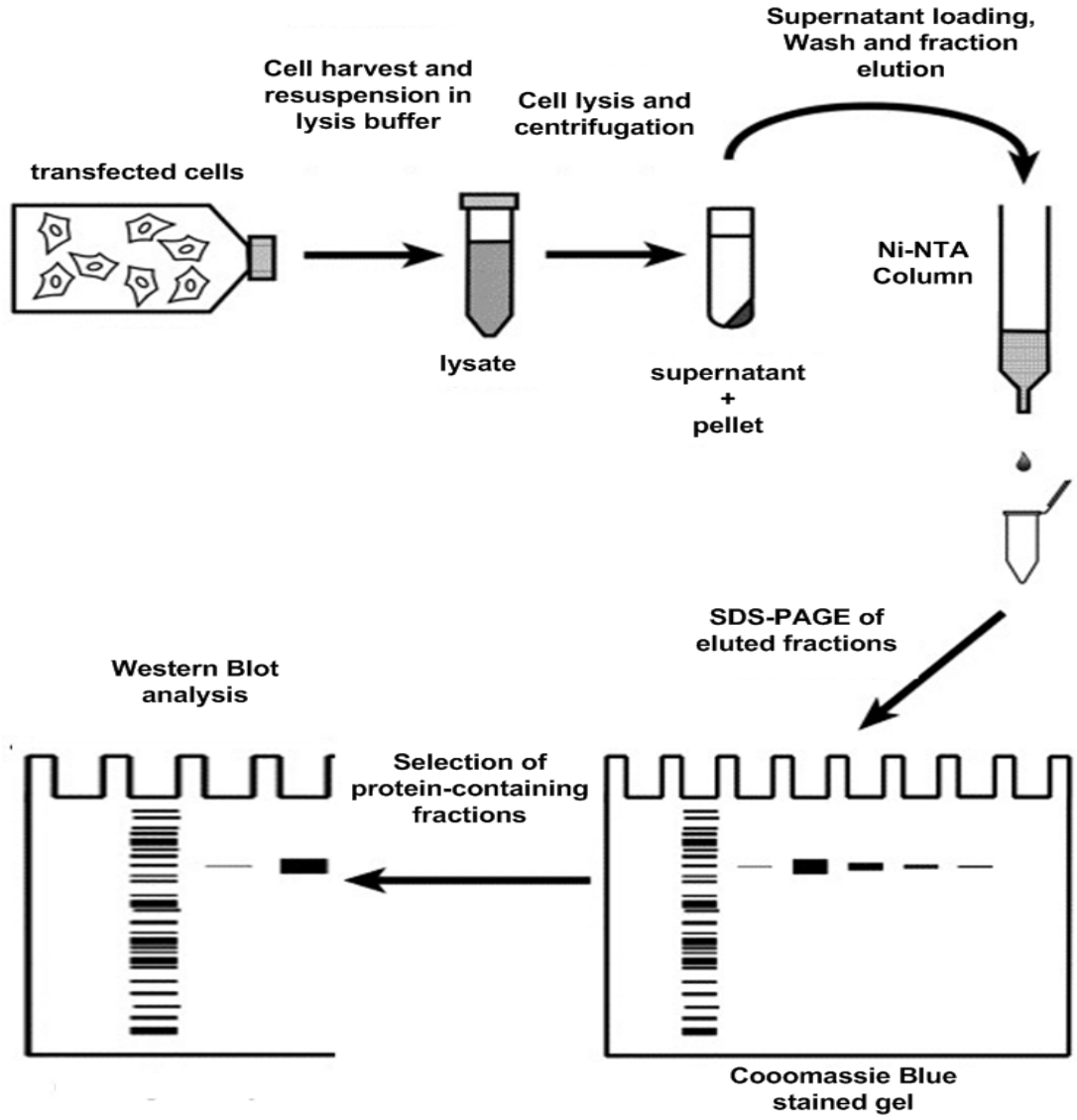

Figure 2.1: Schematic diagram of the protein purification protocol.

2.3.3 Protein Purification using Immobilized metal ion affinity chromatography (IMAC)

A polyhistidine-tag (6xHis-tag) is an amino acid motif in proteins that consists of at least five histidine (*His*) residues, often at the N- or C-terminus of the protein (Hengen, 1995). Polyhistidine-tags are often used for affinity purification of 6xHis-tagged recombinant proteins expressed in *E.coli* and other prokaryotic expression systems. Bacterial cells are harvested via centrifugation and the resulting cell pellet lysed either by physical means or by means of detergents and enzymes such as lysozyme. At this stage raw lysate contains the recombinant protein among many other proteins originating from the bacterial host. This mixture is incubated with affinity media which in this case was Ni-NTA. This affinity media contains bound nickel ions to which the polyhistidine-tag binds with micro molar affinity. The resin is then washed with phosphate buffers to remove proteins that do not specifically interact with the nickel ion. Finally, the protein is eluted from the column using elution buffers. The purity and amount of protein can be assessed by SDS-PAGE and Western blotting.

The TRIM28 and CerS5 cell pellets were thawed on ice for 15 min and then re-suspended in lysis buffer A (see appendix 1 for composition of buffers) at 5mL per gram wet weight. The cells were then lysed by gently vortexing them, taking care to avoid foaming, and lysis is complete when the solution becomes translucent. The lysates were then centrifuged (Eppendorf Centrifuge 5810R) at 10,000 x g for 20 min to pellet the cellular debris. The supernatant was saved for purification. Ni-NTA slurry was loaded onto the purification columns at approximately 1mL of 50% Ni-NTA slurry to 4mL lysate. The TRIM28 and CerS5 lysates were then loaded into separate Ni-NTA columns. The bottom caps were removed and the flow-through was collected. The samples were then washed once with 4mL of buffer B, and twice with 4mL of buffer C. Then the

recombinant proteins were eluted 4 times with 0.5mL of buffer D and 4 times with 0.5mL with buffer E. All of the wash and elution fractions (0.5mL aliquots) were collected and stored at -20ºC for SDS-PAGE and Western blot analysis.

2.3.4 SDS-PAGE

The separation of macromolecules in an electric field is called electrophoresis. Sodium dodecyl sulphate polyacrylamide gel electrophoresis (SDS-PAGE), describes a technique widely used in biochemistry, genetics and molecular biology to separate proteins according to differences in the electrophoretic mobility (a function of the length of a polypeptide chain and its charge). SDS is an anionic detergent meaning that, when dissolved, its molecules have a net negative charge within a wide pH range. A polypeptide chain binds amounts of SDS in proportion to its relative molecular mass. The sample to be analysed is mixed with SDS, which denatures secondary and non–disulphide–linked tertiary structures, and applies a negative charge to each protein in proportion to its mass. Heating the samples to 95°C further promotes protein denaturation, helping SDS to bind. Polyacrylamide gels restrain larger molecules from migrating as fast as smaller molecules. Because the charge-to-mass ratio is nearly the same among SDS-denatured polypeptides, the final separation of proteins is dependent almost entirely on the relative molecular mass of polypeptides (Schägger and von Jagow, 1987).

Regardless of the system, preparation requires casting two different layers of acrylamide between glass plates. The lower layer (separating, or resolving, gel) is responsible for actually separating polypeptides by size. The upper layer (stacking gel) includes the sample wells, where the samples are applied. Free radical-induced polymerisation of the resolving gel acrylamide (See table 2.2 above) was catalysed by addition of ammonium persulphate and the accelerator TEMED and the gel was added to the space between

the plates and covered with a layer of ethanol. Following polymerisation of the gel, the ethanol was removed and the stacking gel placed directly onto the resolving gel. A plastic comb was placed in this gel creating the wells for sample application. Once the gel had fully polymerised, the plates were then placed in an electrophoresis chamber, the comb was removed, the chamber and wells filled with electrophoresis buffer (25mM Tris, 250 mM glycine (electrophoresis grade), pH 8.3 and 0.1% (w/v) SDS) and samples were loaded and run at 100V for 1-2 hrs. The gel was then removed from the casting tray apparatus and stained using Coomassie blue solution for 1 hour. The gel was transferred to destain solution and incubated until the protein bands were clearly visible (approximately 1 hr).

2.3.5 Western Blotting

Western blotting is an analytical technique widely used to detect specific proteins in the given sample of tissue homogenate or extract. Proteins were separated by SDS as described previously. The proteins were then transferred to a nitrocellulose membrane where they were probed with antibodies specific to the target protein. After an SDS-PAGE gel has been resolved, it is incubated in transfer buffer for 20 min, along with thick blotting paper and nitrocellulose membrane. The proteins were transferred to the nitrocellulose membrane at 15V for 20 min. When the transfer is complete the nitrocellulose membrane is carefully removed from the apparatus and placed in 5% (w/v) Milk Marvel blocking solution in 1X PBS for 1 hour to block the non-specific binding. The membrane is then washed and incubated with the primary antibody dissolved in 1% (w/v) Milk Marvel in PBS-Tween for 1 hour. The membrane is then washed again and incubated with the secondary antibody dissolved in 1% (w/v) Milk Marvel in 1X PBS-Tween for 30 min. Finally the membrane is washed 3 times in PBS, followed by 1X PBS-Tween for 5 min each and then detection takes place using the appropriate substrate. Two detection methods were used in this project; colorimetric and enhanced

chemiluminescence (ECL). Colorimetric detection utilises the reaction of the conjugated label with a compatible substrate. When the conjugated enzyme reacts with the substrate a colour change occurs. The TMB (3,3′,5,5′-Tetramethylbenzidine) substrate was used for all colorimetric detection analyses. ECL involves the reaction of the conjugate with a luminol and hydrogen peroxide solution, emitting a photon of light. The intensity of light emitted is detected by a charge-coupled device camera which captures a digital image of the Western blot.

2.3.6 Lowry Assay

The Lowry assay is a commonly used technique for protein quantification. The total protein concentration is exhibited by a colour change of the sample solution in proportion to protein concentration, which can then be measured using colorimetric techniques. The procedure involves the reaction of protein with cupric sulphate and tartrate in an alkaline solution, resulting in the formation of tetradenate copper-protein complexes. When the Folin-Ciocalteu Reagent is added, it is effectively reduced in proportion to these chelated copper complexes, producing a water-soluble product whose blue colour can be measured at 750nm. In this project the Lowry assay was used to determine the levels of protein in the SW480 and SW620 cell lines, enabling the same amount of protein for each cell line to be loaded to the gel when carrying out SDS-PAGE and Western Blot analysis. This then allows for the comparison of TRIM28 expression between the cell lines.

Bovine serum albumin (BSA) protein standards were made up in the same lysis buffer that was used to prepare the cell lysates in the range of 0-500µg/mL. Dilutions of the cell lysate samples were also made up in lysis buffer. 1X Folin-Ciocalteu was prepared fresh on the day of use by diluting the supplied 2X reagent 1:1 with ultrapure water. Each standard (40µL) and unknown sample replicate was added into a well of a 96-well plate.

Modified Lowry Reagent (200µL) was added to each well at nearly the same moment using a multi-channel pipette. The micro plate was covered and incubated at room temperature for exactly 10 minutes. The prepared 1X Folin-Ciocaltau Reagent (20µL) was added to each well using a multi-channel pipette and the plate was mixed immediately on a plate mixer for 30 seconds. The micro plate was covered and incubated at room temperature for 30 minutes. The absorbance was then measured at 750nm on a plate reader. The average 750nm absorbance of the blank standard replicates was subtracted from the average from the 750nm value for all individual standards and unknown sample replicates. A standard curve was prepared by plotting the average blank corrected 750nm value for each BSA standard versus its concentration in µg/mL. This standard curve was then used to determine the protein concentration of each unknown sample.

2.4 Histological Methods

2.4.1 Ethical Approval, Study Cohort and Sample Collection

The research conducted in this PhD thesis was approved by the Ethics (Medical) Research Committee at Beaumont Hospital, Dublin, Ireland and informed consent was obtained from all patients. Patients undergoing colonoscopy were screened prospectively, with the clinical notes of all patients attending for colonoscopies being reviewed daily by the clinical research nurses. Patients with a history of cancer or systemic inflammatory disease and patients taking immunosuppressive medication were excluded from the study. In total, 156 Caucasian patients with newly diagnosed CRC fulfilled the inclusion criteria. A pathologist sampled an area of invasive carcinoma from the tumour mass and an adjacent area of uninvolved colonic/rectal mucosa was also sampled.

A representative section of archived formalin-fixed and paraffin-embedded (FFPE) CRC tissue specimens for each of the patients in the cohort was retrieved for the study. Each block was sectioned and stained with haematoxylin and eosin (H&E). The case was reviewed by a pathologist to confirm pathological stage. The relevant tumour areas were marked and used as the donor cores for TMA construction.

2.4.2 Tissue Microarrays (TMA)

Tissue microarrays are produced by a method of re-locating tissue from conventional histologic paraffin blocks such that tissue from multiple patients or tissue blocks can be seen on the same slide. This is done by using a needle to biopsy a standard histologic tissue block and placing the core into an array on a recipient paraffin block. This technique was originally described in 1987 by Wan, Fortuna and Furmanski in the Journal of Immunological Methods (Wen-Hui *et al.*, 1987). The group published a modification of Battifora's "sausage" block technique whereby tissue cores were placed in specific spatially fixed positions in a solid paraffin block (Battifora, 1986). The technique was further developed by Kononen and colleagues in the laboratory of Ollie Kallioneimi and published in Nature Medicine in 1998, (Kononen *et al.*, 1998).

The major advantage of TMAs is that they allow the performance of tissue-based assays (immunohistochemistry, in situ hybridization, Fluorescent-in-situ-hybridisation, etc.) on a large number of patient samples in an efficient and cost-effective manner. With TMA technology, several hundred representative cores from several hundred patients may be included on a single glass slide for analysis at the same time. Thus, significantly more tissue can be conserved than if the full sections of blocks were to be sectioned serially. TMAs have been generated from all tissue types including decalcified bone and core biopsies. The major disadvantage of TMAs is that each core (or set of cores) represents a fraction of the lesion. This was considered a major weakness, particularly in the early days of the TMA. However, multiple studies in different organ systems have now

demonstrated that consistent and comparable results can be obtained using multiple-TMA cores as with whole sections (Henriksen *et al.*, 2007; Kyndi *et al.*, 2008; Thomson *et al.*, 2009). In this study the TMA construction was performed as previously described (Kononen *et al.*, 1998; Kay *et al.*, 2004) using the Beecher Instruments Tissue Microarrayer (Beecher Instruments, Silver Spring, MD, USA). Cores of 1.0 mm diameter were sampled in quadruplicate for each case. Of the 137 CRC cases, 126 were incorporated into the TMAs and a further 11 cases, that could not be included into the TMAs for various reasons, were investigated using whole sections of tissue. Normal mucosa from surgical margins was incorporated into the TMAs for 28 cases and a further 10 cases were investigated using whole tissue sections. All 19 cases of the RPPA cohort were also investigated for CerS5 expression using IHC in FFPE whole tissue sections. The TMA construction process is shown schematically in Fig. 2.2.

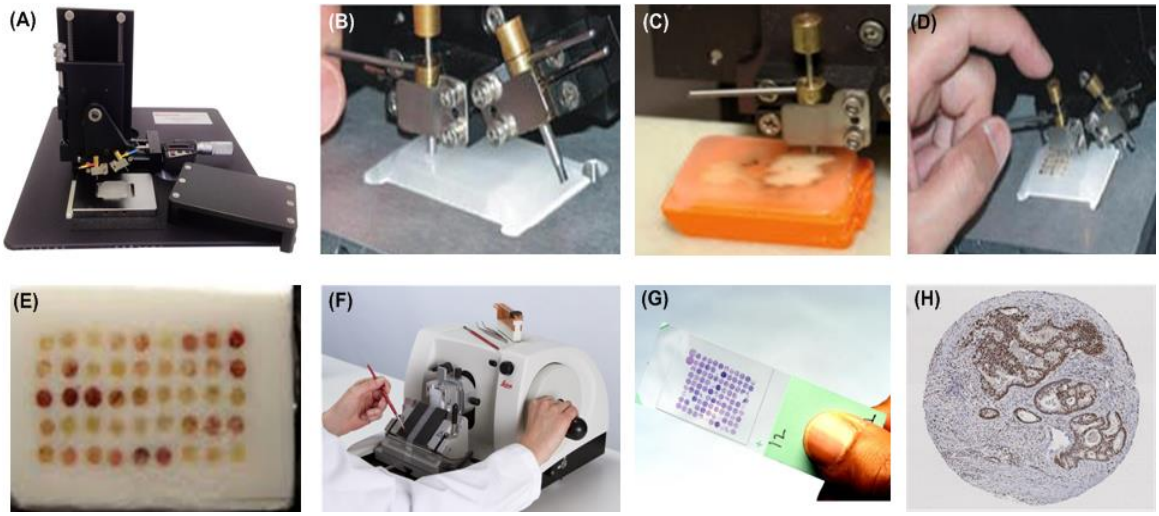

Figure 2.2: Pictorial representation of the TMA construction process. Cylindrical cores are obtained from a number of individual formalin-fixed, paraffin-embedded tissue blocks using the Beecher Instrument Manual Tissue Arrayer (A-C). These are transferred to a recipient TMA block (D&E). Sections (4µm) are cut from the TMA using a microtome and transferred to a glass slide (F&G). All resulting TMA slides have the same tissues in the same coordinate positions. The individual slides can be used for a variety of analyses including immunohistochemistry (H). Individual images (A-G) taken and adapted from images.google.com.

2.4.3 Immunohistochemical Staining

Sections of 4 µm thickness were cut from all TMA blocks and from the whole section blocks for the purpose of immunohistochemistry. Sections were immunostained with an anti-TRIM28 rabbit monoclonal antibody (mAb) (C42G12, Cell Signalling Technology Inc, Danvers, MA, USA), anti-p53 mouse mAb (DO-7, Dako, Glostrup, Denmark), or anti-CerS5 human polyclonal (pAb) (LS-B3152, LifeSpan Biosciences, Inc. Seattle, WA, USA) on an automated platform (Bond system – Leica Microsystems, Bannockburn, IL, USA). Briefly, cut sections were subjected to on-board dewaxing. For each antibody varying antigen retrieval conditions and antibody dilutions were used, which are given below. Detection of the antibody–antigen complex was achieved using a polymer-based kit (Bond Refine) with 3, 3'-diaminobenzadine (DAB) as the chromogen. All sections were counterstained with haematoxylin. Negative controls were included for all sections by omitting the primary antibody and positive controls were also used for each antibody. The positive control tissue included tonsil and colonic adenocarcinoma for TRIM28 and CerS5 and bladder cancer tissue for p53.

For the anti-TRIM28 antibody, the optimal conditions were as follows: antigen retrieval in tri-sodium citrate buffer (Bond Epitope Retrieval 1 solution) for 20 mins and 1:50 antibody dilution. For the anti-CerS5 antibody, the optimal conditions were as follows: antigen retrieval in tri-sodium citrate buffer (Bond Epitope Retrieval 1 solution) for 20 mins and 1:300 antibody dilution. The optimal conditions for anti-p53 antibody were as follows: antigen retrieval in tri-sodium citrate buffer (Bond Epitope Retrieval 1 solution) for 30 mins and 1:100 antibody dilution.

2.4.4 Immunohistochemical Analysis and Assessment

Immunohistochemistry scoring was performed independently by two reviewers blinded to the clinicopathological details and clinical outcome of the cohort. In cases where there were discrepancies between the scorers, a consensus was reached after a joint review using a multi-headed microscope. A previous study in our labatory has shown that the inter-observer variability of immunohistochemistry scoring is as low as 7%, (Kay *et al.*, 1996).

The degree of nuclear TRIM28 staining was evaluated for epithelial and stromal tissue. The intensity of the TRIM28 staining (negative = 0; weak = 1+; moderate = 2+; strong = 3+) was recorded for both epithelial and stromal tissue. The relationship between the epithelial and stromal intensity was calculated by determining the ratio of TRIM28 expression between the two compartments. A High TRIM28 expression ratio was defined as at least 2 units of difference in staining intensity (e.g. epithelium strong (3+) and stroma weak (1+), or epithelium moderate (2+) and stroma negative (0). A Low TRIM28 expression ratio was defined as 1 or 0 units of difference in staining intensity (e.g. epithelium moderate (2+) and stroma weak (1+).

The degree of membranous CerS5 staining was evaluated. The intensity of the CerS5 staining (negative = 0; weak = 1+; moderate = 2+; strong = 3+) was recorded for all tumour and normal tissue sections. The p53 staining and scoring was carried out previously by a research team from our group.

Nuclear p53 staining was evaluated and the intensity of expression was recorded (negative = 0; weak = 1+; moderate = 2+; strong = 3+).

2.4.5 Frozen Tissue Sectioning

Fresh tissue samples for RPPA analysis were rapidly processed and snap-frozen in liquid nitrogen. The time from removal of a colectomy specimen to snap-freezing of samples was < 20 mins. Prompt preservation of the sample limits protein and RNA degradation as a result of protease and RNase activity, respectively, and limits reactive changes in phosphorylated proteins (Botling *et al.*, 2009; Espina *et al.*, 2011). Tissue stabilization and preservation methods should be compatible with the intended downstream analysis. Preservation of tissue histology and morphology is essential for verification of tissue type and cellular content. Fresh-frozen tissue samples were stored at −80°C.

The frozen tissue samples are first embedded in optimal cutting temperature compound (OCT). The bottom of a cryomold is covered with OCT to a depth of 2-4mm and the frozen tissue specimen is placed on top of the OCT in the cryomold and orientated in the desired position, keeping in mind that the side facing down will be the first tissue surface cut. The tissue is completely covered with OCT and placed in a container of dry ice immediately. The frozen tissue is stored at −70° to −80°C.

When carrying out frozen tissue sectioning the cryomold is removed from the O.C.T. tissue block and the block is placed directly onto a chuck at room temperature. The chuck is then immediately placed in liquid nitrogen, allowing the O.C.T. to freeze and forming a bond between the tissue block and the chuck. A new blade is placed in the knife holder and the chuck containing the tissue block is placed in the chuck holder. The micrometre is set to the desired thickness (5-8μm is optimal for laser capture microdissection) and frozen sections are cut and discarded until a full tissue section is obtained. These tissue sections are then placed on a glass slide at room temperature. The tissue block and frozen section slides are then stored at −80°C.

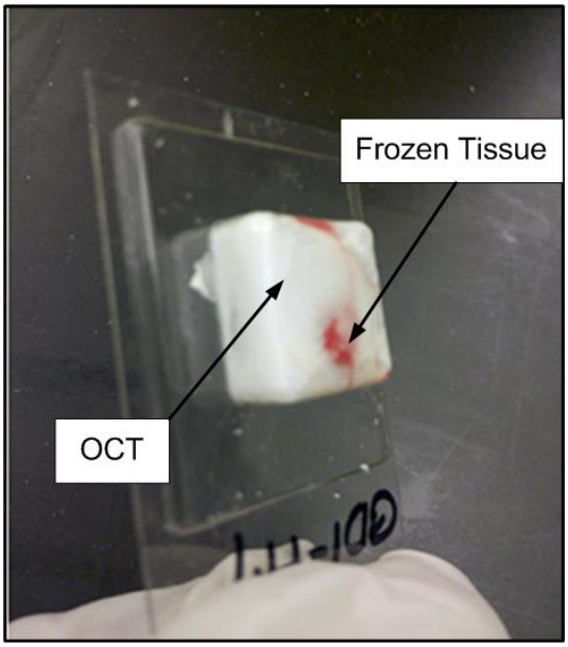

Figure 2.3: Tissue Embedded in OCT. This image shows a piece of frozen human tissue embedded in OCT, contained with a cryomold.

2.4.6 Haematoxylin Staining for LCM

Haematoxylin stains cellular nuclear material bluish/purple while eosin stains cytoplasmic proteins pink, allowing the visual distinction between cytoplasmic and nuclear cellular elements (Wittmann, 1965). This process is often called blueing. Haematin, a product of oxidation of haematoxylin, is the compound that combines with aluminium ions to form the active dye-metal complex. Alum haematoxylin solutions (Mayer's Haematoxylin) impart to the nuclei of cells a light transparent red stain that rapidly turns blue on exposure to any neutral or alkaline liquid (Scott's Tap Water Substitute). Haematoxylin and Eosin (H&E) stains are compatible with Laser Capture Microdissection (LCM) and are suitable for general histological examination of tissue sections. To reduce potential dye-cellular protein interactions, Eosin-Y is not included in the staining protocol for tissue that will be microdissected. Thus, only nuclei will be stained blue with these haematoxylin staining protocols (Kiernan, 2010).

Frozen sections slides are immediately fixed in 70% (v/v) ethanol. OCT is then dissolved by soaking the slide in water, followed by nucleic acid staining with Mayer's Haematoxylin. Excess dye is removed by rinsing the slide in water. The blue colour of the dye develops in a basic solution (Scott's Tap Water Substitute). The final staining steps are dehydration in graded alcohols (70%, 95% and 100% (v/v) ethanol) followed by clearing in xylene. The slides are allowed to air dry at room temperature after the final rinse in xylene.

2.4.7 Laser Capture Microdissection

Cellular heterogeneity of tissue is a common problem encountered by both genomic and proteomic researchers during tissue analysis. Molecular and proteomic analysis of heterogeneous tissue is hindered by extreme variability and inaccuracy because it is impossible to discern which cells contribute which cellular constituents to a given tissue lysate (Wulfkuhle *et al.*, 2008). Laser capture microdissection (LCM) is a technology invented and pioneered by Dr. Lance Liotta that allows the identification, selection and isolation of pure cell populations from a heterogeneous tissue section or cytological preparation under direct microscopic visualization of the cells (Emmert-Buck *et al.*, 1996; Bonner *et al.*, 1997). Using LCM researchers are able to isolate normal, pre-malignant, and malignant cells without contamination from surrounding cells (Nakazono *et al.*, 2003; Angeles *et al.*, 2006; Nakamura *et al.*, 2007). Molecular profiling of pure cell populations, which is reflective of the cell population's *in vivo* genomic and proteomic state, can determine molecular signatures in normal and diseased tissue (Wulfkuhle *et al.*, 2002; Petricoin *et al.*, 2005; Petricoin *et al.*, 2007).

The fundamental components of LCM technology are (i) visualization of the cells of interest via microscopy, (ii) transfer of laser energy to a thermolabile polymer with formation of a polymer-cell composite (Infrared system) or photo volatilization of cells surrounding a selected area (Ultraviolet system), and (iii) removal of the cells of interest from the heterogeneous tissue section. The Arcturus*XT*™ system (Applied Biosystems/Life Technologies) discussed herein incorporates both laser types in one instrument providing options as to the type of microdissection to be performed. For the purpose of this study only the Infrared laser type was used.

A stationary near-infrared laser mounted in the optical axis of the microscope stage is used for melting a thermolabile polymer film. The polymer film is manufactured on the bottom surface of an optical-quality plastic support cap. The cap acts as an optic for focusing the laser in the same plane as the tissue section. The polymer melts only in the vicinity of the laser pulse, forming a polymer-cell composite. Lifting the polymer from the tissue surface shears the embedded cells of interest away from the heterogeneous tissue section. The exact cellular morphology, as well as the DNA, RNA and proteins of the procured cells, remain intact and bound to the polymer. Following microdissection, extraction buffer directly applied to the polymer film solubilizes the cells, allowing the collection of the molecules of interest for downstream analysis of DNA, RNA or proteins.

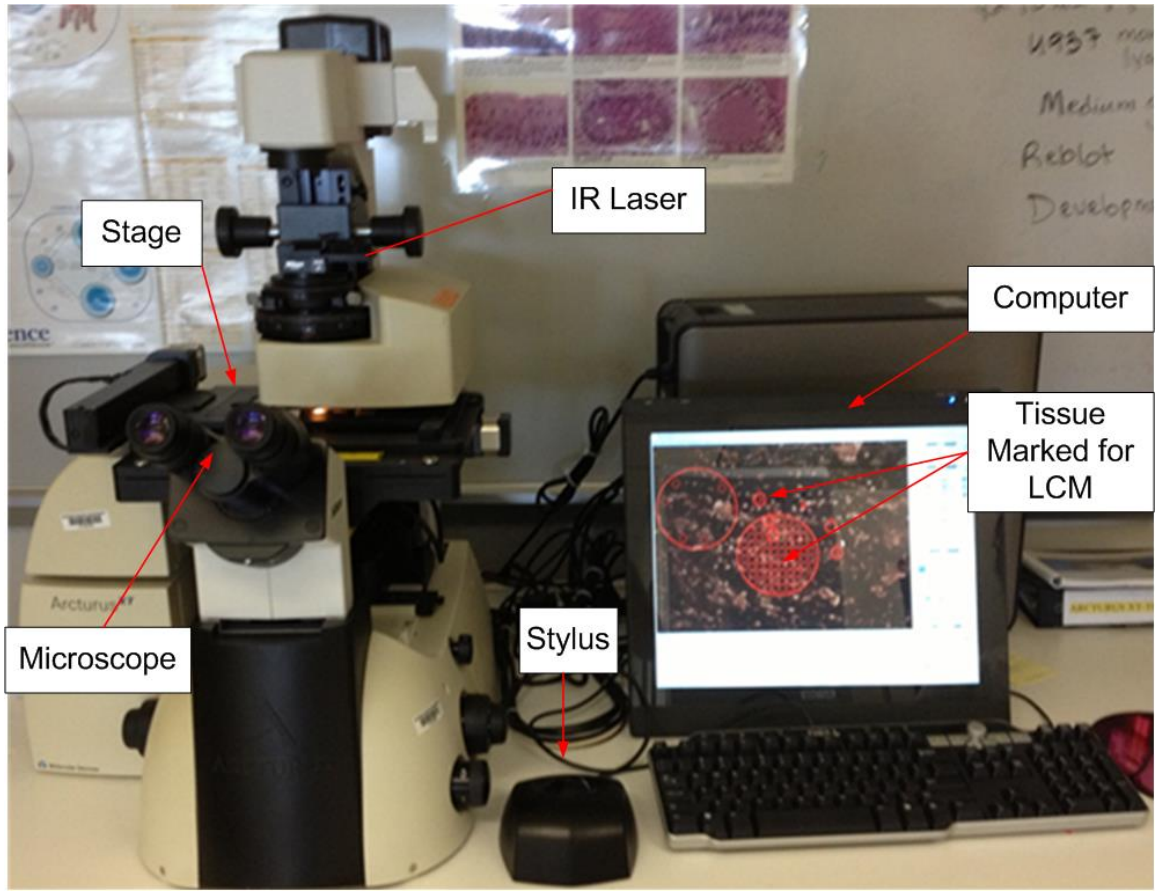

Figure 2.4: The ArcturusXT™ Laser Capture Microdissection System. The system is composed of a microscope, an IR laser, and a computer. The stage holds the slide containing the tissue sample and the LCM caps. The stylus allows the user to navigate around the tissue sample and find cells of interest. Cells to be microdissected are marked on the computer screen.

In this study, LCM was performed to isolate separate populations of epithelial and stromal cells for signalling analysis (Fig. 2.5). Using the LCM apparatus (Arcturus *XT*, Life Technologies, San Francisco, CA, USA) (Emmert-Buck *et al.*, 1996), approximately 15000 - 20000 laser shots (estimated >20 000 cells) of epithelium and stroma were removed for each frozen tissue sample, from consecutive cryostat sections. No attempt was made to target specific regions of carcinoma cells within the tumour and multiple separate areas of tissue were dissected so that signalling analysis could be performed on a cell population-wide scale within each patient sample. Tissue processing and

preparation of tissue lysates have been described previously (Wulfkuhle *et al.*, 2003; Sheehan *et al.*, 2005).

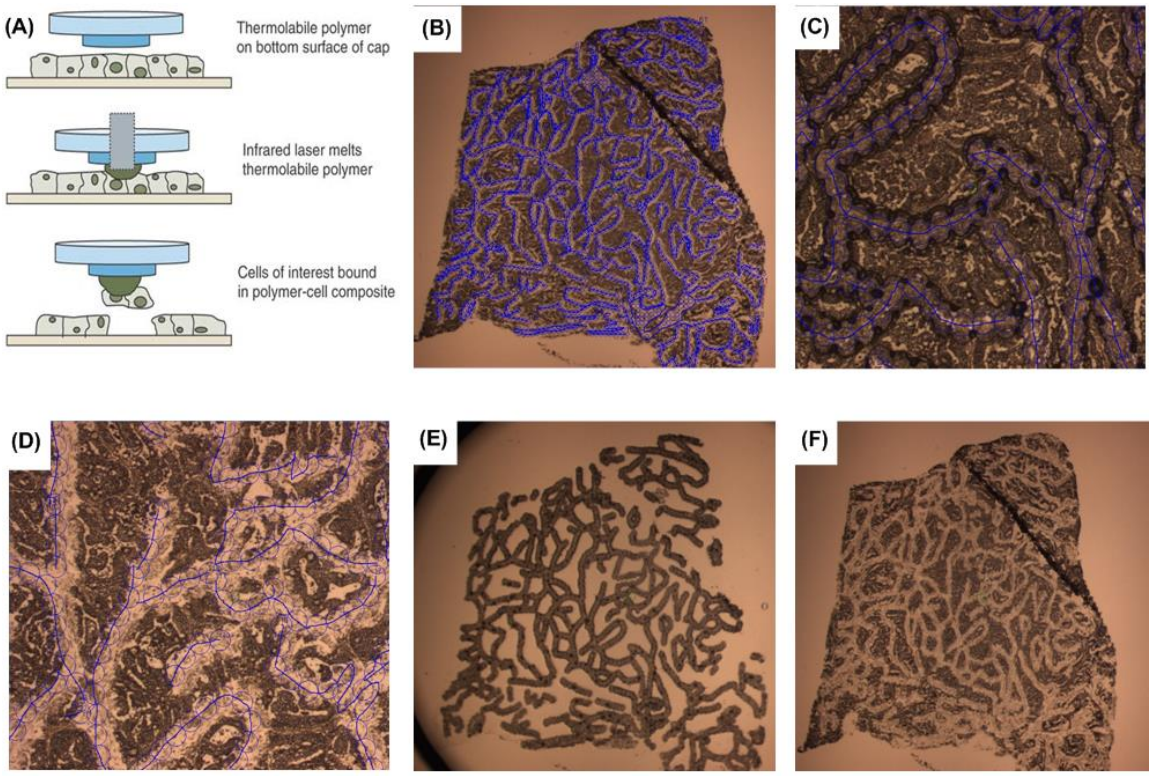

Figure 2.5: Pictorial Representation of the LCM Process. (A): An overview of the LCM process. (B): Stromal Cells marked (In Blue) for LCM prior to the laser being 'fired'. (C): A close-up of the stromal cells after the laser has been fired. *Note the circles along the blue lines corresponding to a 'shot' of the laser. (D): A close up of the tissue remaining (epithelial cells) after the stromal cells have been removed. (E): A picture of the LCM Cap, with the stromal cells attached. (F): The remaining Epithelial cells on the tissue section. (Image (A) taken and adapted from Espina *et al*., 2006).

2.4.8 Protein Extraction of Microdissected Material for Downstream Analysis

The LCM cap, containing microdissected cells for protein analysis, can be stored at -80°C for extraction at a later date. Extraction of proteins from microdissected cells should be performed just prior to the downstream analysis to prevent aggregation of proteins, degradation of proteins, or binding of protein to the walls of the micro-centrifuge tube during prolonged storage. Microdissected samples for Western blotting and/or reverse phase protein array analysis can be prepared with the following denaturing cell lysis/protein extraction buffer:

2x SDS Tris-glycine sample buffer	450µL
TCEP (Tris(2-carboxyethyl)phosphine)	100µL
T-PER (Tissue Protein Extraction Reagent)	450µL

Each LCM cap is first thawed at room temperature and then 30µL of extraction buffer is added directly onto the cap film and incubated for 1 min. The extraction buffer is pipetted up and down on the surface of the cap to solubilize the cells. The extraction buffer containing the solubilized cells is collected in a 0.5mL microcentrifuge tube. If more than one CapSure cap is used to microdissect the cells of interest, solubilized cells from these caps are collected in the same microcentrifuge tube. The samples are then denatured by heating the microcentrifuge tubes at 100°C for 5-8 minutes prior to downstream proteomic analysis. The samples are stored at –80°C.

2.5 Reverse-Phase Protein Microarrays

Reverse phase protein microarrays (RPPAs) are a multiplexed proteomic platform used to evaluate cell signalling protein levels or phosphoprotein profiles in many samples printed on one array for one specific endpoint per array (Paweletz *et al.*, 2001; Espina *et al.*, 2003; Belluco *et al.*, 2005; Petricoin *et al.*, 2007; VanMeter *et al.*, 2007; Wulfkuhle *et al.*, 2008). Over 100 array slides can be printed with 40µL of protein lysate and each array is probed with a single antibody. In addition to printing sample lysates, it is also essential to print control lysates such as commercial cell lysates, recombinant peptides, or peptide mixtures that are known to contain the antigens being investigated. All samples are printed in a range of concentrations, which permits the selection of the optimal sample protein concentration for individual antibodies having varying affinities.

The Aushon 2470 arrayer utilizes a solid pin format for the application of cell lysates or other protein containing fluids onto a matrix of nitrocellulose mounted on a glass microscope slide. Prior to printing cell lysates on a RPPA, the number of cells required should be optimized preceding the final array construction. The arrays are subsequently stained using a Dako CSA (Catalysed Signal Amplification) System that includes blocking and signal amplification reagents that are compatible with chromogenic (DAB), chemiluminescent, or fluorescent (Li-Cor® IRDye680) detection reagents (Fig. 2.6).

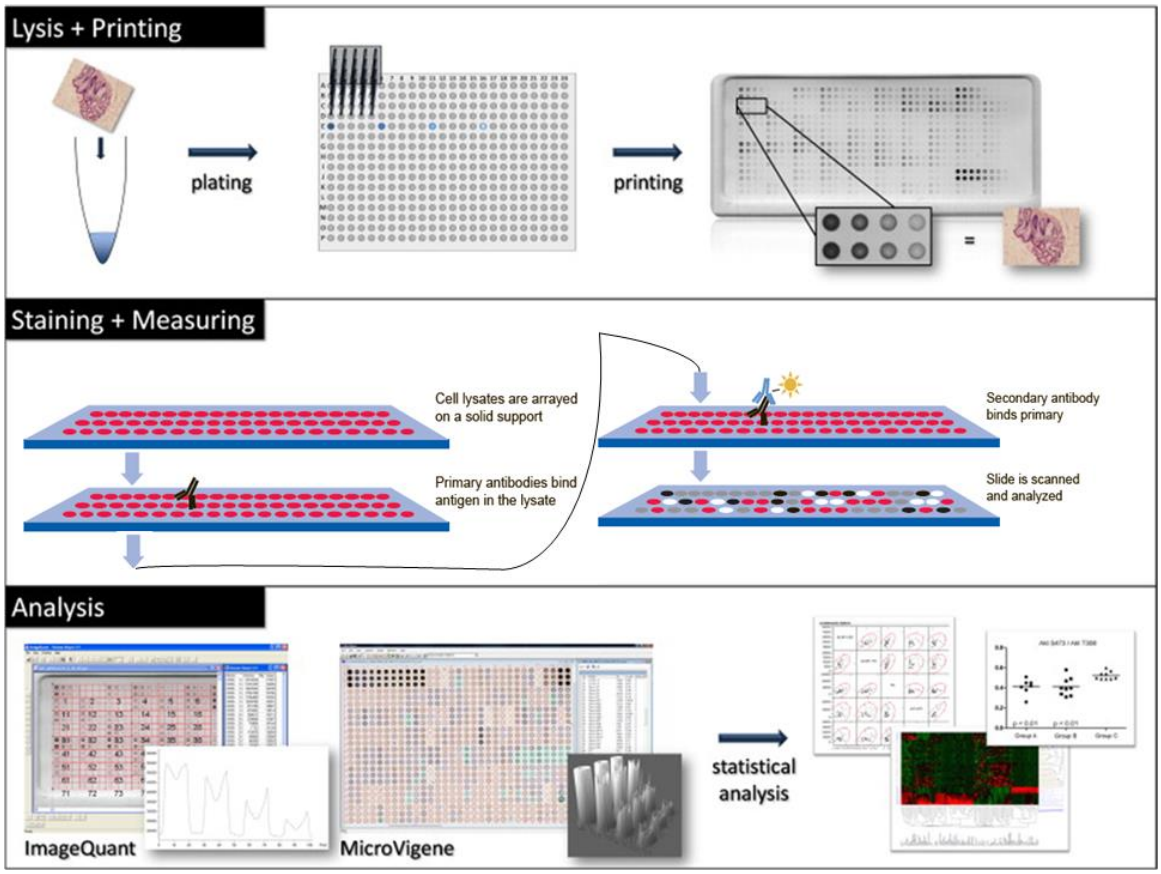

Figure 2.6: Schematic overview of the RPPA Construction Process. Laser capture microdissected cells are lysed and immobilized onto nitrocellulose slides at distinct positions. Each sample is arrayed in duplicate and in a range of concentrations. After arraying these slides are incubated with a primary antibody, allowing the antibody to bind the antigen in the lysate. Bound antibodies are detected by secondary tagging and signal amplification and these can then be detected by chemiluminescencent, fluorescence-based, or colorimetric assays. The intensity of the signal is proportional to the concentration of the target protein. This data can then be analysed using specially designed software to analyse the results (Taken and adapted from www.capmm.gmu.edu).

Reverse-phase protein microarrays (RPPA) were generated as described previously (Paweletz *et al.*, 2001; Liotta *et al.*, 2003; Espina *et al.*, 2007; Mueller *et al.*, 2010). LCM-enriched epithelium lysates were printed in triplicate on ONCYTE Avid nitrocellulose film-slides (GRACE Bio-Labs, Bend, OR) using an Aushon 2470 arrayer equipped with 350 µm pins (Aushon Biosystems, Billerica, MA). Each array contained epithelium lysates for all 19 cases and each lysate was printed in a 2-fold dilution curve representing undiluted lysate, 1:2, 1:4 and 1:8 dilutions. Control lysates were printed in a 2-fold dilution curve. All RPPAs were baked for 2 hrs at 80°C to allow fixation and then stored with desiccant at −20°C. Quality control samples, including A431 cell lines (±EGF stimulation; BD Pharmingen, San Diego, CA, USA) and Bovine serum albumin (BSA) standards, were printed on the RPPA to ensure protein deposition and immunostaining reactivity (reviewed in Gulmann *et al*., 2006).

2.5.1 RPPA immunostaining, image acquisition and data analysis

RPPA slides were blocked (I-Block, Applied Biosystems) for 2 hours before immunostaining. Immunostaining was conducted on a Dako Autostainer using a Dako Catalysed Signal Amplification (CSA) kit, (Fig. 2.7). Each slide was incubated with a single primary antibody at room temperature for 30 minutes. The negative control slide was incubated with antibody diluent (Dako). For each immunostaining run, 1 slide was incubated with anti-ssDNA antibody (1:15,000; IBL International GmbH). Secondary antibody was goat anti-rabbit (1:10,000; Vector Laboratories), or rabbit anti-mouse IgG (1:10; Dako), that were amplified via horseradish peroxidase-mediated biotinyl tyramide with chromogenic detection (diaminobenzidine; Dako). In total 30 primary antibodies specific to known signalling endpoints were used to measure phosphorylation and total protein levels using RPPAs (Table 2.4).

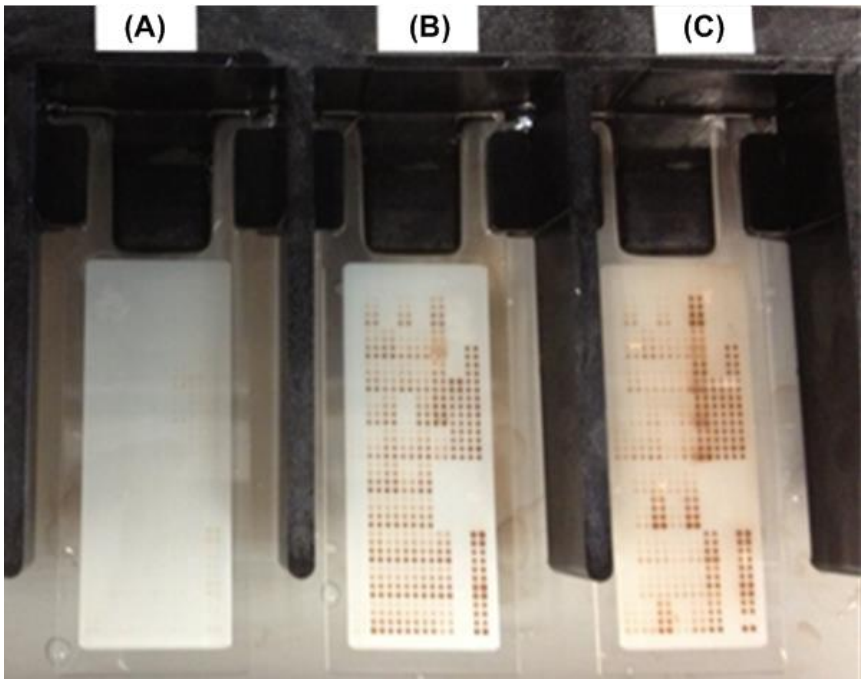

Figure 2.7: RPPA slides stained using the Dako Autostainer. (A) = A negative control slide incubated with antibody diluent (Dako). (B & C) = Examples of stained RPPA slides stained with (B) anti-Sphingosine Kinase 1 and (C) anti-Acid Ceramidase antibodies.

RPPA slides were scanned on a UMAX 2100XL flatbed scanner (white balance 255, black 0, middle tone 1.37, 600 dpi, 14 bit). Spot intensity was analysed by Image Quant v5.2 software (Molecular Dynamics). Data reduction was carried out with a VBA Excel macro, RPPA Analysis Suite (Mueller, 2013). To normalize data, the relative intensity for each protein spot was divided by the ssDNA relative intensity for the corresponding spot (Chiechi *et al.*, 2012).

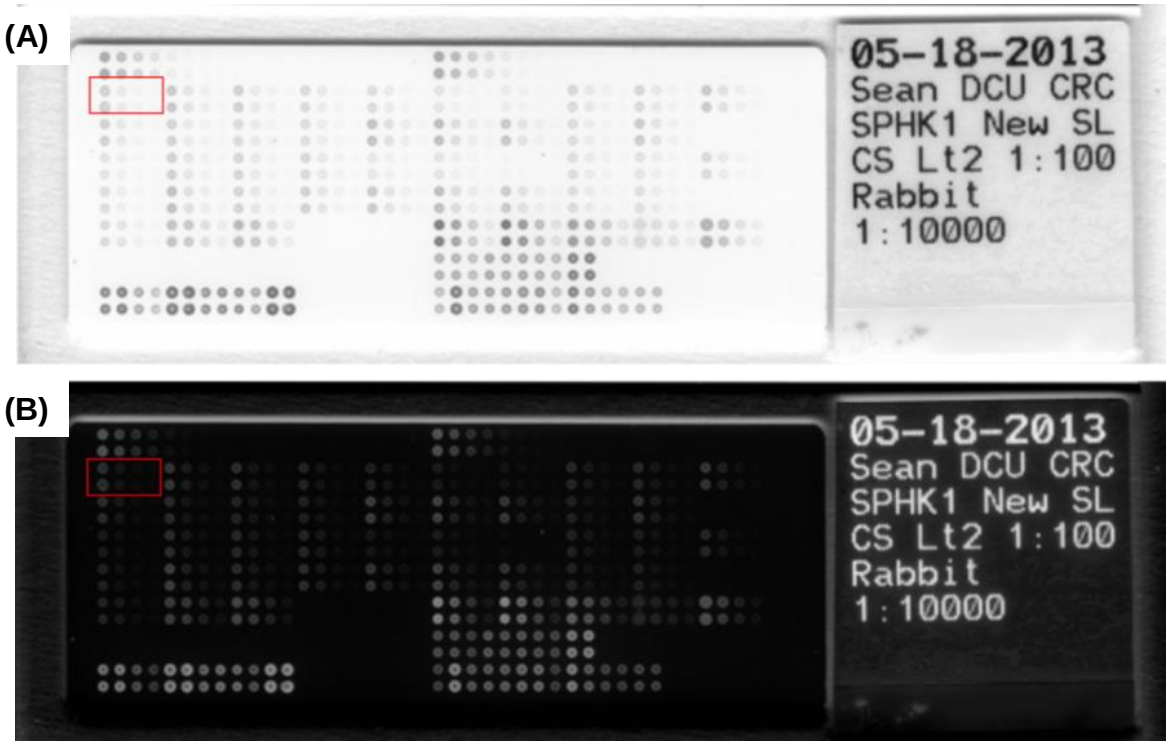

Figure 2.8: An example of an RPPA slide stained with the anti-Sphingosine Kinase 1 antibody. (A) shows the scanned image of the slide. (B) shows the corresponding inverted image that is used for measuring spot intensity. The red box in both cases indicates the first tissue sample, printed in duplicate in a range of concentrations.

2.6 Cell Culture Techniques and Protein Analysis

2.6.1 Cell Lines

In this project two colorectal cancer cell lines were used, SW480 and SW620. The two CRC cell lines were purchased from the European Collection of Cell Cultures (ECACC/Sigma Aldrich). SW480 cells were originally isolated from a primary colon carcinoma, while the SW620 line was established from a metastasis that arose in the same patient one year later. The stromal fibroblast cell line, CCD-18Co (ECACC/Sigma Aldrich), was derived from normal colon tissue. This cell line was used in this project to represent the tumour microenvironment. SW480 and SW620 cell lines were cultured in RPMI medium supplemented with 10% (v/v) fetal bovine serum (FBS) and 1% (v/v) penicillin. The CCD-18Co cell line was cultured in Minimal Essential Media (MEM) supplemented with 2X essential and non-essential amino acids, 2X vitamins, 2mM L-glutamine, 15% (v/v) inactivated Foetal Bovine Serum (FBS) and 1% penicillin-streptomycin.

2.6.2 Sub-culturing

Old media was removed and discarded from the cell culture flasks. The cell layer was rinsed (30secs) with 1.5mL of 1X Trypsin (0.25%). This was then removed and replaced with 3mL 1X Trypsin. Cells were monitored under the microscope until the cell layer had come off the bottom of the flask. The cell suspension was removed from the flask and added to 7mL of the appropriate media in a 15mL tube to inactivate the 1X Trypsin. Cells

were pelleted at 1200 RPM for 5 minutes, supernatant was removed and the cell pellets were re-suspended in 2mL of fresh medium. One millilitre of the cell suspension was added to 2 new T75 cell culture flasks and incubated at 37°C.

2.6.3 Resuscitation of frozen cell line stocks

An aliquot of cells was thawed, when new cultures were required, or when the viability of the cells after cryopreservation needed to be assessed. Ten millilitres of the appropriate medium was pre-warmed to 37°C. The cryovial was thawed at 37ºC in a water bath. The contents of the vial were slowly transferred to the pre-warmed medium, which was then placed in the incubator. Cell growth was monitored by examining the cells, under a Nikon® inverted microscope. After 72-96 hrs, the regular subculture routine was initiated to ensure that the optimal cell concentration and conditions were maintained.

2.6.4 Cell lysis

The lysis buffer was prepared as described in 2.2.6. PBS was refrigerated overnight. Medium was removed from cells and replaced with 20mL of cold PBS. PBS was removed from the flask and 2mL of lysis buffer was added. The cells were scraped from the bottom of the flask and transferred to a new receptacle. The sample consistency should be viscous. The cells were sonicated at 20% amplitude for 30 seconds using the Branson Sonifier™ S-450 Digital Sonicator. The cell lysate was then aliquoted.

2.6.5 Cell counting

Cells were counted and their viability assessed using trypan blue exclusion. Trypan blue is negatively charged, so it is excluded from viable cells. Therefore, only the cells with

damaged cell membranes (e.g. dead cells) will stain blue. To count the cells, 10µL of cell suspension was added to 90µL of 0.04 % (v/v) trypan blue solution. The sample was loaded into the chamber of a Neubauer haemocytometer. Using a UV visible light microscope, cells were counted in 5 squares of either side of the chamber (10 in total). The concentration of the cells in the suspension (cells/mL) was calculated by multiplying the total number of cells in all 10 squares x dilution factor x 1,000.

2.6.6 Long-term storage of cell lines

Cells were prepared by aliquoting into 1mL cryovials at a concentration of 5-10 x 10^6cells/mL in freeze medium. Freeze medium consisted of 95% (v/v) of the appropriate medium and 5% (v/v) dimethyl sulfoxide (DMSO). Once dispensed, the vials were immediately transferred to a Nalgene® Mr. Frosty and placed in a -80ºC freezer for slow freezing. Once frozen, the vials were transferred to liquid nitrogen for long-term storage.

2.6.7 Mycoplasma Testing

Testing for Mycoplasma was carried out using MycoAlert® Mycoplasma Detection Kit (Lonza), as per the manufacturer's instructions. This luminescence-based technique is based on the measurement of adenosine triphosphate (ATP) in a culture supernatant. Enzymes released from viable Mycoplasma react with the kit substrate (Luciferin), catalysing the conversion of ADP to ATP. By measuring the level of ATP in a sample both before and after the addition of the MycoAlert™ substrate, a ratio can be obtained

which is indicative of the presence or absence of mycoplasma (<0.9 = Negative; 0.9-1.2 = Borderline and >1.2 = Positive). If these enzymes are not present, the second reading shows no increase over the first, while reaction of mycoplasmal enzymes with their specific substrates in the MycoAlert™ substrate, leads to elevated ATP levels.

2.6.8 Fluorescence Microscopy

Fluorescence microscopy has become an essential tool in biology and the biomedical sciences, as well as in materials science due to attributes that are not readily available in other contrast modes with traditional optical microscopy. The application of an array of fluorochromes has made it possible to identify cells and sub-microscopic cellular components with a high degree of specificity amid non-fluorescing material. In fact, the fluorescence microscope is capable of revealing the presence of a single molecule. Through the use of multiple fluorescence labels, different probes can simultaneously identify several target molecules simultaneously. Although the fluorescence microscope cannot provide spatial resolution below the diffraction limit of specific specimen features, the detection of fluorescing molecules below such limits is readily achieved. Fluorescence microscopy uses fluorescence to generate an image. The sample to be tested is labelled with a secondary (2^{o}) antibody chemically linked to flurophores, which is specific for the target protein. A flurophore is a fluorescent chemical compound which can re-emit light upon excitation. The sample is illuminated with light of a specific wavelength, which is absorbed by the fluorophores, causing them to emit light of a

longer wavelength. This technique was used in the project to look at the expression of TRIM28 and *β*-Actin in the cancer cell lines.

Cover-slips (0.13mm-0.16mm thickness) were sterilized by placing in 100% (v/v) EtOH and flamed through a Bunsen. The cover-slips were placed in a 6-well plate and placed under UV light for 30 minutes. SW480 and SW620 cell lines were trypsinsed (section 3.2) and re-suspended in 10mL of media. The cell suspension (100µL) was added to 1.9mL of media in the 6 well plate and cells were left to adhere to the coverslip overnight at 37^{o}C. The media was removed and 1mL of 3% platelet-activating factor (PAF) solution was added, covered and left on ice for 20 minutes. The reaction was quenched with 1mL of 50 mM ammonium chloride solution. Perma block buffer solution (1mL) was added to the wells and left for 1h at RT. The blocking solution was removed and a square was drawn around the cover-slip using a wax pen. The primary antibody (100µL), made up in perma block, was added to the cover-slip and incubated at 37^{o}C for 1h. The cover-slip was washed 3 times with perma block solution. Fluorescently labelled secondary antibody, made up in perma block (100µL), was added to the cover-slip and incubated at 37^{0}C for 1 hour in the dark. Antibody dilutions are indicated in Table 2.6. The cover-slip was washed with perma block and 7µL of fluorescence mounting media (DAKO) was added, the cover-slip turned and stuck to a glass slide and stored in a dark box. The cover-slip was sealed with nail varnish and left at 4^{o}C until imaging. The cells were imaged using the OPTIKA XDS-2FL Inverted trinocular EPI fluorescence microscope

HBO illumination system with OPTIKAM Pro 3, 3.1Mpixels PC camera and the optika vision pro software.

Table 2.6: Antibody dilutions for use in fluorescence microscopy

Antibody	Primary Antibody	Secondary Antibody
β-Actin	1 in 40	1 in 2,000
TRIM28	1 in 100	1 in 2,000

2.6.9 Cell Scratch Assay

Moving cell fronts are features of tissue repair and tumour spreading. Monitoring cell fronts give an insight into wound healing, development and disease (Stetler-Stevenson *et al.*, 1993). The rate at which the front of a population of cells moves is influenced by the rate at which individual cells within the population migrate and proliferate. Cell scratch assays are a commonly used method to investigate the motion of cell fronts by creating a scratch in a cell monolayer and observing the motion of the cell front (Teppo *et al.*, 2013). Images of the cell front are then taken over a period of time. The most cost-effective and convenient means of analysis is to monitor the location of the cell front as a function of time. This method of analysis is convenient as it is non-destructive and does not require labelling, tracking or counting individual cells amongst a population. Reporting in this manner presents a qualitative visual comparison between a control assay and a different assay where a treatment was applied. Cell scratch assays can be used to monitor how drugs which inhibit proliferation will reduce tumour spreading, while steroid treatment can be used to analyse wound healing (Johnston *et al.*, 2014). In this project a cell scratch assay was used to monitor the movement of the cell front in the SW480 and SW620 cell lines, once a scratch had been applied. The scratch assay

protocol was taken and amended from a protocol which had previously been described (Liang *et al.*, 2007).

SW480 and SW620 cell lines were trypsinised and centrifuged as discussed in section 2.6.2 and resuspended in 2mL of media. The cell suspension (50µL) was added to 1.95mL of media in a 6 well cell culture plate. The cells were incubated at 37^{o}C until they reached at least 80% confluency. Once this had occurred the cell monolayer of appropriate wells was scratched in a straight line using a p200 pipette tip. The cellular debris was removed by washing the wells twice with 2mL of PBS and twice with the appropriate media. Finally 2mL of media was added to each well. At various time-points (0, 24, 48, or 72hr), the migration associated with wound closure was assessed and quantified using a microscope. Images of the front were captured over the 4 day period using the OPTIKA XDS-2FL microscope, with images being taken every 24hr.

2.7 Proteomic Network Analysis

Proteomic network analysis was performed as previously described (Chiechi *et al.*, 2013). Briefly, Spearman ρ correlation analysis with $\rho \geq 0.75$ and $p \leq 0.01$ was used to build proteomic network graphs (Gephi 0.8.2 beta, The Gephi Consortium, Paris, France, www.gephi.org). Nodes in the network represent RPPA endpoint molecules. The bigger the node the more significant correlations it has with other endpoint molecules. Each line connecting 2 nodes represents a significant correlation between the nodes; the thicker the line, the higher the Spearman ρ correlation. Proteins are grouped on the basis of Spearman ρ values and the number of connections among a group of nodes; strongly correlated nodes are represented close to each other and with the same colour.

2.8 Statistical Analysis

Association between discrete variables was assessed using the χ^2 test. Five-year survival and five-year 'recurrence-free' survival were analysed and survival curves were plotted according to the Kaplan-Meier method using the generalized log-rank test to compare survival curves. Prognostic factors for 5-year survival and 5-year 'recurrence-free' survival were evaluated by univariate and multivariate analyses for TNM stages, gender and lymphovascular invasion (Cox proportional hazard regression model). For both Kaplan-Meier and Cox regression analyses, patients who had follow-up information for more than 5-years, were censored at 5-years post-diagnosis. In survival analysis, the hazard ratio (HR) is the ratio of the hazard rates corresponding to the conditions described by two levels of an explanatory variable. The confidence interval (CI) indicates the level of uncertainty around the measure of effect (precision of the effect estimate) which in this case is expressed as CI. Confidence intervals are used because a study recruits only a small sample of the overall population so by having an upper and lower confidence limit it infers that the true population effect lies between these two points. The CI for this study was 95% with is consistent with most other studies. All tests were analysed using SPSS 19.0 software (SPSS, Chicago, IL, USA) and the findings were considered statistically significant at $P < 0.05$.

Unsupervised hierarchical clustering of the RPPA dataset was conducted using JMP 5.1.2 (SAS Institute Inc. USA). The Spearman rank correlation coefficient, ρ, was calculated for each protein pair in the RPPA cohort; $\rho \geq 0.75$ with $P \leq 0.01$ considered significant.

Chapter 3

Colorectal Cancer Patient Cohort

3.1 Introduction

Large bio-repositories of formalin-fixed paraffin-embedded tissue already exist in many hospitals and are typically used for immunohistochemical analysis. When tissue samples are accompanied by a patient's medical, genetic, clinical, pathological, and follow-up information it provides researchers with an invaluable resource for studying the aetiology of the disease. These patient cohorts can also help to identify novel biomarkers of diagnosis, disease progression, prognosis, response to therapy etc. These bio-specimens are now being used to better examine the determinants of cancer prognosis and patient survival, as newer proteomic and genomic technologies emerge. Next-generation sequencing technologies have been used to successfully assess copy number variation in as little as 5 ng of DNA extracted from FFPE samples (Wood *et al.*, 2010; Kerick *et al.*, 2011) and have recently been used to evaluate predictive biomarkers in CRC (Peeters *et al.*, 2013). This highlights the importance of having a strong patient cohort that accurately reflects the aetiology of the disease, when studying potentially novel biomarkers.

In the current study, we developed a large database containing information on the familial history, medical history, clinical and pathological information, treatment regimen, disease recurrence and patient outcome for all of the patients in our cohort. This provided us with large volumes of information that could then be correlated with the levels of expression of antigens of interest to see if there were any significant links to CerS5 and TRIM28 expression levels.

3.2 Patient Recruitment

The research conducted in this Ph.D. thesis was approved by the Ethics (Medical) Research Committee at Beaumont Hospital, Dublin, Ireland and informed consent was obtained from all patients. The recruitment of patients into the colorectal cancer study was performed within the Clinical Research Centre, Beaumont Hospital, Dublin, with the assistance of full-time clinical research nurses. Patients were recruited either at the time of their diagnostic colonoscopy or when they were hospitalized for surgical management of their disease. All patients attending for colonoscopy in the hospital's endoscopy unit received a Patient Information Leaflet (PIL) with their appointment. During admission to the unit the admitting doctor was required to confirm that the patient had read and understood the contents of the PIL, and invite the patient to sign a research consent form. Patients were assured that participation was voluntary and that refusal to participate would not affect their treatment in any way.

The clinical notes of all patients attending for colonoscopies were reviewed daily by the clinical research nurses. Following the procedure the colonoscopy findings were reviewed and patients that were eligible to participate, and who had signed consent, were asked to provide a blood sample, if appropriate. If a lesion was identified during the colonoscopy additional tissue samples could be taken from consenting patients for research purposes.

3.3 Results

3.3.1 Clinicopathological Features

A total of 137 cases with a diagnosis of CRC met the inclusion criteria and were included in the initial study cohort. The median age of the patients at the time of first diagnosis was 68 years (range 34-87 years). The cohort included 85 male and 52 female patients with a median follow up of 54 months (range 1-122 months). In total, 89 patients had colonic carcinoma, whereas 48 had rectal carcinoma. Table 3.1 shows the clinicopathological demographics of the patient cohort, along with the follow-up information.

Chemotherapy can alter the balance of sphingolipid metabolism, as previously mentioned. Therefore, in the CerS5 arm of the study the cohort was split into neo-adjuvant and non-neoadjuvantly treated patients. No correlation has been found to date between TRIM28 expression and chemotherapy or radiation treatment and therefore all 137 patients were included.

In order to characterize the signalling protein networks associated with both TRIM28 and CerS5, reverse-phase protein microarray (RPPA) analysis was performed in fresh-frozen tissue from an additional 19 patients with colorectal cancer (RPPA cohort). Patients in the RPPA cohort were diagnosed with colorectal cancer between 2012 and 2013 and met the same inclusion criteria as those of the IHC cohort. Clinical and pathological parameters of all patients are presented in Table 3.1.

Table 3.1: Clinicopathological details of patient cohorts

	IHC cohort		RPPA cohort	
Factor	**Number of patients = 137**	**%**	**Number of patients = 19**	**%**
Gender				
Female	52	37.96	10	52.6
Male	85	62.04	9	47.4
Age (years)				
Median	68	-	67	-
Range	34-87	-	47-88	-
<65	59	43.1	8	42.1
≥65	78	56.9	11	57.9
Tumour site				
Colon	89	65.0	15	78.9
Rectum	48	35.0	4	21.1
Tumour stage				
Tis	2	1.5		
T1	9	6.6	0	0
T2	20	14.6	0	0
T3	87	63.5	13	68.4
T4	19	13.9	6	31.6
Not Stated†	2	1.5	-	-
Node stage				
N0	75	54.7	11	57.9
N1	37	27.0	2	10.5
N2	23	16.8	6	31.6
Not Stated†	2	1.5	-	-
Metastasis stage				
M0	126	92.0	17	89.5
M1	11	8.0	2	10.5
Lymphovascular invasion				
Yes	30	21.9	7	36.8
No	105	76.6	12	63.2
Not Stated†	2	1.5		
Differentiation				
Well	3	2.2	0	0
Moderately	119	86.9	17	89.5
Poorly	15	10.9	2	10.5
Follow-up (months)				
Median	54.3	-	N/A*	-
Range	1-122	-	N/A*	-

Abbreviations: n = number of patients; T = tumour; N = node; M = metastasis; †These patients presented with terminal metastatic disease and only had biopsies taken; thus, their T and N stage could not be accurately determined. *Follow-up information was not available for these patients as they were diagnosed with CRC in 2012/13.

3.3.2 Reported Symptoms in Colorectal Cancer Patients

The most common presenting symptom amongst our cohort was rectal bleeding; i.e. bleeding from lower colon or rectum. Almost half (48%) of the patients reported having suffered from rectal bleeding prior to diagnosis of CRC. Other common symptoms reported were abdominal pain, anaemia, altered bowel habit and weight loss. Often these symptoms are reported in combination with each other, as well as the other symptoms mentioned in Fig. 3.1 below. Interestingly, only 7% of patients diagnosed with CRC were discovered by screening for CRC, highlighting the need for a novel diagnostic device or biomarker capable of accurately detecting CRC.

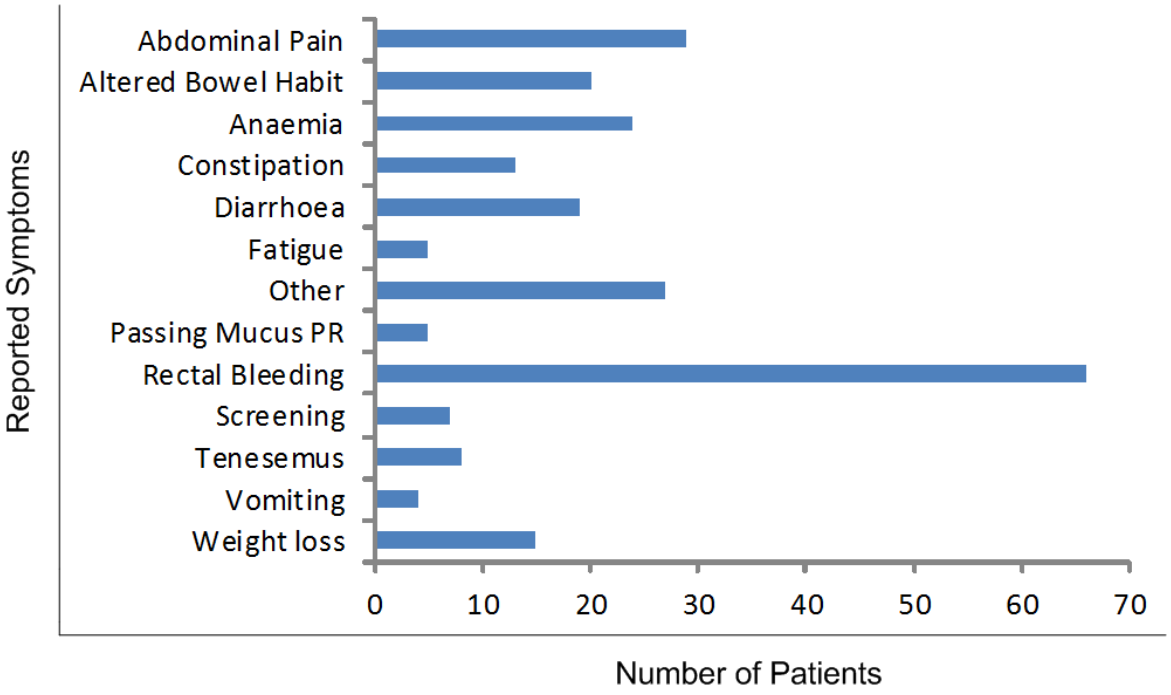

Figure 3.1: Most Common Presenting Symptoms in CRC Cohort. The presenting symptoms of all the CRC patients in the cohort (*n*=137) were assessed to find the most commonly reported symptoms.

3.3.3 Distribution of Tumour sites in Colorectal Cancer Patients

The majority of patients included in this study presented with tumour localised on the left side (65%), which includes the descending colon, sigmoid colon, recto-sigmoid junction and the rectum. 29% of patients presented with a tumour localised to the right colon, including the caecum and ascending colon. Only 3% of patients presented with a tumour in the transverse colon which joins the left and right colon (Fig. 3.2). The location of the tumour within the colorectum can affect both patient outcome and response to therapy, (Elsaleh *et al.*, 2000; Wray *et al.*, 2009).

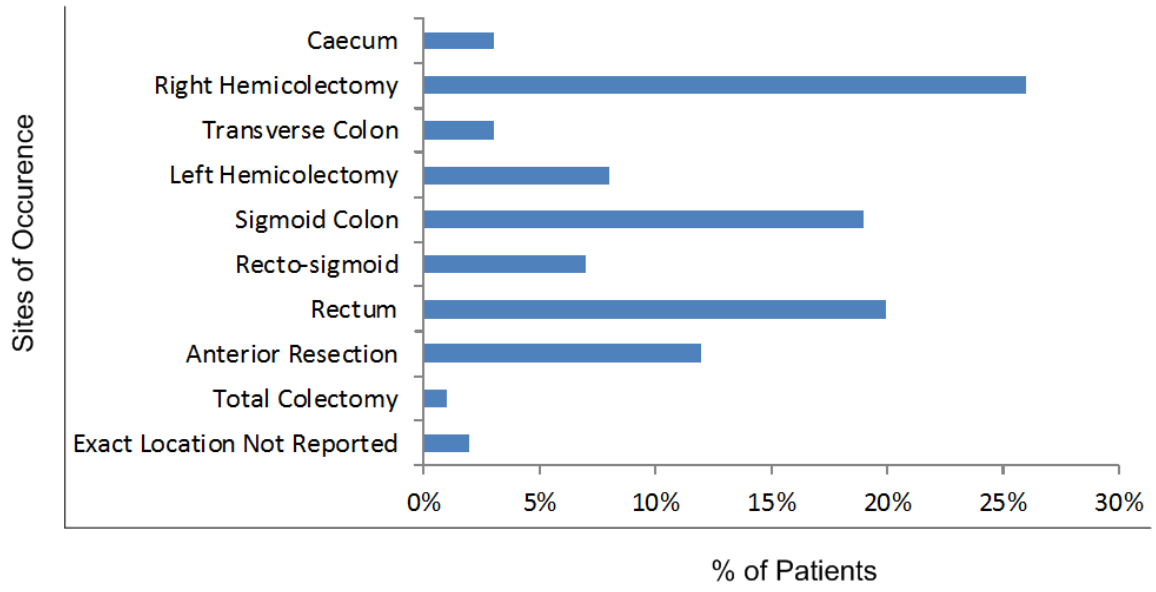

Figure 3.2: Distribution of Sites of Occurrence in CRC patients. The location of the tumour within the colon or rectum was reported for the CRC patients in the cohort (*n*=156).

3.3.4 Patient History Information

The patient history of all cases in the cohort was also recorded. This information, together with the physical examination, enables the physician and other health professionals to form a diagnosis and treatment plan. A number of genetic syndromes are also associated with higher rates of colorectal cancer (e.g. hereditary nonpolyposis colorectal cancer) and 33% of patients in our cohort reported a family history of CRC. Smoking is also known to increase a person's risk of developing cancer and 39% of the patients in this cohort are or previously were smokers.

Table 3.2: Patient History Information from CRC Cohort

Parameter	Measurement	Number of Patients = 137	(%)
Drink	Yes	104	76
	No	33	24
Smoke	Yes	53	39
	No	84	61
Aspirin	Yes	44	32
	No	93	68
History of Polyps	Yes	20	15
	No	117	85
Family History of Polyps	Yes	15	11
	No	122	89
Family History of CRC	Yes	45	33
	No	92	67
Family History of other Cancers	Yes	91	66
	No	46	34

3.3.5 The Correlation between Dukes Stage and Survival

Advanced CRC, represented by increasing Dukes stages, correlated significantly (*P* = 0.000) with the overall survival of the patients in our cohort. Dukes A patients had the best overall survival, with 100% patient survival (25/25). 15% (7/48) of Dukes B and 34% (18/53) Dukes C patients died as a result of their disease. The poorest survival rates were seen in Dukes D patients, with only 19% (2/11) of patients surviving for 5-years.

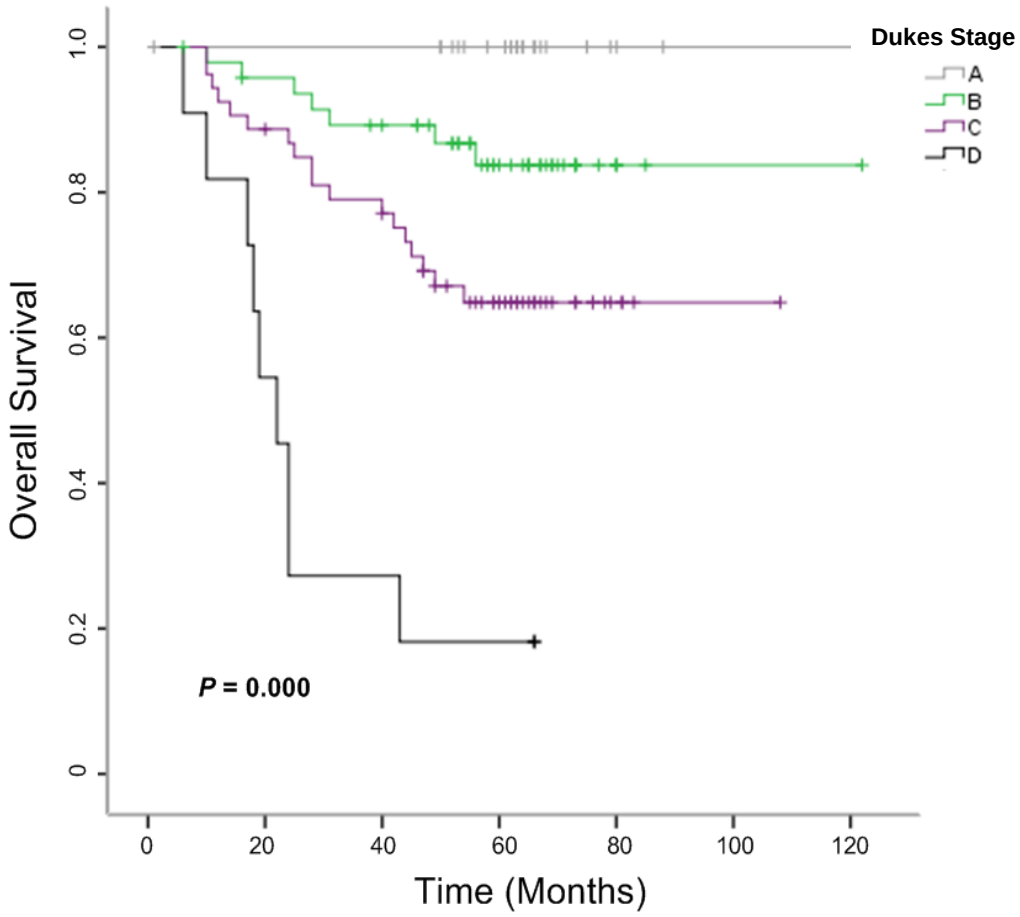

Figure 3.3: Dukes Stage predicts survival in colorectal cancer. The Kaplan-Meier plot of colorectal cancer specimens (n=137) demonstrates significantly (log-rank test) lower survival is associated with increasing Dukes stages.

3.3.6 The Correlation between T-Stage and Survival

The increasing extent of the primary tumour, represented by increasing T-Stages, correlated significantly (P = 0.000) with the overall survival of the patients in our cohort. Primary tumours that were confined to the colon or rectum (Tis-T2) had the best overall survival, with none (0/29) of these patients dying as a result of CRC. T3 cases, where the tumour had grown completely through the muscularis propria into the serosa layer but not into any neighbouring tissues, had the next best survival rate with 25% (22/87) of patients dying as a result of CRC. Finally, T4 cases, where the tumour has grown through the colon wall and breached the peritoneal layer or invaded other organs or tissues, had the worst overall survival rate with 53% (10/19) of patients dying as a result of their disease.

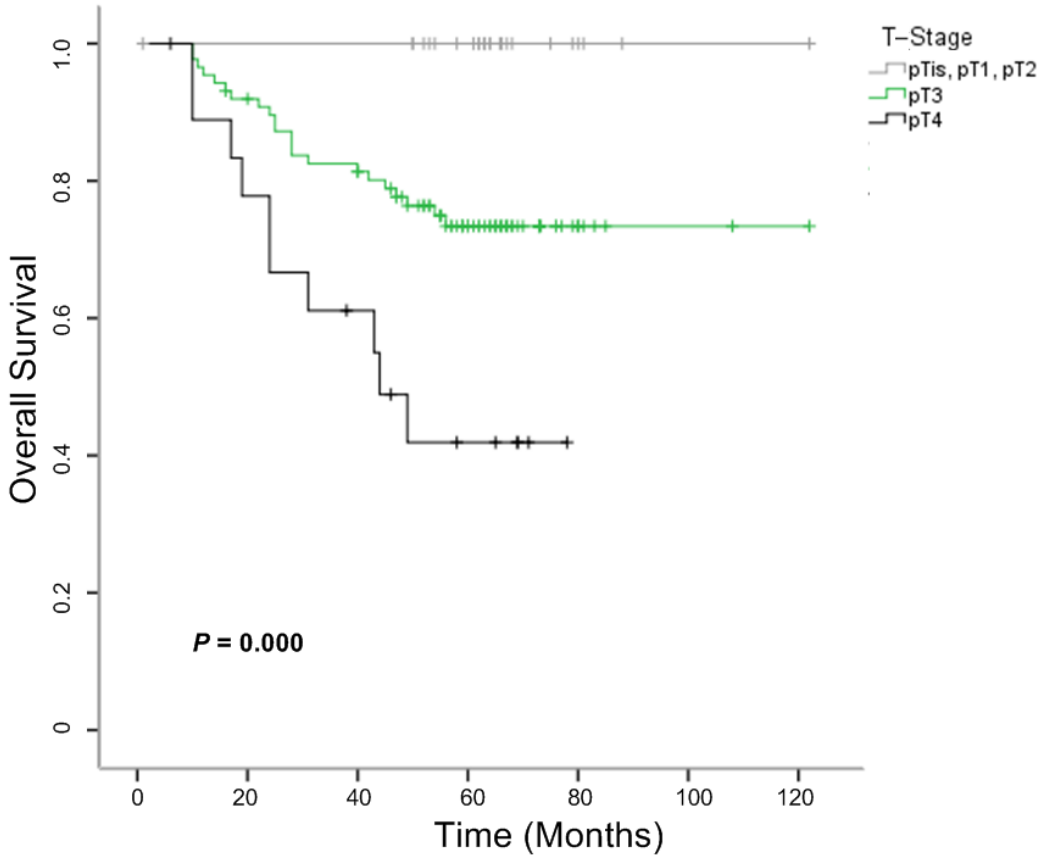

Figure 3.4: T-Stage predicts survival in colorectal cancer. The Kaplan-Meier plot of colorectal cancer specimens (n=135*) demonstrates significantly (log-rank test) lower survival is associated with increasing T-Stages. *2 patients presented with terminal metastatic disease and only had biopsies taken; thus, their T-Stage could not be accurately determined.

3.3.7 The Correlation between N-Stage and Survival

The amount of lymph node involvement, represented by increasing N-Stages, correlated significantly (*P* = 0.000) with the overall survival of the patients in our cohort. In cases where there was no lymph node involvement (N0), the patients survived the longest. 11% (8/75) of these patients died as a result of CRC. In cases where cancer cells were present in local lymph nodes (N1), 35% (13/37) patients died as a result of their disease. Finally, in cases where cancer cells were found in distant lymph nodes (N2), 48% (11/23) of patients died as a result of CRC.

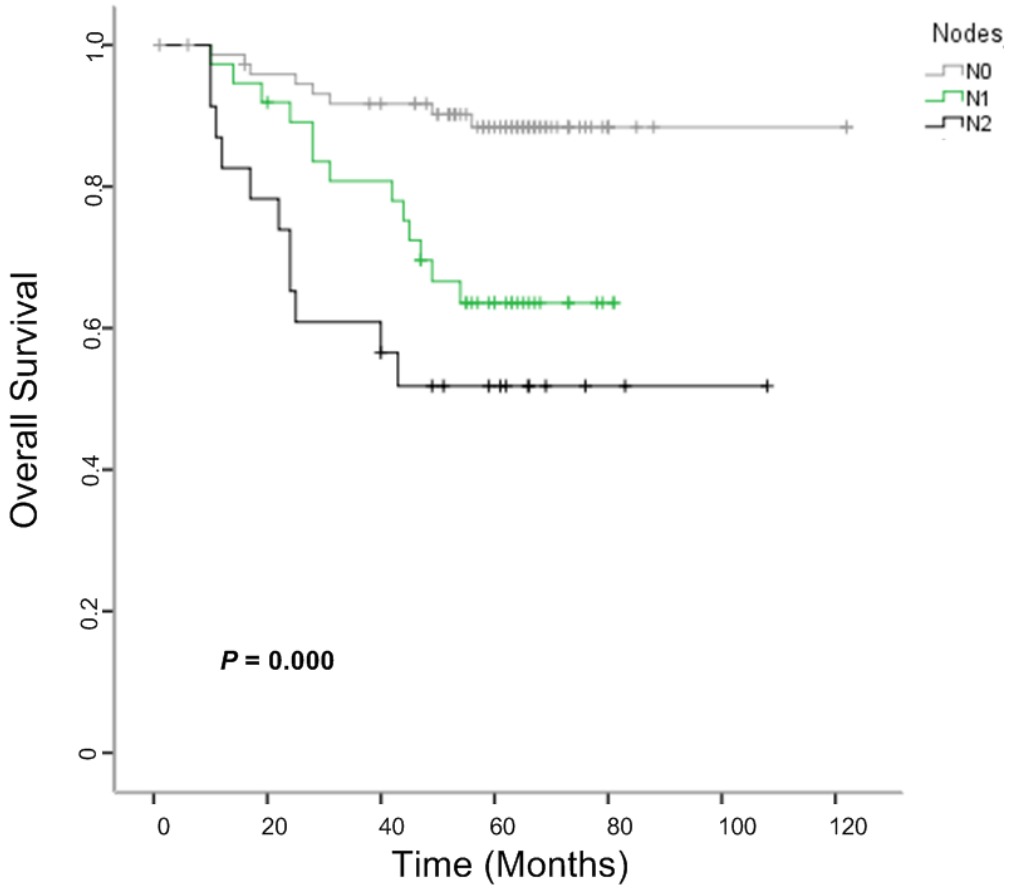

Figure 3.5: N-Stage predicts survival in colorectal cancer. The Kaplan-Meier plot of colorectal cancer specimens (n=135*) demonstrates significantly (log-rank test) lower survival is associated with increasing N-Stages. *2 patients presented with terminal metastatic disease and only had biopsies taken; thus, their N-Stage could not be accurately determined.

3.3.8 The Correlation between M-Stage and Survival

The presence or absence of metastases in patients with CRC correlated significantly (*P* = 0.000) with the overall survival of the patients in our cohort. In cases where there were no metastases present (M0), the patients survived the longest, with 80% of patients without metastases present, surviving 5 or more years after their initial diagnosis. In cases where metastases were present (M1), only 18% of patients survived 5 or more years after their initial diagnosis.

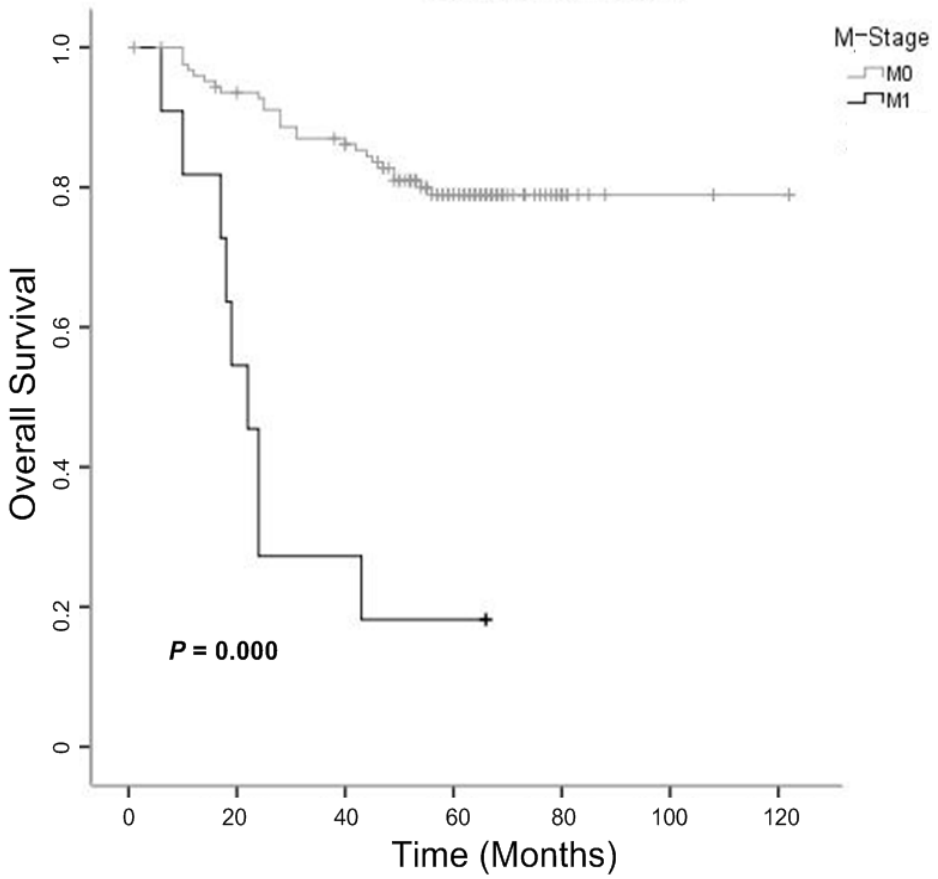

Figure 3.6: M-Stage predicts survival in colorectal cancer. The Kaplan-Meier plot of colorectal cancer specimens (n=137) demonstrates significantly (log-rank test) lower survival is associated with increasing M-Stages.

3.3.9 The Correlation between Differentiation and Survival

The degree to which a cancer cell differs from a normal cell, represented by decreasing stages of differentiation (Well → Moderately → Poorly), correlated significantly (*P* = 0.000) with the overall survival of the patients in our cohort (Figure 3.7). Too few patients had well differentiated tumours (*n* = 3) to obtain reliable results and therefore were excluded from this analysis. The patients who had poorly differentiated tumours had the worst overall survival with 64% of them dying as a result of their disease.

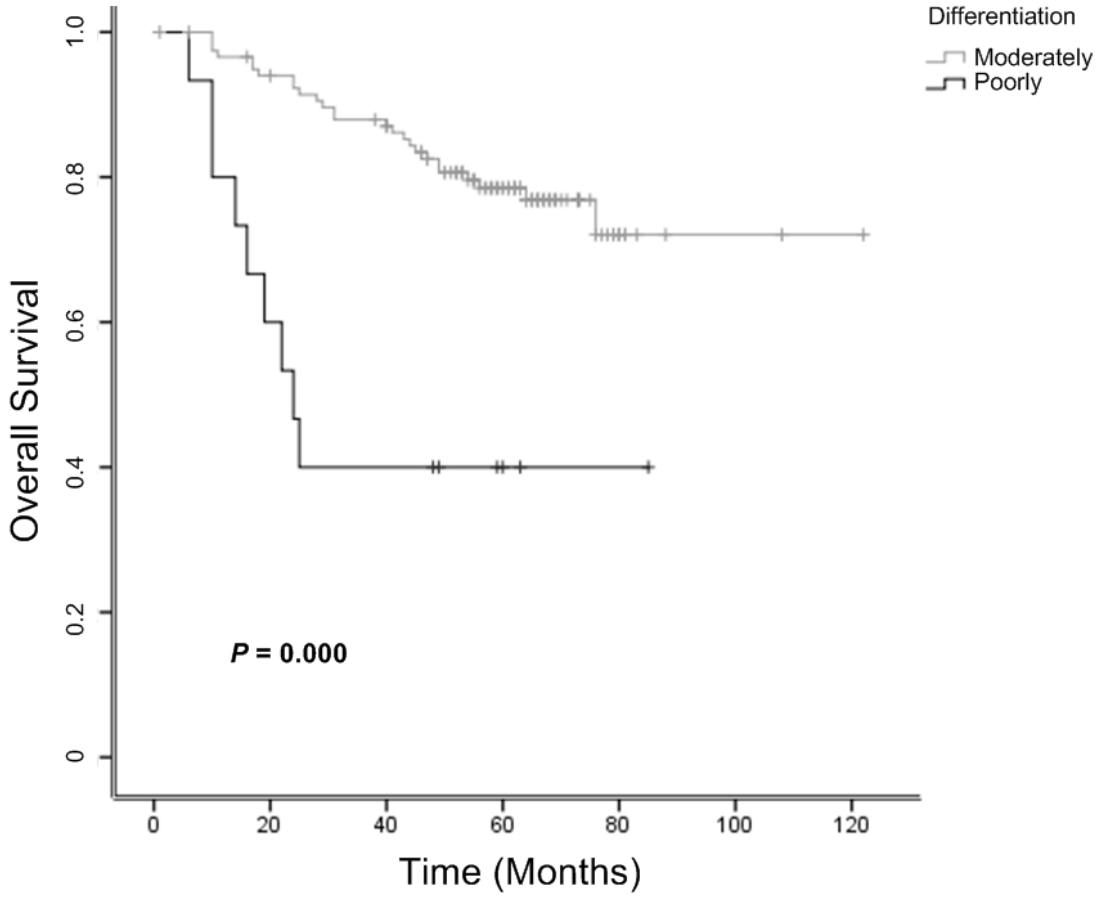

Figure 3.7: Differentiation predicts survival in colorectal cancer. The Kaplan-Meier plot of colorectal cancer specimens (n=137) demonstrates significantly (log-rank test) lower survival is associated with increasing differentiation.

3.3.10 The Correlation Between Age and Survival

Advancing age, represented by patients over/under 75 years of age, correlated significantly (*P* = 0.017) with the overall survival of the patients in our cohort. CRC patients, who were 75 years or older at the time of their diagnosis had a significantly shorter survival than patients who were diagnosed under the age of 75.

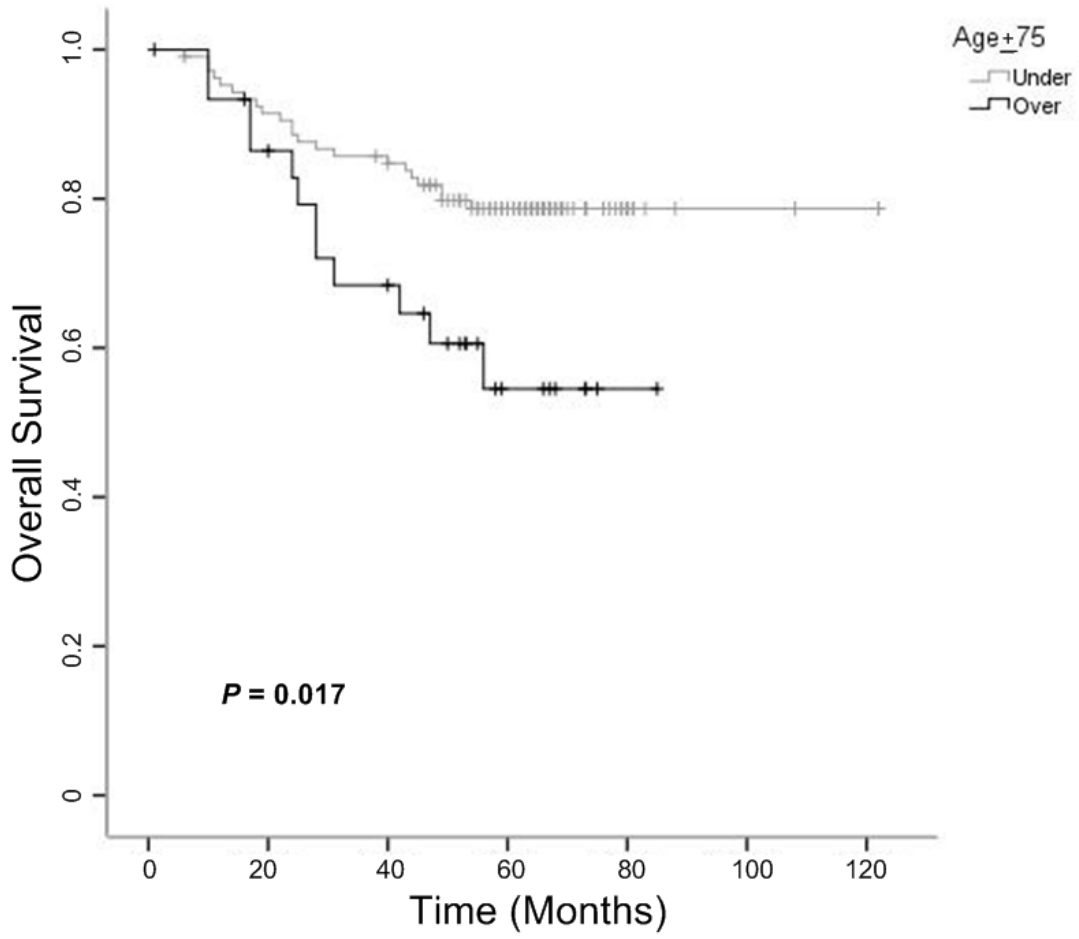

Figure 3.8: Age predicts survival in colorectal cancer. The Kaplan-Meier plot of colorectal cancer specimens (n=137) demonstrates significantly (log-rank test) lower survival is associated with increasing age.

3.4 Discussion

Evaluation of the historical, clinical, pathological and patient outcome data for each patient in the cohort showed a broad distribution of sex, age, Dukes stage, TNM stage, differentiation, disease recurrence, outcome etc. The median age at diagnosis of our IHC and RPPA cohorts was 68 and 67, respectively, and the age range across both cohorts was 34-88, which is in agreement with previous studies (Maughan *et al.*, 2011; Howlader, 2012; Zauber *et al.*, 2012). In general the incidences of colorectal cancer are about 35% to 40% higher in men than women (American Cancer Society, 2011), and this was also true of our cohort as there were 96 men and 62 women included. The reported symptoms and distribution of sites of occurrence in our cohort as depicted graphically in Figs. 3.1 & 3.2, respectively, were also consistent with previous studies (Austoker, 1994; Davies *et al.*, 2005). These results are important because they demonstrate that our cohort is following the same epidemiological patterns of previous cohorts and therefore our findings are comparable.

There was also an even distribution of pathological parameters such as site, TNM-stages, lymphovascular invasion etc. across the cohort, with the exception of differentiation which is generally moderate in CRC adenocarcinomas. These parameters were then used to investigate potential correlations with expression levels of the antigens in the corresponding CRC tissue samples.

In conclusion, the patient cohort constructed in this study provided us with an invaluable resource from which to accurately investigate the expression levels of the cancer specific antigens CerS5 and TRIM28.

Chapter 4

CerS5 and its Role in Colorectal Cancer

4.1 Introduction

CerS5 plays a crucial role in ceramide biosynthesis and is expressed ubiquitously in mammalian tissue in an organ specific distribution pattern (Levy and Futerman, 2010; Mullen *et al.*, 2012). CerS5 was found to be up-regulated on a gene level in CRC patients (Kijanka *et al.*, 2010), and recent studies have shown that reduced gene expression levels of CerS2, CerS4 and CerS6 are associated with tumour grade, lymph node status and cell proliferation in breast cancer (Ruckhaberle *et al.*, 2009a; Schiffmann *et al.*, 2009; Hartmann *et al.*, 2012); while in head and neck tumours, CerS1 has been shown to negatively regulate tumour growth (Koybasi *et al.*, 2004). While most of these studies were based on gene expression analysis and silencing studies of specific CerS enzymes, the expression of the ceramide synthases in cancer tissue has not yet been well characterised. The aim was to investigate the protein expression levels of CerS5 in human CRC tissue and correlate this with clinicopathological data and patient outcome.

An immunohistochemical study of CerS5 in CRC using tissue microarrays generated from a well characterised CRC patient cohort (*n*=102) was performed. Survival analysis was carried out based on CerS5 expression levels in CRC tissue. A TMA with 24 normal mucosa cases from surgical margins and further cohort of 10 normal whole sections from surgical margins were used to assess the CerS5 staining in normal tissue and used for comparison with CRC tissue. The effect of neoadjuvant therapy on patient survival in a subset of neoadjuvantly treated patients (*n*=23) was also investigated. Neoadjuvant therapy generally consisted of both chemotherapy (5-FU) and radiation therapy. CerS5 was further characterised using reverse-phase protein microarrays generated from laser capture microdissection-enriched carcinoma cells, enabling measurements of phosphorylation and total levels of known signalling proteins involved in apoptosis,

autophagy and other cancer related pathways. The quantitative RPPA data was used to design protein networks associated with high and Low CerS5 protein expression levels.

4.2 Results

4.2.1 Antibody Validation

Western blot analysis was carried out in order to determine if the anti-CerS5 antibody was specific. A band was obtained at the expected molecular weight of 57 kDa in both the cell lines (SW480 & SW620), suggesting that the anti-CerS5 antibody was binding specifically to CerS5. There is more CerS5 present in the metastatic SW620 cell line.

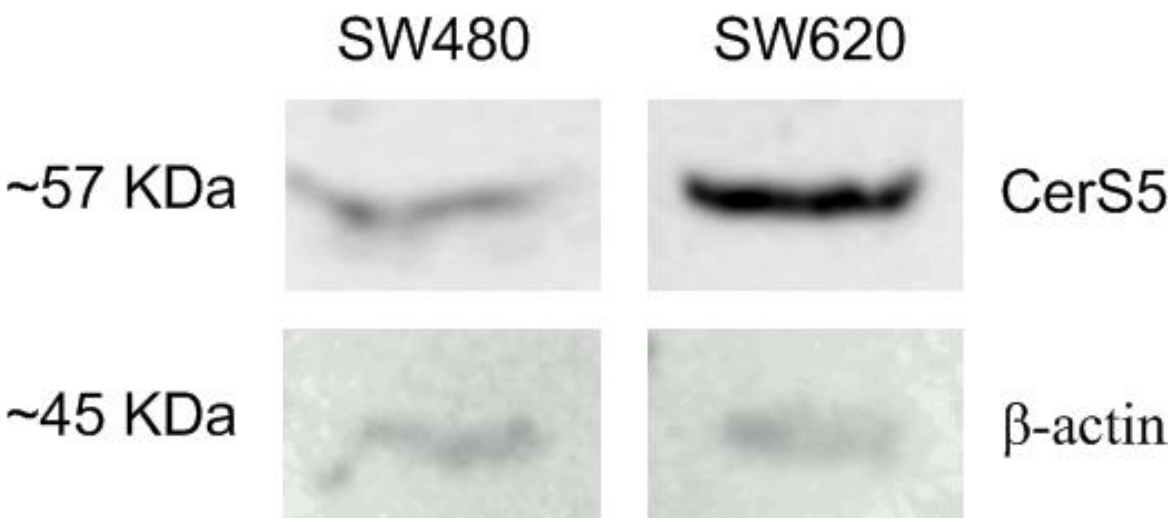

Figure 4.1: Western blot validation of the anti-CerS5 antibody (LS-B3152). Whole-cell lysate was prepared from human colon cancer cell lines SW480 and SW620 and standard Western blot analysis with the anti-CerS5 (LS-B3152) and anti-*β*-Actin antibodies was performed.

4.2.2 CerS5 is expressed in both normal and cancerous colorectal tissue

In previous studies, it was shown that CerS5 is upregulated at a gene level in colorectal cancer (Kijanka *et al.*, 2010). Although CerS5 has been shown to be expressed at low basal levels in most non-cancerous tissues, studies have yet to show protein expression levels of CerS5 in colorectal cancer. The results show distinct membranous CerS5 staining in both the normal mucosa and cancerous tissue (Figs. 4.2 & 4.3). In the 34 cases which had matched normal mucosa and cancerous tissue, high membranous CerS5 staining intensity (2+ & 3+) was found in 55.9% (19/34) of cancerous tissue samples when compared with patient-matched adjacent normal mucosa. In the total IHC cohort, Low CerS5 staining (0 & 1+) was observed in 45.1% (46/102) and High CerS5 staining (2+ & 3+) was observed in 54.9% (56/102) of CRC patient tissue in the IHC cohort. The RPPA cohort was also evaluated by immunohistochemistry with 42.1% (8/19) of CRC patient tissue demonstrating low staining intensity (0 & 1+) and 57.9% (11/19) showing high (2+ & 3+) staining intensity of CerS5.

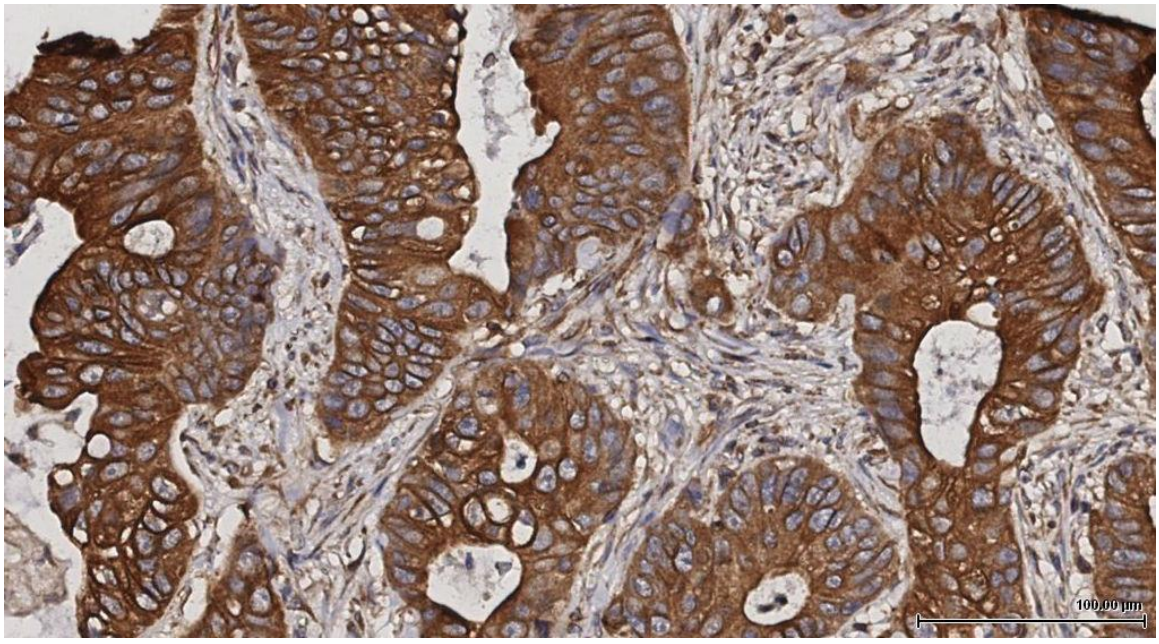

Figure 4.2: Membranous staining for CerS5 in colorectal adenocarcinoma. CerS5 staining was seen in the membrane and in the cytoplasm.

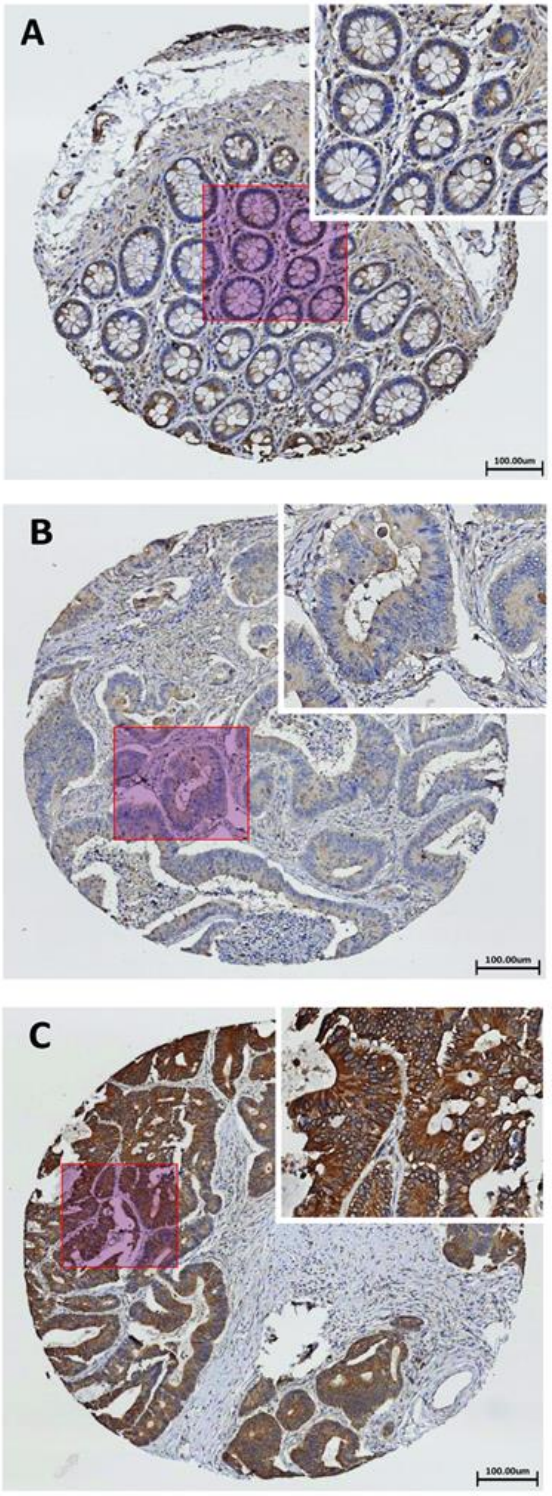

Figure 4.3: IHC staining for CerS5 in colorectal adenocarcinoma and normal colorectal mucosa. (A) Normal colorectal mucosa from tumour-free adjacent surgical margins with negative membranous CerS5 staining. (B) Colorectal cancer tissue with weak membranous CerS5 staining. (C) Colorectal cancer tissue with strong membranous CerS5 staining.

4.2.3 High CerS5 expression in colorectal cancer tissue correlates with poor patient survival

To assess if CerS5 staining intensity correlated with patient survival, the 5-year follow-up data of the 102 non-neoadjuvantly treated cases in the IHC cohort was analysed. Kaplan-Meier analysis showed (Fig. 4.4) that High CerS5 staining in colorectal cancer was found to have a significant negative prognostic value. Overall 5-year survival rates for patients with High CerS5 membranous intensity were significantly lower than those with Low CerS5 membranous intensity (P = 0.001, Fig. 4.4A). Five-year 'recurrence-free' survival was also significantly lower for patients with High CerS5 membranous intensity, when compared with those showing Low CerS5 membranous intensity (P = 0.002, Fig. 4.4B).

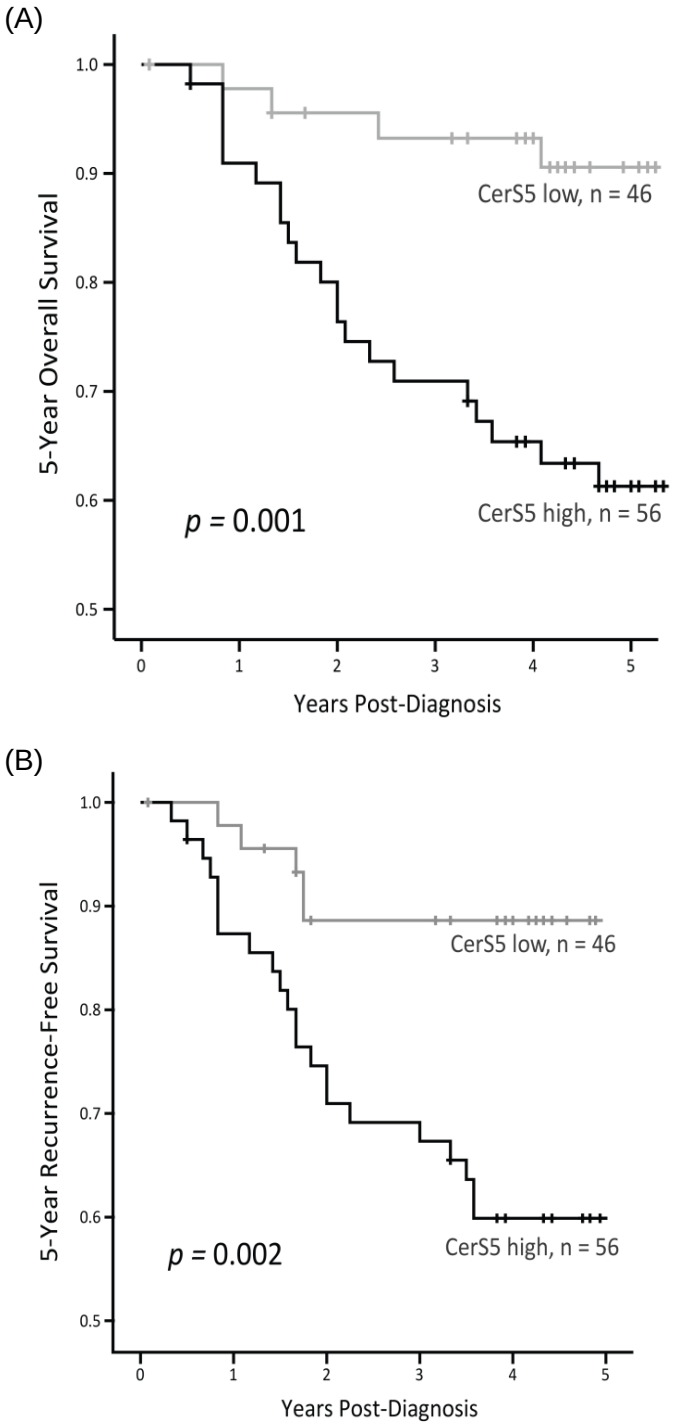

<u>Figure 4.4:</u> High CerS5 expression is associated with poor prognosis in non-neoadjuvantly treated CRC patients. (A) Kaplan-Meier analysis revealed that High CerS5 expression correlates significantly with lower 5-year overall survival (log-rank test, *P* = 0.001) and (B) lower 5-year 'recurrence-free' survival (log-rank test, *P* = 0.002).

4.2.4 CerS5 expression is an independent predictor of survival and disease recurrence

Multivariate analysis showed that the intensity of membranous CerS5 expression was an independent predictor of 5-year overall survival and 5-year 'recurrence-free' survival (*P* = 0.019 & *P* = 0.011, respectively) in CRC patients (Tables 4.1 & 4.2). Membranous CerS5 expression was independent of TNM stage, gender, differentiation and lymphovascular invasion in its ability to predict prognosis. The hazard ratio for 5-year overall survival in CerS5 High patients was 4.7 times higher than in CerS5 Low patients and for 5-year 'recurrence-free' survival the hazard ratio in CerS5 High patients was 4.3 times higher than in CerS5 Low patients.

Table 4.1: Cox uni- and multivariate analysis of relative risk of death from colorectal cancer within 5 years

5-Year Overall Survival								
	Univariate				Multivariate			
Variable	***p* value**	**HR**	**95% CI for HR**		***p* value**	**HR**	**95% CI for HR**	
CerS5 High/Low	0.004	4.855	1.666	14.152	0.019	4.712	1.287	17.250
Gender	0.460	1.373	0.592	3.183	0.939	1.040	0.382	2.829
T-stage	0.000	4.062	1.984	8.317	0.053	2.226	0.989	5.007
N-stage	0.002	2.017	1.284	3.170	0.530	1.259	0.613	2.587
M-stage	0.000	8.140	3.515	18.851	0.464	1.600	0.455	5.620
Differentiation	0.000	4.903	2.037	11.801	0.041	3.165	1.049	9.547
Lymphovascular invasion	0.001	3.612	1.642	7.946	0.381	1.715	0.514	5.721

Table 4.2: Cox uni- and multivariate analysis of relative risk of recurrence of colorectal cancer within 5 years

5-Year Recurrence-Free Survival								
	Univariate				Multivariate			
Variable	***p* value**	**HR**	**95% CI for HR**		***p* value**	**HR**	**95% CI for HR**	
CerS5 High/Low	0.005	4.047	1.532	10.690	0.011	4.322	1.407	13.280
Gender	0.551	1.275	0.573	2.840	0.870	1.079	0.434	2.681
T-stage	0.002	2.809	1.455	5.424	0.131	1.721	0.851	3.479
N-stage	0.004	2.883	1.221	2.903	0.677	1.152	0.591	2.246
M-stage	-	*N/A	-	-	-	*N/A	-	-
Differentiation	0.002	3.920	1.667	9.224	0.046	2.667	1.018	6.987
Lymphovascular invasion	0.001	3.455	1.621	7.362	0.132	2.359	0.773	7.194

Abbreviations: HR = Hazard Ratio; CI = confidence interval; T = tumour; N = node; M = metastasis; *5-year Recurrence-Free Survival analysis not applicable for patients with metastatic disease.

4.2.5 Unsupervised hierarchical clustering analysis identifies two distinct groups of patients

On the basis of the results thus far, the aim was to understand the underlying molecular interplay associated with the significant effects of CerS5 expression levels on patient outcomes. The RPPA cohort was applied to investigate protein networks associated with sphingolipid metabolism, apoptosis, autophagy and other cancer related pathways in CerS5 High and Low tumours. 30 antibody substrates were quantified in the RPPA patient cohort for proteomic analysis. Unsupervised hierarchical clustering analysis of RPPA signalling endpoint-measurements identified two distinct clusters as represented by a heat map in Fig. 4.5. These two clusters support the results seen by immunohistochemical analyses; the first cluster (red) on the dendrogram is composed mainly of CerS5 High patients (9 cases) and with three CerS5 Low patients. The second cluster on the dendrogram (green) contains mainly CerS5 Low patients (5 cases) and with 2 CerS5 High cases.

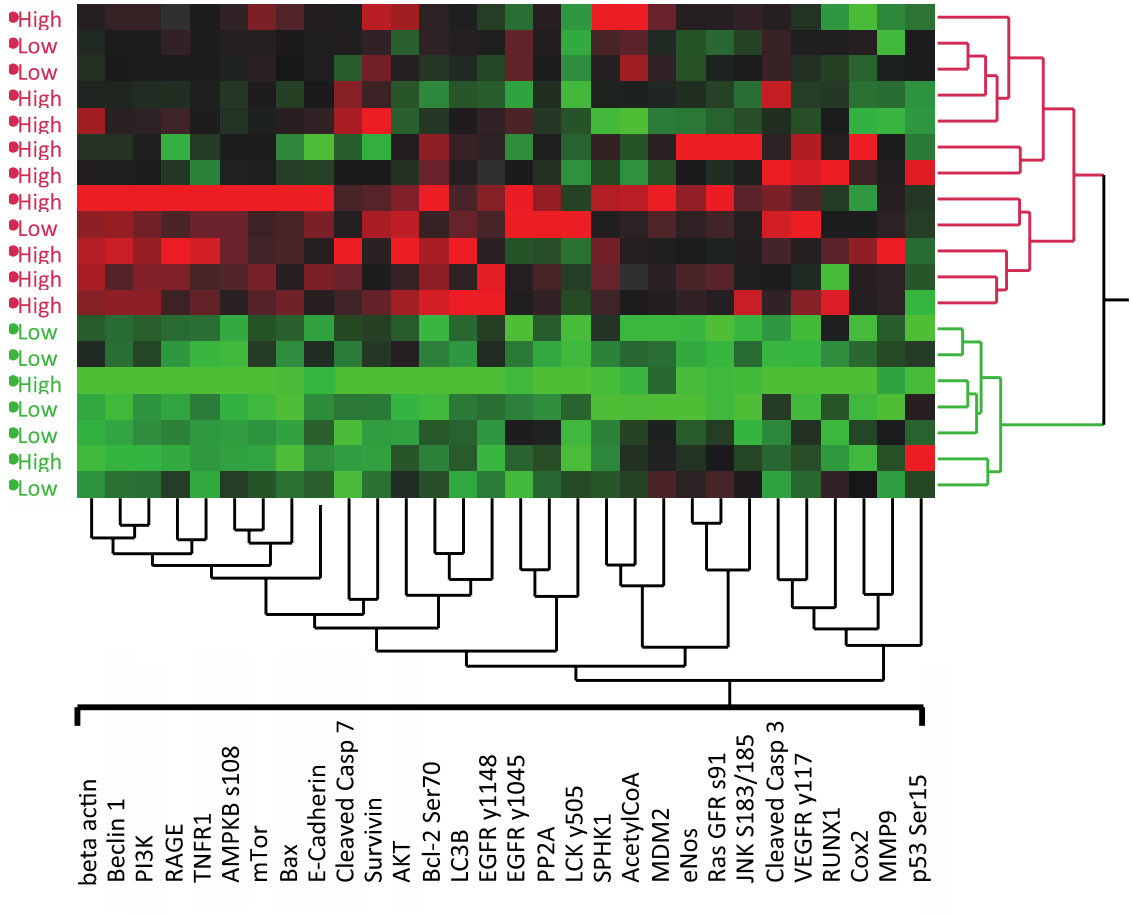

Figure 4.5: Unsupervised hierarchical cluster analysis in 19 CRC patients based on RPPA measurements of 30 endpoints. Patients (CerS5 High and CerS5 Low) are shown on the vertical axis, 30 endpoints are outlined on the horizontal axis. Higher relative levels of signal are represented in red; intermediate in black and lower levels are in green. The analysis identifies two groups of patients; the first cluster (red) is mainly composed of CerS5 High patients, whereas the second cluster contains mainly CerS5 Low patients.

4.2.6 CerS5 High and CerS5 Low proteomic networks differ in colorectal cancer

Spearman ρ rank correlation analysis was used to determine significant protein interactions identified by RPPA measurements. The analysis of 30 signalling endpoints revealed that 49 of 435 protein pairs were positively and significantly correlated ($\rho > 0.75$, $P \leq 0.01$) in both CerS5 High and Low patients (Appendix; Supplementary Table 2 & 3). Sixty three positive significant correlations were found exclusively in the CerS5 Low group (Fig. 4.6A, Appendix; Supplementary Table 2), whereas 54 protein pairs showed a significant Spearman ρ value exclusively in the CerS5 High group (Fig. 4.6B, Appendix; Supplementary Table 3). No significant RPPA protein interactions that correlated negatively were observed. The protein interaction network of colorectal cancer specimens associated with a CerS5 High IHC staining intensity was distinctly different from the CerS5 Low network (Fig. 4.6).

4.2.7 CerS5 Low proteomic network is associated with apoptosis

The CerS5 Low proteomic network constructed from the Spearman ρ rank correlation analysis revealed four main sub-networks (Fig. 4.6A, Appendix; Supplementary Table 2). The sub-networks were defined by proteins strongly correlated with and in close proximity to each other and these were represented by the same colour in the network. The four main CerS5 Low sub-networks were dominated by proteins linked to apoptosis, including PP2A, survivin and the cleaved caspases 3 and 7. These dominant nodes radiated outward to interconnect with other cancer-associated molecules within their respective sub-networks. These results provide evidence for the activation of the ceramide driven apoptotic pathways in CerS5 Low tumours, potentially resulting in better outcomes seen in colorectal cancer patients with weak membranous CerS5 staining.

4.2.8 CerS5 High proteomic network is associated with autophagy

The CerS5 High proteomic network was composed of 3 main sub-networks as shown (Fig. 4.6B, Appendix; Supplementary Table 3). When the CerS5 High and CerS5 Low proteomic networks were compared, it was found that the CerS5 High network is not dominated by proteins associated with apoptosis, as seen in the CerS5 Low network. However, in CerS5 High patients, one sub-network mostly composed of proteins linked to autophagy was identified (Fig. 4.6B light blue). The autophagy sub-network is composed of the initiators of autophagy beclin-1 and JNK and the autophagy regulators Akt, AMPK and LC3B. Interestingly, the autophagy sub-network is linked through mTOR, to the sphingolipid metabolism proteins PP2A and SPHK1, both associated with autophagy through mTOR pathway activation (Taniguchi *et al.*, 2012). Taken together these results suggest a dysregulation of the ceramide-driven apoptotic pathways and activation of autophagy in CerS5 High patients, which may account for the correlation of strong CerS5 expression and poor survival.

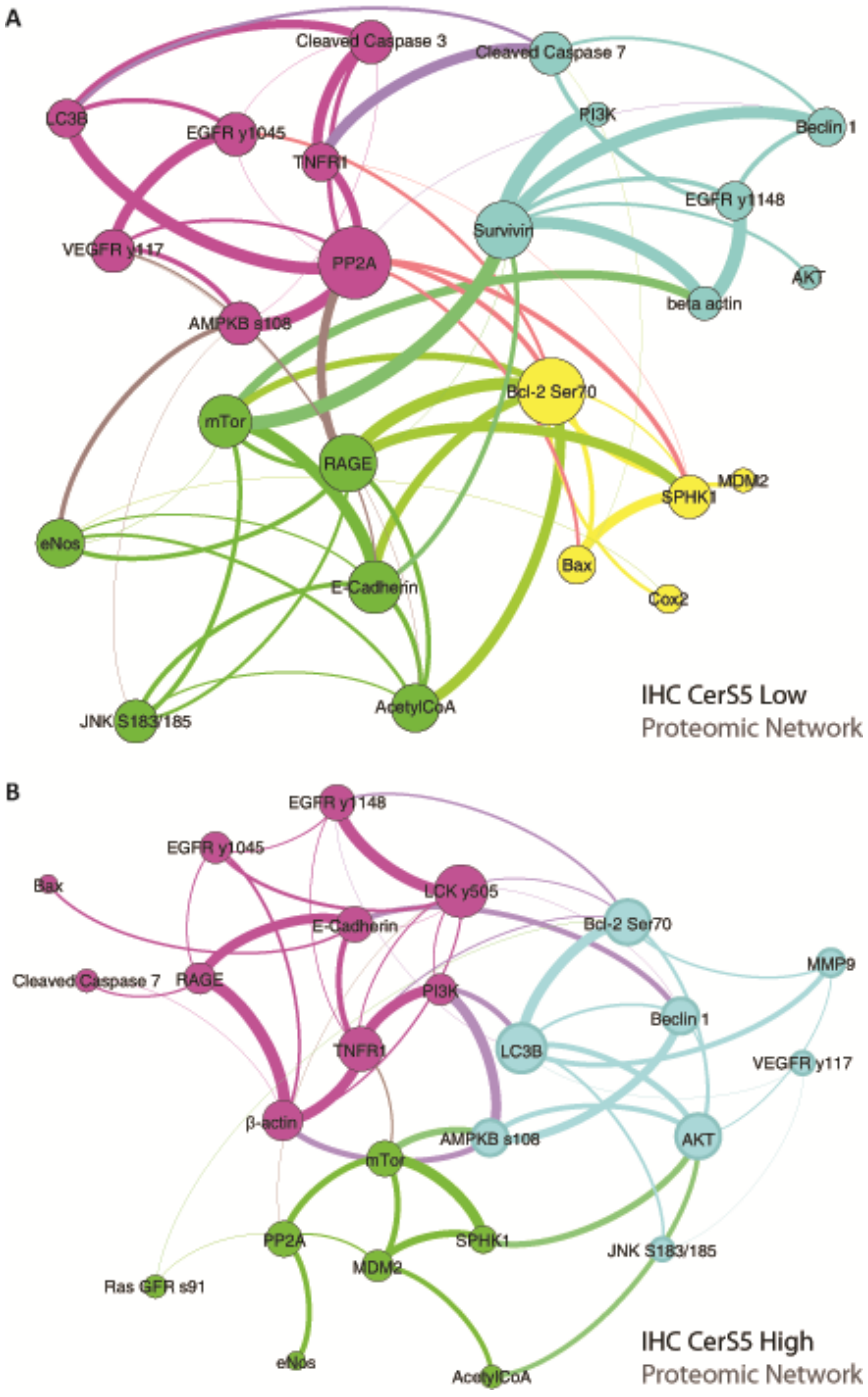

<u>Figure 4.6:</u> RPPA analysis identifies distinct proteomic networks in CerS5 High and low CRC patients. (**A**) CerS5 Low proteomic network consists of four main sub-networks dominated by proteins linked to apoptosis; including PP2A, survivin and the cleaved caspases 3 and 7. (**B**) CerS5 High proteomic network consists of three sub-networks with one sub-network mainly composed of proteins linked to the autophagy (blue); including the initiators of autophagy beclin-1 and JNK and the autophagy regulators Akt, AMPK, and LC3B**.**

4.2.9 CerS5 expression levels appear to have opposing prognostic values in Neoadjuvant treated patients

Tissue samples from a small number of neoadjuvantly treated patients (*n* = 23) had been incorporated onto the TMAs and these were used to investigate the prognostic significance of CerS5 expression levels in these patients. It was found that the 5-year overall-survival and 5-year 'recurrence-free' survival for neoadjuvantly treated patients with High CerS5 membranous intensity was better than the neoadjuvantly treated patients with Low CerS5 membranous intensity, (Fig. 4.7, *P* = 0.089 & *P* = 0.201). This was the opposite of what had been seen previously in the non-neoadjuvantly treated patients.

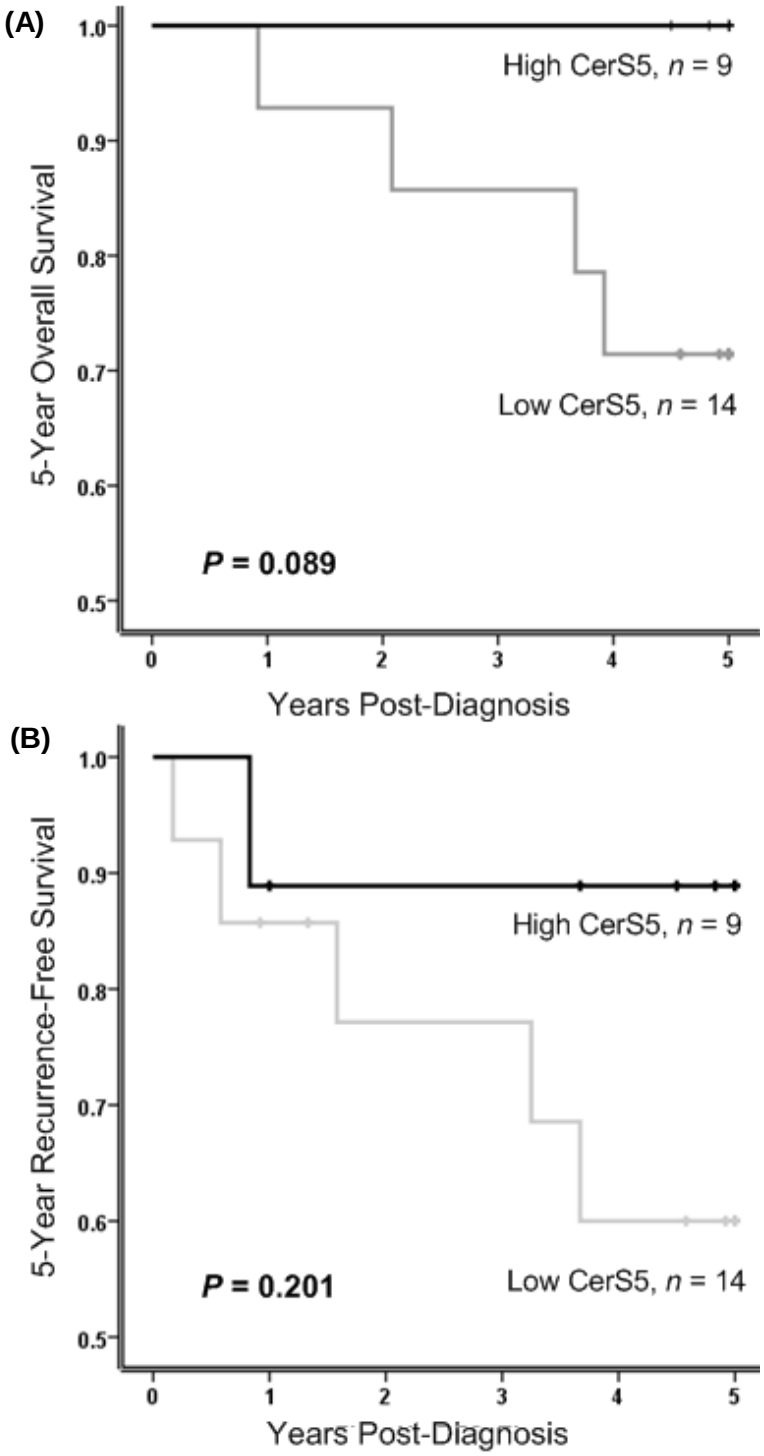

Figure 4.7: CerS5 expression levels have different prognostic values in Neoadjuvant treated patients. In neoadjuvantly treated colorectal cancer patients, High CerS5 expression is indicative of; (A) better 5-year overall survival (*P* = 0.089) and (B) better 5-year 'recurrence-free' survival (*P* = 0.201).

4.2.10 CerS5 expression levels are predictive of response to Neoadjuvant therapy

The survival of the neoadjuvantly treated CerS5 High patients was then compared with the non-neoadjuvantly treated CerS5 High patients and found that the neoadjuvantly treated CerS5 High patients had a significantly better 5-year overall survival, (Fig. 4.8A, *P* = 0.037). The survival of CerS5 Low patients with and without neo-adjuvant treatment was also compared and it was found that the neoadjuvantly treated CerS5 Low patients had a significantly poorer 5-year 'recurrence-free' survival when compared with the non-neoadjuvantly treated CerS5 Low patients, (Fig. 4.8D, *P* = 0.017). Neo-adjuvant therapy has a significant positive influence on survival in CerS5 High patients and has a significant negative influence on 'recurrence-free' survival in CerS5 Low patients.

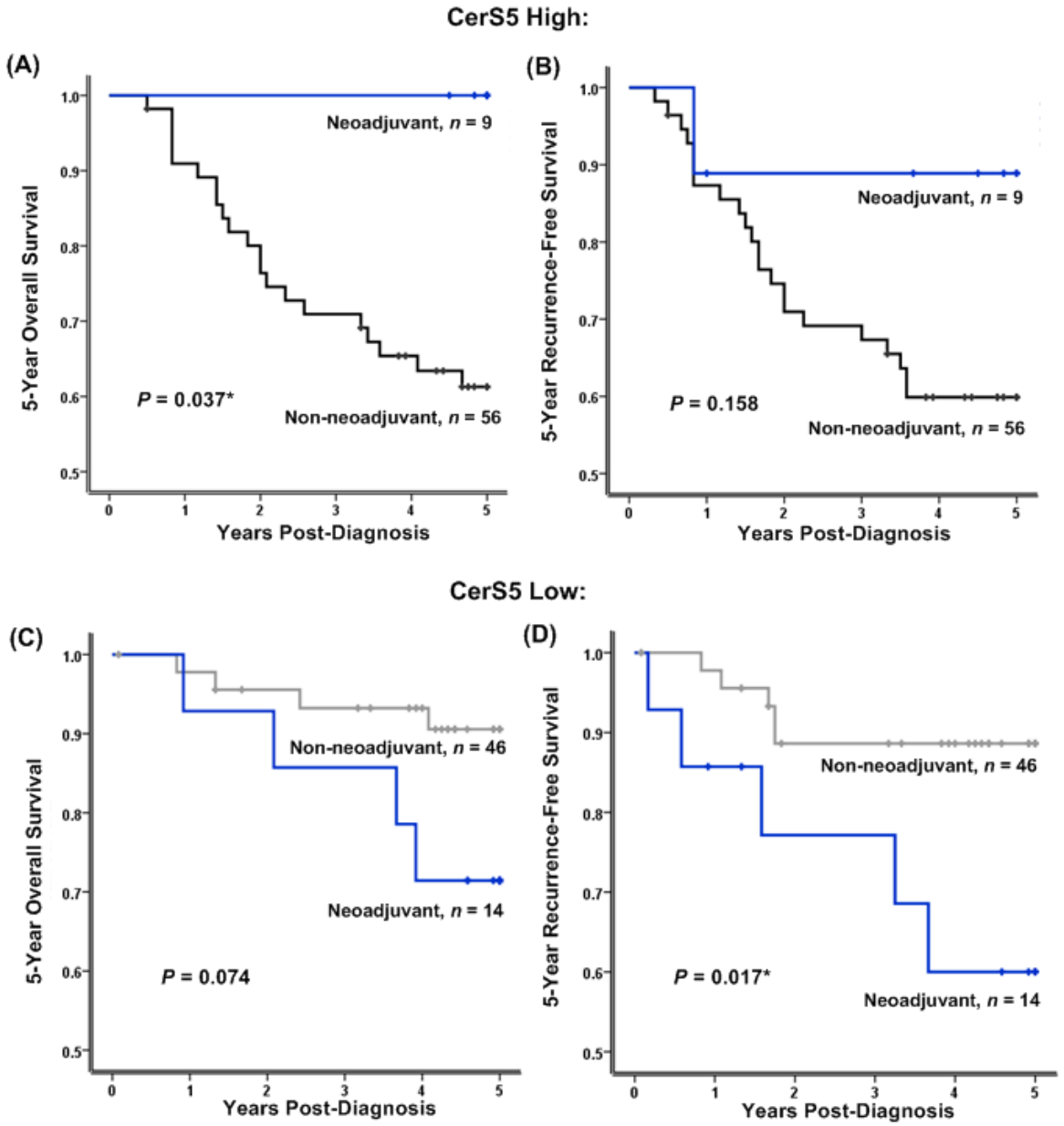

Figure 4.8: CerS5 expression levels are predictive of response to therapy. (A&B): In CerS5 High patients only, neoadjuvant treated patients had; (A) significantly better 5-year overall survival (*P* = 0.037*) and (B) better 5-year 'recurrence-free' survival (*P* = 0.158), compared with non-neoadjuvantly treated patients. (C&D): In CerS5 Low patients only, neoadjuvant treated patients had; (C) poorer 5-year overall survival (*P* = 0.074) and (D) significantly poorer 5-year 'recurrence-free' survival (*P* = 0.017*) compared with non-neoadjuvantly treated patients.

4.2.11 Potential of RPPA technology to stratify patients based on antigen expression levels

Up until now we have used IHC to stratify the patients in our cohort into CerS5 High or Low groups. However, RPPA is a viable alternative to IHC for rapid experimental screening and validation of candidate biomarkers in tissue samples. Robust quantification is achieved through having serial dilutions of each tissue sample. To investigate the potential of RPPA to stratify patients based on the level of expression of a biomarker, we calculated the median CerS5 RPPA intensity value from our RPPA cohort of 18 patients. We assigned with an RPPA intensity score on or above the median as being RPPA CerS5 High (n=10) and with an RPPA intensity score below the median as RPPA CerS5 Low (n=8).

Unsupervised hierarchical clustering analysis identified three distinct clusters as represented by a heat map in Figure 4.9. The first cluster (red) on the dendrogram is composed of RPPA CerS5 High patients only (5 cases). The second cluster on the dendrogram (green) is composed mainly of RPPA CerS5 High patients (5) and only 2 RPPA CerS5 Low patients. The third cluster (blue) contains only RPPA CerS5 Low patients (6 cases).

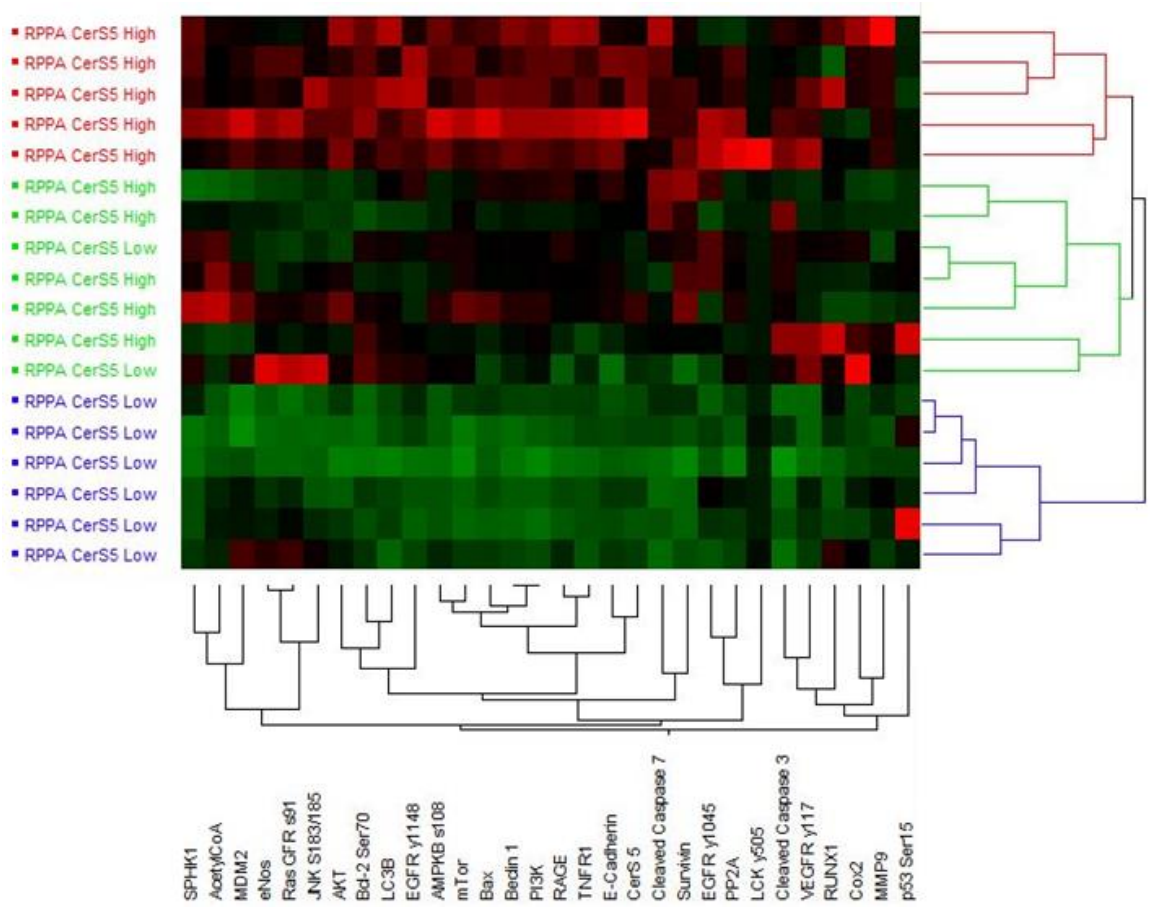

<u>Figure 4.9:</u> Unsupervised hierarchical cluster analysis in 18 CRC patients based on RPPA measurements of 30 endpoints. Patients (RPPA CerS5 High and CerS5 Low) are shown on the vertical axis, 30 endpoints are outlined on the horizontal axis. Higher relative levels of signal are represented in red; intermediate in black and lower levels are in green. The analysis identifies three groups of patients; the first cluster (red) is composed only of CerS5 High patients, the second cluster (green) is also mainly composed of CerS5 High patients, whereas the third cluster contains only CerS5 Low patients.

4.2.12 Unsupervised hierarchical clustering analysis of patients based on sphingolipid signalling

To investigate what effect the differing expression levels of CerS5 was having on the other members of the sphingolipid metabolic pathway, the RPPA cohort was again applied. The relative expression levels of ceramide, as well as the other Ceramide Synthases (CerS 1, 2, 3, 6), Acid Ceramidase, Sphinosine-1-kinase, Sphingosine-1-phosphate phosphatase were probed. The CerS4 antibody did not work on the RPPAs and so was excluded from this study. Unsupervised hierarchical clustering analysis identified three distinct clusters as represented by a heat map in Figure 4.10. The first cluster (red) on the dendrogram is composed mainly of CerS5 High patients (5 cases), with only 1 CerS5 Low patient. The second cluster on the dendrogram (blue) has 5 CerS5 High patients and 2 CerS5 Low patients. The third cluster (green) contains mainly CerS5 Low patients (4 cases) and 2 CerS5 High cases. However, not all of the antibodies (CerS 6, Acid Ceramidase, Sphingosine-1-phosphatase) have been validated using Western blot analysis and, therefore, no definitive conclusions can been drawn until the antibody validation is complete.

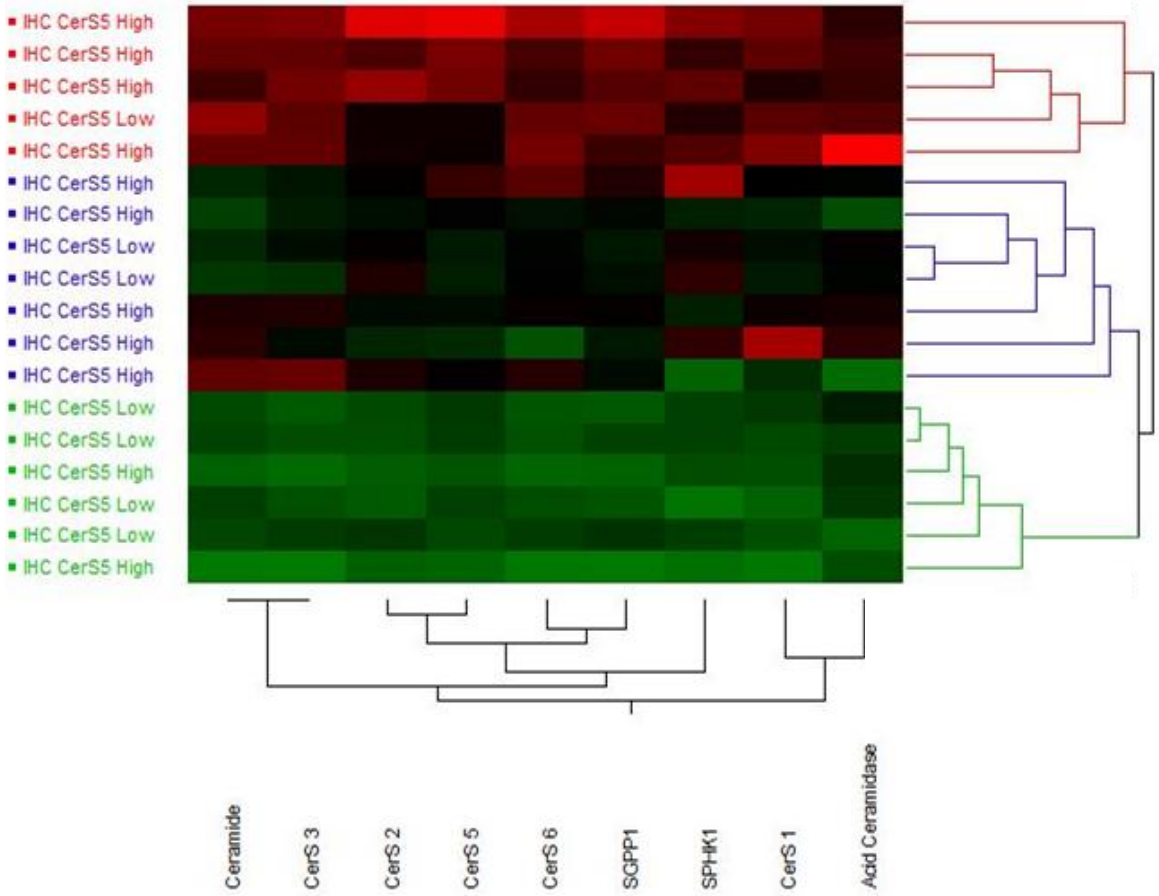

Figure 4.10: Unsupervised hierarchical cluster analysis in 18 CRC patients based on RPPA measurements of 9 endpoints. Patients (CerS5 High and CerS5 Low) are shown on the vertical axis. Nine endpoints are outlined on the horizontal axis. Higher relative levels of signal are represented in red, intermediate in black and lower levels are in green. The analysis identified three groups of patients: the first cluster (red) is primarily composed of CerS5 High patients (4 CerS5 High and 1 CerS5 Low patients), the second cluster (blue) is also predominantly composed of CerS5 High patients (5 CerS5 High and 2 CerS5 Low patients), whereas the third cluster contains mainly CerS5 Low patients (4 CerS5 Low and 2 CerS5 High patients).

4.2.13 CerS5 High and CerS5 Low proteomic networks differ in colorectal cancer

Spearman ρ rank correlation analysis was again used to determine significant protein interactions between members of the sphingolipid metabolic pathway identified by RPPA measurements. The analysis of 9 signalling endpoints revealed that 19 of 36 protein pairs were positively and significantly correlated ($\rho > 0.75$, $P \leq 0.01$) in CerS5 High patients and 21 positive significant correlations were found in the CerS5 Low group (Fig. 4.11). No significant RPPA protein interactions that correlated negatively were observed. The protein interaction network of colorectal cancer specimens associated with a CerS5 High IHC staining intensity was distinctly different from the CerS5 Low network (Fig. 4.11).

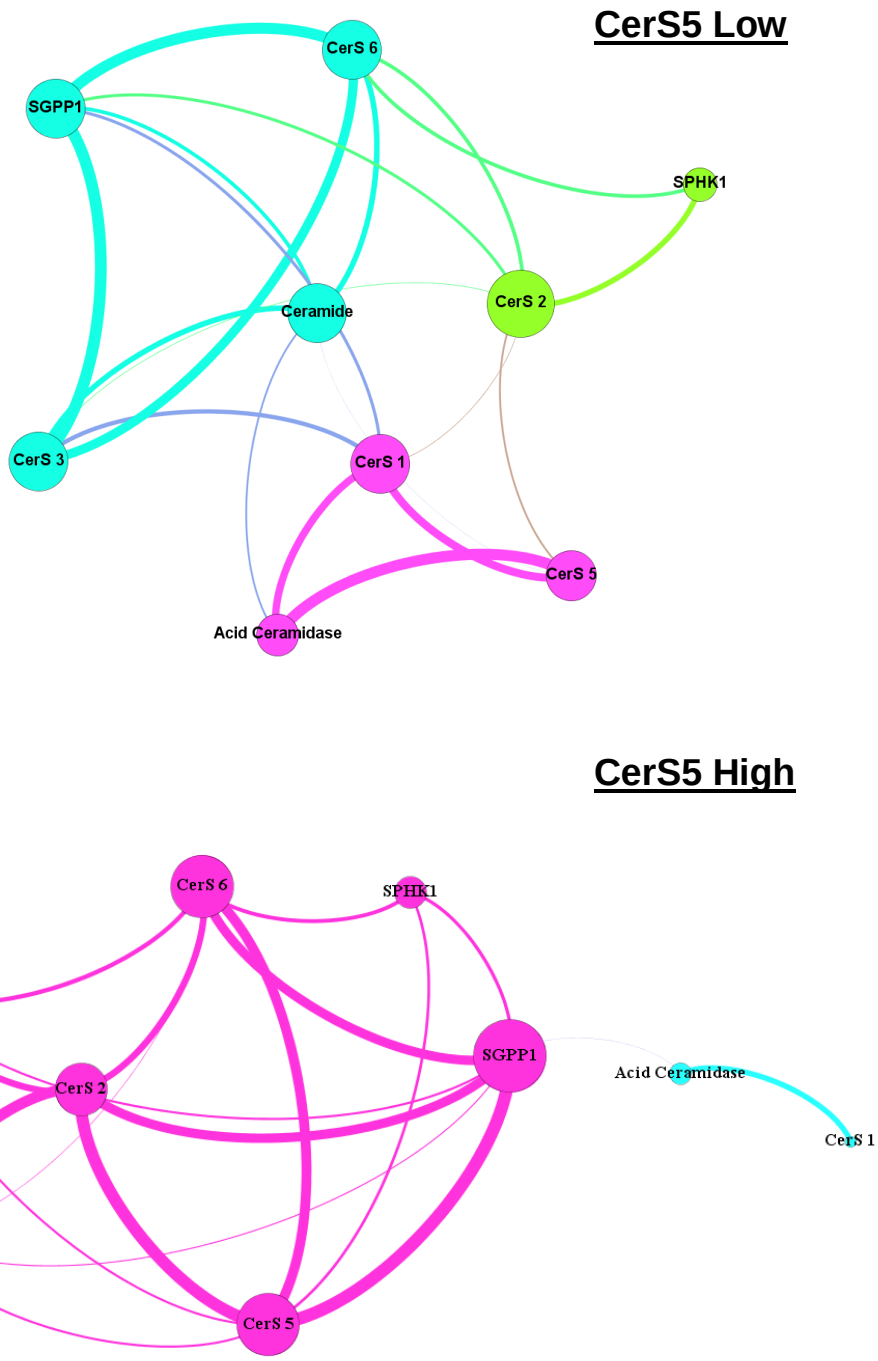

Figure 4.11: RPPA analysis identifies distinct proteomic networks in CerS5 High and Low CRC patients. (A) CerS5 Low proteomic network consists of two main inter-connected sub-networks. (B) CerS5 High proteomic network consists of one dominant network and a separate minor sub-network.

4.3 DISCUSSION

The results indicate that strong membranous CerS5 staining correlates with poor prognosis in patients with CRC. A favourable prognosis was observed in CRC patients with negative or weak CerS5 staining, which was also found in the majority of normal colorectal mucosae. CerS5 staining intensity was also found to be independent of disease stage in its ability to predict prognosis. This data suggests that elevated CerS5 expression is associated with increased tumour aggressiveness, which may be regulated by altered levels of bioactive ceramides, though the mechanisms involved have yet to be elucidated. Interestingly, altered expression levels of CerS5 in colon cancer may distort the balance of ceramides, thereby contributing to tumour progression (Hartmann *et al.*, 2012). Proteomic network analysis in this study demonstrates a shift from apoptosis-related pathways in CerS5 Low cases to autophagy in CerS5 High cases, suggesting a causative link between poor survival in CerS High cases and a dysregulation of programmed cell-death pathways. Finally, it was shown that CerS5 expression levels are predictive of response to neoadjuvant therapy.

CerS5 was previously identified as a marker in CRC and showed that it is upregulated at a gene level (Kijanka *et al.*, 2010). Other studies have shown CerS5 expression at low basal levels in non-cancerous tissues (Levy and Futerman, 2010; Mullen *et al.*, 2012). However, there is a paucity of literature on protein expression of CerS5 in cancer tissue. It was shown that down-regulation of the CerS2 gene in breast cancer is associated with poor patient outcomes (Fan *et al.*, 2013). In addition, the overexpression of specific enzymes of sphingolipid metabolism has been shown to have both a negative prognostic value (ceramide kinase) and a positive prognostic value (galactosyl ceramide synthase, ganglioside GD3 synthase) in breast cancer (Ruckhaberle *et al.*, 2009b). In the current study, elevated protein levels of CerS5 in CRC tissue were confirmed using immunohistochemistry with CerS5 overexpression shown to correlate with poor

prognosis in patients with CRC and this was found to be a stage-independent predictor of prognosis. This suggests that elevated CerS5 expression is associated with increased tumour aggressiveness and therefore, CerS5 could be used as a novel prognostic biomarker in CRC.

Ceramides are generally assumed to be pro-apoptotic (Bose *et al.*, 1995; Veret *et al.*, 2011); and as such, one would expect that increased CerS would lead to increased ceramides in tumour tissue with resultant cell death. However, the data presented in this study suggests that strong membranous CerS5 staining in CRC tissue is associated with tumour progression. Recent studies support our findings demonstrating that elevated levels of ceramides increase tumour growth in SCID mice, and that silencing rather than overexpression of the CerS6 gene can lead to apoptosis in cancer cell lines (Senkal *et al.*, 2010; Senkal *et al.*, 2011). Furthermore, Hartmann *et al*. demonstrated that overexpression of CerS2, despite having no direct impact on ceramide levels, leads to increased cell proliferation in breast and colon cancer cell lines (Hartmann *et al.*, 2012). These studies, in conjunction with our findings, suggest that although apoptosis is a recognised feature of ceramides, specific ceramide synthase expression levels and ceramide fatty acid chain lengths in different tissues may provide alternative survival modes in cancer.

The proteomic data presented in this study offer some insights into the tumour suppressive and tumour promoting effects of CerS5 in CRC. Analysis of the RPPA results revealed two distinct signalling networks for CerS5; a CerS5 Low proteomic network associated with apoptosis and a CerS5 High proteomic network associated with autophagy. The apoptotic pathway which emerged from our CerS5 Low network included apoptosis-related proteins such as PP2A, Survivin and Caspases 3 and 7. Veret *et al*. recently showed that overexpression of CerS4 in pancreatic β-cell-induced

apoptosis and was associated with increased caspase 3 and 7 activities through *de novo* synthesis of C18:0 ceramide species (Veret *et al.*, 2011). By contrast, another study showed that down-regulation of CerS6 in SCID mice was linked to caspase 3 activation and subsequent apoptosis (Senkal *et al.*, 2011). In our CerS5 High proteomic network, LC3B, Beclin-1 and JNK were identified as key signalling molecules for autophagy, a phagolysosome process whereby damaged proteins and organelles are removed to prevent cell damage and intracellular molecules are sequestered for cell survival (Maes *et al.*, 2013). Espina *et al.* have recently shown that autophagy is required to promote abnormal breast cancer progenitor cells into invasive breast cancer by providing necessary survival mechanisms under stress (Espina *et al.*, 2010). Another study in pancreatic cancer showed that autophagy was required for tumour growth (Yang *et al.*, 2011). LC3B dominates a central node in our CerS5 High network and has been previously been shown to induce mitochondrial autophagy in human cancer cells by directly binding to ceramides (Sentelle *et al.*, 2012). Although CerS5 has not been linked to autophagy in cancer, a model of diabetic cardiomyopathy showed that CerS5 promoted cardiac autophagy through de novo synthesis of C14-ceramide (Russo *et al.*, 2012). Furthermore, cardiac autophagy required CerS5 for sphingolipid-mediated induction of Beclin 1 protein and overexpression of LC3B, both of which dominate central nodes in our CerS5 High proteomic network.

Although two distinct signalling networks associated with apoptosis and autophagy are identified, there are also dominant nodes common to both networks such as Bcl-2 and Sphingosine Kinase 1 (SPHK1). This may be explained by the fact that apoptosis and autophagy are intimately linked through common signalling pathways. Binding of Bcl-2 to phosphorylated Beclin1 induces autophagy while cleavage of Beclin1 by effector caspases is pro-apoptotic (Delgado *et al.*, 2014). SPHK1, a central enzyme in sphingolipid metabolism, activates anti-apoptotic signal transduction in a model of

Kaposi's sarcoma in SCID mice (Qin *et al.*, 2014); while other studies have shown that overexpression of SPHK1 stimulates autophagy in breast cancer cells by increasing the formation of LC3B-positive autophagosomes (Lavieu *et al.*, 2006).

Cancer is ultimately the uncontrolled growth of cells coupled with malignant behaviour, such as invasion and metastasis. The BCL2 family of proteins and bioactive sphingolipids are intricately linked during apoptotic cell death with many chemotherapeutic drugs known to cause accumulation of the pro-apoptotic sphingolipid ceramide (Beverly *et al.*, 2013). A recent study, has demonstrated that treatment with ABT-263, a potent inhibitor of three anti-apoptotic BCL2-like proteins; BCL2, BCLxL and BCLw (Mérino *et al.*, 2012), induces the generation of C16-ceramide in multiple cell lines. They also present a feed-forward model by which activation of CerS by chemotherapeutic drugs leads to elevated ceramide levels that result in synergistic channel formation by ceramide (or one of its metabolites) and BAX/BAK, (Beverly *et al.*, 2013). In support of this it was found that non-neoadjuvantly treated CerS5 High CRC patients had poorer overall survival and rates of recurrence, suggesting that, in the cancer cells, pro-survival signals outweighed the pro-apoptotic signals. Conversely, patients with High CerS5 after neoadjuvant treatment had better overall survival and rates of recurrence, suggesting that neoadjuvant therapy stimulates the apoptotic pathway and ceramide-driven apoptosis is restored (Figure 4.12). In the CerS5 Low cohort, non-neoadjuvantly treated patients had good 5-year overall survival and rates of recurrence, suggesting that the pro-apoptotic cell signals outweighed the pro-survival signals and tissue homeostasis is working correctly. However, patients with Low CerS5 after neoadjuvant treatment had significantly higher rates of recurrence, suggesting that neoadjuvant therapy has an overall negative effect on these patients. In non-neoadjuvantly treated CerS5 Low patients, the levels of the pro-apoptotic ceramide and Sphingosine and the pro-survival Sphingosine-1-phosphate seem to be balanced,

replicating normal tissue homeostasis (Sliva *et al.*, 2000). However, when these patients receive possibly unnecessary chemotherapy treatment, the balance between pro-apoptotic and pro-survival signals is disturbed potentially accounting for the poorer survival and 'recurrence-free' survival seen in the neoadjuvant-treated patients. These results suggest that CerS5 membranous intensity could potentially identify CRC patients that would benefit from neoadjuvant therapy (CerS5 High) and patients that neoadjuvant therapy would have a negative effect on their survival (CerS5 Low). This would need to be evaluated further in a larger patient cohort to confirm these findings.

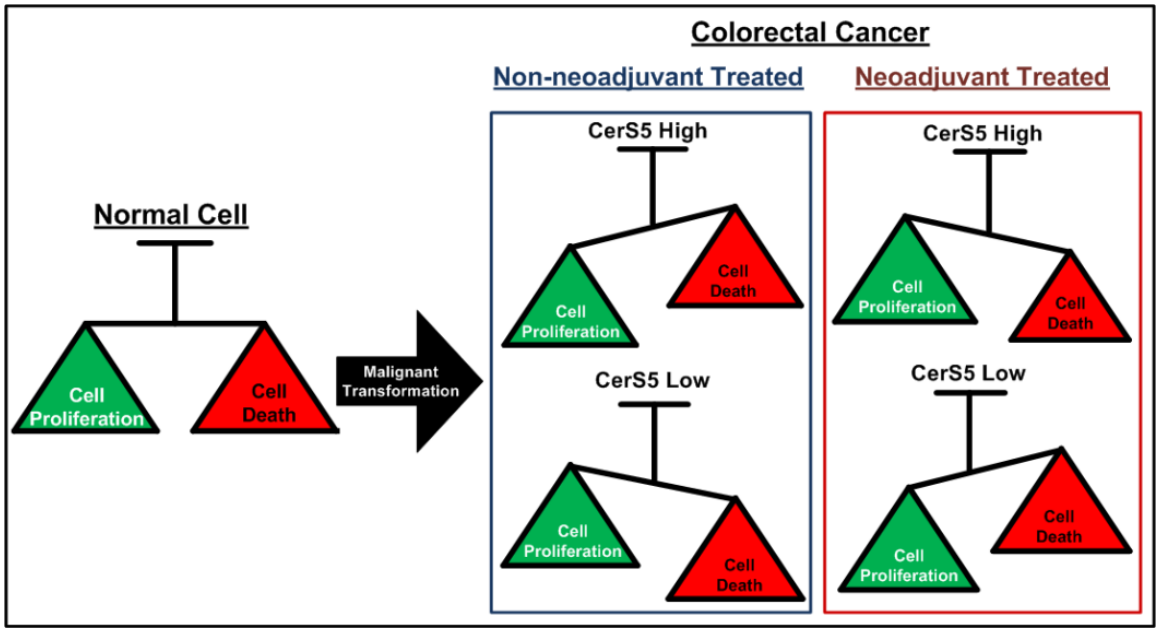

Figure 4.12: Neoadjuvant therapy reverses cell survival in CerS5 High and Low patients. Under normal circumstances, tissue homeostasis is a perfectly choreographed process balancing pro-survival and death signals. When shifted in favour of proliferative signals, the imbalance leads to deregulated cell growth that contributes to malignancy, as happens in colorectal cancer. Non-neoadjuvantly treated CerS5 High CRC patients had poor overall survival and rates of recurrence, suggesting that the pro-survival cell signals outweighed the pro-apoptotic signals. Conversely, patients with High CerS5 after neoadjuvant treatment had better overall survival and lower rates of recurrence, suggesting that neoadjuvant therapy stimulates the apoptotic pathway. Contrastingly, in the CerS5 Low cohort, non-neoadjuvantly treated patients had good overall survival and rates of recurrence, suggesting that the pro-apoptotic cell signals outweighed the pro-survival signals. However, patients with Low CerS5 after neoadjuvant treated had poorer overall survival and rates of recurrence, suggesting that neoadjuvant therapy has an overall negative effect on these patients. Therefore, CerS5 membranous intensity can identify CRC patients that would benefit from neoadjuvant therapy (CerS5 High) and patients in whom neoadjuvant therapy would have a negative effect on their survival (CerS5 Low).

CerS5 is part of a family of ceramide synthases which along with other enzymes such as Acid Ceramidase, Sphingosine-1-kinase and Sphingosine-1-phosphate phosphatase regulate the sphingolipid metabolic pathway. Abnormalities in sphingolipid metabolism disturb the balance between these various sphingolipid species and in order to investigate what effect the differing expression levels of CerS5 was having on the other members of the sphingolipid metabolic pathway, the RPPA cohort was again applied. The results from the unsupervised hierarchical clustering analysis suggest that there is deregulation and high expression levels of the sphingolipid metabolic enzymes in CerS5 High patients. This supports our earlier unsupervised hierarchical clustering analysis finding that analysis of signalling endpoints linked to apoptosis, autophagy and other cancer related pathways, splits the cohort into 2 clusters of patients, one mainly composed of CerS5 High patients and a second composed of CerS5 Low patients. The proteomic networks constructed from the endpoints linked to the sphingolipid metabolic pathway also differed between CerS5 High and Low patients. Taken together these findings suggest that, in addition to the previous findings that linked the proteomic network of CerS5 High patients to autophagy, there is also deregulation and high expression levels of the sphingolipid metabolic enzymes in these patients. Whether the imbalance of sphingolipid enzymes causes the changes seen in apoptotic, autophagic and other cancer related pathways in CerS5 High patients or *vice versa* is yet to be elucidated. However, as previously mentioned, not all of the sphingolipid antibodies (CerS 6, Acid Ceramidase, Sphingosine-1-phosphatase) have been validated using Western blot analysis and therefore no definitive conclusions can been drawn until the antibody validation is complete.

Immunohistochemistry is no longer a technique used solely for diagnosis as often a semi-quantitative evaluation of the level of expression of a diagnostic/therapeutic biomarker is now required. There are many factors that can affect the immunohistochemical staining intensity of an antigen including tissue fixation, antigen retrieval, detection systems, and different scoring systems and hence, RPPA is emerging as a promising novel approach for the quantitative assessment of antigens in human tissue (Charboneau *et al.*, 2002). In this study we crudely assigned patients as being RPPA CerS5 High or Low based solely on whether their RPPA CerS5 expression levels were above or below the median CerS5 expression level of the eighteen patients in the cohort. We found that unsupervised hierarchical clustering analysis stratified the patients into three main clusters, the first cluster being composed of RPPA CerS5 High patients only, while the second cluster is composed mainly of RPPA CerS5 High patients (5) and only 2 RPPA CerS5 Low patients. The third cluster contains only RPPA CerS5 Low patients. When this heatmap (Fig. 4.9) is compared with the previous heatmap where patients are labelled based on IHC CerS5 intensity (Fig. 4.5), we can see that using RPPA analysis stratifies the patients more accurately. This may be due to the fact that RPPA is a quantitative analysis method and IHC is a subjective semi-quantitative method of analysis. RPPA has already been used to show that the activating state of the PI3K-AKT pathway can stratify patients who could benefit from neoadjuvant treatment in CRC (Mammano *et al.*, 2012). RPPAs have the potential to accurately stratify patients based on antigen expression levels and this could prove to be an invaluable resource for accurately assessing the expression levels of prognostic and predictive biomarkers, such as CerS5, in clinical samples.

In conclusion, it is shown for the first time that CerS5 is expressed in CRC tissue and that CerS5 High expression is associated with poor patient survival. Two distinct signalling CerS5 protein networks which may influence the fate of the cancer cell by switching between apoptosis and autophagy are delineated. This study highlights the importance of CerS5 in the tumourigenic process and that selective targeting of products of sphingolipid metabolism may prove beneficial in the therapeutic treatment of colorectal cancer. Targeting the sphingolipid biosynthesis pathway is emerging as a novel method for treating tumour progression in colorectal cancer, and most chemotherapeutic drugs ultimately work by stimulating apoptosis. The results of our study suggest that as well as being a novel prognostic marker of apoptosis, CerS5 expression can identify colorectal cancer patients that would benefit from neoadjuvant therapy (CerS5 High) and patients that neoadjuvant therapy would have an overall negative effect on (CerS5 Low).

4.4 Future Work

As previously described, membranous staining intensity of CerS5 could potentially identify CRC patients that would benefit from neoadjuvant therapy (CerS5 High) and patients that neoadjuvant therapy would have a negative effect on their survival (CerS5 Low). Ideally, in order to use this to the benefit of patients the findings need to be verified in a larger patient cohort. Furthermore, the over-expression of the CerS5 gene in HEK293 cells has previously been shown to increase sensitivity to doxorubicin and vincristine, but not to cisplatin and carboplatin (Min *et al.*, 2007). Therefore it would also be interesting to determine if the overexpression of CerS5 in CRC tissue can predict a response to a particular drug, family of drugs, or combination of drugs.

Chapter 5

TRIM28 and its Role in Colorectal Cancer

5.1 Introduction

Tumour cells generally modulate their stromal microenvironment by producing stroma-modulating growth factors, which disrupt normal tissue homeostasis and activate surrounding stromal cells, such as fibroblasts, smooth-muscle cells and adipocytes. Fibroblasts, in particular, can affect the stromal microenvironment leading to an increase in tumour aggressiveness (Stuelten *et al.*, 2010). Although numerous studies have investigated the tumour-promoting and tumour-suppressor activity of TRIM28 in cancer, little is known about the expression of TRIM28 in the tumour microenvironment. The balance of TRIM28 expression in cancer epithelium and the surrounding stroma may be a critical determinant of the tumour-promoting or tumour-suppressing phenotype of the protein. By dissecting the effects of TRIM28 in stromal fibroblasts and epithelial tumour cells, the aim was to elucidate the complex relationship between stromal and epithelial compartments in colorectal cancer as it was previously shown that the TRIM28 gene is overexpressed in CRC (Kijanka *et al.*, 2010).

An immunohistochemistry-based study to investigate the levels of expression of TRIM28 in both epithelial and stromal compartments using tissue microarrays was performed. Fluorescence microscopy was used to confirm the nuclear location of TRIM28. Survival analysis was performed based on TRIM28 expression ratios between epithelial and stromal cells in CRC tissue. TRIM28 was further characterised using Reverse-Phase Protein Microarrays generated from laser capture microdissected epithelial and stromal cells. The quantitative RPPA data was used to design protein networks associated with High and Low TRIM28 expression ratios.

5.2 Results

5.2.1 TRIM28 Antibody Validation

The TRIM28 protein was expressed in *E.coli* and purified using IMAC purification as outlined in the methods chapter (2.3.1-2.3.3). SDS-PAGE and Western blot analyses were run in parallel to ensure that the TRIM28 protein was successfully expressed and purified to give an approximate location of the size of the protein and also to validate that the anti-TRIM28 antibody used binds specifically to TRIM28. As seen in Figure 5.1. (A), the TRIM28 protein was successfully expressed and purified, with bands believed to represent TRIM28 observed at approximately 100 kDa. The anti-TRIM28 antibody (C42G12, Cell Signalling Technology Inc) also detected the band at 100 kDa in lane 2 of the Western Blot (Figure 5.1B). Thus, it would appear that the anti-TRIM28 antibody was binding specifically to TRIM28.

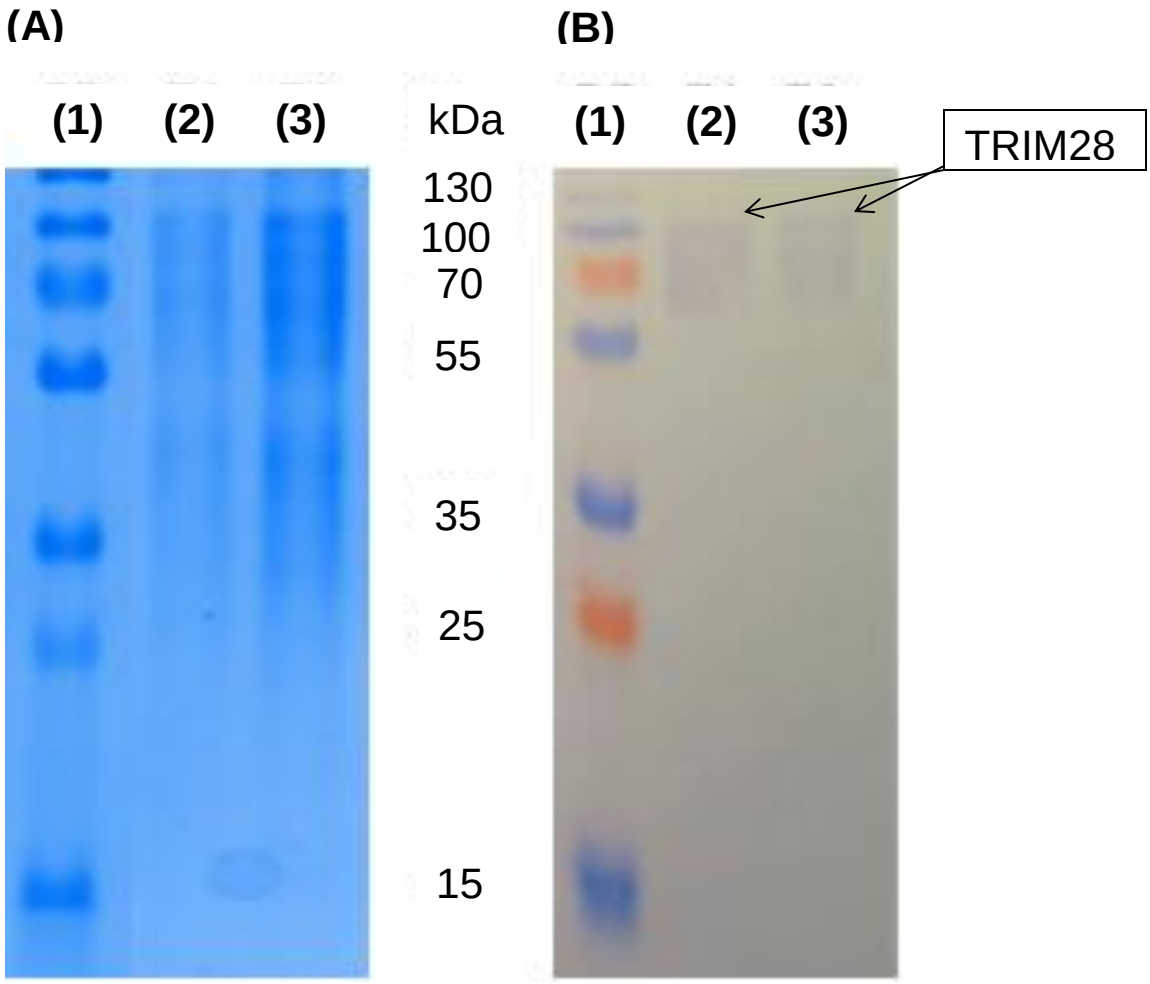

Figure 5.1: Validation of the anti-TRIM28 antibody using SDS-PAGE and Western Blotting. (A) SDS-PAGE Gel: Lane 1 represents the Fermentas pageruler^{TM} marked for protein size determination; lanes 2 and 3 represent the eluted samples containing the TRIM28 protein. (B) Western Blot using TMB chromogenic substrate for detection: Gel: Lane 1 represents the Fermentas pageruler^{TM} marked for protein size determination; lanes 2 and 3 represent the eluted samples containing the TRIM28 protein.

5.2.2 Investigation of the level of expression of TRIM28 in CRC cancer cell lines.

The cells were lysed using cell lysis buffer as described previously in section 2.6.4. A Lowry assay was then carried out in order to quantify the levels of protein in two CRC cell lines (SW480 and SW620). This was done to ensure that the same amount of protein (50µg/ml) would be loaded onto the lanes when carrying out SDS-PAGE and Western Blot analysis to ensure an accurate comparison of TRIM28 expression between cell lines. Standard concentrations of BSA were used to construct a protein standard curve and curve-linear regression was used to extrapolate the unknown protein concentrations of the SW480 and SW620 cell lines from the standard curve. A 1 in 5 dilution of both cell lines (SW480 and SW620) was used to calculate the protein concentration, as it best fit the linear region of the curve. The results of the Lowry Assay indicated that there was a slightly higher protein content in the SW480 cell lines (Fig. 5.2). Therefore it was calculated that 10.9µls of the SW480 cells and 17.8µls of the SW620 cells needed to be added to each lane of the SDS-PAGE gel, which corresponded to 50µg/ml.

(A)

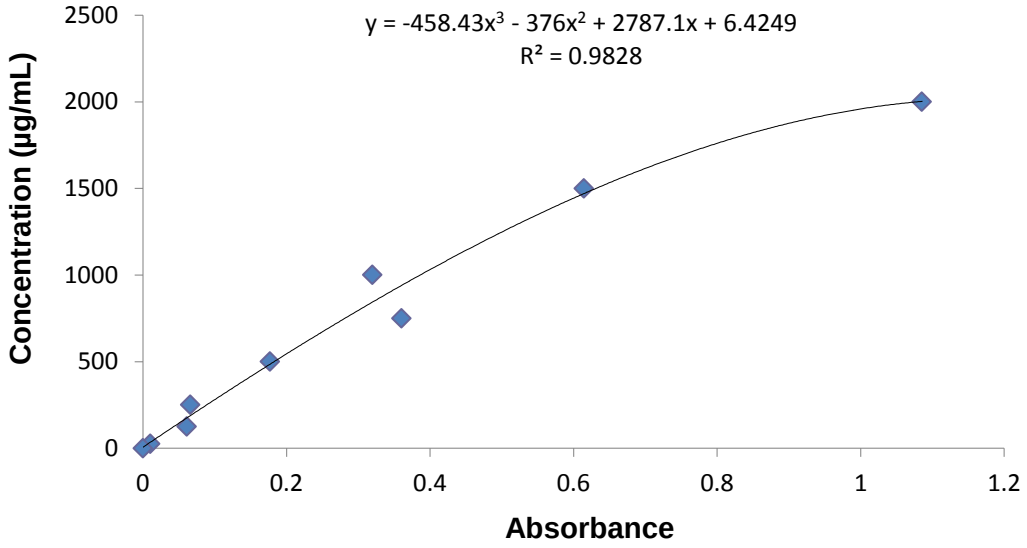

(B)

	SW480 Protein Concentration:								
	Neat	1:2	1:5	1:8	1:10	1:12	1:15	1:20	1:100
Final Conc. mg/mL	1.8	3.3	4.6	4.8	3.5	6	5.9	8	20.6
	SW620 Protein Concentration:								
	Neat	1:2	1:5	1:8	1:10	1:12	1:15	1:20	1:100
Final Conc. mg/mL	1.9	3.4	2.8	3.2	5	4.9	3.9	3.2	6.4

Figure 5.2: Lowry Assay for Protein Quantification in cell lines. (A) Standard Curve using various concentrations of BSA Standards versus absorbance at A_{750nm}. (B) Protein Concentration in varying dilutions of the SW480 and SW620 cell lines, extrapolated from standard curve.

β-Actin and TRIM28 expression levels were evaluated using Western Blot analysis based on the information which had been obtained from the Lowry Assay. *β*-Actin was chosen as the housekeeping, control protein, as it is found in abundance in all eukaryotic cells. Housekeeping proteins are used as an internal control for protein loading as well as reference in Western blotting analysis (Ruan and Lai, 2007). The SDS-PAGE results indicate that similar amounts of protein are present for both cell lines (Fig. 5.3 C). The Western Blot analysis for *β*-Actin confirmed this as the level of expression was very similar for both cell lines, indicating that the correct amount of protein had been loaded to each well (Fig. 5.3 A). The Western Blot analysis for TRIM28 shows a slightly higher level of TRIM28 expression in the SW620 cell line, when compared with the SW480 cell line (Fig. 5.3 B).

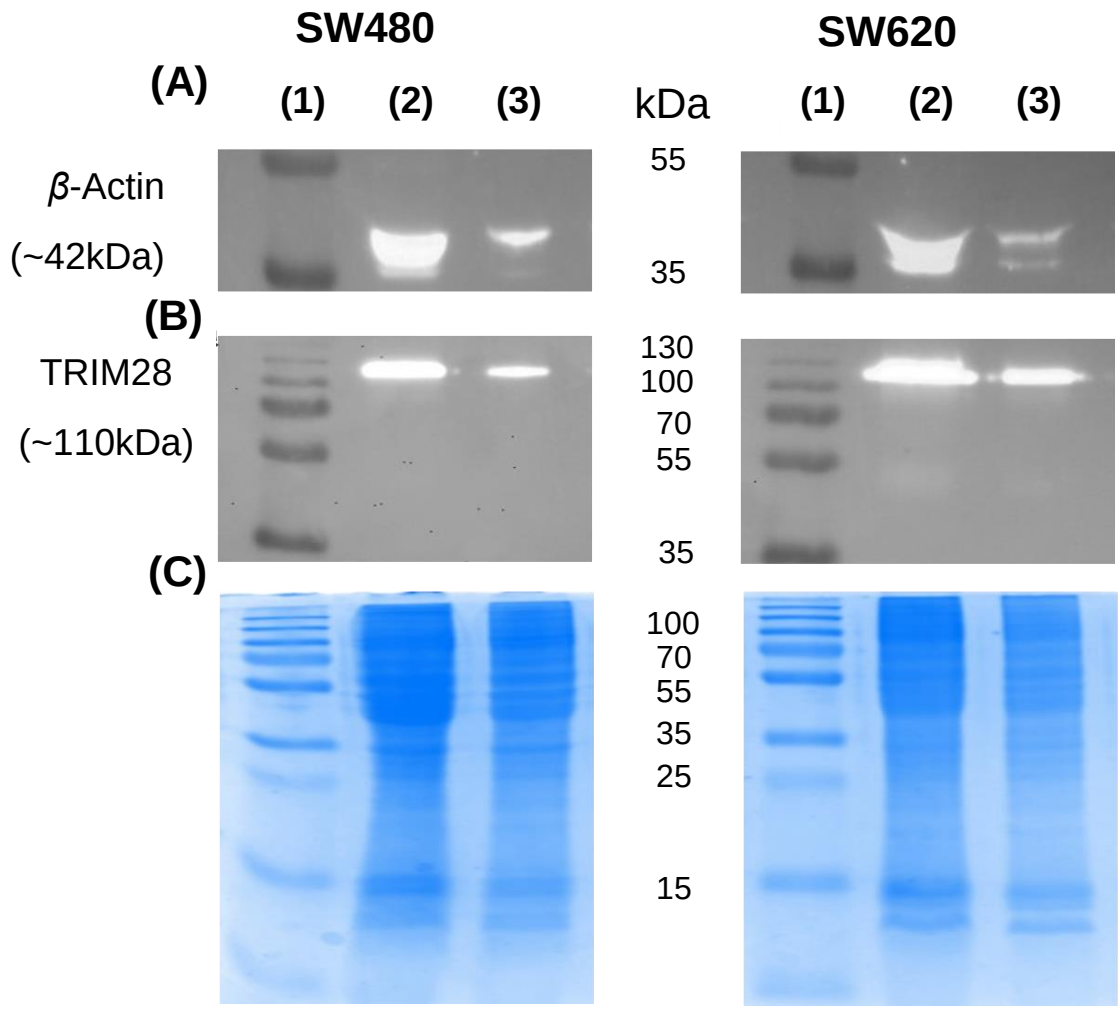

Figure 5.3: Detection of TRIM28 and *β*-Actin in cancer cell lines, using SDS-PAGE and Western Blotting. (A) Western Blot for *β*-Actin in cancer cell lines. (B) Western Blot for TRIM28 in cancer cell lines. (C) SDS-PAGE gel for validation of protein content in cell lysates. In each case; lane 1 represents the page ruler marked for protein size determination; lane 2 represents a neat sample SW480 or SW620 cell lysates; lane 3 represents a 1:2 dilution of SW480 or SW620 cell lysates.

5.2.3 TRIM28 expression determined to be in the cell nuclei

The expression of TRIM28 and *β*-Actin was evaluated in the cancer cell lines using fluorescence microscopy. *β*-Actin was chosen as the housekeeping, control protein as homogenous levels are found in all eukaryotic cells. *β*-Actin is expressed uniformly throughout the cells, while TRIM28 expression is localised to the nucleus (Fig. 5.4).

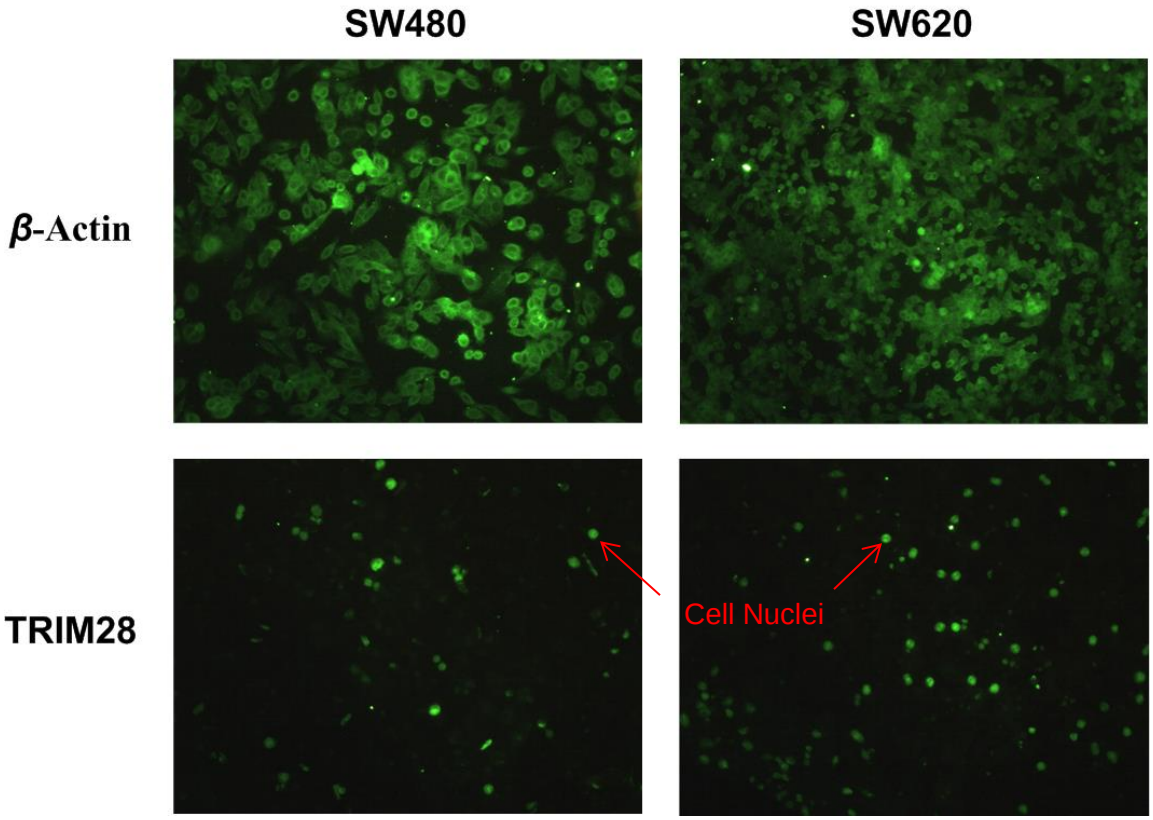

Figure 5.4: *β*-Actin and TRIM28 expression in SW480 and SW620 cells. The cells were fixed with PAF solution and incubated with the primary antibodies (anti-*β*-Actin or anti-TRIM28) overnight, followed by incubation with the fluorescently labelled secondary antibody (Alexo-Fluoro 488) Anti-Rabbit IgG for 1 hour. The red arrows highlight the cell nuclei.

5.2.4 TRIM28 is overexpressed in epithelial CRC tissue

The tissue sections were evaluated using immunohistochemical staining for the expression of the TRIM28 within the epithelium and the surrounding stroma, in both cancerous tissue and adjacent normal mucosa. There was distinct nuclear staining for TRIM28 and the intensity and staining distribution was usually homogeneous within a case (Fig. 5.5). In both the normal and cancerous epithelial tissue TRIM28 staining was confined to cell nuclei. In normal stromal tissue TRIM28 expression was also nuclear and was predominantly found in lamina propria fibroblasts and occasionally in lymphoid cells in the germinal centres of lymphoid follicles. In tumour stromal tissue the nuclear TRIM28 expression was present in fibroblasts and was occasionally present in lymphocytes.

The majority of normal epithelial and stromal tissue showed weak to moderate TRIM28 positivity (83.3% and 91.8%, respectively). However, markedly higher TRIM28 expression levels were found in the epithelium of CRC tissue, when compared with normal colorectal epithelium. A total of 57 out of 137 (42%) CRC cases showed strong epithelial TRIM28 staining (intensity 3+) in the nuclei of epithelial cells (Fig. 5.5). The TRIM28 expression was independent of any clinicopathological features investigated, including survival and 'recurrence-free' survival.

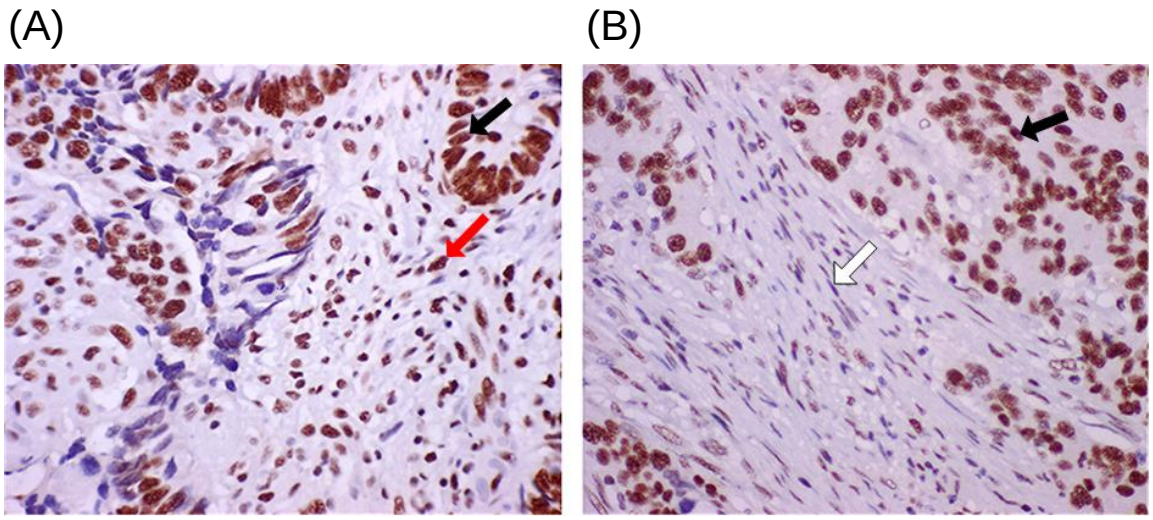

Figure 5.5: Sections from colorectal cancer tissue demonstrating epithelial and stromal staining for TRIM28. Panel (A) shows strong expression of TRIM28 in epithelial cells (black arrow) and moderate expression in stromal compartments, particularly in fibroblasts (red arrow). Panel (B) shows strong expression of TRIM28 in epithelial cells (black arrows) and weak expression in stromal compartments, fibroblasts (white arrow). (x400).

5.2.5 TRIM28 expression ratios

The relationship between the epithelial and stromal intensity was calculated by determining the ratio of TRIM28 expression between the two compartments (Fig. 5.6). A High TRIM28 expression ratio was defined as at least 2 units of difference in staining intensity (e.g. epithelium strong (3+) and stroma weak (1+), or epithelium moderate (2+) and stroma negative (0)). A Low TRIM28 expression ratio was defined as 1 or 0 units of difference in staining intensity (e.g. epithelium moderate (2+) and stroma weak (1+), or epithelium weak (1+) and stroma weak (1+)).

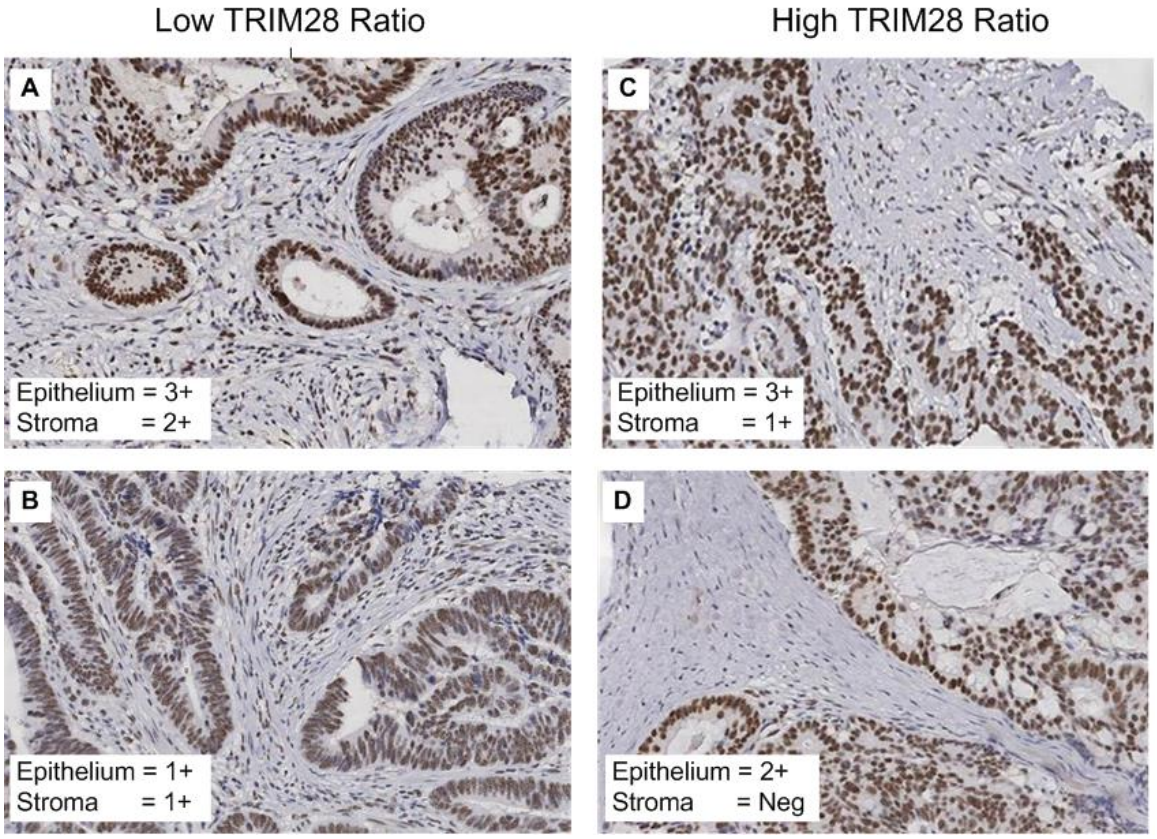

Figure 5.6. Epithelial to stromal TRIM28 expression ratios in colorectal cancer tissue. Negative (0), weak (1+), moderate (2+) or strong (3+) TRIM28 expression was found in cell nuclei of epithelial and stromal colorectal cancer tissue. Panel (A) shows strong expression of TRIM28 in epithelial cells and moderate expression in stromal compartments resulting in a low epithelial to stromal TRIM28 expression ratio. Panel (B) shows weak expression of TRIM28 in both epithelial and stromal cells resulting in a low epithelial to stromal TRIM28 expression ratio. Panel (C) shows strong expression of TRIM28 in epithelial cells and weak expression in stromal compartments resulting in a High epithelial to stromal TRIM28 expression ratio. Panel (D) shows moderate expression of TRIM28 in epithelial cells and negative staining in stromal compartments resulting in a High epithelial to stromal TRIM28 expression ratio. (x200).

In total, 103 cases had a Low ratio of epithelial to stromal TRIM28 expression and 34 cases had a High ratio of epithelial to stromal TRIM28 expression (Fig. 5.7).

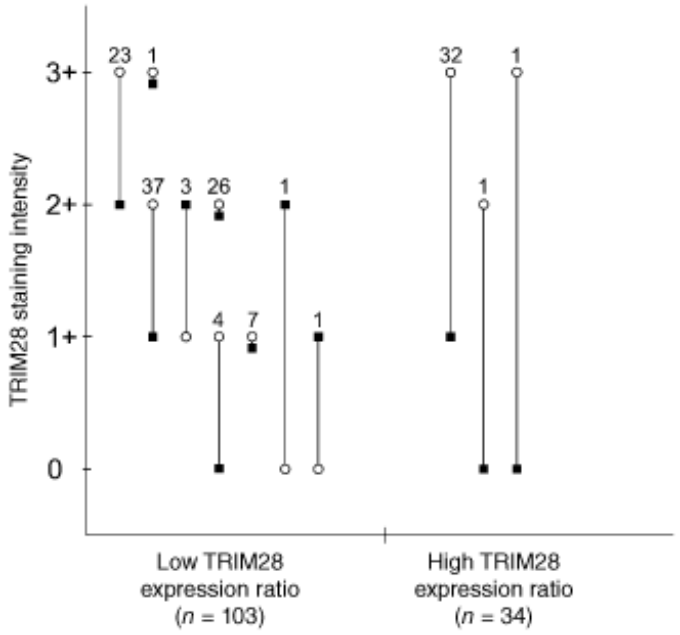

Figure 5.7: Graphical representation of the epithelial to stromal TRIM28 expression ratios in the colorectal cancer cohort. Negative (0), weak (1+), moderate (2+), or strong (3+) TRIM28 staining intensities were found in both epithelial and stromal tissue compartments. The TRIM28 expression ratios are labelled by (○) epithelial and (■) stromal symbols, which are linked with straight lines for matched cases. The numbers above the connection lines depict the total number of cases for each specific distribution of epithelial to stromal TRIM28 expression ratios.

5.2.6 A High TRIM28 expression ratio is associated with shorter survival

Kaplan-Meier curves for patients with colorectal carcinoma, categorized according to High or Low TRIM28 expression ratios between the epithelium and patient-matched stromal tissue are shown in Fig. 5.8. The ratio of the intensity of TRIM28 expression in patient-matched epithelial and stromal tissue had a significant prognostic value. Overall 5-year survival rates (OS) for patients with a High TRIM28 expression ratio (≥2 units of difference) were significantly lower than those with a Low TRIM28 expression ratio (≤1 units of difference), (P = 0.033). Five-year 'recurrence-free' survival (RFS) was also significantly lower for patients with a High intensity ratio of TRIM28 expression (≥2 units of difference) than those with a Low TRIM28 expression ratio (≤1 units of difference), (P = 0.043).

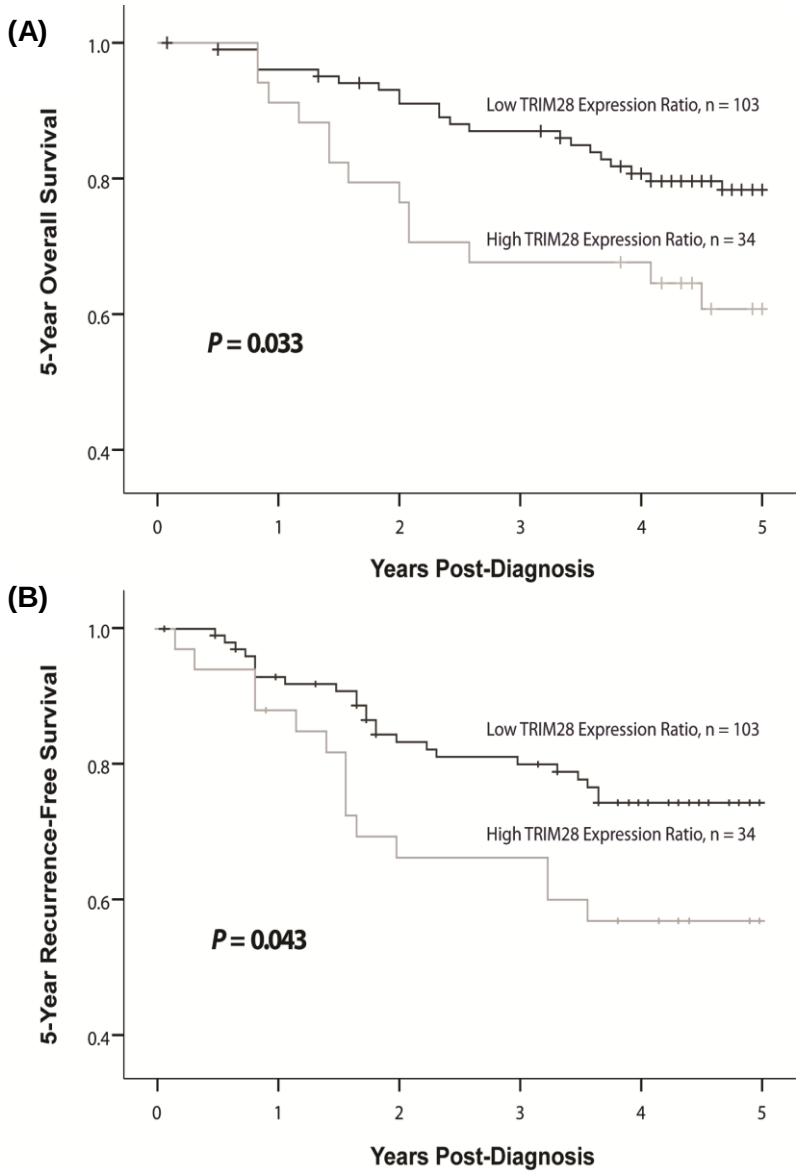

Figure 5.8: Epithelial to stromal TRIM28 expression ratios predict survival in colorectal cancer. (A) High TRIM28 expression ratio in colorectal cancer correlates with lower 5-year overall survival (OS). The Kaplan-Meier plot of colorectal cancer specimens (n = 137) demonstrates significantly lower (P = 0.033; log-rank test) survival associated with High TRIM28 expression ratios. (B) High TRIM28 expression ratio in colorectal cancer correlates with lower 5-year 'recurrence-free' survival (RFS). The Kaplan-Meier plot of colorectal cancer specimens (n=137) demonstrates significantly lower (*P* = 0.043; log-rank test) 'recurrence-free' survival associated with High TRIM28 expression ratio.

5.2.7 TRIM28 Expression is an Independent Predictor of Prognosis

In addition, multivariate analysis showed that the epithelial to stromal TRIM28 expression ratio was an independent predictor of 5-year overall survival (*P* = 0.046; Table 5.1) and 5-year 'recurrence-free' survival (*P* = 0.035; Table 5.2).

Table 5.1. Cox uni- and multivariate analysis of relative risk of death from colorectal cancer within 5 years

5-year Overall Survival				
	Univariate		Multivariate	
Variable	**Hazard Ratio (95% CI)**	**p Value**	**Hazard Ratio (95% CI)**	**p Value**
TRIM28 Ratio	2.070 (1.036-4.137)	0.039	2.136 (1.015-4.498)	0.046
Age <75>	2.398 (1.184-4.858)	0.015	4.119 (1.825-9.293)	0.001
Gender	1.094 (.542-2.211)	0.802	0.998 (0.441-2.260)	0.997
T-Stage	2.092 (1.203-3.641)	0.009	2.628 (1.315-5.255)	0.006
N-Stage	2.390 (1.561-3.658)	0.000	2.243 (1.392-3.615)	0.001
M-Stage	8.091 (3.699-17.697)	0.000	3.879 (1.440-10.453)	0.007

Abbreviations: CI = confidence interval; T = tumour; N = node; M = metastasis.

Table 5.2. Cox uni- and multivariate analysis of relative risk of recurrence of colorectal cancer within 5 years

5-year Recurrence-Free Survival				
	Univariate		Multivariate	
Variable	**Hazard Ratio (95% CI)**	**p Value**	**Hazard Ratio (95%CI)**	**p Value**
TRIM28 Ratio	1.944 (1.005-3.759)	0.048	2.100 (1.052-4.191)	0.035
Age <75>	2.084 (1.050-4.139)	0.036	2.979 (1.404-6.321)	0.004
Gender	1.135 (.581-2.220)	0.710	1.297 (0.609-2.760)	0.500
T-Stage	1.709 (1.040-2.807)	0.034	2.267 (1.232-4.173)	0.009
N-Stage	2.053 (1.386-3.040)	0.000	2.055 (1.340-3.151)	0.001
M-Stage	*N/A		*N/A	

Abbreviations: CI = confidence interval; T = tumour; N = node; M = metastasis; *5-year Recurrence-Free Survival analysis not applicable for patients with metastatic disease.

5.2.8 Cell Scratch Assay to Monitor CRC Cancer Cells Migration Patterns

A cell scratch assay was performed, as described previously (2.6.9), to investigate the migration capabilities of the SW480 and SW620 CRC cancer cell lines. The SW480 cell line appeared to migrate more rapidly than the SW620 cell line (Fig. 5.9). By 48hr, the SW480 cell line had almost completely closed the scratch and by 72hr the scratch was no longer visible. The SW620 cell line also showed cell migration following the scratch. However, the scratch had not closed by 48hr and at 72hr the scratch was still clearly visible.

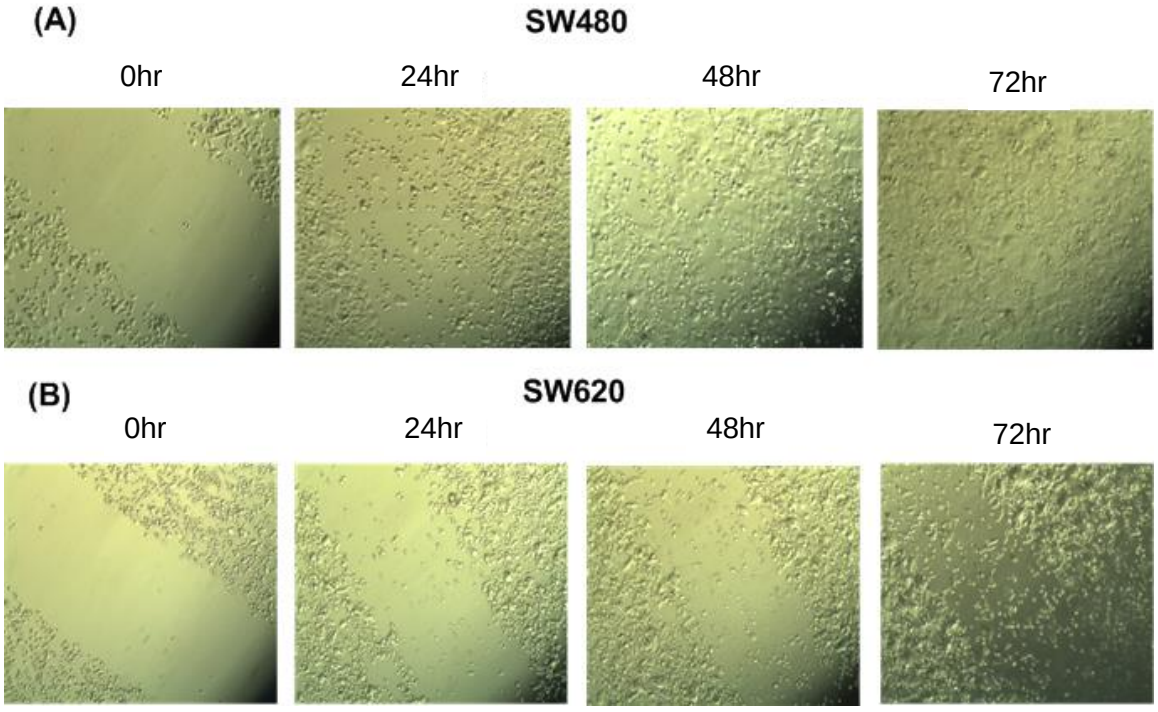

Figure 5.9: Cell Scratch Assay to monitor Cancer Cell Migration. (A) SW480 and (B) SW620 cells were grown and subjected to an *in vitro* scratch assay, with images captured at 0, 24, 48, and 72 h incubation. The rate of migration was measured by the closing of the scratch, (n = 1).

5.2.9 Cancer Cell Co-Culture with Fibroblasts affects cancer cell growth

To determine the effect that fibroblasts have on cancer cell growth, the cancer cell lines were co-cultured with fibroblasts (CCD-18Co) and cell growth was monitored at various time-points (0, 24 and 48hr). Cell growth was not effected in either of the SW480 and SW620 cell lines at 24hr, (Fig. 5.10). At 48hr, there is to be cell death occurring in both the SW480 and SW620 control groups, which had not been co-cultured with fibroblasts (Fig. 5.10). After 48hr in the co-culture there was no noticeable level of cell death, and the cancer cell lines were continuing to grow (Fig. 5.10). This suggests that the fibroblast cells are affecting the rate of growth of both the primary (SW480) and metastatic (SW620) cell lines.

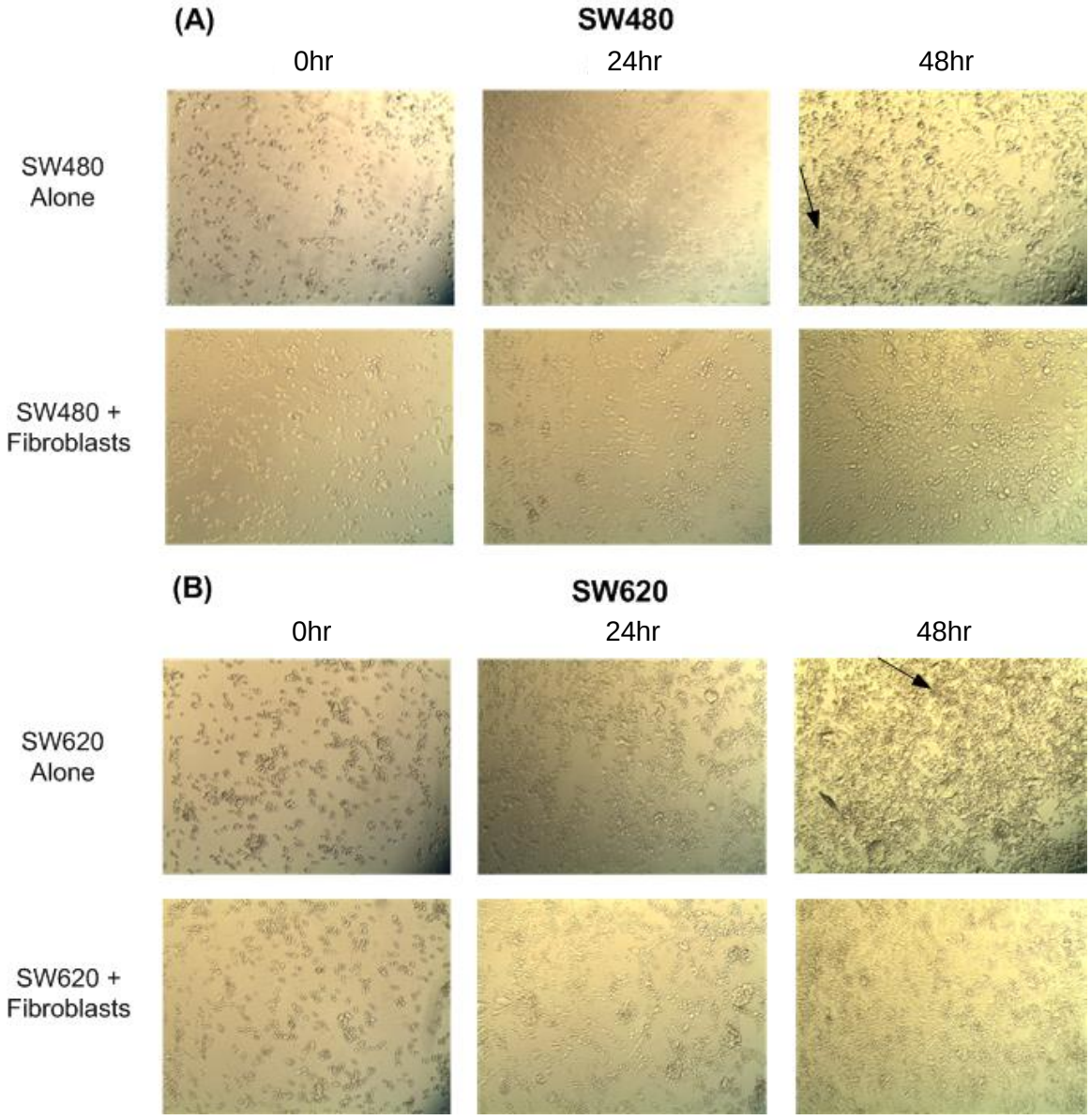

Figure 5.10: Cancer Cell Growth when co-cultured with Fibroblasts. (A) SW480 and (B) SW620 cell lines were cultured alone or in the presence of fibroblasts. The black arrows highlight areas of cell death, (n = 1).

5.2.10 RPPA expression levels of antibodies included in the proteomic analysis

The underlying molecular interactions at play in the tumour microenvironment were investigated in order to further understand the significant effects of TRIM28 expression ratios on patient outcome. The RPPA cohort was used to investigate protein networks associated with apoptosis, autophagy and other cancer related pathways in TRIM28 High and Low ratio tumours. The TRIM28 staining intensity was high (2+ or 3+) in the epithelium of all TRIM28 High and Low ratio cases and hence, all of these samples were grouped together (*n* = 14). The stromal cases were split into TRIM28 High Ratio cases (*n*=8) and TRIM28 Low Ratio cases (*n*=6) (Fig. 5.11).

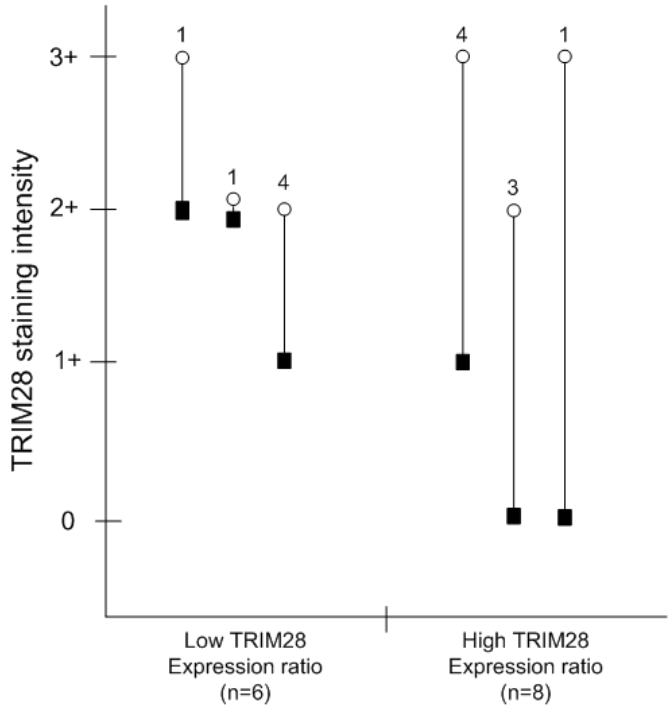

Figure 5.11: Graphical representation of the epithelial to stromal TRIM28 expression ratios in the CRC proteomic cohort. Negative (0), weak (1+), moderate (2+), or strong (3+) TRIM28 staining intensities were found in both epithelial and stromal tissue compartments. The TRIM28 expression ratios are labelled by (○) epithelial and (■) stromal symbols, which are linked with straight lines for matched cases. The numbers above the connection lines depict the total number of cases for each specific distribution of epithelial to stromal TRIM28 expression ratios.

The level of expression of each of the 26 endpoints in pure populations of cells isolated from epithelial and stromal tissue samples following laser capture microdissection was investigated. The expression level of each endpoint, in each tissue type is shown graphically in the box-plot image in figure 5.12. In the stroma of TRIM28 High and Low ratio patients, the difference in expression levels of a numbers of endpoints are approaching significance: Cleaved Caspase 3 (p=0.067); Cleaved Caspase 7 (p=0.091); EGFR1148 (p=0.082) and RUNX1 (p=0.065).

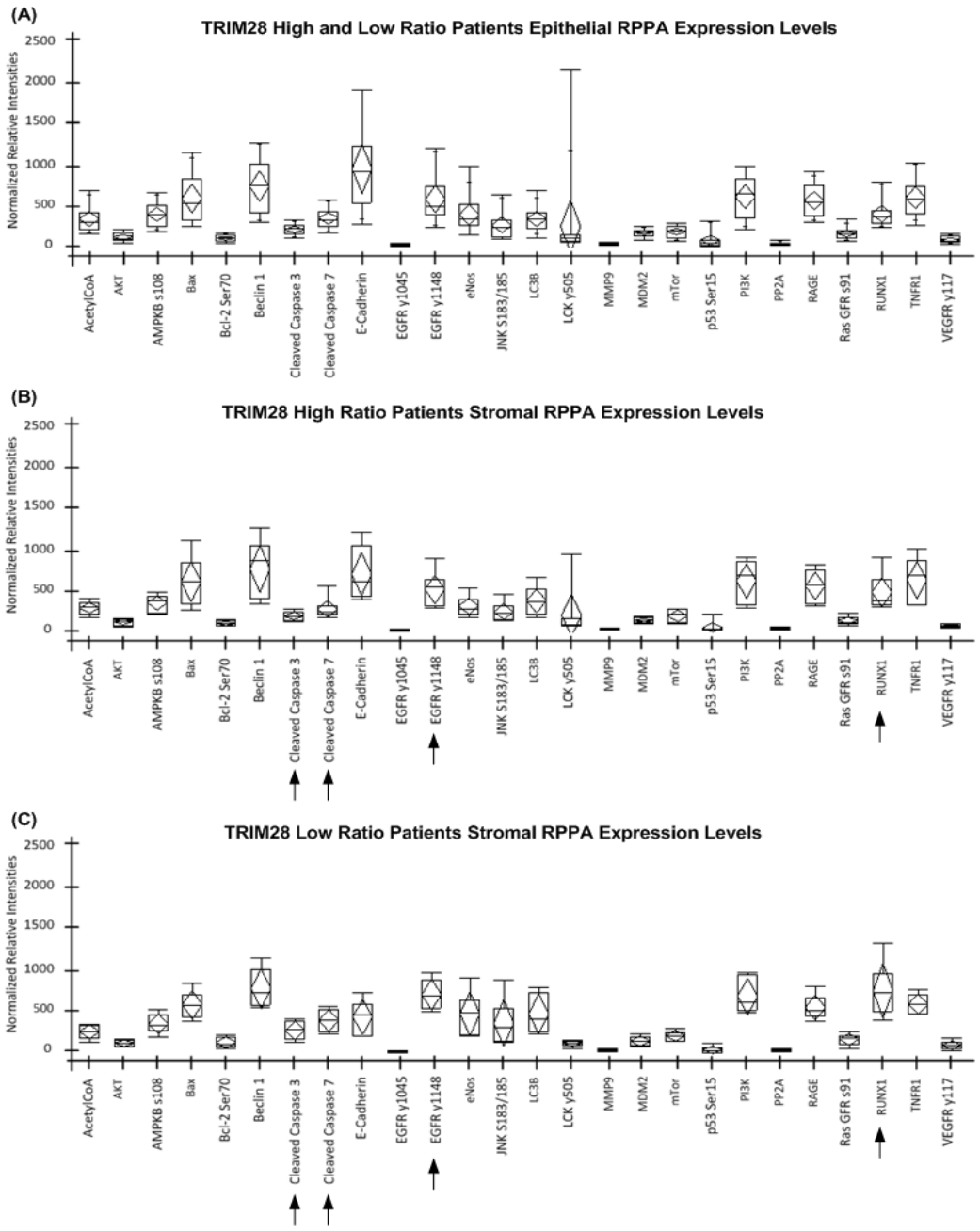

<u>Figure 5.12:</u> Box plot diagram showing RPPA expression levels of all 26 endpoints included in the proteomic analysis. (A): TRIM28 High and Low Ratio Patients Epithelium RPPA Expression Levels (B): TRIM28 High Ratio and (C): TRIM28 Low Ratio Patients Stroma RPPA Expression Levels. The median (line within the box), mean (centre of the diamond), 25th and 75th percentiles and maximum and minimum values are all displayed on each box-plot. The black arrows represent endpoints where the difference in expression levels between the stromal cells is approaching significance.

5.2.11 MDM2 expression is significantly lower in TRIM28 High Ratio patients

In the TRIM28 High ratio cases, there is significantly less MDM2 expressed in the stroma than in the epithelium (p = 0.017, Fig. 5.13). There is no significant difference in MDM2 intensity between the epithelium and stroma in TRIM28 Low ratio cases (p = 0.873, Fig. 5.13). MDM2 is a RING domain ubiquitin E3 ligase and a major regulator of the p53 tumour suppressor. Importantly, TRIM28 was previously identified as an MDM2-binding protein and shown to form a complex with MDM2 and p53 *in vivo (Wang et al., 2005).* The binding is mediated by the N-terminal coiled-coil domain of TRIM28 and the central acidic domain of MDM2. This is an important finding as it supports our previous finding that there is less TRIM28 in the stroma of TRIM28 High ratio patients and, taken together, these results suggest that there is a dysregulation of the p53 tumour suppressor in these patients. This may account for their significantly poorer 5-year overall survival and 5-year 'recurrence-free' survival. Interestingly, no significant correlations were seen in the TRIM28 Low ratio cases.

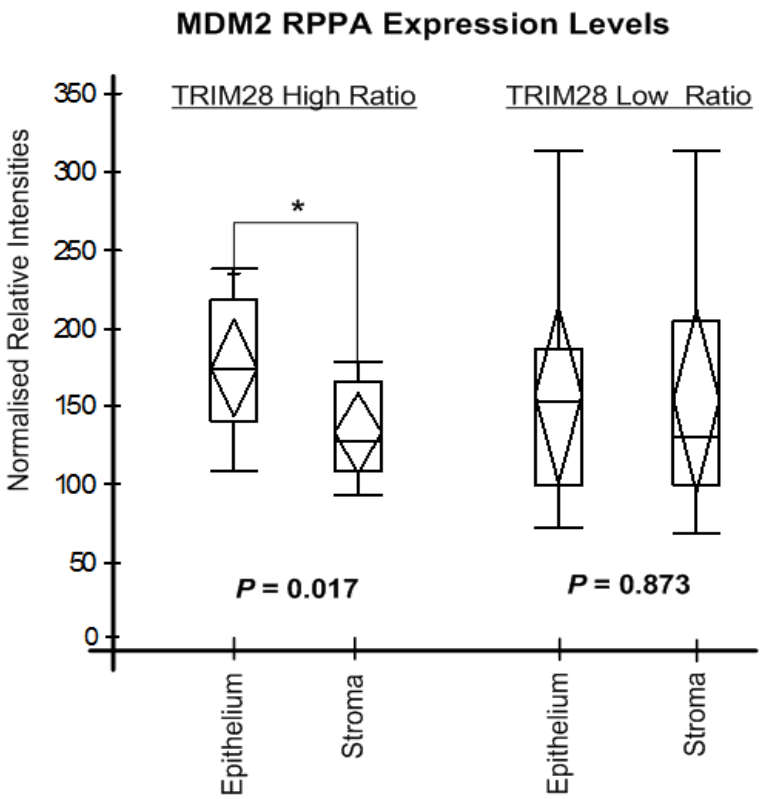

Figure 5.13: Box plot diagram showing MDM2 RPPA intensity levels. MDM2 RPPA intensity levels in the epithelium and stroma of TRIM28 High and Low ratio patients are represented by box-plot diagrams. There is significantly less MDM2 expressed in the stroma than in the epithelium of TRIM28 High ratio patients (p = 0.017). There is no significant difference in MDM2 intensity between the epithelium and stroma in TRIM28 Low ratio cases (p = 0.873). The median (line within the box), mean (centre of the diamond), 25th and 75th percentiles and maximum and minimum values are all displayed on each box-plot.

5.2.12 Proteomic Networks in the tumour microenvironment of TRIM28 High and Low ratio patients

Spearman ρ rank correlation analyses were used to determine significant protein interactions identified by RPPA measurements. No significant RPPA protein interactions that correlated negatively were observed. As the IHC score was always 2+ or 3+ in the epithelial cells, a proteomic network composed of the significant positive correlations in all of the epithelial tissue samples (both TRIM28 High and Low ratio) was constructed.

The analysis of 26 signalling endpoints revealed that 101 of 325 protein pairs were positively and significantly correlated ($\rho > 0.75$, $P \leq 0.01$) in the epithelium of both TRIM28 High and Low ratio patients (Fig. 5.14, Appendix; Supplementary Table 4).

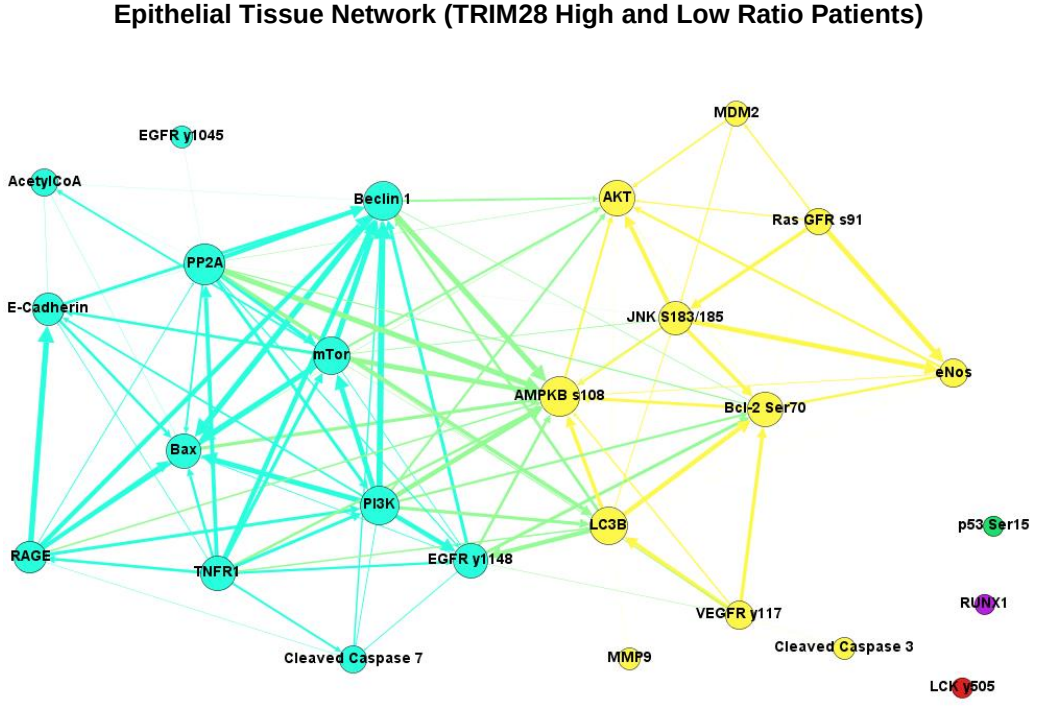

Figure 5.14: Proteomic network identified from the epithelial tissue of TRIM28 High and Low ratio patients. The epithelial proteomic network consists of two main sub-networks (blue and yellow).

124 positive significant correlations were found exclusively in the stroma of the TRIM28 High ratio group (Fig. 5.15 A, Appendix; Supplementary Table 5), whereas 152 protein pairs showed a significant Spearman ρ value exclusively in the stroma of the TRIM28 Low ratio group (Fig. 5.15 B, Appendix; Supplementary Table 6).

(A) **TRIM28 High Ratio Patients Stromal Tissue Network:**

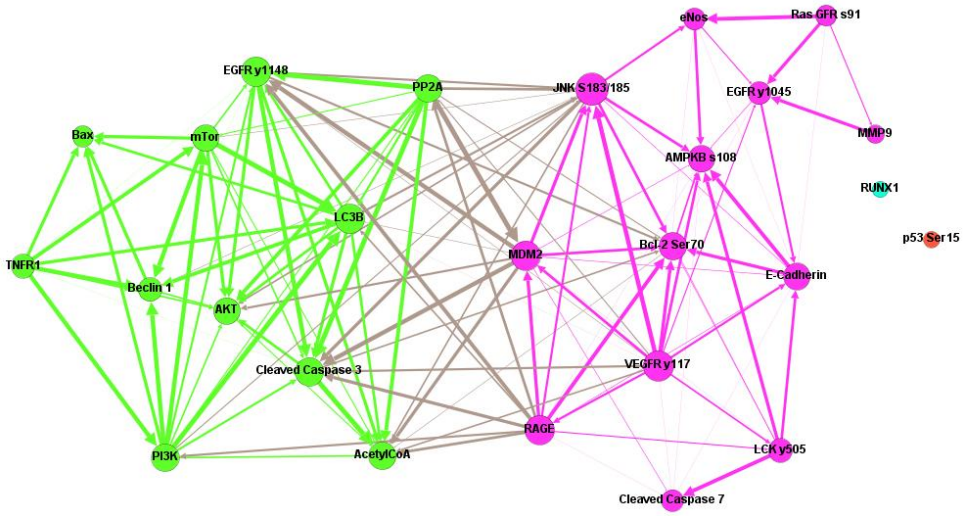

TRIM28 Low Ratio Patients Stromal Tissue Network:

(B)

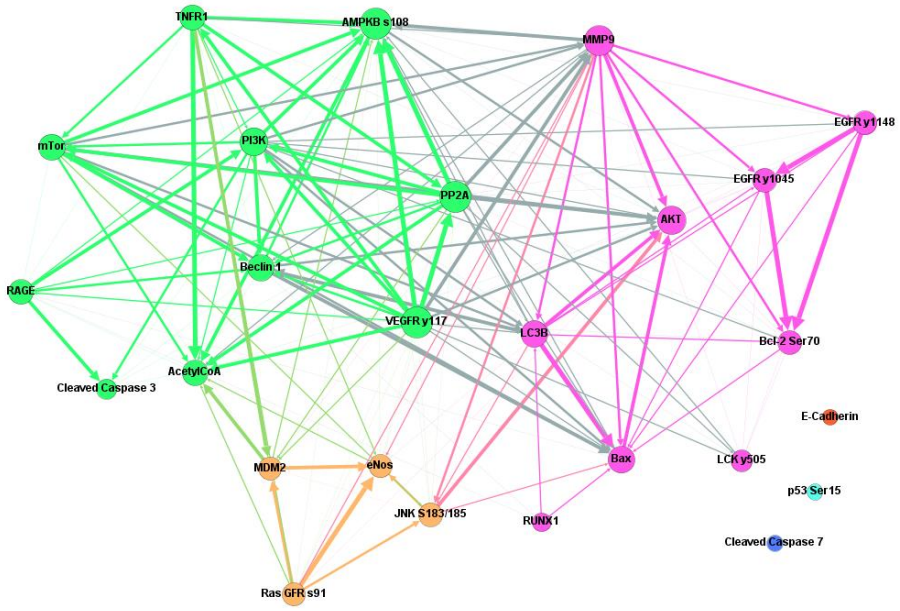

<u>Figure 5.15:</u> Proteomic networks identified from the stromal tissue of TRIM28 High and Low ratio patients. (**A**) TRIM28 High ratio stromal network consists of 2 main sub-networks (green and pink). (**B**) TRIM28 Low ratio stromal network consists of 3 main sub-networks (green, pink and cyan).

Interestingly the proteomic network constructed from the stromal tissue of the TRIM28 High ratio cases is very similar to that of the proteomic network constructed from the epithelial samples. The TRIM28 High ratio stromal proteomic network also consists of two main sub-networks (green and pink). As can be seen from the Venn-diagram in figure 5.16, 18 of the 26 endpoints are located in the same sub-networks in both of these proteomic networks. Only 12 of the 26 endpoints are located in the same sub-networks in the epithelial and TRIM28 Low ratio stromal proteomic networks (Fig 5.16). This suggests that protein networks in epithelium and stroma of TRIM28 High ratio cases are similar, indicating that the epithelial cells may potentially have undergone epithelium to mesenchymal transition (EMT).

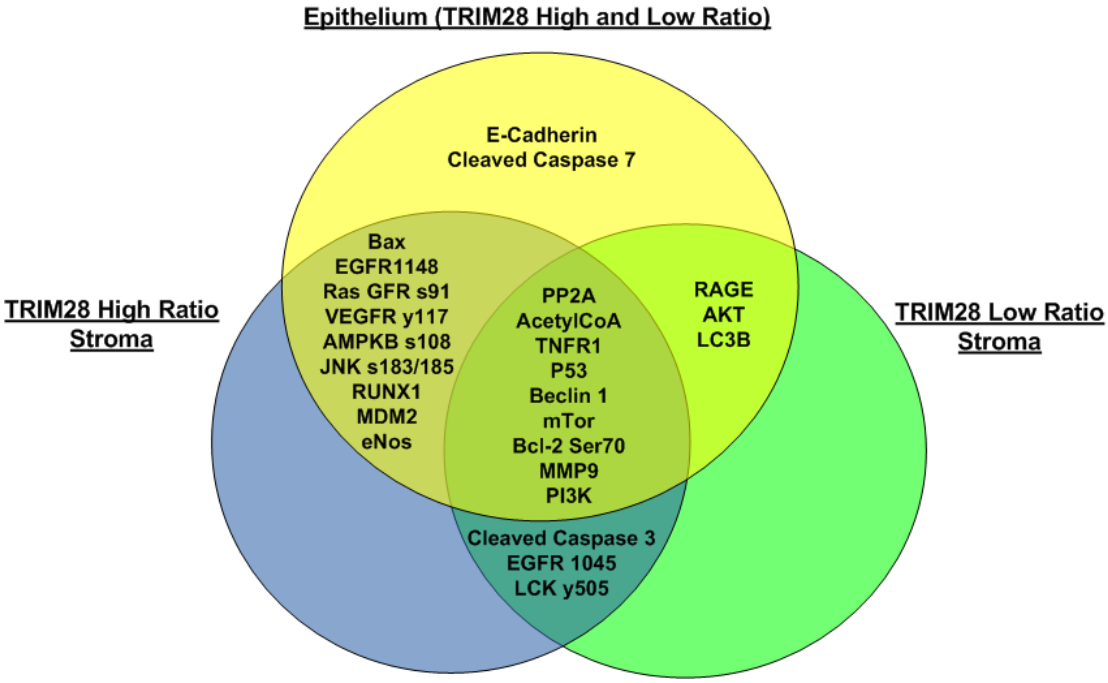

Figure 5.16: Venn-diagram showing the overlap between each of the proteomic networks. Eighteen of the 26 endpoints are located in the same sub-networks in both the epithelial and High ratio stroma networks. Only 12 of the 26 endpoints are located in the same sub-networks in the epithelial and Low ratio stromal proteomic networks.

5.3 Discussion

An accumulating body of evidence suggests that the crosstalk between the epithelial and stromal microenvironment plays a crucial role in tumour progression (Tlsty and Hein, 2001; Buhrmann *et al.*, 2014). Fibroblasts and tumour cells act on each other and on other cellular components of the tumour microenvironment through the secretion of cytokines and growth factors (Bhowmick *et al.*, 2004). Several studies have previously shown that altered protein expression in cells of the stromal tissue compartment, rather than tumour cells alone, can influence survival in lung, prostate and breast cancer (Ogawa *et al.*, 2004; Sloan *et al.*, 2009; Hagglof *et al.*, 2010). These interactions, however, are complex, reciprocal and stage-dependent. Since the molecular and cellular basis of this crosstalk is not yet fully understood, it warrants further in-depth investigation.

Immunohistochemical analysis was used to demonstrate that TRIM28 is overexpressed in human colorectal cancer and TRIM28 expression was localised to the nuclei of CRC cells. It was found that the epithelial to stromal TRIM28 expression ratio correlates significantly with patient survival. Furthermore, Cox regression analyses revealed that high epithelial to stromal TRIM28 expression ratio is an independent prognostic factor for both poor survival and poor 'recurrence-free' survival. RPPA analysis showed that the proteomic networks of TRIM28 High and Low ratio patients differ and MDM2 expression is significantly lower in the stroma than in the epithelium of TRIM28 High ratio patients. To our knowledge, this is the first study to examine the correlation between TRIM28 expression in CRC tissue and patient survival.

Based on these novel findings we propose that the pathophysiological role of TRIM28 in carcinogenesis is highly dependent on the expression of the protein in specific types of cells and that the balance of TRIM28 expression in cancer epithelium and the surrounding stroma may be a critical determinant of the tumour-promoting or tumour-suppressing phenotype of the protein. In addition, we speculate that TRIM28 may act on different pathways in stromal fibroblasts and tumour epithelial cells, resulting in an altered molecular outcome in each compartment.

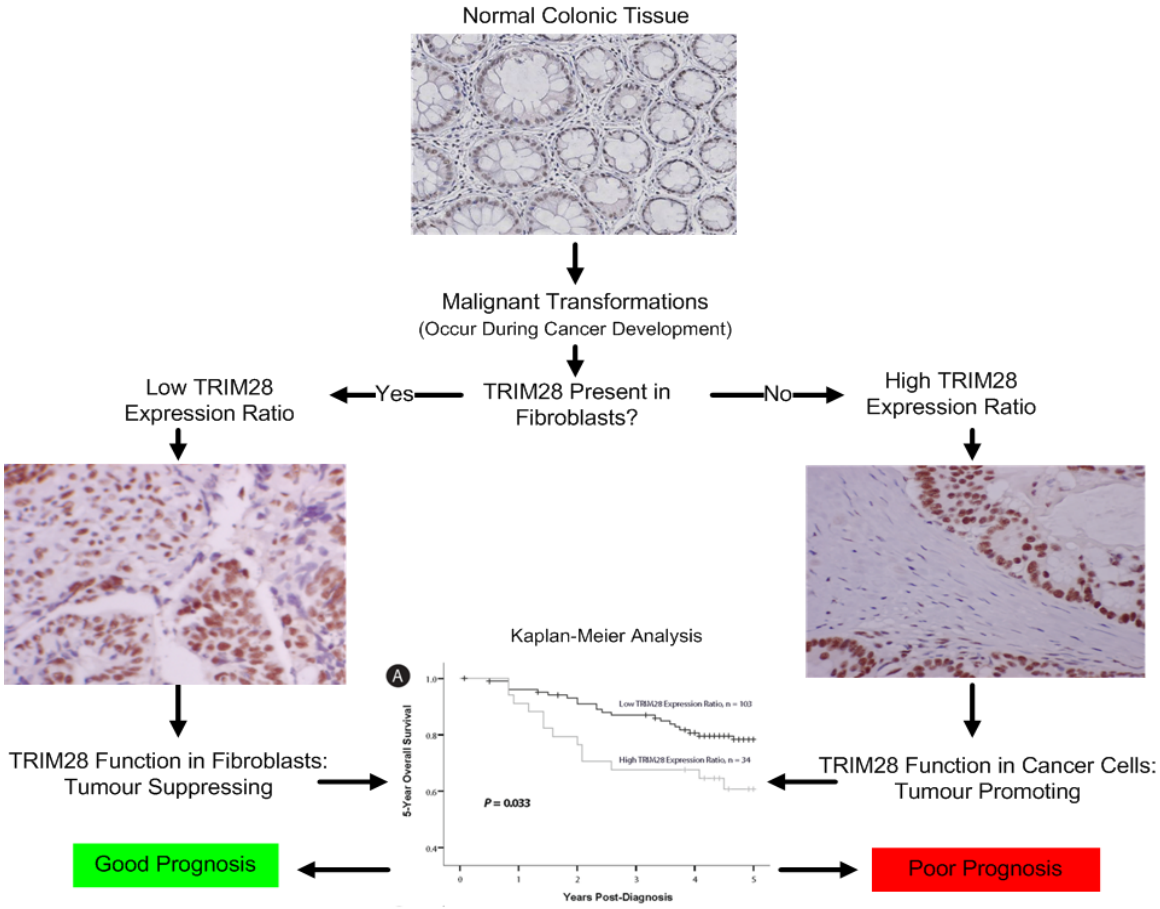

Figure 5.17: Schematic Representation of the proposed model of TRIM28. The balance of TRIM28 expression in cancer epithelium and the surrounding stroma may be a critical determinant of the tumour-promoting or tumour-suppressing phenotype of the protein.

In order to investigate this further laser capture microdissection was employed to isolate pure populations of epithelial and stromal cells from TRIM28 High and Low ratio cases. The isolated cell lysates were used to make RPPAs, which were stained with the antibodies against the endpoints of interest and finally used to investigate the underlying molecular interactions at play in the tumour microenvironment. Recent studies from our group propose that during the epithelial to mesenchymal transformation of tumour cells, a carcinoma cell can take on some characteristics of stromal fibroblasts (Sheehan *et al.*, 2007). EMT is thought to be required physiologically during embryogenesis, but its persistence in tumour cells is suggested to play a role in the promotion of an invasive phenotype. The proteomic network constructed from the significant protein correlations in the stroma of TRIM28 High ratio patients was almost identical to that of the proteomic network of the epithelial cells. This suggests that that EMT may have taken place in the stroma of the TRIM28 High ratio patients which could account for the poorer patient survival seen in this cohort. By dissecting the effects of TRIM28 in stromal fibroblasts and epithelial tumour cells, we were able to elucidate the complex relationship between stromal and epithelial compartments in CRC and the proteomic data offers some insights into the tumour suppressive and tumour promoting effects of the TRIM28 protein in the stroma of CRC patients.

The tumour-suppressor p53 has previously been shown through immunohistochemical analysis to be accumulated in between 42-55% of CRC tissue samples (Scott *et al.*, 1991). In our patient cohort, p53 was overexpressed in 50% of CRC samples, which is consistent with previous studies (Appendix; Supplementary Table 1). Wang demonstrated that TRIM28 does not interact with p53 on its own, but through its co-operation with MDM2 *(Wang et al., 2005).* The MDM2 protein regulates the stability of p53 and the abnormal accumulation of the MDM2 protein is observed in many tumours (Onel and Cordon-Cardo, 2004). TRIM28 can influence p53 acetylation, stimulate p53

ubiquitination and inhibit p53 transcription and apoptotic functions *(Wang et al., 2005)*. In the TRIM28 High ratio cases, there is significantly less MDM2 expressed in the stroma than in the epithelium (p = 0.017). This is an important finding as it supports our previous finding that there is less TRIM28 in the stroma of TRIM28 High ratio patients. This indicates that either the level of TRIM28 in the stroma affects the level of MDM2 or *vice versa*. Taken together these results suggest that the low levels of TRIM28 and MDM2 seen in the stroma of TRIM28 High ratio patients are involved in the dysregulation of the p53 tumour suppressor in these patients.

Western blot analysis suggested that higher levels of TRIM28 are present in the metastatic SW620 cell line than in the primary SW480 cell line and this could affect the aggressiveness of the CRC cell lines. In order to investigate if the higher levels of TRIM28 expression had an impact on the migration of CRC cells a cell scratch assay was carried out. The results suggest that the primary cell line (SW480) showed a greater migratory capacity than the metastatic cell line (SW620). This could be explained by the fact that throughout the course of the project the SW480 cells grew faster in culture than the SW620 cell line. Therefore, the closing of the scratch could be as a result of faster cell growth and not cell migration, so it cannot be definitively concluded that the marginally higher levels of TRIM28 present in the SW620 cell line affect the aggressiveness of CRC cells.

In conclusion, the pathophysiological role of TRIM28 in carcinogenesis may be contextual, depending on cell type of expression and the balance of expression levels between epithelial and stromal compartments, determining the tumour-promoting or tumour-suppressing phenotype. As multiple cellular processes including normal cell development, cell differentiation, neoplastic transformation, DNA repair and apoptosis, converge on this evolutionary conserved TRIM28 protein, it may emerge as a key player in the proliferation and differentiation of both normal and tumour cells. With this study demonstrating both TRIM28 expression in the tumour microenvironment and its potential as a prognostic marker, a combinatorial approach assessing the tumour cells as well as the corresponding stromal cells may prove to be a more effective way of predicting survival in human cancers.

5.4 Future Work

In order to fully elucidate the effects that TRIM28 is having on CRC aggressiveness, TRIM28 would need to be silenced and/or over-expressed in both cell lines (SW480 & SW620) and then cell migration monitored using scratch assays and appropriate controls. The co-culture model could also be improved by using cell culture inserts with porous membranes to keep the co-cultivated cell populations separated. This *in vitro* study would allow for the carcinoma and stromal cells to be separated and each component to be examined separately. This would mimic the *in vivo* isolation of separate populations of cells using LCM. In order to investigate the link between TRIM28 and MDM2 further we intend to carry out qPCR analysis on the epithelial and stromal cells extracted from TRIM28 High and Low ratio CRC cases to detect and quantitate the gene expression levels of MDM2 and TRIM28.

Chapter 6

General Discussion

Although KRAS mutations, B-RAF mutations and mismatch repair deficiency have all demonstrated their utility as prognostic biomarkers in CRC (Andreyev *et al.*, 2001; Popat *et al.*, 2005; Richman *et al.*, 2009), disease stage at diagnosis remains the most accurate predictor of prognosis. However, using the TNM stage to predict response to therapy is not as accurate owing to the fact that CRC is a heterogeneous disease that results in differences in disease progression and response to therapy. For example 20–30% of patients with locally restricted stage II colon cancer will suffer from disease recurrence and TNM staging alone cannot identify these high-risk patients (Strambu *et al.*, 2014) and in metastatic CRC, a significant proportion of patients receiving various chemotherapy regimens do not respond. Therefore, there is a niche for both novel prognostic biomarkers and novel predictive biomarkers that can identify subgroups of patients who may benefit from specific treatment regimens. Advances in genomic and proteomic technologies have enhanced our understanding of CRC and identified many potentially useful biomarkers. The challenge now is to determine which of these biomarkers are clinically useful and the research and validation of these novel biomarkers is key in terms of the development of optimized and personalized regimens for the treatment of CRC (Van Schaeybroeck *et al.*, 2011).

In this study two potential novel biomarkers have been identified and validated. In a previous study in this group, high-density protein arrays were used to screen serum samples and auto-antibodies to the antigens CerS5 and TRIM28 were found in colorectal cancer patients. In this study it was demonstrated using immunohistochemistry that both proteins are also overexpressed in the tumour tissue of CRC patients. Differing expression patterns of both proteins in CRC cancer tissue have also been shown to correlate significantly with both overall-patient survival and ‘recurrence-free’ survival and the underlying molecular interplay associated with the significant effects of both CerS5 and TRIM28 were elucidated using proteomic analysis.

Cancer therapy resistance is another major problem leading to treatment failure and results from a variety of factors including individual variations in patients and somatic cell genetic differences in tumours (Gottesman, 2002). The ability of cancer cells to avoid the generation and/or accumulation of intracellular pro-apoptotic ceramide, coupled with the knowledge that exogenously increasing ceramide can induce apoptosis, suggests that drug resistance may be linked to the sphingolipid metabolism and targeting the related pathways may provide new insights in cancer therapy. Neoadjuvant treatment in colorectal cancer is administered for rectal cancer management as determined by the treating physician. In addition, colon cancer patients usually do not receive neoadjuvant treatment due to risks associated with the treatment outweighing potential benefits. Currently there are no molecular biomarkers available supporting clinical decision-making to identify responders and non-responders to neoadjuvant therapy. There is an evident need for novel biomarkers capable of predicting a patient's likelihood to respond to a particular therapy.

This study identifies CerS5 as a novel biomarker of response to current adjuvant therapy, as well as being a prognostic biomarker. CerS5 can be used as a biomarker to support the clinical decision-making and identify responsive rectal cancer patients that benefit from neoadjuvant treatment and non-responsive rectal cancer patients that benefit from exclusion from neoadjuvant treatment. Furthermore, colon cancer patients are generally not treated neoadjuvantly even though it has been suggested that certain colon cancer patients may benefit from it. CerS5 may help to change this clinical decision-making process as it could potentially identify responsive colon cancer patients that would benefit from neoadjuvant treatment and non-responsive colon cancer patients that would benefit from exclusion from neoadjuvant treatment.

The traditional focus in cancer research has been on the malignantly transformed cell, but in recent years there has been increasing interest in the role of the tumour stroma in the development and progression of tumours. In the process of tumour progression, the initial local growth of a tumour, the subsequent spreading of the malignant cells into the vasculature and/or lymphatic system, and finally the establishment of a distant metastasis are all processes in which host-derived factors are highly involved (Kalluri and Zeisberg, 2006). However, the tumour-microenvironment surrounding the malignant cells also affects the growth of the tumour. Although the stromal cells appear to be non-malignant in the sense of genetic mutations, they do exhibit epigenetic changes, which affect their behaviour and protein expression (Kalluri and Zeisberg, 2006; Polyak, 2007). For example, cancer-associated fibroblasts and tumour-associated macrophages have been shown to have a significant prognostic value (Finak *et al.*, 2008). Therefore, the expression levels of tumour biomarkers in the tumour microenvironment, together with the cancer cell-derived biomarkers, are areas of cancer research that are gaining a lot of interest in recent years.

We found variations in the expression of TRIM28 in stromal fibroblast cells correspond significantly with both 5-year survival and 'recurrence-free' survival. The ratio of the intensity of TRIM28 expression in patient-matched epithelial and stromal tissue had a significant prognostic value. Overall 5-year survival and 5-year 'recurrence-free' survival for patients with a High TRIM28 expression ratio were significantly lower than those with a Low TRIM28 expression ratio. We propose that the pathophysiological role of TRIM28 in carcinogenesis is highly dependent on the expression of the protein in specific types of cells. TRIM28 may act on different pathways in stromal fibroblasts and tumour epithelial cells, resulting in an altered molecular outcome in each compartment. In addition, the balance of TRIM28 expression in cancer epithelium and the surrounding stroma may be a critical determinant of the tumour-promoting or tumour-suppressing

phenotype of the protein. Therefore, a combinatorial approach, measuring the levels of TRIM28 in the stromal fibroblasts and comparing it with the levels of expression in the cancerous epithelial cells, may prove TRIM28 to be a good biomarker for predicting prognosis and recurrence in CRC patients.

Laser capture microdissection is an extremely useful tool for investigating the tumour microenvironment. It facilitates the analysis of individual populations of cells isolated from tissue samples. This is particularly important in light of the aforementioned recent shift in focus of cancer research from the malignantly transformed cell to a more comprehensive analysis that incorporates the tumour microenvironment. RPPA technology allows for the quantitative analysis of numerous phosphorylated, glycosylated, cleaved, or total cellular proteins from a limited amount of sample and can be used for tissue samples, cells, serum and body fluids. Understanding protein networks is important because most drugs currently in development and on the market today are designed to target proteins, not genes and this makes RPPA an extremely powerful tool as we move towards an era of personalised medicine. For example proteomic network analysis in this study demonstrated a shift from apoptosis-related pathways in CerS5 Low cases to autophagy in CerS5 High cases. This suggests a causative link between poor survival in CerS High cases and a dysregulation of programmed cell-death pathways. Therefore, CerS5 High patients could potentially be treated using an autophagy inhibitor and/or agents that stimulate apoptosis.

In conclusion, the data in this thesis suggests that both TRIM28 and CerS5 will prove to be very useful prognostic biomarkers of CRC and may also prove to be useful for measuring the aggressiveness of the tumour, predicting ‘recurrence-free’ prognosis and response to therapy of CRC patients, and, possibly, may even be novel therapeutic targets for the treatment of CRC.

Chapter 7

Bibliography of References

Agricola, E., Randall, R.A., Gaarenstroom, T., Dupont, S. & Hill, C.S. 2011. Recruitment of TIF1gamma to chromatin via its PHD finger-bromodomain activates its ubiquitin ligase and transcriptional repressor activities. *Mol. Cell,* 43**,** 85-96.

Amado, R.G., Wolf, M., Peeters, M., Van Cutsem, E., Siena, S., Freeman, D.J., Juan, T., Sikorski, R., Suggs, S., Radinsky, R., Patterson, S.D. & Chang, D.D. 2008. Wild-Type KRAS Is Required for Panitumumab Efficacy in Patients With Metastatic Colorectal Cancer. *J. Clin. Oncol.,* 26**,** 1626-1634.

American Cancer Society 2011. Colorectal Cancer Facts & Figures 2011-2013. American Cancer Society.

Andreyev, H.J.N., Norman, A.R., Cunningham, D., Oates, J., Dix, B.R., Iacopetta, B.J., Young, J., Walsh, T., Ward, R., Hawkins, N., Beranek, M., Jandik, P., Benamouzig, R., Jullian, E., Laurent-Puig, P., Olschwang, S., Muller, O., Hoffmann, I. & Rabes, H.M. 2001. Kirsten ras mutations in patients with colorectal cancer: the 'RASCAL II' study. *Br. J. Cancer,* 85**,** 692.

Angeles, G., Berrio-Sierra, J., Joseleau, J.P., Lorimier, P., Lefebvre, A. & Ruel, K. 2006. Preparative laser capture microdissection and single-pot cell wall material preparation: a novel method for tissue-specific analysis. *Planta,* 224**,** 228-32.

Astler, V.B. & Coller, F.A. 1954. The Prognostic Significance of Direct Extension of Carcinoma of the Colon and Rectum. *Ann. Surg.,* 139**,** 846-851.

Austoker, J. 1994. *Cancer Prevention in Primary Care Screening for colorectal cancer*.

Barsky, S.H., Green, W.R., Grotendorst, G.R. & Liotta, L.A. 1984. Desmoplastic breast carcinoma as a source of human myofibroblasts. *Am. J. Pathol.,* 115**,** 329-33.

Battifora, H. 1986. The multitumor (sausage) tissue block: novel method for immunohistochemical antibody testing. *Laboratory investigation; a journal of technical methods and pathology,* 55**,** 244-248.

Belluco, C., Mammano, E., Petricoin, E., Prevedello, L., Calvert, V., Liotta, L., Nitti, D. & Lise, M. 2005. Kinase substrate protein microarray analysis of human colon cancer and hepatic metastasis. *Clin. Chim. Acta,* 357**,** 180-3.

Besser, M.J., Shapira-Frommer, R., Treves, A.J., Zippel, D., Itzhaki, O., Schallmach, E., Kubi, A., Shalmon, B., Hardan, I., Catane, R., Segal, E., Markel, G., Apter, S., Nun, A.B., Kuchuk, I., Shimoni, A., Nagler, A. & Schachter, J. 2009. Minimally cultured or selected autologous tumor-infiltrating lymphocytes after a lympho-depleting chemotherapy regimen in metastatic melanoma patients. *J. Immunother.,* 32**,** 415-23.

Beverly, L.J., Howell, L.A., Hernandez-Corbacho, M., Casson, L., Chipuk, J.E. & Siskind, L.J. 2013. BAK activation is necessary and sufficient to drive ceramide synthase-dependent ceramide accumulation following inhibition of BCL2-like proteins. *The Biochemical journal,* 452**,** 111-9.

Bhowmick, N.A., Neilson, E.G. & Moses, H.L. 2004. Stromal fibroblasts in cancer initiation and progression. *Nature,* 432**,** 332-337.

Biomarkers Definition Working Group. 2001. Biomarkers and surrogate endpoints: preferred definitions and conceptual framework. Clin. Pharmacol. Ther., 69, 89-95.

Bond, J.H. 2003. Colon polyps and cancer. *Endoscopy,* 35**,** 27-35.

Bonner, R.F., Emmert-Buck, M., Cole, K., Pohida, T., Chuaqui, R., Goldstein, S. & Liotta, L.A. 1997. Laser capture microdissection: molecular analysis of tissue. *Science,* 278**,** 1481,1483.

Bose, R., Verheij, M., Haimovitz-Friedman, A., Scotto, K., Fuks, Z. & Kolesnick, R. 1995. Ceramide synthase mediates daunorubicin-induced apoptosis: an alternative mechanism for generating death signals. *Cell,* 82**,** 405-414.

Botling, J., Edlund, K., Segersten, U., Tahmasebpoor, S., Engstrom, M., Sundstrom, M., Malmstrom, P.U. & Micke, P. 2009. Impact of thawing on RNA integrity and gene expression analysis in fresh frozen tissue. *Diagn. Mol. Pathol.,* 18**,** 44-52.

Brown, L.F., Guidi, A.J., Schnitt, S.J., Van De Water, L., Iruela-Arispe, M.L., Yeo, T.-K., Tognazzi, K. & Dvorak, H.F. 1999. Vascular stroma formation in carcinoma in situ, invasive carcinoma, and metastatic carcinoma of the breast. *Clin. Cancer Res.,* 5**,** 1041-1056.

Buhrmann, C., Kraehe, P., Lueders, C., Shayan, P., Goel, A. & Shakibaei, M. 2014. Curcumin Suppresses Crosstalk between Colon Cancer Stem Cells and Stromal Fibroblasts in the Tumor Microenvironment: Potential Role of EMT. *PLoS One,* 9**,** e107514.

Cancer, A.J.C.O. 2006. *AJCC Cancer Staging Atlas.* American Joint Committee on Cancer.

Cann, K.L. & Dellaire, G. 2010. Heterochromatin and the DNA damage response. *Biochem. Cell Biol.,* 89**,** 45-60.

Chan, A.T., Giovannucci, E.L., Meyerhardt, J.A., Schernhammer, E.S., Curhan, G.C. & Fuchs, C.S. 2005. Long-term use of aspirin and nonsteroidal anti-inflammatory drugs and risk of colorectal cancer. *JAMA,* 294**,** 914-23.

Chang, H.Y., Chi, J.-T., Dudoit, S., Bondre, C., Van De Rijn, M., Botstein, D. & Brown, P.O. 2002. Diversity, topographic differentiation, and positional memory in human fibroblasts. *Proc. Natl. Acad. Sci. U. S. A.,* 99**,** 12877-12882.

Charboneau, L., Scott, H., Chen, T., Winters, M., Petricoin, E.F., Liotta, L.A. & Paweletz, C.P. 2002. Utility of reverse phase protein arrays: Applications to signalling pathways and human body arrays. *Briefings in Functional Genomics & Proteomics,* 1**,** 305-315.

Chauvier, D., Morjani, H. & Manfait, M. 2002. Ceramide involvement in homocamptothecin- and camptothecin-induced cytotoxicity and apoptosis in colon HT29 cells. *International journal of oncology,* 20**,** 855-63.

Chen, L., Muñoz-Antonia, T. & Cress, W.D. 2014. Trim28 Contributes to EMT via Regulation of E-Cadherin and N-Cadherin in Lung Cancer Cell Lines. *PLoS One,* 9**,** e101040.

Chiechi, A., Mueller, C., Boehm, K.M., Romano, A., Benassi, M.S., Picci, P., Liotta, L.A. & Espina, V. 2012. Improved data normalization methods for reverse phase protein microarray analysis of complex biological samples. *BioTechniques,* 0**,** 1-7.

Chiechi, A., Novello, C., Magagnoli, G., Petricoin, E.F., 3rd, Deng, J., Benassi, M.S., Picci, P., Vaisman, I., Espina, V. & Liotta, L.A. 2013. Elevated TNFR1 and serotonin in bone metastasis are correlated with poor survival following bone metastasis diagnosis for both carcinoma and sarcoma primary tumors. *Clin. Cancer Res.,* 19**,** 2473-85.

Ciechanover, A. 1998. The ubiquitin–proteasome pathway: on protein death and cell life. *The EMBO journal,* 17**,** 7151-7160.

Cuvillier, O., Pirianov, G., Kleuser, B., Vanek, P.G., Coso, O.A., Gutkind, S. & Spiegel, S. 1996. Suppression of ceramide-mediated programmed cell death by sphingosine-1-phosphate. *Nature,* 381**,** 800-3.

Davies, R.J., Miller, R. & Coleman, N. 2005. Colorectal cancer screening: prospects for molecular stool analysis. *Nat. Rev. Cancer,* 5**,** 199-209.

De Mattos-Arruda, L., Dienstmann, R. & Tabernero, J. 2011. Development of molecular biomarkers in individualized treatment of colorectal cancer. *Clin. Colorectal Cancer,* 10**,** 279-89.

Delgado, M.E., Dyck, L., Laussmann, M.A. & Rehm, M. 2014. Modulation of apoptosis sensitivity through the interplay with autophagic and proteasomal degradation pathways. *Cell Death Dis.,* 5**,** e1011.

Denoix, P. 1946. Enquete permanent dans les centres anticancereaux. *Bull Inst Nat Hyg* 70–5.

Devroede, G.J. & Phillips, S.F. 1969. Conservation of Sodium, Chloride, and Water by the Human Colon. *Gastroenterology,* 56**,** 101-109.

Dimanche-Boitrel, M.T., Rebillard, A. & Gulbins, E. 2011. Ceramide in chemotherapy of tumors. *Recent patents on anti-cancer drug discovery,* 6**,** 284-93.

Dukes, C.E. 1932. The classification of cancer of the rectum. *The Journal of Pathology and Bacteriology,* 35**,** 323-332.

Dvorak, H.F. 1986. Tumors: wounds that do not heal: similarities between tumor stroma generation and wound healing. *The New England journal of medicine,* 315**,** 1650-1659.

Edge, S. & Compton, C. 2010. The American Joint Committee on Cancer: the 7th Edition of the AJCC Cancer Staging Manual and the Future of TNM. *Ann. Surg. Oncol.,* 17**,** 1471-1474.

Elsaleh, H., Joseph, D., Grieu, F., Zeps, N., Spry, N. & Iacopetta, B. 2000. Association of tumour site and sex with survival benefit from adjuvant chemotherapy in colorectal cancer. *The Lancet,* 355**,** 1745-1750.

Emmert-Buck, M.R., Bonner, R.F., Smith, P.D., Chuaqui, R.F., Zhuang, Z., Goldstein, S.R., Weiss, R.A. & Liotta, L.A. 1996. Laser Capture Microdissection. *Science,* 274**,** 998-1001.

Engels, B., Rowley, D.A. & Schreiber, H. 2012. Targeting stroma to treat cancers. *Semin. Cancer Biol.,* 22**,** 41-9.

Espina, V., Mariani, B.D., Gallagher, R.I., Tran, K., Banks, S., Wiedemann, J., Huryk, H., Mueller, C., Adamo, L., Deng, J., Petricoin, E.F., Pastore, L., Zaman, S., Menezes, G., Mize, J., Johal, J., Edmiston, K. & Liotta, L.A. 2010. Malignant precursor cells pre-exist in human breast DCIS and require autophagy for survival. *PLoS One,* 5**,** e10240.

Espina, V., Mehta, A.I., Winters, M.E., Calvert, V., Wulfkuhle, J., Petricoin, E.F., 3rd & Liotta, L.A. 2003. Protein microarrays: molecular profiling technologies for clinical specimens. *Proteomics,* 3**,** 2091-100.

Espina, V., Mueller, C. & Liotta, L.A. 2011. Phosphoprotein Stability in Clinical Tissue and Its Relevance for Reverse Phase Protein Microarray Technology. *Methods in molecular biology (Clifton, N.J.),* 785**,** 23-43.

Espina, V., Wulfkuhle, J.D., Calvert, V.S., Petricoin, E.F., 3rd & Liotta, L.A. 2007. Reverse phase protein microarrays for monitoring biological responses. *Methods Mol. Biol.,* 383**,** 321-36.

Espina, V., Wulfkuhle, J.D., Calvert, V.S., Vanmeter, A., Zhou, W., Coukos, G., Geho, D.H., Petricoin, E.F. & Liotta, L.A. 2006. Laser-capture microdissection. *Nat. Protocols,* 1**,** 586-603.

Fan, S., Niu, Y., Tan, N., Wu, Z., Wang, Y., You, H., Ke, R., Song, J., Shen, Q., Wang, W., Yao, G., Shu, H., Lin, H., Yao, M., Zhang, Z., Gu, J. & Qin, W. 2013. LASS2 enhances chemosensitivity of breast cancer by counteracting acidic tumor microenvironment through inhibiting activity of V-ATPase proton pump. *Oncogene,* 32**,** 1682-90.

Ferlay, J., Soerjomataram, I., Ervik, M., Dikshit, R., Eser, S., Mathers, C., Rebelo, M., Parkin, D., Forman, D. & Bray, F. 2014. GLOBOCAN 2012 v1. 0, Cancer Incidence and Mortality Worldwide: IARC CancerBase No. 11 [Internet]. Lyon,

France: International Agency for Research on Cancer. c2013 [cited 2013 Oct 17]. *globocan. iarc. fr*.

Ferlay, J., Steliarova-Foucher, E., Lortet-Tieulent, J., Rosso, S., Coebergh, J.W.W., Comber, H., Forman, D. & Bray, F. 2013. Cancer incidence and mortality patterns in Europe: Estimates for 40 countries in 2012. *Eur. J. Cancer,* 49**,** 1374-1403.

Finak, G., Bertos, N., Pepin, F., Sadekova, S., Souleimanova, M., Zhao, H., Chen, H., Omeroglu, G., Meterissian, S., Omeroglu, A., Hallett, M. & Park, M. 2008. Stromal gene expression predicts clinical outcome in breast cancer. *Nat. Med.,* 14**,** 518-527.

Fleming, M., Ravula, S., Tatishchev, S.F. & Wang, H.L. 2012. Colorectal carcinoma: Pathologic aspects. *J. Gastrointest. Oncol.,* 3**,** 153-173.

Friedman, J.R., Fredericks, W.J., Jensen, D.E., Speicher, D.W., Huang, X.P., Neilson, E.G. & Rauscher, F.J., 3rd 1996. KAP-1, a novel corepressor for the highly conserved KRAB repression domain. *Genes Dev.,* 10**,** 2067-78.

Futerman, A.H. & Riezman, H. 2005. The ins and outs of sphingolipid synthesis. *Trends Cell Biol.,* 15**,** 312-318.

Gallagher, P.G., Bao, Y., Prorock, A., Zigrino, P., Nischt, R., Politi, V., Mauch, C., Dragulev, B. & Fox, J.W. 2005. Gene expression profiling reveals cross-talk between melanoma and fibroblasts: implications for host-tumor interactions in metastasis. *Cancer Res.,* 65**,** 4134-46.

Giantonio, B.J., Catalano, P.J., Meropol, N.J., O'dwyer, P.J., Mitchell, E.P., Alberts, S.R., Schwartz, M.A. & Benson, A.B. 2007. Bevacizumab in Combination With Oxaliplatin, Fluorouracil, and Leucovorin (FOLFOX4) for Previously Treated

Metastatic Colorectal Cancer: Results From the Eastern Cooperative Oncology Group Study E3200. *J. Clin. Oncol.,* 25**,** 1539-1544.

Gillen, C.D., Walmsley, R.S., Prior, P., Andrews, H.A. & Allan, R.N. 1994. Ulcerative colitis and Crohn's disease: a comparison of the colorectal cancer risk in extensive colitis. *Gut,* 35**,** 1590-1592.

Glimelius, B. 2002. Radiotherapy in rectal cancer. *Br. Med. Bull.,* 64**,** 141-157.

Goodarzi, A.A., Noon, A.T., Deckbar, D., Ziv, Y., Shiloh, Y., Lobrich, M. & Jeggo, P.A. 2008. ATM signaling facilitates repair of DNA double-strand breaks associated with heterochromatin. *Mol. Cell,* 31**,** 167-77.

Gottesman, M.M. 2002. Mechanisms of cancer drug resistance. *Annu. Rev. Med.,* 53**,** 615-27.

Graslund, S., Nordlund, P., Weigelt, J., Hallberg, B.M., Bray, J., Gileadi, O., Knapp, S., Oppermann, U., Arrowsmith, C., Hui, R., Ming, J., Dhe-Paganon, S., Park, H.W., Savchenko, A., Yee, A., Edwards, A., Vincentelli, R., Cambillau, C., Kim, R., Kim, S.H., Rao, Z., Shi, Y., Terwilliger, T.C., Kim, C.Y., Hung, L.W., Waldo, G.S., Peleg, Y., Albeck, S., Unger, T., Dym, O., Prilusky, J., Sussman, J.L., Stevens, R.C., Lesley, S.A., Wilson, I.A., Joachimiak, A., Collart, F., Dementieva, I., Donnelly, M.I., Eschenfeldt, W.H., Kim, Y., Stols, L., Wu, R., Zhou, M., Burley, S.K., Emtage, J.S., Sauder, J.M., Thompson, D., Bain, K., Luz, J., Gheyi, T., Zhang, F., Atwell, S., Almo, S.C., Bonanno, J.B., Fiser, A., Swaminathan, S., Studier, F.W., Chance, M.R., Sali, A., Acton, T.B., Xiao, R., Zhao, L., Ma, L.C., Hunt, J.F., Tong, L., Cunningham, K., Inouye, M., Anderson, S., Janjua, H., Shastry, R., Ho, C.K., Wang, D., Wang, H., Jiang, M., Montelione, G.T., Stuart, D.I., Owens, R.J., Daenke, S., Schutz, A., Heinemann, U., Yokoyama, S., Bussow, K. & Gunsalus, K.C. 2008. Protein production and purification. *Nat. Methods,* 5**,** 135-46.

Green, B.L., Marshall, H.C., Collinson, F., Quirke, P., Guillou, P., Jayne, D.G. & Brown, J.M. 2013. Long-term follow-up of the Medical Research Council CLASICC trial of conventional versus laparoscopically assisted resection in colorectal cancer. *Br. J. Surg.,* 100**,** 75-82.

Green, D.R. & Kroemer, G. 2009. Cytoplasmic functions of the tumour suppressor p53. *Nature,* 458**,** 1127-30.

Guillem, J.G., Paty, P.B. & Cohen, A.M. 1997. Surgical treatment of colorectal cancer. *CA Cancer J. Clin.,* 47**,** 113-128.

Gulmann, C., Sheehan, K.M., Kay, E.W., Liotta, L.A. & Petricoin, E.F., 3rd 2006. Array-based proteomics: mapping of protein circuitries for diagnostics, prognostics, and therapy guidance in cancer. *J. Pathol.,* 208**,** 595-606.

Gutman, M. & Fidler, I.J. 1995. Biology of human colon cancer metastasis. *World J. Surg.,* 19**,** 226-234.

Hagglof, C., Hammarsten, P., Josefsson, A., Stattin, P., Paulsson, J., Bergh, A. & Ostman, A. 2010. Stromal PDGFRbeta expression in prostate tumors and non-malignant prostate tissue predicts prostate cancer survival. *PLoS One,* 5**,** e10747.

Hait, N.C., Oskeritzian, C.A., Paugh, S.W., Milstien, S. & Spiegel, S. 2006. Sphingosine kinases, sphingosine 1-phosphate, apoptosis and diseases. *Biochimica et Biophysica Acta (BBA) - Biomembranes,* 1758**,** 2016-2026.

Hanahan, D. & Weinberg, R.A. 2000. The hallmarks of cancer. *Cell,* 100**,** 57-70.

Hartmann, D., Lucks, J., Fuchs, S., Schiffmann, S., Schreiber, Y., Ferreiros, N., Merkens, J., Marschalek, R., Geisslinger, G. & Grosch, S. 2012. Long chain ceramides and very long chain ceramides have opposite effects on human breast and colon cancer cell growth. *Int. J. Biochem. Cell Biol.,* 44**,** 620-8.

Hatakeyama, S. 2011. TRIM proteins and cancer. *Nat. Rev. Cancer,* 11**,** 792-804.

Hengen, P. 1995. Purification of His-Tag fusion proteins from Escherichia coli. *Trends Biochem. Sci.,* 20**,** 285-6.

Henriksen, K.L., Rasmussen, B.B., Lykkesfeldt, A.E., Møller, S., Ejlertsen, B. & Mouridsen, H.T. 2007. Semi-quantitative scoring of potentially predictive markers for endocrine treatment of breast cancer: a comparison between whole sections and tissue microarrays. *J. Clin. Pathol.,* 60**,** 397-404.

Herquel, B., Ouararhni, K. & Davidson, I. 2011a. The TIF1alpha-related TRIM cofactors couple chromatin modifications to transcriptional regulation, signaling and tumor suppression. *Transcription,* 2**,** 231-6.

Herquel, B., Ouararhni, K., Khetchoumian, K., Ignat, M., Teletin, M., Mark, M., Bchade, G., Van Dorsselaer, A., Sanglier-Cianfrani, S., Hamiche, A., Cammas, F., Davidson, I. & Losson, R. 2011b. Transcription cofactors TRIM24, TRIM28, and TRIM33 associate to form regulatory complexes that suppress murine hepatocellular carcinoma. *Proceedings of the National Academy of Sciences*.

Howlader, N. 2012. SEER Cancer Statistics Review, 1975–2009 (Vintage 2009 Populations). *http://seer.cancer.gov/csr/1975_2009_pops09/, based on November 2011 SEER data submission, posted to the SEER web site,*.

Hunt, I. 2005. From gene to protein: a review of new and enabling technologies for multi-parallel protein expression. *Protein Expr. Purif.,* 40**,** 1-22.

Huntley, S., Baggott, D.M., Hamilton, A.T., Tran-Gyamfi, M., Yang, S., Kim, J., Gordon, L., Branscomb, E. & Stubbs, L. 2006. A comprehensive catalog of human KRAB-associated zinc finger genes: insights into the evolutionary history of a large family of transcriptional repressors. *Genome Res.,* 16**,** 669-677.

Iyengar, S. & Farnham, P.J. 2011. KAP1 protein: an enigmatic master regulator of the genome. *J. Biol. Chem.,* 286**,** 26267-76.

Johnston, S.T., Simpson, M.J. & Mcelwain, D.L.S. 2014. How much information can be obtained from tracking the position of the leading edge in a scratch assay? *Journal of The Royal Society Interface,* 11.

Jorge, J. & Wexner, S. 1997. Anatomy and physiology of the rectum and anus. *The European journal of surgery= Acta chirurgica,* 163**,** 723-731.

Joyce, J.A. & Pollard, J.W. 2009. Microenvironmental regulation of metastasis. *Nat. Rev. Cancer,* 9**,** 239-252.

Kalluri, R. & Zeisberg, M. 2006. Fibroblasts in cancer. *Nat. Rev. Cancer,* 6**,** 392-401.

Kay, E.W., O'grady, A., Morgan, J.M., Wozniak, S. & Jasani, B. 2004. Use of tissue microarray for interlaboratory validation of HER2 immunocytochemical and FISH testing. *J. Clin. Pathol.,* 57**,** 1140-1144.

Kay, E.W., Barry Walsh, C.J., Whelan, D., O'grady, A. & Leader, M.B. 1996. Inter-observer variation of p53 immunohistochemistry--an assessment of a practical problem and comparison with other studies. *British journal of biomedical science,* 53**,** 101-107.

Kelly, C. & Cassidy, J. 2007. Chemotherapy in metastatic colorectal cancer. *Surg. Oncol.,* 16**,** 65-70.

Kepkay, R., Attwood, K.M., Ziv, Y., Shiloh, Y. & Dellaire, G. 2011. KAP1 depletion increases PML nuclear body number in concert with ultrastructural changes in chromatin. *Cell cycle,* 10**,** 308-22.

Kerick, M., Isau, M., Timmermann, B., Sultmann, H., Herwig, R., Krobitsch, S., Schaefer, G., Verdorfer, I., Bartsch, G., Klocker, H., Lehrach, H. & Schweiger, M.R. 2011. Targeted high throughput sequencing in clinical cancer settings: formaldehyde fixed-paraffin embedded (FFPE) tumor tissues, input amount and tumor heterogeneity. *BMC Med. Genomics,* 4**,** 68.

Kiernan, J.A. 2010. *Histological and histochemical methods : theory and practice,* Banbury, Scion Publishing Limited.

Kijanka, G., Hector, S., Kay, E.W., Murray, F., Cummins, R., Murphy, D., Maccraith, B.D., Prehn, J.H. & Kenny, D. 2010. Human IgG antibody profiles differentiate between symptomatic patients with and without colorectal cancer. *Gut,* 59**,** 69-78.

Kim, S.S., Chen, Y.M., O'leary, E., Witzgall, R., Vidal, M. & Bonventre, J.V. 1996. A novel member of the RING finger family, KRIP-1, associates with the KRAB-A transcriptional repressor domain of zinc finger proteins. *Proc. Natl. Acad. Sci. U. S. A.,* 93**,** 15299-304.

Kindler, H. & Shulman, K. 2001. Metastatic colorectal cancer. *Curr. Treat. Options Oncol.,* 2**,** 459-471.

Kirklin, J.W., Dockerty, M.B. & Waugh, J.M. 1949. The role of the peritoneal reflection in the prognosis of carcinoma of the rectum and sigmoid colon. *Surg. Gynecol. Obstet.,* 88**,** 326-31.

Knudson, A.G. 2002. Cancer genetics. *Am. J. Med. Genet.,* 111**,** 96-102.

Kolesnick, R. & Fuks, Z. 2003. Radiation and ceramide-induced apoptosis. *Oncogene,* 22**,** 5897-906.

Kononen, J., Bubendorf, L., Kallioniemi, A., Barlund, M., Schraml, P., Leighton, S., Torhorst, J., Mihatsch, M.J., Sauter, G. & Kallioniemi, O.P. 1998. Tissue microarrays for high-throughput molecular profiling of tumor specimens. *Nat. Med.,* 4**,** 844-7.

Koybasi, S., Senkal, C.E., Sundararaj, K., Spassieva, S., Bielawski, J., Osta, W., Day, T.A., Jiang, J.C., Jazwinski, S.M., Hannun, Y.A., Obeid, L.M. & Ogretmen, B. 2004. Defects in cell growth regulation by C18:0-ceramide and longevity assurance gene 1 in human head and neck squamous cell carcinomas. *J. Biol. Chem.,* 279**,** 44311-9.

Kyndi, M., Sørensen, F.B., Knudsen, H., Overgaard, M., Nielsen, H.M., Andersen, J. & Overgaard, J. 2008. Tissue microarrays compared with whole sections and biochemical analyses. A subgroup analysis of DBCG 82 b&c. *Acta Oncol.,* 47**,** 591-599.

Lahiri, S. & Futerman, A.H. 2005. LASS5 Is a Bona Fide Dihydroceramide Synthase That Selectively Utilizes Palmitoyl-CoA as Acyl Donor. *J. Biol. Chem.,* 280**,** 33735-33738.

Lavieu, G., Scarlatti, F., Sala, G., Carpentier, S., Levade, T., Ghidoni, R., Botti, J. & Codogno, P. 2006. Regulation of autophagy by sphingosine kinase 1 and its role in cell survival during nutrient starvation. *J. Biol. Chem.,* 281**,** 8518-27.

Le Douarin, B., You, J., Nielsen, A.L., Chambon, P. & Losson, R. 1998. TIF1α: A possible link between KRAB zinc finger proteins and nuclear receptors1. *The Journal of Steroid Biochemistry and Molecular Biology,* 65**,** 43-50.

Lee, G.H., Malietzis, G., Askari, A., Bernardo, D., Al-Hassi, H.O. & Clark, S.K. 2014. Is right-sided colon cancer different to left-sided colorectal cancer? – A systematic review. *European Journal of Surgical Oncology (EJSO)*.

Levy, M. & Futerman, A.H. 2010. Mammalian ceramide synthases. *IUBMB Life,* 62**,** 347-356.

Liang, C.C., Park, A.Y. & Guan, J.-L. 2007. In vitro scratch assay: a convenient and inexpensive method for analysis of cell migration in vitro. *Nat. Protoc.,* 2**,** 329-333.

Lièvre, A., Bachet, J.-B., Le Corre, D., Boige, V., Landi, B., Emile, J.-F., Côté, J.-F., Tomasic, G., Penna, C., Ducreux, M., Rougier, P., Penault-Llorca, F. & Laurent-Puig, P. 2006. KRAS Mutation Status Is Predictive of Response to Cetuximab Therapy in Colorectal Cancer. *Cancer Res.,* 66**,** 3992-3995.

Lim, S.B., Yu, C.S., Jang, S.J., Kim, T.W., Kim, J.H. & Kim, J.C. 2010. Prognostic significance of lymphovascular invasion in sporadic colorectal cancer. *Dis. Colon Rectum,* 53**,** 377-84.

Liotta, L.A., Espina, V., Mehta, A.I., Calvert, V., Rosenblatt, K., Geho, D., Munson, P.J., Young, L., Wulfkuhle, J. & Petricoin Iii, E.F. 2003. Protein microarrays: Meeting analytical challenges for clinical applications. *Cancer Cell,* 3**,** 317-325.

Liotta, L.A. & Kohn, E.C. 2001. The microenvironment of the tumour-host interface. *Nature,* 411**,** 375-9.

Logan, C.Y. & Nusse, R. 2004. THE WNT SIGNALING PATHWAY IN DEVELOPMENT AND DISEASE. *Annu. Rev. Cell Dev. Biol.,* 20**,** 781-810.

Maas, M., Rutten, I.G., Nelemans, P., Lambregts, D.J., Cappendijk, V., Beets, G. & Beets-Tan, R.H. 2011. What is the most accurate whole-body imaging modality for assessment of local and distant recurrent disease in colorectal cancer? A meta-analysis. *Eur. J. Nucl. Med. Mol. Imaging,* 38**,** 1560-1571.

Maes, H., Rubio, N., Garg, A.D. & Agostinis, P. 2013. Autophagy: shaping the tumor microenvironment and therapeutic response. *Trends Mol. Med.,* 19**,** 428-46.

Mammano, E., Galdi, F., Pierobon, M., Tessari, E., Deng, J., Pucciarelli, S., Agostini, M., De Marchi, F., Canzonieri, V., De Paoli, A., Belluco, C., Liotta, L., Petricoin, E., Pilati, P. & Nitti, D. 2012. Multiplexed protein signal pathway mapping identifies patients with rectal cancer that responds to neoadjuvant treatment. *Clin. Colorectal Cancer,* 11**,** 268-74.

Mao, C., Xu, R., Bielawska, A. & Obeid, L.M. 2000. Cloning of an Alkaline Ceramidase from Saccharomyces cerevisiae : AN ENZYME WITH REVERSE (CoA-INDEPENDENT) CERAMIDE SYNTHASE ACTIVITY. *Journal of Biological Chemistry,* 275**,** 6876-6884.

Mariadason, J.M., Arango, D., Shi, Q., Wilson, A.J., Corner, G.A., Nicholas, C., Aranes, M.J., Lesser, M., Schwartz, E.L. & Augenlicht, L.H. 2003. Gene Expression Profiling-Based Prediction of Response of Colon Carcinoma Cells to 5-Fluorouracil and Camptothecin. *Cancer Res.,* 63**,** 8791-8812.

Martenson, J.A., Willett, C.G., Sargent, D.J., Mailliard, J.A., Donohue, J.H., Gunderson, L.L., Thomas, C.R., Fisher, B., Benson, A.B., Myerson, R. & Goldberg, R.M. 2004. Phase III Study of Adjuvant Chemotherapy and Radiation Therapy Compared With Chemotherapy Alone in the Surgical Adjuvant Treatment of Colon Cancer: Results of Intergroup Protocol 0130. *J. Clin. Oncol.,* 22**,** 3277-3283.

Maughan, T.S., Adams, R.A., Smith, C.G., Meade, A.M., Seymour, M.T., Wilson, R.H., Idziaszczyk, S., Harris, R., Fisher, D., Kenny, S.L., Kay, E., Mitchell, J.K., Madi, A., Jasani, B., James, M.D., Bridgewater, J., Kennedy, M.J., Claes, B., Lambrechts, D., Kaplan, R. & Cheadle, J.P. 2011. Addition of cetuximab to oxaliplatin-based first-line combination chemotherapy for treatment of advanced colorectal cancer: results of the randomised phase 3 MRC COIN trial. *The Lancet,* 377**,** 2103-2114.

Mellert, H.S., Stanek, T.J., Sykes, S.M., Rauscher, F.J., 3rd, Schultz, D.C. & Mcmahon, S.B. 2011. Deacetylation of the DNA-binding domain regulates p53-mediated apoptosis. *J Biol Chem,* 286**,** 4264-70.

Mérino, D., Khaw, S.L., Glaser, S.P., Anderson, D.J., Belmont, L.D., Wong, C., Yue, P., Robati, M., Phipson, B., Fairlie, W.D., Lee, E.F., Campbell, K.J., Vandenberg, C.J., Cory, S., Roberts, A.W., Ludlam, M.J.C., Huang, D.C.S. & Bouillet, P. 2012. Bcl-2, Bcl-xL, and Bcl-w are not equivalent targets of ABT-737 and navitoclax (ABT-263) in lymphoid and leukemic cells. *Blood,* 119**,** 5807-5816.

Meroni, G. & Diez-Roux, G. 2005. TRIM/RBCC, a novel class of single protein RING finger E3 ubiquitin ligases. *Bioessays,* 27**,** 1147-1157.

Merrill, A.H. 2002. De Novo Sphingolipid Biosynthesis: A Necessary, but Dangerous, Pathway. *J. Biol. Chem.,* 277**,** 25843-25846.

Messerschmidt, D.M., De Vries, W., Ito, M., Solter, D., Ferguson-Smith, A. & Knowles, B.B. 2012. Trim28 is required for epigenetic stability during mouse oocyte to embryo transition. *Science,* 335**,** 1499-502.

Min, J., Mesika, A., Sivaguru, M., Van Veldhoven, P.P., Alexander, H., Futerman, A.H. & Alexander, S. 2007. (Dihydro)ceramide synthase 1 regulated sensitivity to cisplatin is associated with the activation of p38 mitogen-activated protein kinase and is abrogated by sphingosine kinase 1. *Mol. Cancer Res.,* 5**,** 801-12.

Mizutani, Y., Kihara, A. & Igarashi, Y. 2005. Mammalian Lass6 and its related family members regulate synthesis of specific ceramides. *Biochem. J.,* 390**,** 263-271.

Mizutani, Y., Kihara, A. & Igarashi, Y. 2006. LASS3 (longevity assurance homologue 3) is a mainly testis-specific (dihydro)ceramide synthase with relatively broad substrate specificity. *Biochem. J.,* 398**,** 531-8.

Moertel, C.G., Fleming, T.R., Macdonald, J.S., Haller, D.G., Laurie, J.A., Goodman, P.J., Ungerleider, J.S., Emerson, W.A., Tormey, D.C. & Glick, J.H. 1990. Levamisole and fluorouracil for adjuvant therapy of resected colon carcinoma. *N. Engl. J. Med.,* 322**,** 352-358.

Moosmann, P., Georgiev, O., Le Douarin, B., Bourquin, J.P. & Schaffner, W. 1996. Transcriptional repression by RING finger protein TIF1 beta that interacts with the KRAB repressor domain of KOX1. *Nucleic Acids Res.,* 24**,** 4859-67.

Morales, A., Lee, H., Goni, F.M., Kolesnick, R. & Fernandez-Checa, J.C. 2007. Sphingolipids and cell death. *Apoptosis : an international journal on programmed cell death,* 12**,** 923-39.

Mueller, C., Liotta, L.A. & Espina, V. 2010. Reverse phase protein microarrays advance to use in clinical trials. *Mol. Oncol.,* 4**,** 461-81.

Mueller, C. 2013. Reverse Phase Protein Microarray Analysis Suite. http://capmm.gmu.edu/rpma-analysis-suite.

Mullen, T.D., Hannun, Y.A. & Obeid, L.M. 2012. Ceramide synthases at the centre of sphingolipid metabolism and biology. *Biochem. J.,* 441**,** 789-802.

Mullen, T.D. & Obeid, L.M. 2012. Ceramide and apoptosis: exploring the enigmatic connections between sphingolipid metabolism and programmed cell death. *Anticancer Agents Med. Chem.,* 12**,** 340-63.

Nakamura, N., Ruebel, K., Jin, L., Qian, X., Zhang, H. & Lloyd, R.V. 2007. Laser capture microdissection for analysis of single cells. *Methods Mol. Med.,* 132**,** 11-8.

Nakazono, M., Qiu, F., Borsuk, L.A. & Schnable, P.S. 2003. Laser-capture microdissection, a tool for the global analysis of gene expression in specific plant cell types: identification of genes expressed differentially in epidermal cells or vascular tissues of maize. *Plant Cell,* 15**,** 583-96.

National Cancer Registry Ireland 2006. Trends in Irish cancer incidence 1994-2002, with projections to 2020.

Nawa, T., Kato, J., Kawamoto, H., Okada, H., Yamamoto, H., Kohno, H., Endo, H. & Shiratori, Y. 2008. Differences between right- and left-sided colon cancer in patient characteristics, cancer morphology and histology. *J. Gastroenterol. Hepatol.,* 23**,** 418-23.

Ogawa, E., Takenaka, K., Yanagihara, K., Kurozumi, M., Manabe, T., Wada, H. & Tanaka, F. 2004. Clinical significance of VEGF-C status in tumour cells and stromal macrophages in non-small cell lung cancer patients. *Br. J. Cancer,* 91**,** 498-503.

Ogretmen, B. & Hannun, Y.A. 2004. Biologically active sphingolipids in cancer pathogenesis and treatment. *Nat. Rev. Cancer,* 4**,** 604-616.

Okamoto, K., Kitabayashi, I. & Taya, Y. 2006. KAP1 dictates p53 response induced by chemotherapeutic agents via Mdm2 interaction. *Biochem Biophys Res Commun,* 351**,** 216-22.

Olivera, A., Rosenthal, J. & Spiegel, S. 1994. Sphingosine Kinase from Swiss 3T3 Fibroblasts: A Convenient Assay for the Measurement of Intracellular Levels of Free Sphingoid Bases. *Anal Biochem,* 223**,** 306-312.

Onel, K. & Cordon-Cardo, C. 2004. MDM2 and Prognosis. *Mol. Cancer Res.,* 2**,** 1-8.

Ozato, K., Shin, D.-M., Chang, T.-H. & Morse, H.C. 2008. TRIM family proteins and their emerging roles in innate immunity. *Nat. Rev. Immunol.,* 8**,** 849-860.

Paweletz, C.P., Charboneau, L., Bichsel, V.E., Simone, N.L., Chen, T., Gillespie, J.W., Emmert-Buck, M.R., Roth, M.J., Petricoin, I.E. & Liotta, L.A. 2001. Reverse phase protein microarrays which capture disease progression show activation of pro-survival pathways at the cancer invasion front. *Oncogene,* 20**,** 1981-9.

Peeters, M., Oliner, K.S., Parker, A., Siena, S., Van Cutsem, E., Huang, J., Humblet, Y., Van Laethem, J.-L., André, T., Wiezorek, J., Reese, D. & Patterson, S.D. 2013. Massively Parallel Tumor Multigene Sequencing to Evaluate Response to Panitumumab in a Randomized Phase III Study of Metastatic Colorectal Cancer. *Clin. Cancer Res.,* 19**,** 1902-1912.

Peng, H., Zheng, L., Lee, W.H., Rux, J.J. & Rauscher, F.J., 3rd 2002. A common DNA-binding site for SZF1 and the BRCA1-associated zinc finger protein, ZBRK1. *Cancer Res.,* 62**,** 3773-81.

Petricoin, E.F., 3rd, Bichsel, V.E., Calvert, V.S., Espina, V., Winters, M., Young, L., Belluco, C., Trock, B.J., Lippman, M., Fishman, D.A., Sgroi, D.C., Munson, P.J., Esserman, L.J. & Liotta, L.A. 2005. Mapping molecular networks using

proteomics: a vision for patient-tailored combination therapy. *J. Clin. Oncol.,* 23**,** 3614-21.

Petricoin, E.F., 3rd, Espina, V., Araujo, R.P., Midura, B., Yeung, C., Wan, X., Eichler, G.S., Johann, D.J., Jr., Qualman, S., Tsokos, M., Krishnan, K., Helman, L.J. & Liotta, L.A. 2007. Phosphoprotein pathway mapping: Akt/mammalian target of rapamycin activation is negatively associated with childhood rhabdomyosarcoma survival. *Cancer Res.,* 67**,** 3431-40.

Pewzner-Jung, Y., Ben-Dor, S. & Futerman, A.H. 2006. When Do Lasses (Longevity Assurance Genes) Become CerS (Ceramide Synthases)? *J. Biol. Chem.,* 281**,** 25001-25005.

Polyak, K. 2007. Breast cancer: origins and evolution. *The Journal of Clinical Investigation,* 117**,** 3155-3163.

Ponz De Leon, M. & Percesepe, A. 2000. Pathogenesis of colorectal cancer. *Dig. Liver Dis.,* 32**,** 807-821.

Popat, S., Hubner, R. & Houlston, R.S. 2005. Systematic review of microsatellite instability and colorectal cancer prognosis. *J. Clin. Oncol.,* 23**,** 609-618.

Program, N.T. 2011. NTP 12th Report on Carcinogens. *Report on carcinogens: carcinogen profiles/US Dept. of Health and Human Services, Public Health Service, National Toxicology Program,* 12**,** iii.

Pyne, N.J. & Pyne, S. 2010. Sphingosine 1-phosphate and cancer. *Nat Rev Cancer,* 10**,** 489-503.

Qin, Z., Dai, L., Trillo-Tinoco, J., Senkal, C., Wang, W., Reske, T., Bonstaff, K., Del Valle, L., Rodriguez, P., Flemington, E., Voelkel-Johnson, C., Smith, C.D., Ogretmen, B. & Parsons, C. 2014. Targeting sphingosine kinase induces apoptosis and tumor regression for KSHV-associated primary effusion lymphoma. *Mol. Cancer Ther.,* 13**,** 154-64.

Renert, A.F., Leprince, P., Dieu, M., Renaut, J., Raes, M., Bours, V., Chapelle, J.P., Piette, J., Merville, M.P. & Fillet, M. 2009. The proapoptotic C16-ceramide-dependent pathway requires the death-promoting factor Btf in colon adenocarcinoma cells. *Journal of proteome research,* 8**,** 4810-22.

Reymond, A., Meroni, G., Fantozzi, A., Merla, G., Cairo, S., Luzi, L., Riganelli, D., Zanaria, E., Messali, S., Cainarca, S., Guffanti, A., Minucci, S., Pelicci, P.G. & Ballabio, A. 2001. The tripartite motif family identifies cell compartments. *The EMBO Journal,* 20**,** 2140-2151.

Richman, S.D., Seymour, M.T., Chambers, P., Elliott, F., Daly, C.L., Meade, A.M., Taylor, G., Barrett, J.H. & Quirke, P. 2009. KRAS and BRAF Mutations in Advanced Colorectal Cancer Are Associated With Poor Prognosis but Do Not Preclude Benefit From Oxaliplatin or Irinotecan: Results From the MRC FOCUS Trial. *J. Clin. Oncol.,* 27**,** 5931-5937.

Riebeling, C., Allegood, J.C., Wang, E., Merrill, A.H. & Futerman, A.H. 2003. Two Mammalian Longevity Assurance Gene (LAG1) Family Members, trh1 and trh4, Regulate Dihydroceramide Synthesis Using Different Fatty Acyl-CoA Donors. *J. Biol. Chem.,* 278**,** 43452-43459.

Ronnov-Jessen, L., Petersen, O.W. & Bissell, M.J. 1996. Cellular changes involved in conversion of normal to malignant breast: importance of the stromal reaction. *Physiol. Rev.,* 76**,** 69-125.

Rosenberg, S.A. 2010. CAR T Cell Receptor Immunotherapy Targeting VEGFR2 for Patients With Metastatic Cancer. *ClinicalTrials.gov,* National Cancer Institute (NCI). Bethesda, MD, US. **,** NLM Identifier: NCT01218867.

Rowe, H.M., Jakobsson, J., Mesnard, D., Rougemont, J., Reynard, S., Aktas, T., Maillard, P.V., Layard-Liesching, H., Verp, S., Marquis, J., Spitz, F., Constam,

D.B. & Trono, D. 2010. KAP1 controls endogenous retroviruses in embryonic stem cells. *Nature,* 463**,** 237-40.

Ruan, W. & Lai, M. 2007. Actin, a reliable marker of internal control? *Clin. Chim. Acta,* 385**,** 1-5.

Ruckhaberle, E., Holtrich, U., Engels, K., Hanker, L., Gatje, R., Metzler, D., Karn, T., Kaufmann, M. & Rody, A. 2009a. Acid ceramidase 1 expression correlates with a better prognosis in ER-positive breast cancer. *Climacteric : the journal of the International Menopause Society,* 12**,** 502-13.

Ruckhaberle, E., Karn, T., Rody, A., Hanker, L., Gatje, R., Metzler, D., Holtrich, U. & Kaufmann, M. 2009b. Gene expression of ceramide kinase, galactosyl ceramide synthase and ganglioside GD3 synthase is associated with prognosis in breast cancer. *J. Cancer Res. Clin. Oncol.,* 135**,** 1005-13.

Russo, S.B., Baicu, C.F., Van Laer, A., Geng, T., Kasiganesan, H., Zile, M.R. & Cowart, L.A. 2012. Ceramide synthase 5 mediates lipid-induced autophagy and hypertrophy in cardiomyocytes. *J. Clin. Invest.,* 122**,** 3919-30.

Ryan, G.B., Cliff, W.J., Gabbiani, G., Irle, C., Statkov, P.R. & Majno, G. 1973. Myofibroblasts in an avascular fibrous tissue. *Lab. Invest.,* 29**,** 197-206.

Schägger, H. & Von Jagow, G. 1987. Tricine-sodium dodecyl sulfate-polyacrylamide gel electrophoresis for the separation of proteins in the range from 1 to 100 kDa. *Anal. Biochem.,* 166**,** 368-379.

Schiffmann, S., Sandner, J., Birod, K., Wobst, I., Angioni, C., Ruckhaberle, E., Kaufmann, M., Ackermann, H., Lotsch, J., Schmidt, H., Geisslinger, G. & Grosch, S. 2009. Ceramide synthases and ceramide levels are increased in breast cancer tissue. *Carcinogenesis,* 30**,** 745-52.

Schiffmann, S., Ziebell, S., Sandner, J., Birod, K., Deckmann, K., Hartmann, D., Rode, S., Schmidt, H., Angioni, C., Geisslinger, G. & Grösch, S. 2010. Activation of

ceramide synthase 6 by celecoxib leads to a selective induction of C16:0-ceramide. *Biochemical Pharmacology,* 80**,** 1632-1640.

Schmoll, H.J., Van Cutsem, E., Stein, A., Valentini, V., Glimelius, B., Haustermans, K., Nordlinger, B., Van De Velde, C.J., Balmana, J., Regula, J., Nagtegaal, I.D., Beets-Tan, R.G., Arnold, D., Ciardiello, F., Hoff, P., Kerr, D., Köhne, C.H., Labianca, R., Price, T., Scheithauer, W., Sobrero, A., Tabernero, J., Aderka, D., Barroso, S., Bodoky, G., Douillard, J.Y., El Ghazaly, H., Gallardo, J., Garin, A., Glynne-Jones, R., Jordan, K., Meshcheryakov, A., Papamichail, D., Pfeiffer, P., Souglakos, I., Turhal, S. & Cervantes, A. 2012. ESMO Consensus Guidelines for management of patients with colon and rectal cancer. A personalized approach to clinical decision making. *Ann. Oncol.,* 23**,** 2479-2516.

Schor, S.L., Schor, A.M., Grey, A.M. & Rushton, G. 1988. Foetal and cancer patient fibroblasts produce an autocrine migration-stimulating factor not made by normal adult cells. *J. Cell Sci.,* 90 (Pt 3)**,** 391-9.

Schultz, D.C., Ayyanathan, K., Negorev, D., Maul, G.G. & Rauscher, F.J. 2002. SETDB1: a novel KAP-1-associated histone H3, lysine 9-specific methyltransferase that contributes to HP1-mediated silencing of euchromatic genes by KRAB zinc-finger proteins. *Genes Dev.,* 16**,** 919-932.

Schultz, D.C., Friedman, J.R. & Rauscher, F.J., 3rd 2001. Targeting histone deacetylase complexes via KRAB-zinc finger proteins: the PHD and bromodomains of KAP-1 form a cooperative unit that recruits a novel isoform of the Mi-2alpha subunit of NuRD. *Genes Dev.,* 15**,** 428-43.

Scott, N., Sagar, P., Stewart, J., Blair, G.E., Dixon, M.F. & Quirke, P. 1991. p53 in colorectal cancer: clinicopathological correlation and prognostic significance. *Br. J. Cancer,* 63**,** 317-319.

Selzner, M., Bielawska, A., Morse, M.A., Rüdiger, H.A., Sindram, D., Hannun, Y.A. & Clavien, P.-A. 2001. Induction of Apoptotic Cell Death and Prevention of Tumor Growth by Ceramide Analogues in Metastatic Human Colon Cancer. *Cancer Research,* 61**,** 1233-1240.

Senkal, C.E., Ponnusamy, S., Bielawski, J., Hannun, Y.A. & Ogretmen, B. 2010. Antiapoptotic roles of ceramide-synthase-6-generated C16-ceramide via selective regulation of the ATF6/CHOP arm of ER-stress-response pathways. *FASEB J.,* 24**,** 296-308.

Senkal, C.E., Ponnusamy, S., Manevich, Y., Meyers-Needham, M., Saddoughi, S.A., Mukhopadyay, A., Dent, P., Bielawski, J. & Ogretmen, B. 2011. Alteration of ceramide synthase 6/C16-ceramide induces activating transcription factor 6-mediated endoplasmic reticulum (ER) stress and apoptosis via perturbation of cellular Ca2+ and ER/Golgi membrane network. *J. Biol. Chem.,* 286**,** 42446-58.

Sentelle, R.D., Senkal, C.E., Jiang, W., Ponnusamy, S., Gencer, S., Selvam, S.P., Ramshesh, V.K., Peterson, Y.K., Lemasters, J.J., Szulc, Z.M., Bielawski, J. & Ogretmen, B. 2012. Ceramide targets autophagosomes to mitochondria and induces lethal mitophagy. *Nat. Chem. Biol.,* 8**,** 831-8.

Seung, L.P., Seung, S.K. & Schreiber, H. 1995. Antigenic cancer cells that escape immune destruction are stimulated by host cells. *Cancer Res.,* 55**,** 5094-5100.

Sheehan, K.M., Calvert, V.S., Kay, E.W., Lu, Y., Fishman, D., Espina, V., Aquino, J., Speer, R., Araujo, R., Mills, G.B., Liotta, L.A., Petricoin, E.F., 3rd & Wulfkuhle, J.D. 2005. Use of reverse phase protein microarrays and reference standard development for molecular network analysis of metastatic ovarian carcinoma. *Mol. Cell. Proteomics,* 4**,** 346-55.

Sheehan, K.M., Gulmann, C., Eichler, G.S., Weinstein, J.N., Barrett, H.L., Kay, E.W., Conroy, R.M., Liotta, L.A. & Petricoin, E.F., Iii 2007. Signal pathway profiling of

epithelial and stromal compartments of colonic carcinoma reveals epithelial-mesenchymal transition. *Oncogene,* 27**,** 323-331.

Shinya, H. & Wolff, W.I. 1979. Morphology, anatomic distribution and cancer potential of colonic polyps. *Ann. Surg.,* 190**,** 679-683.

Sliva, D., Mason, R., Xiao, H. & English, D. 2000. Enhancement of the Migration of Metastatic Human Breast Cancer Cells by Phosphatidic Acid. *Biochem. Biophys. Res. Commun.,* 268**,** 471-479.

Sloan, E.K., Ciocca, D.R., Pouliot, N., Natoli, A., Restall, C., Henderson, M.A., Fanelli, M.A., Cuello-Carrion, F.D., Gago, F.E. & Anderson, R.L. 2009a. Stromal cell expression of caveolin-1 predicts outcome in breast cancer. *Am. J. Pathol.,* 174**,** 2035-43.

Stetler-Stevenson, W.G., Aznavoorian, S. & Liotta, L.A. 1993. Tumor cell interactions with the extracellular matrix during invasion and metastasis. *Annu. Rev. Cell Biol.,* 9**,** 541-573.

Strambu, V., Garofil, D., Pop, F., Radu, P., Bratucu, M. & Popa, F. 2014. Translating clinical research of Molecular Biology into a personalized, multidisciplinary approach of colorectal cancer patients. *J. Med. Life,* 7**,** 17-26.

Stuelten, C.H., Busch, J.I., Tang, B., Flanders, K.C., Oshima, A., Sutton, E., Karpova, T.S., Roberts, A.B., Wakefield, L.M. & Niederhuber, J.E. 2010. Transient tumor-fibroblast interactions increase tumor cell malignancy by a TGF-Beta mediated mechanism in a mouse xenograft model of breast cancer. *PLoS One,* 5**,** e9832.

Taniguchi, M., Kitatani, K., Kondo, T., Hashimoto-Nishimura, M., Asano, S., Hayashi, A., Mitsutake, S., Igarashi, Y., Umehara, H., Takeya, H., Kigawa, J. & Okazaki, T. 2012. Regulation of Autophagy and Its Associated Cell Death by “Sphingolipid Rheostat”: RECIPROCAL ROLE OF CERAMIDE AND SPHINGOSINE 1-

PHOSPHATE IN THE MAMMALIAN TARGET OF RAPAMYCIN PATHWAY. *J. Biol. Chem.,* 287**,** 39898-39910.

Teppo, S., Sundquist, E., Vered, M., Holappa, H., Parkkisenniemi, J., Rinaldi, T., Lehenkari, P., Grenman, R., Dayan, D., Risteli, J., Salo, T. & Nyberg, P. 2013. The hypoxic tumor microenvironment regulates invasion of aggressive oral carcinoma cells. *Exp. Cell Res.,* 319**,** 376-89.

Thomson, T.A., Zhou, C., Chu, C. & Knight, B. 2009. Tissue Microarray for Routine Analysis of Breast Biomarkers in the Clinical Laboratory. *Am. J. Clin. Pathol.,* 132**,** 899-905.

Tlsty, T.D. & Hein, P.W. 2001. Know thy neighbor: stromal cells can contribute oncogenic signals. *Current Opinion in Genetics & Development,* 11**,** 54-59.

Tosato, M., Zamboni, V., Ferrini, A. & Cesari, M. 2007. The aging process and potential interventions to extend life expectancy. *Clin. Interv. Aging,* 2**,** 401-412.

Turnbull, R.B., Jr., Kyle, K., Watson, F.R. & Spratt, J. 1967. Cancer of the colon: the influence of the no-touch isolation technic on survival rates. *Ann. Surg.,* 166**,** 420-7.

Van Brocklyn, J.R. & Williams, J.B. 2012. The control of the balance between ceramide and sphingosine-1-phosphate by sphingosine kinase: Oxidative stress and the seesaw of cell survival and death. *Comparative Biochemistry and Physiology Part B: Biochemistry and Molecular Biology,* 163**,** 26-36.

Van Schaeybroeck, S., Allen, W.L., Turkington, R.C. & Johnston, P.G. 2011. Implementing prognostic and predictive biomarkers in CRC clinical trials. *Nat. Rev. Clin. Oncol.,* 8**,** 222-232.

Vanmeter, A., Signore, M., Pierobon, M., Espina, V., Liotta, L.A. & Petricoin, E.F., 3rd 2007. Reverse-phase protein microarrays: application to biomarker discovery and translational medicine. *Expert Rev Mol Diagn,* 7**,** 625-33.

Venable, M.E. & Yin, X. 2009. Ceramide induces endothelial cell senescence. *Cell Biochem. Funct.,* 27**,** 547-551.

Venkataraman, K. & Futerman, A.H. 2002. Do longevity assurance genes containing Hox domains regulate cell development via ceramide synthesis? *FEBS Lett.,* 528**,** 3-4.

Venkataraman, K., Riebeling, C., Bodennec, J., Riezman, H., Allegood, J.C., Sullards, M.C., Merrill, A.H. & Futerman, A.H. 2002. Upstream of Growth and Differentiation Factor 1 (uog1), a Mammalian Homolog of the Yeast Longevity Assurance Gene 1 (LAG1), RegulatesN-Stearoyl-sphinganine (C18-(Dihydro)ceramide) Synthesis in a Fumonisin B1-independent Manner in Mammalian Cells. *J. Biol. Chem.,* 277**,** 35642-35649.

Venkov, C., Plieth, D., Ni, T., Karmaker, A., Bian, A., George, A.L., Jr. & Neilson, E.G. 2011. Transcriptional Networks in Epithelial-Mesenchymal Transition. *PLoS One,* 6**,** e25354.

Venkov, C.D., Link, A.J., Jennings, J.L., Plieth, D., Inoue, T., Nagai, K., Xu, C., Dimitrova, Y.N., Rauscher, F.J. & Neilson, E.G. 2007. A proximal activator of transcription in epithelial-mesenchymal transition. *J. Clin. Invest.,* 117**,** 482-91.

Veret, J., Coant, N., Berdyshev, E.V., Skobeleva, A., Therville, N., Bailbe, D., Gorshkova, I., Natarajan, V., Portha, B. & Le Stunff, H. 2011. Ceramide synthase 4 and de novo production of ceramides with specific N-acyl chain lengths are involved in glucolipotoxicity-induced apoptosis of INS-1 beta-cells. *Biochem. J.,* 438**,** 177-89.

Vogelstein, B. & Kinzler, K.W. 2004. Cancer genes and the pathways they control. *Nat. Med.,* 10**,** 789-799.

Wang, C., Ivanov, A., Chen, L., Fredericks, W.J., Seto, E., Rauscher, F.J. & Chen, J. 2005. MDM2 interaction with nuclear corepressor KAP1 contributes to p53 inactivation. *EMBO J.,* 24**,** 3279-3290.

Wang, C., Rauscher, F.J., 3rd, Cress, W.D. & Chen, J. 2007. Regulation of E2F1 function by the nuclear corepressor KAP1. *J. Biol. Chem.,* 282**,** 29902-9.

Weber, F., Xu, Y., Zhang, L., Patocs, A., Shen, L., Platzer, P. & Eng, C. 2007. Microenvironmental genomic alterations and clinicopathological behavior in head and neck squamous cell carcinoma. *JAMA,* 297**,** 187-95.

Weinberg, R.A. 1996. How cancer arises. *Sci. Am.,* 275**,** 62-71.

Wen-Hui, W., Fortuna, M.B. & Furmanski, P. 1987. A rapid and efficient method for testing immunohistochemical reactivity of monoclonal antibodies against multiple tissue samples simultaneously. *J. Immunol. Methods,* 103**,** 121-129.

Whalen, J.P. 1975. Anatomy Of The Colon: Guide to Intra-abdominal Pathology Hickey Lecture, 1975. *American Journal of Roentgenology,* 125**,** 2-20.

White-Gilbertson, S., Mullen, T., Senkal, C., Lu, P., Ogretmen, B., Obeid, L. & Voelkel-Johnson, C. 2009. Ceramide synthase 6 modulates TRAIL sensitivity and nuclear translocation of active caspase-3 in colon cancer cells. *Oncogene,* 28**,** 1132-1141.

White, D.E., Negorev, D., Peng, H., Ivanov, A.V., Maul, G.G. & Rauscher, F.J., 3rd 2006. KAP1, a novel substrate for PIKK family members, colocalizes with numerous damage response factors at DNA lesions. *Cancer Res.,* 66**,** 11594-9.

Winter, E. & Ponting, C.P. 2002. TRAM, LAG1 and CLN8: members of a novel family of lipid-sensing domains? *Trends Biochem. Sci.,* 27**,** 381-383.

Wittmann, W. 1965. Aceto-Iron-Haematoxylin-Chloral Hydrate for Chromosome Staining. *Biotech. Histochem.,* 40**,** 161-164.

Wood, H.M., Belvedere, O., Conway, C., Daly, C., Chalkley, R., Bickerdike, M., Mckinley, C., Egan, P., Ross, L., Hayward, B., Morgan, J., Davidson, L., Maclennan, K., Ong, T.K., Papagiannopoulos, K., Cook, I., Adams, D.J., Taylor, G.R. & Rabbitts, P. 2010. Using next-generation sequencing for high resolution multiplex analysis of copy number variation from nanogram quantities of DNA from formalin-fixed paraffin-embedded specimens. *Nucleic Acids Res.,* 38**,** e151.

Wray, C.M., Ziogas, A., Hinojosa, M.W., Le, H., Stamos, M.J. & Zell, J.A. 2009. Tumor Subsite Location Within the Colon Is Prognostic for Survival After Colon Cancer Diagnosis. *Dis. Colon Rectum,* 52**,** 1359-1366 10.1007/DCR.0b013e3181a7b7de.

Wulfkuhle, J.D., Aquino, J.A., Calvert, V.S., Fishman, D.A., Coukos, G., Liotta, L.A. & Petricoin, E.F., 3rd 2003. Signal pathway profiling of ovarian cancer from human tissue specimens using reverse-phase protein microarrays. *Proteomics,* 3**,** 2085-90.

Wulfkuhle, J.D., Sgroi, D.C., Krutzsch, H., Mclean, K., Mcgarvey, K., Knowlton, M., Chen, S., Shu, H., Sahin, A., Kurek, R., Wallwiener, D., Merino, M.J., Petricoin, E.F., 3rd, Zhao, Y. & Steeg, P.S. 2002. Proteomics of human breast ductal carcinoma in situ. *Cancer Res.,* 62**,** 6740-9.

Wulfkuhle, J.D., Speer, R., Pierobon, M., Laird, J., Espina, V., Deng, J., Mammano, E., Yang, S.X., Swain, S.M., Nitti, D., Esserman, L.J., Belluco, C., Liotta, L.A. & Petricoin, E.F. 2008. Multiplexed Cell Signaling Analysis of Human Breast Cancer Applications for Personalized Therapy. *J. Proteome Res.,* 7**,** 1508-1517.

Yang, B., O'herrin, S.M., Wu, J., Reagan-Shaw, S., Ma, Y., Bhat, K.M., Gravekamp, C., Setaluri, V., Peters, N., Hoffmann, F.M., Peng, H., Ivanov, A.V., Simpson, A.J. & Longley, B.J. 2007. MAGE-A, mMage-b, and MAGE-C proteins form complexes

with KAP1 and suppress p53-dependent apoptosis in MAGE-positive cell lines. *Cancer Res.,* 67**,** 9954-62.

Yang, S., Wang, X., Contino, G., Liesa, M., Sahin, E., Ying, H., Bause, A., Li, Y., Stommel, J.M., Dell'antonio, G., Mautner, J., Tonon, G., Haigis, M., Shirihai, O.S., Doglioni, C., Bardeesy, N. & Kimmelman, A.C. 2011. Pancreatic cancers require autophagy for tumor growth. *Genes Dev.,* 25**,** 717-29.

Yokoe, T., Toiyama, Y., Okugawa, Y., Tanaka, K., Ohi, M., Inoue, Y., Mohri, Y., Miki, C. & Kusunoki, M. 2010. KAP1 is associated with peritoneal carcinomatosis in gastric cancer. *Ann. Surg. Oncol.,* 17**,** 821-8.

Young, G.P., John, D.J.B.S., Winawer, S.J. & Rozen, P. 2002. Choice of fecal occult blood tests for colorectal cancer screening: recommendations based on performance characteristics in population studies. *Am. J. Gastroenterol.,* 97**,** 2499-2507.

Yu, Y., Lu, H., Pan, H., Ma, J.-H., Ding, Z.-J. & Li, Y.-Y. 2006. Expression of LASS2 controlled by LAG1 or ADH1 promoters cannot functionally complement Lag1p. *Microbiol. Res.,* 161**,** 203-211.

Zauber, A.G., Winawer, S.J., O'brien, M.J., Lansdorp-Vogelaar, I., Van Ballegooijen, M., Hankey, B.F., Shi, W., Bond, J.H., Schapiro, M., Panish, J.F., Stewart, E.T. & Waye, J.D. 2012. Colonoscopic Polypectomy and Long-Term Prevention of Colorectal-Cancer Deaths. *N. Engl. J. Med.,* 366**,** 687-696.

Zhang, Q.J., Holland, W.L., Wilson, L., Tanner, J.M., Kearns, D., Cahoon, J.M., Pettey, D., Losee, J., Duncan, B., Gale, D., Kowalski, C.A., Deeter, N., Nichols, A., Deesing, M., Arrant, C., Ruan, T., Boehme, C., Mccamey, D.R., Rou, J., Ambal, K., Narra, K.K., Summers, S.A., Abel, E.D. & Symons, J.D. 2012. Ceramide Mediates Vascular Dysfunction in Diet-Induced Obesity by PP2A-Mediated Dephosphorylation of the eNOS-Akt Complex. *Diabetes,* 61**,** 1848-1859.

Ziv, Y., Bielopolski, D., Galanty, Y., Lukas, C., Taya, Y., Schultz, D.C., Lukas, J., Bekker-Jensen, S., Bartek, J. & Shiloh, Y. 2006. Chromatin relaxation in response to DNA double-strand breaks is modulated by a novel ATM-and KAP-1 dependent pathway. *Nat. Cell Biol.,* 8**,** 870-876.

Appendix 1: Buffers for protein purification under denaturing conditions

IMAC purification involves the following steps:

- Incubation of the cell lysate with Ni-NTA resin to allow the target molecule in the sample to bind to the immobilized ligand
- Washing away of non-bound sample components from the column using appropriate wash buffers that maintain the binding interaction between target and ligand
- Elution of the target molecule from the immobilized ligand by altering the buffer conditions so that the binding interaction no longer occurs.

Under denaturing conditions, the 6xHis tag on a protein will be fully exposed so that binding to the Ni-NTA matrix will improve and the efficiency of the purification procedure will be maximized by reducing the potential for nonspecific binding. Elution of the tagged proteins from the column can be achieved either by reducing the pH, or by competition with imidazole.

Lysis buffer:

Buffer A (Denaturing lysis/binding buffer, 1 Litre):

8 M Urea	480.5 g urea (60.06 g/mol)
100 mM NaH2PO4	13.80 g NaH2PO4·H2O (MW 137.99 g/mol)
100 mM Tris·Cl	12.10 g Tris base (MW 121.1 g/mol)

Adjust pH to 8.0 using HCl.

Wash buffer:

Buffer B (Denaturing wash buffer, 1 litre):

8 M Urea	480.5 g urea (60.06 g/mol)
100 mM NaH2PO4	13.80 g NaH2PO4·H2O (MW 137.99 g/mol)
100 mM Tris·Cl	12.10 g Tris base (MW 121.1 g/mol)

Adjust pH to 6.3 using HCl.

Elution buffer:

Buffer C (Denaturing elution buffer, 1 litre):

8 M Urea	480.50 g urea (60.06 g/mol)
100 mM NaH2PO4	13.80 g NaH2PO4·H2O (MW 137.99 g/mol)
100 mM Tris·Cl	12.10 g Tris base (MW 121.1 g/mol)

Adjust pH to 4.5 using HCl.

Appendix 2: Supplementary Data

In a sub-cohort of 38 patients, p53 was found to be overexpressed in 50% of CRC samples, which is consistent with previous studies.

Supplementary Table 1: p53 Immunohistochemistry Scores:

Patient No:	Tissue p53 IHC:	Tissue p53 IHC Neg=0, Weak=1, Mod=2, Strong=3
CR00213	Moderate	2
CR00240	Strong	3
CR00035	Strong	3
CR00036	Strong	3
CR00202	Strong	3
CR00223	Strong	3
CR00225	Strong	3
CR00034	Strong	3
CR00060	Strong	3
CR00227	Weak	1
CR00009	Moderate	2
CR00208	Moderate	2
CR00214	Moderate	2
CR00237	Moderate	2
CR00008	Strong	3
CR00210	Strong	3
CR00216	Strong	3
CR00222	Strong	3
CR00226	Strong	3
CR00231	Strong	3
CR00234	Strong	3
CR00037	Strong	3
CR00209	Strong	3
CR00220	Strong	3
CR00224	Strong	3
CR00022	Negative	0
CR00232	Weak	1
CR00244	Weak	1
CR00018	Weak	1
CR00253	Weak	1
CR00204	Moderate	2
CR00228	Moderate	2
CR00251	Moderate	2
CR00067	Moderate	2
CR00219	Moderate	2
CR00217	Negative	0
CR00250	Negative	0
CR00238	Negative	0

Supplementary Table 2: Spearman's Rho correlation analysis results for CerS5 Low Patients, using RPMA data.

CerS5 Low			
Source	**Target**	**Spearman ρ**	**Prob>|ρ|**
Beclin 1	Bax	0.976190476	3.3144E-05
JNK S183/185	eNos	0.976190476	3.3144E-05
MDM2	eNos	0.976190476	3.3144E-05
PI3K	mTor	0.976190476	3.3144E-05
Survivin	PI3K	0.976190476	3.3144E-05
PI3K	Beclin 1	0.952380952	0.0002604
RAGE	AMPKB s108	0.952380952	0.0002604
RAGE	Bax	0.952380952	0.0002604
Ras GFR s91	MDM2	0.952380952	0.0002604
Survivin	mTor	0.952380952	0.0002604
Bcl-2 Ser70	AMPKB s108	0.928571429	0.000862968
MDM2	JNK S183/185	0.928571429	0.000862968
Ras GFR s91	eNos	0.928571429	0.000862968
mTor	E-Cadherin	0.928571429	0.000862968
PP2A	AMPKB s108	0.928571429	0.000862968
PP2A	LC3B	0.928571429	0.000862968
RAGE	Bcl-2 Ser70	0.928571429	0.000862968
Survivin	Beclin 1	0.928571429	0.000862968
eNos	Bcl-2 Ser70	0.904761905	0.002008276
mTor	Beclin 1	0.904761905	0.002008276
PI3K	Bax	0.904761905	0.002008276
TNFR1	LC3B	0.904761905	0.002008276
VEGFR y117	Bcl-2 Ser70	0.904761905	0.002008276
Bax	SPHK1	0.904761905	0.002008276
RAGE	SPHK1	0.904761905	0.002008276
TNFR1	Cleaved Caspase 3	0.904761905	0.002008276
TNFR1	Cleaved Caspase 7	0.904761905	0.002008276
VEGFR y117	EGFR y1045	0.904761905	0.002008276
JNK S183/185	Bcl-2 Ser70	0.880952381	0.00385032
mTor	Bax	0.880952381	0.00385032
RAGE	Beclin 1	0.880952381	0.00385032
Ras GFR s91	JNK S183/185	0.880952381	0.00385032
Survivin	Bax	0.880952381	0.00385032
E-Cadherin	Bcl-2 Ser70	0.880952381	0.00385032
LC3B	Cleaved Caspase 3	0.880952381	0.00385032
RAGE	PP2A	0.880952381	0.00385032
TNFR1	PP2A	0.880952381	0.00385032
EGFR y1045	E-Cadherin	0.857142857	0.006530017

mTor	AKT	0.857142857	0.006530017
PI3K	E-Cadherin	0.857142857	0.006530017
Beclin 1	SPHK1	0.857142857	0.006530017
mTor	Bcl-2 Ser70	0.857142857	0.006530017
AMPKB s108	SPHK1	0.833333333	0.01017554
Bax	AMPKB s108	0.833333333	0.01017554
PI3K	AKT	0.833333333	0.01017554
Bcl-2 Ser70	Bax	0.833333333	0.01017554
EGFR y1148	Beclin 1	0.833333333	0.01017554
EGFR y1148	Cleaved Caspase 7	0.833333333	0.01017554
eNos	AMPKB s108	0.833333333	0.01017554
JNK S183/185	E-Cadherin	0.833333333	0.01017554
LC3B	EGFR y1045	0.833333333	0.01017554
MDM2	Bcl-2 Ser70	0.833333333	0.01017554
mTor	JNK S183/185	0.833333333	0.01017554
PP2A	SPHK1	0.833333333	0.01017554
PP2A	Bcl-2 Ser70	0.833333333	0.01017554
PP2A	Cleaved Caspase 3	0.833333333	0.01017554
RAGE	eNos	0.833333333	0.01017554
RAGE	mTor	0.833333333	0.01017554
Survivin	E-Cadherin	0.833333333	0.01017554
Survivin	EGFR y1148	0.833333333	0.01017554
VEGFR y117	AMPKB s108	0.833333333	0.01017554
EGFR y1045	Bcl-2 Ser70	0.80952381	0.014902668
RAGE	PI3K	0.80952381	0.014902668
VEGFR y117	Cox2	0.80952381	0.014902668
Cleaved Caspase 7	Beclin 1	0.80952381	0.014902668
Cox2	Bcl-2 Ser70	0.80952381	0.014902668
LC3B	Cleaved Caspase 7	0.80952381	0.014902668
PP2A	Bax	0.80952381	0.014902668
RAGE	JNK S183/185	0.80952381	0.014902668
Survivin	AKT	0.80952381	0.014902668
VEGFR y117	PP2A	0.80952381	0.014902668
Beclin 1	Bcl-2 Ser70	0.785714286	0.020815127
JNK S183/185	AKT	0.785714286	0.020815127
PI3K	Bcl-2 Ser70	0.785714286	0.020815127
PI3K	EGFR y1148	0.785714286	0.020815127
TNFR1	AMPKB s108	0.785714286	0.020815127
TNFR1	Bax	0.785714286	0.020815127
Bcl-2 Ser70	SPHK1	0.785714286	0.020815127
eNos	E-Cadherin	0.785714286	0.020815127
VEGFR y117	E-Cadherin	0.785714286	0.020815127
LC3B	AMPKB s108	0.761904762	0.028004939

PI3K	SPHK1	0.761904762	0.028004939
TNFR1	Beclin 1	0.761904762	0.028004939
TNFR1	RAGE	0.761904762	0.028004939
VEGFR y117	eNos	0.761904762	0.028004939
Cleaved Caspase 3	AMPKB s108	0.761904762	0.028004939
Cleaved Caspase 7	Bax	0.761904762	0.028004939
EGFR y1045	Cleaved Caspase 3	0.761904762	0.028004939
eNos	Cox2	0.761904762	0.028004939
JNK S183/185	AMPKB s108	0.761904762	0.028004939
MDM2	AMPKB s108	0.761904762	0.028004939
mTor	eNos	0.761904762	0.028004939
PP2A	Beclin 1	0.761904762	0.028004939
PP2A	EGFR y1045	0.761904762	0.028004939
Survivin	RAGE	0.761904762	0.028004939
TNFR1	SPHK1	0.761904762	0.028004939
Beclin 1	AMPKB s108	0.738095238	0.036552761
Cox2	AMPKB s108	0.738095238	0.036552761
E-Cadherin	AKT	0.738095238	0.036552761
E-Cadherin	Beclin 1	0.738095238	0.036552761
EGFR y1148	Bax	0.738095238	0.036552761
LC3B	Beclin 1	0.738095238	0.036552761
mTor	SPHK1	0.738095238	0.036552761
RAGE	E-Cadherin	0.738095238	0.036552761
RAGE	MDM2	0.738095238	0.036552761
Ras GFR s91	Bcl-2 Ser70	0.738095238	0.036552761
Ras GFR s91	Cox2	0.738095238	0.036552761
Survivin	Cleaved Caspase 7	0.738095238	0.036552761
VEGFR y117	LC3B	0.738095238	0.036552761
VEGFR y117	MDM2	0.738095238	0.036552761
VEGFR y117	RAGE	0.738095238	0.036552761
Cleaved Caspase 7	Cleaved Caspase 3	0.714285714	0.046528232
E-Cadherin	AMPKB s108	0.714285714	0.046528232
E-Cadherin	Bax	0.714285714	0.046528232
EGFR y1045	AMPKB s108	0.714285714	0.046528232
JNK S183/185	Bax	0.714285714	0.046528232
JNK S183/185	Cox2	0.714285714	0.046528232
LC3B	SPHK1	0.714285714	0.046528232
LC3B	Bax	0.714285714	0.046528232
MDM2	E-Cadherin	0.714285714	0.046528232
mTor	AMPKB s108	0.714285714	0.046528232
mTor	EGFR y1045	0.714285714	0.046528232
mTor	EGFR y1148	0.714285714	0.046528232
PI3K	JNK S183/185	0.714285714	0.046528232

RAGE	LC3B	0.714285714	0.046528232
Ras GFR s91	LCK y505	0.714285714	0.046528232
Survivin	SPHK1	0.714285714	0.046528232
Survivin	Bcl-2 Ser70	0.714285714	0.046528232
Beclin 1	AKT	0.69047619	0.057990318
eNos	AKT	0.69047619	0.057990318
eNos	Bax	0.69047619	0.057990318
LC3B	Bcl-2 Ser70	0.69047619	0.057990318
MDM2	Cox2	0.69047619	0.057990318
PI3K	Cleaved Caspase 7	0.69047619	0.057990318
PI3K	EGFR y1045	0.69047619	0.057990318
PP2A	Cleaved Caspase 7	0.69047619	0.057990318
RUNX1	RAGE	0.69047619	0.057990318
VEGFR y117	JNK S183/185	0.69047619	0.057990318
Bax	AKT	0.666666667	0.070987654
MDM2	AKT	0.666666667	0.070987654
mTor	MDM2	0.666666667	0.070987654
PI3K	AMPKB s108	0.666666667	0.070987654
PI3K	LC3B	0.666666667	0.070987654
PP2A	PI3K	0.666666667	0.070987654
RAGE	Cox2	0.666666667	0.070987654
Ras GFR s91	AMPKB s108	0.666666667	0.070987654
Survivin	JNK S183/185	0.666666667	0.070987654
TNFR1	Survivin	0.666666667	0.070987654
VEGFR y117	Ras GFR s91	0.666666667	0.070987654
Cleaved Caspase 7	SPHK1	0.642857143	0.085558891
EGFR y1045	Beclin 1	0.642857143	0.085558891
JNK S183/185	Beclin 1	0.642857143	0.085558891
LCK y505	eNos	0.642857143	0.085558891
PI3K	eNos	0.642857143	0.085558891
PP2A	eNos	0.642857143	0.085558891
PP2A	mTor	0.642857143	0.085558891
RAGE	Cleaved Caspase 3	0.642857143	0.085558891
RAGE	EGFR y1045	0.642857143	0.085558891
Ras GFR s91	E-Cadherin	0.642857143	0.085558891
RUNX1	Bax	0.642857143	0.085558891
Survivin	EGFR y1045	0.642857143	0.085558891
TNFR1	EGFR y1045	0.642857143	0.085558891
TNFR1	PI3K	0.642857143	0.085558891
VEGFR y117	Cleaved Caspase 3	0.642857143	0.085558891
VEGFR y117	mTor	0.642857143	0.085558891
Cleaved Caspase 3	Bcl-2 Ser70	0.619047619	0.101733037
LCK y505	JNK S183/185	0.619047619	0.101733037

MMP9	AKT	0.619047619	0.101733037
MDM2	LCK y505	0.619047619	0.101733037
MDM2	MMP9	0.619047619	0.101733037
PP2A	E-Cadherin	0.619047619	0.101733037
RAGE	Cleaved Caspase 7	0.619047619	0.101733037
RUNX1	AMPKB s108	0.619047619	0.101733037
Survivin	AMPKB s108	0.619047619	0.101733037
Survivin	LC3B	0.619047619	0.101733037
TNFR1	Bcl-2 Ser70	0.619047619	0.101733037
Bcl-2 Ser70	AKT	0.595238095	0.119529806
Cleaved Caspase 3	SPHK1	0.595238095	0.119529806
Cleaved Caspase 3	Bax	0.595238095	0.119529806
E-Cadherin	SPHK1	0.595238095	0.119529806
E-Cadherin	Cleaved Caspase 3	0.595238095	0.119529806
E-Cadherin	Cox2	0.595238095	0.119529806
EGFR y1045	Bax	0.595238095	0.119529806
eNos	SPHK1	0.595238095	0.119529806
eNos	Beclin 1	0.595238095	0.119529806
LC3B	E-Cadherin	0.595238095	0.119529806
mTor	LC3B	0.595238095	0.119529806
PP2A	MDM2	0.595238095	0.119529806
RAGE	AKT	0.595238095	0.119529806
Ras GFR s91	RAGE	0.595238095	0.119529806
RUNX1	SPHK1	0.595238095	0.119529806
RUNX1	JNK S183/185	0.595238095	0.119529806
Survivin	PP2A	0.595238095	0.119529806
TNFR1	EGFR y1148	0.595238095	0.119529806
VEGFR y117	Bax	0.595238095	0.119529806
Cleaved Caspase 3	Beclin 1	0.571428571	0.138959957
EGFR y1045	Cox2	0.571428571	0.138959957
EGFR y1148	E-Cadherin	0.571428571	0.138959957
eNos	EGFR y1045	0.571428571	0.138959957
JNK S183/185	SPHK1	0.571428571	0.138959957
LCK y505	AMPKB s108	0.571428571	0.138959957
MDM2	Bax	0.571428571	0.138959957
mTor	Cleaved Caspase 7	0.571428571	0.138959957
RUNX1	Cox2	0.571428571	0.138959957
RUNX1	eNos	0.571428571	0.138959957
Survivin	Cleaved Caspase 3	0.571428571	0.138959957
Survivin	eNos	0.571428571	0.138959957
TNFR1	mTor	0.571428571	0.138959957
VEGFR y117	SPHK1	0.571428571	0.138959957
VEGFR y117	Beclin 1	0.571428571	0.138959957

VEGFR y117	PI3K	0.571428571	0.138959957
Cleaved Caspase 7	AMPKB s108	0.547619048	0.160025643
EGFR y1045	SPHK1	0.547619048	0.160025643
EGFR y1045	Cleaved Caspase 7	0.547619048	0.160025643
JNK S183/185	EGFR y1045	0.547619048	0.160025643
LC3B	EGFR y1148	0.547619048	0.160025643
PI3K	Cleaved Caspase 3	0.547619048	0.160025643
PI3K	MDM2	0.547619048	0.160025643
PP2A	Cox2	0.547619048	0.160025643
PP2A	JNK S183/185	0.547619048	0.160025643
RAGE	EGFR y1148	0.547619048	0.160025643
VEGFR y117	TNFR1	0.547619048	0.160025643
Cox2	SPHK1	0.523809524	0.182720751
EGFR y1148	AKT	0.523809524	0.182720751
EGFR y1148	EGFR y1045	0.523809524	0.182720751
LCK y505	Cleaved Caspase 3	0.523809524	0.182720751
MDM2	EGFR y1045	0.523809524	0.182720751
mTor	Cleaved Caspase 3	0.523809524	0.182720751
Ras GFR s91	AKT	0.523809524	0.182720751
Ras GFR s91	mTor	0.523809524	0.182720751
RUNX1	Bcl-2 Ser70	0.523809524	0.182720751
EGFR y1148	SPHK1	0.5	0.20703125
LCK y505	Bcl-2 Ser70	0.5	0.20703125
LCK y505	Cox2	0.5	0.20703125
LCK y505	E-Cadherin	0.5	0.20703125
MMP9	eNos	0.5	0.20703125
PI3K	MMP9	0.5	0.20703125
RUNX1	Beclin 1	0.5	0.20703125
TNFR1	E-Cadherin	0.5	0.20703125
VEGFR y117	MMP9	0.5	0.20703125
Cox2	Bax	0.476190476	0.232935535
EGFR y1148	Bcl-2 Ser70	0.476190476	0.232935535
MMP9	E-Cadherin	0.476190476	0.232935535
MMP9	EGFR y1045	0.476190476	0.232935535
MDM2	SPHK1	0.476190476	0.232935535
MDM2	Beclin 1	0.476190476	0.232935535
mTor	Cox2	0.476190476	0.232935535
mTor	MMP9	0.476190476	0.232935535
RUNX1	LCK y505	0.476190476	0.232935535
VEGFR y117	LCK y505	0.476190476	0.232935535
VEGFR y117	Survivin	0.476190476	0.232935535
Cleaved Caspase 7	Bcl-2 Ser70	0.452380952	0.260404767
MMP9	Bcl-2 Ser70	0.452380952	0.260404767

MMP9	JNK S183/185	0.452380952	0.260404767
MMP9	LC3B	0.452380952	0.260404767
PP2A	MMP9	0.452380952	0.260404767
Survivin	MDM2	0.452380952	0.260404767
AKT	SPHK1	0.428571429	0.289403225
AMPKB s108	AKT	0.428571429	0.289403225
E-Cadherin	Cleaved Caspase 7	0.428571429	0.289403225
eNos	Cleaved Caspase 3	0.428571429	0.289403225
PP2A	EGFR y1148	0.428571429	0.289403225
RAGE	LCK y505	0.428571429	0.289403225
Ras GFR s91	EGFR y1045	0.428571429	0.289403225
Ras GFR s91	MMP9	0.428571429	0.289403225
Ras GFR s91	PP2A	0.428571429	0.289403225
RUNX1	MDM2	0.428571429	0.289403225
RUNX1	mTor	0.428571429	0.289403225
RUNX1	Ras GFR s91	0.428571429	0.289403225
LC3B	eNos	0.404761905	0.319888641
Survivin	RUNX1	0.404761905	0.319888641
TNFR1	RUNX1	0.404761905	0.319888641
Cox2	Beclin 1	0.380952381	0.351812553
EGFR y1045	AKT	0.380952381	0.351812553
EGFR y1148	AMPKB s108	0.380952381	0.351812553
EGFR y1148	Cleaved Caspase 3	0.380952381	0.351812553
LCK y505	EGFR y1045	0.380952381	0.351812553
MMP9	Beclin 1	0.380952381	0.351812553
MDM2	Cleaved Caspase 3	0.380952381	0.351812553
p53 Ser15	Cleaved Caspase 3	0.380952381	0.351812553
p53 Ser15	EGFR y1045	0.380952381	0.351812553
Ras GFR s91	Bax	0.380952381	0.351812553
RUNX1	PP2A	0.380952381	0.351812553
TNFR1	eNos	0.380952381	0.351812553
JNK S183/185	Cleaved Caspase 3	0.357142857	0.385120644
JNK S183/185	EGFR y1148	0.357142857	0.385120644
MDM2	LC3B	0.357142857	0.385120644
RAGE	MMP9	0.357142857	0.385120644
Ras GFR s91	PI3K	0.357142857	0.385120644
RUNX1	PI3K	0.357142857	0.385120644
Survivin	MMP9	0.357142857	0.385120644
VEGFR y117	Cleaved Caspase 7	0.357142857	0.385120644
LC3B	Cox2	0.333333333	0.419753086
LC3B	JNK S183/185	0.333333333	0.419753086
MMP9	AMPKB s108	0.333333333	0.419753086
MMP9	Bax	0.333333333	0.419753086

mTor	LCK y505	0.333333333	0.419753086
p53 Ser15	E-Cadherin	0.333333333	0.419753086
p53 Ser15	LCK y505	0.333333333	0.419753086
PI3K	Cox2	0.333333333	0.419753086
PP2A	AKT	0.333333333	0.419753086
PP2A	LCK y505	0.333333333	0.419753086
Ras GFR s91	SPHK1	0.333333333	0.419753086
RUNX1	EGFR y1148	0.333333333	0.419753086
TNFR1	JNK S183/185	0.333333333	0.419753086
TNFR1	LCK y505	0.333333333	0.419753086
VEGFR y117	AKT	0.333333333	0.419753086
VEGFR y117	EGFR y1148	0.333333333	0.419753086
Cleaved Caspase 7	AKT	0.30952381	0.455644891
RUNX1	Cleaved Caspase 7	0.30952381	0.455644891
Cox2	Cleaved Caspase 3	0.285714286	0.492726245
LCK y505	AKT	0.285714286	0.492726245
MMP9	Cleaved Caspase 3	0.285714286	0.492726245
Ras GFR s91	Cleaved Caspase 3	0.285714286	0.492726245
RUNX1	AKT	0.285714286	0.492726245
RUNX1	E-Cadherin	0.285714286	0.492726245
Survivin	Ras GFR s91	0.285714286	0.492726245
TNFR1	MDM2	0.285714286	0.492726245
LC3B	AKT	0.261904762	0.530922862
LCK y505	Bax	0.261904762	0.530922862
Ras GFR s91	Beclin 1	0.261904762	0.530922862
Survivin	Cox2	0.261904762	0.530922862
Survivin	LCK y505	0.261904762	0.530922862
TNFR1	AKT	0.261904762	0.530922862
TNFR1	Cox2	0.261904762	0.530922862
Cleaved Caspase 3	AKT	0.238095238	0.570156321
eNos	EGFR y1148	0.238095238	0.570156321
p53 Ser15	EGFR y1148	0.238095238	0.570156321
Survivin	p53 Ser15	0.238095238	0.570156321
VEGFR y117	RUNX1	0.238095238	0.570156321
p53 Ser15	Cleaved Caspase 7	0.214285714	0.610344416
TNFR1	p53 Ser15	0.214285714	0.610344416
JNK S183/185	Cleaved Caspase 7	0.19047619	0.651401496
LCK y505	LC3B	0.19047619	0.651401496
MMP9	SPHK1	0.19047619	0.651401496
PI3K	LCK y505	0.19047619	0.651401496
RUNX1	Cleaved Caspase 3	0.19047619	0.651401496
TNFR1	MMP9	0.19047619	0.651401496
Cox2	AKT	0.166666667	0.693238812

eNos	Cleaved Caspase 7	0.166666667	0.693238812
Ras GFR s91	LC3B	0.166666667	0.693238812
EGFR y1148	Cox2	0.142857143	0.73576486
LCK y505	Beclin 1	0.142857143	0.73576486
MMP9	Cleaved Caspase 7	0.142857143	0.73576486
MMP9	EGFR y1148	0.142857143	0.73576486
p53 Ser15	LC3B	0.142857143	0.73576486
p53 Ser15	mTor	0.142857143	0.73576486
LCK y505	SPHK1	0.119047619	0.778885726
p53 Ser15	Cox2	0.119047619	0.778885726
RUNX1	LC3B	0.119047619	0.778885726
TNFR1	Ras GFR s91	0.119047619	0.778885726
VEGFR y117	p53 Ser15	0.119047619	0.778885726
LCK y505	Cleaved Caspase 7	0.095238095	0.82250543
MDM2	EGFR y1148	0.095238095	0.82250543
PI3K	p53 Ser15	0.095238095	0.82250543
MMP9	Cox2	0.071428571	0.866526271
p53 Ser15	Bcl-2 Ser70	0.071428571	0.866526271
Cox2	Cleaved Caspase 7	0.047619048	0.910849169
LCK y505	EGFR y1148	0.047619048	0.910849169
MMP9	LCK y505	0.047619048	0.910849169
MDM2	Cleaved Caspase 7	0.047619048	0.910849169
p53 Ser15	AMPKB s108	0.047619048	0.910849169
RUNX1	EGFR y1045	0.047619048	0.910849169
p53 Ser15	SPHK1	0.023809524	0.955374012
p53 Ser15	Beclin 1	0.023809524	0.955374012
RUNX1	p53 Ser15	0	1
p53 Ser15	Bax	-0.023809524	0.955374012
PP2A	p53 Ser15	-0.023809524	0.955374012
p53 Ser15	JNK S183/185	-0.047619048	0.910849169
RAGE	p53 Ser15	-0.047619048	0.910849169
Ras GFR s91	EGFR y1148	-0.095238095	0.82250543
Ras GFR s91	p53 Ser15	-0.095238095	0.82250543
p53 Ser15	eNos	-0.119047619	0.778885726
p53 Ser15	AKT	-0.142857143	0.73576486
Ras GFR s91	Cleaved Caspase 7	-0.166666667	0.693238812
p53 Ser15	MDM2	-0.238095238	0.570156321
p53 Ser15	MMP9	-0.476190476	0.232935535

The Spearman rank correlation coefficient, ρ, was calculated for each protein pair in the RPMA quantitative expression profiles of the CerS5 Low patients (n= 9) in the fresh-frozen cohort, $\rho \geq 0.75$ with $P \leq 0.01$ was considered significant. Correlations that are unique for the CerS5 Low cohort are marked in Red. Correlations that are consistent in both the CerS5 High and Low cohorts are marked in Blue.

Supplementary Table 3: Spearman's Rho correlation analysis results for CerS5 High Patients, using RPMA data

CerS5 High			
Source	**Target**	**Spearman ρ**	**Prob>|ρ|**
PI3K	Beclin 1	0.990909091	3.76257E-09
LCK y505	EGFR y1148	0.972727273	5.14218E-07
TNFR1	Beclin 1	0.963636364	1.85204E-06
LC3B	Bcl-2 Ser70	0.954545455	4.9889E-06
TNFR1	PI3K	0.954545455	4.9889E-06
TNFR1	RAGE	0.945454545	1.1183E-05
mTor	SPHK1	0.945454545	1.1183E-05
RAGE	Beclin 1	0.936363636	2.20821E-05
Ras GFR s91	eNos	0.936363636	2.20821E-05
PI3K	AMPKB s108	0.936363636	2.20821E-05
RAGE	E-Cadherin	0.936363636	2.20821E-05
Beclin 1	Bax	0.927272727	3.97377E-05
PI3K	Bax	0.918181818	6.66145E-05
RAGE	PI3K	0.909090909	0.000105593
Beclin 1	AMPKB s108	0.909090909	0.000105593
AMPKB s108	SPHK1	0.9	0.000159971
MDM2	SPHK1	0.890909091	0.000233458
JNK S183/185	eNos	0.881818182	0.000330169
Ras GFR s91	MDM2	0.881818182	0.000330169
Ras GFR s91	JNK S183/185	0.881818182	0.000330169
TNFR1	Bax	0.881818182	0.000330169
mTor	AMPKB s108	0.881818182	0.000330169
AKT	SPHK1	0.872727273	0.000454615
PP2A	mTor	0.872727273	0.000454615
Bcl-2 Ser70	AMPKB s108	0.863636364	0.000611694
JNK S183/185	Bcl-2 Ser70	0.863636364	0.000611694
PI3K	Bcl-2 Ser70	0.863636364	0.000611694
TNFR1	AMPKB s108	0.863636364	0.000611694
LC3B	AKT	0.863636364	0.000611694
mTor	MDM2	0.863636364	0.000611694
TNFR1	E-Cadherin	0.863636364	0.000611694
LC3B	AMPKB s108	0.854545455	0.000806674
AMPKB s108	AKT	0.854545455	0.000806674
E-Cadherin	Beclin 1	0.854545455	0.000806674
PI3K	LC3B	0.854545455	0.000806674
EGFR y1045	E-Cadherin	0.845454545	0.001045182
MMP9	LC3B	0.845454545	0.001045182
PP2A	eNos	0.845454545	0.001045182
MDM2	eNos	0.836363636	0.001333185
mTor	Beclin 1	0.827272727	0.001676974
PI3K	mTor	0.818181818	0.002083145
PI3K	AKT	0.818181818	0.002083145
PI3K	E-Cadherin	0.818181818	0.002083145

RAGE	Bax	0.818181818	0.002083145
Bcl-2 Ser70	AKT	0.818181818	0.002083145
LCK y505	EGFR y1045	0.818181818	0.002083145
Beclin 1	Bcl-2 Ser70	0.809090909	0.00255858
mTor	Bax	0.809090909	0.00255858
RAGE	AMPKB s108	0.809090909	0.00255858
LC3B	Beclin 1	0.809090909	0.00255858
LC3B	JNK S183/185	0.809090909	0.00255858
Bax	AMPKB s108	0.8	0.003110428
EGFR y1148	Bcl-2 Ser70	0.8	0.003110428
E-Cadherin	Bax	0.8	0.003110428
MMP9	Bcl-2 Ser70	0.8	0.003110428
eNos	Bcl-2 Ser70	0.790909091	0.003746083
JNK S183/185	AKT	0.790909091	0.003746083
TNFR1	LC3B	0.790909091	0.003746083
Beclin 1	AKT	0.790909091	0.003746083
PP2A	MDM2	0.790909091	0.003746083
RAGE	Cleaved Caspase 7	0.790909091	0.003746083
TNFR1	mTor	0.790909091	0.003746083
PI3K	SPHK1	0.781818182	0.004473162
VEGFR y117	Cox2	0.781818182	0.004473162
VEGFR y117	eNos	0.781818182	0.004473162
EGFR y1148	EGFR y1045	0.781818182	0.004473162
LCK y505	Bcl-2 Ser70	0.781818182	0.004473162
MDM2	AMPKB s108	0.781818182	0.004473162
MMP9	AKT	0.781818182	0.004473162
PI3K	LCK y505	0.781818182	0.004473162
RAGE	EGFR y1045	0.781818182	0.004473162
TNFR1	Bcl-2 Ser70	0.781818182	0.004473162
TNFR1	LCK y505	0.781818182	0.004473162
MDM2	JNK S183/185	0.772727273	0.005299487
mTor	AKT	0.772727273	0.005299487
PI3K	EGFR y1148	0.772727273	0.005299487
Survivin	Bax	0.772727273	0.005299487
Beclin 1	SPHK1	0.772727273	0.005299487
TNFR1	EGFR y1148	0.772727273	0.005299487
VEGFR y117	Bcl-2 Ser70	0.763636364	0.00623306
LCK y505	E-Cadherin	0.763636364	0.00623306
PP2A	LCK y505	0.763636364	0.00623306
LC3B	EGFR y1148	0.754545455	0.007282041
Ras GFR s91	PP2A	0.754545455	0.007282041
VEGFR y117	JNK S183/185	0.754545455	0.007282041
VEGFR y117	LC3B	0.754545455	0.007282041
LCK y505	Beclin 1	0.745454545	0.008454729
Ras GFR s91	Bcl-2 Ser70	0.745454545	0.008454729
EGFR y1148	Beclin 1	0.736363636	0.009759536
LCK y505	AMPKB s108	0.736363636	0.009759536
PI3K	EGFR y1045	0.736363636	0.009759536
PP2A	EGFR y1148	0.736363636	0.009759536

Bax	SPHK1	0.727272727	0.011204967
EGFR y1045	Beclin 1	0.727272727	0.011204967
eNos	AMPKB s108	0.727272727	0.011204967
MDM2	AKT	0.727272727	0.011204967
mTor	eNos	0.727272727	0.011204967
RAGE	LCK y505	0.727272727	0.011204967
TNFR1	Cleaved Caspase 7	0.727272727	0.011204967
Bcl-2 Ser70	Bax	0.718181818	0.012799598
EGFR y1148	E-Cadherin	0.718181818	0.012799598
JNK S183/185	AMPKB s108	0.718181818	0.012799598
LCK y505	LC3B	0.718181818	0.012799598
PP2A	SPHK1	0.718181818	0.012799598
RAGE	mTor	0.718181818	0.012799598
TNFR1	SPHK1	0.718181818	0.012799598
TNFR1	AKT	0.718181818	0.012799598
Bax	AKT	0.709090909	0.014552052
eNos	SPHK1	0.709090909	0.014552052
JNK S183/185	SPHK1	0.709090909	0.014552052
LC3B	Cox2	0.709090909	0.014552052
LC3B	eNos	0.709090909	0.014552052
PP2A	AMPKB s108	0.709090909	0.014552052
VEGFR y117	Cleaved Caspase 3	0.709090909	0.014552052
VEGFR y117	RUNX1	0.709090909	0.014552052
TNFR1	EGFR y1045	0.7	0.016470979
Bcl-2 Ser70	SPHK1	0.690909091	0.018565033
E-Cadherin	Cleaved Caspase 7	0.690909091	0.018565033
LC3B	SPHK1	0.690909091	0.018565033
LC3B	Bax	0.690909091	0.018565033
MMP9	AMPKB s108	0.690909091	0.018565033
MMP9	Cox2	0.690909091	0.018565033
mTor	Bcl-2 Ser70	0.690909091	0.018565033
RUNX1	Cleaved Caspase 3	0.690909091	0.018565033
VEGFR y117	MMP9	0.690909091	0.018565033
EGFR y1148	AMPKB s108	0.681818182	0.020842854
EGFR y1148	Bax	0.681818182	0.020842854
LCK y505	eNos	0.681818182	0.020842854
E-Cadherin	AMPKB s108	0.672727273	0.02331304
mTor	E-Cadherin	0.672727273	0.02331304
PI3K	MMP9	0.672727273	0.02331304
RAGE	EGFR y1148	0.672727273	0.02331304
Ras GFR s91	SPHK1	0.672727273	0.02331304
RUNX1	Cox2	0.672727273	0.02331304
MDM2	Bcl-2 Ser70	0.663636364	0.025984134
PP2A	Bax	0.663636364	0.025984134
PP2A	Bcl-2 Ser70	0.663636364	0.025984134
PP2A	JNK S183/185	0.663636364	0.025984134
Ras GFR s91	AMPKB s108	0.663636364	0.025984134
Survivin	E-Cadherin	0.663636364	0.025984134
Cleaved Caspase 7	Beclin 1	0.654545455	0.028864599

EGFR y1045	Bax	0.654545455	0.028864599
eNos	EGFR y1148	0.654545455	0.028864599
LCK y505	Bax	0.654545455	0.028864599
MMP9	Beclin 1	0.654545455	0.028864599
mTor	LC3B	0.654545455	0.028864599
PP2A	PI3K	0.654545455	0.028864599
Ras GFR s91	mTor	0.654545455	0.028864599
mTor	JNK S183/185	0.645454545	0.031962799
PP2A	Beclin 1	0.645454545	0.031962799
eNos	AKT	0.636363636	0.035286981
JNK S183/185	EGFR y1148	0.636363636	0.035286981
RAGE	SPHK1	0.636363636	0.035286981
RAGE	Bcl-2 Ser70	0.636363636	0.035286981
RAGE	LC3B	0.636363636	0.035286981
TNFR1	PP2A	0.636363636	0.035286981
mTor	LCK y505	0.627272727	0.038845254
PI3K	JNK S183/185	0.627272727	0.038845254
Ras GFR s91	AKT	0.627272727	0.038845254
Ras GFR s91	LC3B	0.627272727	0.038845254
VEGFR y117	Ras GFR s91	0.627272727	0.038845254
EGFR y1045	Bcl-2 Ser70	0.618181818	0.04264557
Ras GFR s91	LCK y505	0.618181818	0.04264557
Survivin	RAGE	0.618181818	0.04264557
PI3K	MDM2	0.609090909	0.046695709
PP2A	E-Cadherin	0.609090909	0.046695709
Survivin	Beclin 1	0.609090909	0.046695709
TNFR1	Survivin	0.609090909	0.046695709
PI3K	Cleaved Caspase 7	0.6	0.051003261
TNFR1	MMP9	0.6	0.051003261
VEGFR y117	AKT	0.6	0.051003261
Cox2	Bcl-2 Ser70	0.590909091	0.055575604
LCK y505	JNK S183/185	0.590909091	0.055575604
MMP9	JNK S183/185	0.590909091	0.055575604
mTor	EGFR y1148	0.590909091	0.055575604
RAGE	AKT	0.590909091	0.055575604
Ras GFR s91	EGFR y1148	0.590909091	0.055575604
RUNX1	LC3B	0.590909091	0.055575604
Cox2	Cleaved Caspase 3	0.581818182	0.060419896
EGFR y1045	AMPKB s108	0.581818182	0.060419896
MMP9	eNos	0.581818182	0.060419896
eNos	Cox2	0.572727273	0.065543053
MMP9	EGFR y1148	0.572727273	0.065543053
MDM2	Beclin 1	0.572727273	0.065543053
Survivin	Cleaved Caspase 7	0.572727273	0.065543053
MDM2	LC3B	0.563636364	0.070951734
PI3K	eNos	0.563636364	0.070951734
Survivin	PI3K	0.563636364	0.070951734
MMP9	SPHK1	0.554545455	0.076652333
PP2A	LC3B	0.554545455	0.076652333

Ras GFR s91	MMP9	0.554545455	0.076652333
VEGFR y117	AMPKB s108	0.554545455	0.076652333
JNK S183/185	Bax	0.545454545	0.082650957
JNK S183/185	Beclin 1	0.545454545	0.082650957
MMP9	LCK y505	0.545454545	0.082650957
TNFR1	MDM2	0.545454545	0.082650957
EGFR y1148	AKT	0.536363636	0.088953418
PP2A	AKT	0.536363636	0.088953418
RAGE	PP2A	0.536363636	0.088953418
MDM2	Bax	0.527272727	0.095565218
TNFR1	JNK S183/185	0.527272727	0.095565218
VEGFR y117	PP2A	0.527272727	0.095565218
Cleaved Caspase 7	Bax	0.518181818	0.10249154
E-Cadherin	Bcl-2 Ser70	0.518181818	0.10249154
LC3B	Cleaved Caspase 3	0.518181818	0.10249154
mTor	MMP9	0.518181818	0.10249154
Survivin	EGFR y1045	0.518181818	0.10249154
VEGFR y117	EGFR y1148	0.518181818	0.10249154
EGFR y1045	Cleaved Caspase 7	0.509090909	0.109737232
JNK S183/185	Cox2	0.509090909	0.109737232
LCK y505	Cleaved Caspase 7	0.509090909	0.109737232
PP2A	EGFR y1045	0.509090909	0.109737232
RAGE	MMP9	0.509090909	0.109737232
E-Cadherin	SPHK1	0.5	0.117306803
eNos	Beclin 1	0.5	0.117306803
LC3B	EGFR y1045	0.5	0.117306803
MDM2	LCK y505	0.5	0.117306803
Ras GFR s91	PI3K	0.5	0.117306803
LCK y505	AKT	0.490909091	0.125204407
MDM2	MMP9	0.490909091	0.125204407
RUNX1	Bcl-2 Ser70	0.490909091	0.125204407
Survivin	mTor	0.490909091	0.125204407
EGFR y1148	Cleaved Caspase 7	0.481818182	0.133433838
EGFR y1148	Cox2	0.481818182	0.133433838
LCK y505	SPHK1	0.481818182	0.133433838
MMP9	Cleaved Caspase 3	0.481818182	0.133433838
TNFR1	eNos	0.481818182	0.133433838
VEGFR y117	LCK y505	0.481818182	0.133433838
Cleaved Caspase 7	AMPKB s108	0.472727273	0.14199852
LCK y505	Cox2	0.472727273	0.14199852
VEGFR y117	PI3K	0.472727273	0.14199852
Cleaved Caspase 3	Bcl-2 Ser70	0.463636364	0.150901499
LC3B	E-Cadherin	0.463636364	0.150901499
VEGFR y117	SPHK1	0.463636364	0.150901499
LC3B	Cleaved Caspase 7	0.454545455	0.160145437
Cleaved Caspase 3	Beclin 1	0.445454545	0.169732605
EGFR y1148	SPHK1	0.445454545	0.169732605
eNos	Bax	0.445454545	0.169732605
MDM2	EGFR y1148	0.445454545	0.169732605

mTor	Cleaved Caspase 3	0.445454545	0.169732605
VEGFR y117	MDM2	0.445454545	0.169732605
Cox2	AKT	0.436363636	0.179664877
Cox2	AMPKB s108	0.436363636	0.179664877
mTor	EGFR y1045	0.436363636	0.179664877
RAGE	MDM2	0.436363636	0.179664877
Ras GFR s91	Cox2	0.436363636	0.179664877
TNFR1	Ras GFR s91	0.436363636	0.179664877
VEGFR y117	mTor	0.436363636	0.179664877
Cleaved Caspase 7	Cleaved Caspase 3	0.427272727	0.189943725
Ras GFR s91	Beclin 1	0.427272727	0.189943725
Cleaved Caspase 3	AMPKB s108	0.418181818	0.200570217
E-Cadherin	AKT	0.418181818	0.200570217
eNos	Cleaved Caspase 3	0.418181818	0.200570217
MMP9	Bax	0.418181818	0.200570217
PP2A	MMP9	0.418181818	0.200570217
RUNX1	MMP9	0.418181818	0.200570217
Survivin	EGFR y1148	0.418181818	0.200570217
VEGFR y117	Beclin 1	0.418181818	0.200570217
Cleaved Caspase 3	SPHK1	0.409090909	0.21154501
PI3K	Cleaved Caspase 3	0.409090909	0.21154501
RUNX1	JNK S183/185	0.409090909	0.21154501
Cleaved Caspase 3	Bax	0.4	0.22286835
PP2A	Cleaved Caspase 3	0.4	0.22286835
Cleaved Caspase 3	AKT	0.390909091	0.234540067
MMP9	EGFR y1045	0.390909091	0.234540067
Survivin	PP2A	0.390909091	0.234540067
Cox2	Cleaved Caspase 7	0.381818182	0.246559576
mTor	Cleaved Caspase 7	0.381818182	0.246559576
Survivin	SPHK1	0.381818182	0.246559576
MDM2	E-Cadherin	0.372727273	0.258925874
RUNX1	AKT	0.372727273	0.258925874
RUNX1	EGFR y1148	0.372727273	0.258925874
TNFR1	Cleaved Caspase 3	0.372727273	0.258925874
RUNX1	Cleaved Caspase 7	0.363636364	0.271637541
Survivin	AMPKB s108	0.363636364	0.271637541
Survivin	LCK y505	0.363636364	0.271637541
MMP9	E-Cadherin	0.354545455	0.284692741
p53 Ser15	MMP9	0.354545455	0.284692741
Ras GFR s91	p53 Ser15	0.354545455	0.284692741
VEGFR y117	Bax	0.354545455	0.284692741
PI3K	Cox2	0.345454545	0.298089221
Ras GFR s91	Bax	0.345454545	0.298089221
EGFR y1045	AKT	0.336363636	0.311824314
p53 Ser15	MDM2	0.336363636	0.311824314
RUNX1	PI3K	0.336363636	0.311824314
VEGFR y117	p53 Ser15	0.336363636	0.311824314
eNos	EGFR y1045	0.327272727	0.325894941
MMP9	Cleaved Caspase 7	0.327272727	0.325894941

p53 Ser15	EGFR y1045	0.327272727	0.325894941
RUNX1	Bax	0.327272727	0.325894941
Survivin	RUNX1	0.327272727	0.325894941
Cleaved Caspase 7	Bcl-2 Ser70	0.318181818	0.340297614
RAGE	Cleaved Caspase 3	0.318181818	0.340297614
RAGE	eNos	0.318181818	0.340297614
Ras GFR s91	EGFR y1045	0.318181818	0.340297614
RUNX1	Beclin 1	0.318181818	0.340297614
Survivin	AKT	0.318181818	0.340297614
VEGFR y117	TNFR1	0.318181818	0.340297614
JNK S183/185	Cleaved Caspase 3	0.309090909	0.35502844
JNK S183/185	EGFR y1045	0.309090909	0.35502844
p53 Ser15	AMPKB s108	0.309090909	0.35502844
RAGE	JNK S183/185	0.309090909	0.35502844
TNFR1	Cox2	0.309090909	0.35502844
Cleaved Caspase 7	SPHK1	0.3	0.370083122
Cox2	Beclin 1	0.3	0.370083122
Cleaved Caspase 7	AKT	0.290909091	0.38545697
EGFR y1045	SPHK1	0.290909091	0.38545697
p53 Ser15	SPHK1	0.281818182	0.401144898
Ras GFR s91	RAGE	0.281818182	0.401144898
VEGFR y117	EGFR y1045	0.281818182	0.401144898
p53 Ser15	eNos	0.272727273	0.417141437
Survivin	Cleaved Caspase 3	0.272727273	0.417141437
TNFR1	RUNX1	0.272727273	0.417141437
Cox2	SPHK1	0.263636364	0.433440738
eNos	E-Cadherin	0.263636364	0.433440738
p53 Ser15	Cleaved Caspase 3	0.263636364	0.433440738
PP2A	Cox2	0.263636364	0.433440738
MDM2	EGFR y1045	0.254545455	0.450036577
RUNX1	LCK y505	0.254545455	0.450036577
Survivin	Bcl-2 Ser70	0.254545455	0.450036577
Survivin	LC3B	0.254545455	0.450036577
RUNX1	eNos	0.245454545	0.466922367
EGFR y1148	Cleaved Caspase 3	0.236363636	0.484091162
p53 Ser15	AKT	0.236363636	0.484091162
p53 Ser15	Bcl-2 Ser70	0.236363636	0.484091162
RUNX1	EGFR y1045	0.236363636	0.484091162
LCK y505	Cleaved Caspase 3	0.227272727	0.501535668
PP2A	Cleaved Caspase 7	0.227272727	0.501535668
Ras GFR s91	E-Cadherin	0.227272727	0.501535668
RUNX1	AMPKB s108	0.227272727	0.501535668
p53 Ser15	Cox2	0.218181818	0.519248248
mTor	Cox2	0.209090909	0.537220935
RAGE	p53 Ser15	0.209090909	0.537220935
JNK S183/185	E-Cadherin	0.2	0.555445442
MDM2	Cleaved Caspase 3	0.2	0.555445442
RAGE	Cox2	0.2	0.555445442
p53 Ser15	mTor	0.190909091	0.573913168

E-Cadherin	Cleaved Caspase 3	0.181818182	0.592615213
MDM2	Cox2	0.181818182	0.592615213
PI3K	p53 Ser15	0.181818182	0.592615213
Ras GFR s91	Cleaved Caspase 3	0.181818182	0.592615213
EGFR y1045	Cleaved Caspase 3	0.172727273	0.611542385
EGFR y1045	Cox2	0.172727273	0.611542385
p53 Ser15	Beclin 1	0.172727273	0.611542385
Survivin	JNK S183/185	0.172727273	0.611542385
VEGFR y117	RAGE	0.172727273	0.611542385
p53 Ser15	JNK S183/185	0.154545455	0.650033965
RUNX1	RAGE	0.154545455	0.650033965
p53 Ser15	LC3B	0.136363636	0.689309021
PP2A	p53 Ser15	0.127272727	0.709214626
Survivin	MDM2	0.127272727	0.709214626
p53 Ser15	E-Cadherin	0.1	0.769875
RUNX1	SPHK1	0.1	0.769875
Cox2	Bax	0.090909091	0.790372738
p53 Ser15	LCK y505	0.090909091	0.790372738
RUNX1	PP2A	0.090909091	0.790372738
RUNX1	mTor	0.072727273	0.831716405
RUNX1	Ras GFR s91	0.072727273	0.831716405
VEGFR y117	Cleaved Caspase 7	0.063636364	0.852539073
VEGFR y117	E-Cadherin	0.054545455	0.873446578
TNFR1	p53 Ser15	0.045454545	0.894426997
Survivin	eNos	0.036363636	0.915468317
eNos	Cleaved Caspase 7	0.027272727	0.936558448
RUNX1	E-Cadherin	0.018181818	0.957685241
E-Cadherin	Cox2	0.009090909	0.9788365
RUNX1	p53 Ser15	0.009090909	0.9788365
VEGFR y117	Survivin	0	1
JNK S183/185	Cleaved Caspase 7	-0.009090909	0.9788365
MDM2	Cleaved Caspase 7	-0.018181818	0.957685241
p53 Ser15	Cleaved Caspase 7	-0.018181818	0.957685241
p53 Ser15	EGFR y1148	-0.027272727	0.936558448
p53 Ser15	Bax	-0.036363636	0.915468317
Survivin	Ras GFR s91	-0.036363636	0.915468317
Survivin	MMP9	-0.063636364	0.852539073
Ras GFR s91	Cleaved Caspase 7	-0.090909091	0.790372738
RUNX1	MDM2	-0.127272727	0.709214626
Survivin	p53 Ser15	-0.154545455	0.650033965
Survivin	Cox2	-0.163636364	0.630685215

The Spearman rank correlation coefficient, ρ, was calculated for each protein pair in the RPMA quantitative expression profiles of the CerS5 High patients (n= 11) in the fresh-frozen cohort, $\rho \geq 0.75$ with $P \leq 0.01$ was considered significant. Correlations that are unique for the CerS5 Low cohort are marked in Red. Correlations that are consistent in both the CerS5 High and Low cohorts are marked in Blue.

Supplementary Table 4: Spearman's Rho correlation analysis results in the Epithelial cells of all TRIM28 Patients (n=14), using RPMA data

Source	Target	Spearman Rho	Prob>|Rho|
PI3K	Beclin 1	0.967857143	3.59654E-09
Beclin 1	Bax	0.960714286	1.30275E-08
RAGE	E-Cadherin	0.95	6.08626E-08
mTor	Beclin 1	0.946428571	9.44794E-08
Beclin 1	AMPKB s108	0.942857143	1.42477E-07
PP2A	AMPKB s108	0.942857143	1.42477E-07
mTor	Bax	0.935714286	3.01065E-07
PI3K	Bax	0.935714286	3.01065E-07
PI3K	mTor	0.928571429	5.86794E-07
mTor	AMPKB s108	0.925	7.98746E-07
Ras GFR s91	eNos	0.925	7.98746E-07
JNK S183/185	eNos	0.921428571	1.07132E-06
PI3K	AMPKB s108	0.917857143	1.4177E-06
PI3K	EGFR y1148	0.917857143	1.4177E-06
TNFR1	Beclin 1	0.917857143	1.4177E-06
RAGE	Beclin 1	0.914285714	1.85311E-06
LC3B	Bcl-2 Ser70	0.910714286	2.39502E-06
PP2A	Beclin 1	0.910714286	2.39502E-06
LC3B	EGFR y1148	0.907142857	3.06331E-06
VEGFR y117	LC3B	0.903571429	3.8805E-06
JNK S183/185	AKT	0.896428571	6.06614E-06
RAGE	Bax	0.892857143	7.49474E-06
TNFR1	PP2A	0.892857143	7.49474E-06
PP2A	mTor	0.889285714	9.19297E-06
JNK S183/185	Bcl-2 Ser70	0.882142857	1.35582E-05
LC3B	AMPKB s108	0.882142857	1.35582E-05
PP2A	LC3B	0.882142857	1.35582E-05
Ras GFR s91	JNK S183/185	0.878571429	1.63153E-05
VEGFR y117	Bcl-2 Ser70	0.878571429	1.63153E-05
TNFR1	mTor	0.871428571	2.32365E-05
Bax	AMPKB s108	0.867857143	2.75181E-05
EGFR y1148	Beclin 1	0.867857143	2.75181E-05
PI3K	LC3B	0.867857143	2.75181E-05
EGFR y1148	Bcl-2 Ser70	0.864285714	3.24337E-05
PP2A	PI3K	0.864285714	3.24337E-05
RAGE	PI3K	0.864285714	3.24337E-05
TNFR1	PI3K	0.864285714	3.24337E-05
RAGE	mTor	0.860714286	3.80553E-05
Bcl-2 Ser70	AMPKB s108	0.857142857	4.446E-05
E-Cadherin	Beclin 1	0.857142857	4.446E-05
LC3B	Beclin 1	0.853571429	5.17314E-05

TNFR1	RAGE	0.85	5.99589E-05
E-Cadherin	Bax	0.846428571	6.92382E-05
EGFR y1148	AMPKB s108	0.846428571	6.92382E-05
mTor	E-Cadherin	0.846428571	6.92382E-05
eNos	Bcl-2 Ser70	0.842857143	7.9672E-05
TNFR1	AMPKB s108	0.842857143	7.9672E-05
TNFR1	Bax	0.842857143	7.9672E-05
eNos	AKT	0.839285714	9.13694E-05
JNK S183/185	AMPKB s108	0.835714286	0.000104447
PI3K	Bcl-2 Ser70	0.835714286	0.000104447
TNFR1	EGFR y1148	0.835714286	0.000104447
AMPKB s108	AKT	0.832142857	0.000119028
mTor	AKT	0.832142857	0.000119028
PI3K	AKT	0.832142857	0.000119028
TNFR1	Cleaved Caspase 7	0.825	0.000153236
Beclin 1	AKT	0.821428571	0.000173148
mTor	AcetylCoA	0.821428571	0.000173148
PI3K	E-Cadherin	0.821428571	0.000173148
PP2A	Bax	0.821428571	0.000173148
MDM2	AKT	0.814285714	0.000219366
RAGE	AMPKB s108	0.810714286	0.000246008
Ras GFR s91	MDM2	0.807142857	0.000275244
TNFR1	LC3B	0.807142857	0.000275244
Cleaved Caspase 7	Beclin 1	0.803571429	0.000307265
VEGFR y117	AMPKB s108	0.803571429	0.000307265
PP2A	EGFR y1148	0.8	0.00034227
PP2A	Bcl-2 Ser70	0.796428571	0.000380468
Ras GFR s91	AKT	0.796428571	0.000380468
MDM2	JNK S183/185	0.792857143	0.000422077
E-Cadherin	AMPKB s108	0.785714286	0.000516455
LC3B	JNK S183/185	0.785714286	0.000516455
RAGE	PP2A	0.785714286	0.000516455
EGFR y1148	Bax	0.782142857	0.00056971
EGFR y1148	Cleaved Caspase 7	0.782142857	0.00056971
eNos	AMPKB s108	0.782142857	0.00056971
mTor	EGFR y1148	0.782142857	0.00056971
PI3K	Cleaved Caspase 7	0.782142857	0.00056971
mTor	JNK S183/185	0.778571429	0.00062735
TNFR1	E-Cadherin	0.778571429	0.00062735
VEGFR y117	PP2A	0.778571429	0.00062735
Beclin 1	Bcl-2 Ser70	0.775	0.000689645
Bax	AKT	0.767857143	0.00082933
mTor	LC3B	0.767857143	0.00082933
PP2A	AKT	0.767857143	0.00082933
VEGFR y117	EGFR y1148	0.767857143	0.00082933

RAGE	Cleaved Caspase 7	0.764285714	0.00090731
Bax	AcetylCoA	0.760714286	0.000991129
E-Cadherin	AcetylCoA	0.760714286	0.000991129
PI3K	JNK S183/185	0.760714286	0.000991129
Bcl-2 Ser70	AKT	0.757142857	0.001081108
PP2A	E-Cadherin	0.757142857	0.001081108
VEGFR y117	Cleaved Caspase 3	0.757142857	0.001081108
LC3B	AKT	0.753571429	0.001177583
PP2A	AcetylCoA	0.753571429	0.001177583
PP2A	JNK S183/185	0.753571429	0.001177583
Beclin 1	AcetylCoA	0.75	0.001280898
LC3B	eNos	0.75	0.001280898
MMP9	LC3B	0.75	0.001280898
PP2A	EGFR y1045	0.75	0.001280898
Ras GFR s91	Bcl-2 Ser70	0.75	0.001280898
mTor	Cleaved Caspase 7	0.742857143	0.001509489
Cleaved Caspase 7	Bax	0.739285714	0.001635511
LC3B	Cleaved Caspase 7	0.739285714	0.001635511
AMPKB s108	AcetylCoA	0.735714286	0.001769869
LC3B	Cleaved Caspase 3	0.735714286	0.001769869
RAGE	AcetylCoA	0.735714286	0.001769869
VEGFR y117	PI3K	0.735714286	0.001769869
JNK S183/185	Beclin 1	0.732142857	0.001912964
LC3B	Bax	0.732142857	0.001912964
mTor	Bcl-2 Ser70	0.732142857	0.001912964
VEGFR y117	MMP9	0.732142857	0.001912964
MDM2	AcetylCoA	0.728571429	0.00206521
JNK S183/185	EGFR y1148	0.725	0.002227032
VEGFR y117	Beclin 1	0.725	0.002227032
VEGFR y117	EGFR y1045	0.725	0.002227032
Cleaved Caspase 7	AMPKB s108	0.717857143	0.002581165
EGFR y1148	AKT	0.717857143	0.002581165
Cleaved Caspase 7	Cleaved Caspase 3	0.714285714	0.002774384
RAGE	EGFR y1045	0.710714286	0.002978995
RAGE	EGFR y1148	0.707142857	0.003195481
eNos	EGFR y1148	0.703571429	0.003424337
MMP9	Bcl-2 Ser70	0.703571429	0.003424337
MDM2	eNos	0.703571429	0.003424337
E-Cadherin	Cleaved Caspase 7	0.7	0.003666068
PP2A	Cleaved Caspase 7	0.7	0.003666068
E-Cadherin	AKT	0.696428571	0.003921191
PI3K	eNos	0.696428571	0.003921191
mTor	MDM2	0.692857143	0.004190233
EGFR y1045	E-Cadherin	0.689285714	0.004473734
MMP9	AKT	0.689285714	0.004473734

MDM2	AMPKB s108	0.689285714	0.004473734
Ras GFR s91	LCK y505	0.689285714	0.004473734
Bcl-2 Ser70	Bax	0.685714286	0.004772245
Cleaved Caspase 3	Beclin 1	0.685714286	0.004772245
LCK y505	AKT	0.685714286	0.004772245
mTor	eNos	0.685714286	0.004772245
VEGFR y117	JNK S183/185	0.685714286	0.004772245
LCK y505	EGFR y1148	0.682142857	0.005086326
TNFR1	AcetylCoA	0.682142857	0.005086326
TNFR1	AKT	0.682142857	0.005086326
EGFR y1045	AMPKB s108	0.678571429	0.00541655
EGFR y1045	Beclin 1	0.678571429	0.00541655
JNK S183/185	Bax	0.678571429	0.00541655
PP2A	eNos	0.678571429	0.00541655
Ras GFR s91	AMPKB s108	0.675	0.005763499
MMP9	eNos	0.667857143	0.006509957
RAGE	AKT	0.667857143	0.006509957
EGFR y1045	AcetylCoA	0.664285714	0.006910683
LC3B	EGFR y1045	0.664285714	0.006910683
PI3K	Cleaved Caspase 3	0.664285714	0.006910683
PI3K	LCK y505	0.664285714	0.006910683
TNFR1	EGFR y1045	0.664285714	0.006910683
LCK y505	Bcl-2 Ser70	0.660714286	0.00733057
VEGFR y117	eNos	0.657142857	0.007770251
AKT	AcetylCoA	0.653571429	0.008230371
eNos	Beclin 1	0.653571429	0.008230371
LCK y505	AMPKB s108	0.653571429	0.008230371
LCK y505	eNos	0.646428571	0.009214551
MMP9	EGFR y1148	0.646428571	0.009214551
PI3K	MMP9	0.646428571	0.009214551
PP2A	MMP9	0.646428571	0.009214551
PP2A	MDM2	0.646428571	0.009214551
RAGE	LC3B	0.642857143	0.009739945
Cleaved Caspase 3	AMPKB s108	0.639285714	0.010288447
LCK y505	JNK S183/185	0.635714286	0.010860746
PI3K	AcetylCoA	0.635714286	0.010860746
TNFR1	Bcl-2 Ser70	0.635714286	0.010860746
TNFR1	Cleaved Caspase 3	0.635714286	0.010860746
EGFR y1148	Cleaved Caspase 3	0.614285714	0.014833955
PI3K	EGFR y1045	0.614285714	0.014833955
VEGFR y117	TNFR1	0.614285714	0.014833955
LCK y505	Beclin 1	0.607142857	0.016381307
EGFR y1045	Cleaved Caspase 3	0.603571429	0.017200138
VEGFR y117	AKT	0.603571429	0.017200138
LCK y505	E-Cadherin	0.6	0.018050088

RAGE	LCK y505	0.6	0.018050088
EGFR y1148	E-Cadherin	0.596428571	0.018931925
JNK S183/185	AcetylCoA	0.596428571	0.018931925
Ras GFR s91	LC3B	0.596428571	0.018931925
VEGFR y117	mTor	0.596428571	0.018931925
MMP9	AMPKB s108	0.592857143	0.019846422
MMP9	Beclin 1	0.592857143	0.019846422
MMP9	JNK S183/185	0.592857143	0.019846422
Ras GFR s91	PP2A	0.592857143	0.019846422
EGFR y1045	Bcl-2 Ser70	0.589285714	0.020794358
LC3B	E-Cadherin	0.589285714	0.020794358
Ras GFR s91	MMP9	0.589285714	0.020794358
TNFR1	JNK S183/185	0.585714286	0.021776518
MDM2	Beclin 1	0.582142857	0.022793687
mTor	Cleaved Caspase 3	0.582142857	0.022793687
RAGE	Bcl-2 Ser70	0.582142857	0.022793687
VEGFR y117	Bax	0.582142857	0.022793687
PP2A	Cleaved Caspase 3	0.578571429	0.023846659
RAGE	Cleaved Caspase 3	0.578571429	0.023846659
TNFR1	LCK y505	0.578571429	0.023846659
Cleaved Caspase 3	Bax	0.575	0.024936228
LCK y505	LC3B	0.575	0.024936228
MDM2	E-Cadherin	0.575	0.024936228
mTor	EGFR y1045	0.567857143	0.027228357
eNos	Bax	0.564285714	0.028432522
PP2A	LCK y505	0.564285714	0.028432522
EGFR y1045	Bax	0.560714286	0.029676496
mTor	LCK y505	0.560714286	0.029676496
Ras GFR s91	mTor	0.560714286	0.029676496
VEGFR y117	LCK y505	0.560714286	0.029676496
VEGFR y117	Ras GFR s91	0.560714286	0.029676496
Cleaved Caspase 3	Bcl-2 Ser70	0.557142857	0.030961087
E-Cadherin	Cleaved Caspase 3	0.557142857	0.030961087
MDM2	Bax	0.557142857	0.030961087
VEGFR y117	Cleaved Caspase 7	0.557142857	0.030961087
Cleaved Caspase 7	Bcl-2 Ser70	0.546428571	0.03506666
PI3K	MDM2	0.539285714	0.038021656
VEGFR y117	RAGE	0.539285714	0.038021656
MDM2	Bcl-2 Ser70	0.535714286	0.039566972
MDM2	LCK y505	0.535714286	0.039566972
Ras GFR s91	PI3K	0.532142857	0.04115858
LC3B	AcetylCoA	0.528571429	0.042797289
E-Cadherin	Bcl-2 Ser70	0.521428571	0.046219234
RUNX1	Bcl-2 Ser70	0.521428571	0.046219234
Cleaved Caspase 7	AKT	0.510714286	0.051725498

EGFR y1148	EGFR y1045	0.510714286	0.051725498
Ras GFR s91	EGFR y1148	0.510714286	0.051725498
RUNX1	EGFR y1148	0.503571429	0.055654517
VEGFR y117	RUNX1	0.5	0.057698841
p53 Ser15	EGFR y1045	0.496428571	0.059797414
RAGE	JNK S183/185	0.496428571	0.059797414
TNFR1	eNos	0.496428571	0.059797414
eNos	Cleaved Caspase 7	0.492857143	0.061951007
JNK S183/185	E-Cadherin	0.492857143	0.061951007
Ras GFR s91	Beclin 1	0.492857143	0.061951007
RUNX1	Cleaved Caspase 3	0.492857143	0.061951007
LCK y505	Bax	0.489285714	0.064160386
LCK y505	EGFR y1045	0.489285714	0.064160386
MMP9	EGFR y1045	0.489285714	0.064160386
RAGE	MDM2	0.489285714	0.064160386
VEGFR y117	E-Cadherin	0.489285714	0.064160386
MMP9	LCK y505	0.485714286	0.066426312
Cleaved Caspase 3	AKT	0.482142857	0.068749538
Bcl-2 Ser70	AcetylCoA	0.478571429	0.071130808
Cleaved Caspase 3	AcetylCoA	0.478571429	0.071130808
MMP9	Bax	0.475	0.073570862
eNos	E-Cadherin	0.471428571	0.076070429
mTor	MMP9	0.471428571	0.076070429
EGFR y1045	AKT	0.467857143	0.078630231
TNFR1	MMP9	0.467857143	0.078630231
RAGE	eNos	0.460714286	0.083933381
Cleaved Caspase 7	AcetylCoA	0.453571429	0.0894859
MMP9	Cleaved Caspase 3	0.45	0.092357375
MMP9	Cleaved Caspase 7	0.45	0.092357375
RUNX1	JNK S183/185	0.442857143	0.098294066
MMP9	E-Cadherin	0.439285714	0.101360571
RAGE	MMP9	0.439285714	0.101360571
MDM2	LC3B	0.435714286	0.104493357
RUNX1	LC3B	0.435714286	0.104493357
TNFR1	MDM2	0.428571429	0.110960214
EGFR y1045	Cleaved Caspase 7	0.425	0.114295475
eNos	AcetylCoA	0.425	0.114295475
VEGFR y117	AcetylCoA	0.425	0.114295475
MDM2	MMP9	0.421428571	0.117699396
JNK S183/185	Cleaved Caspase 3	0.417857143	0.121172536
Ras GFR s91	AcetylCoA	0.417857143	0.121172536
JNK S183/185	Cleaved Caspase 7	0.410714286	0.128328646
VEGFR y117	MDM2	0.410714286	0.128328646
RUNX1	eNos	0.407142857	0.132012664
RUNX1	PI3K	0.4	0.139595129

MDM2	EGFR y1045	0.396428571	0.143494531
Ras GFR s91	E-Cadherin	0.396428571	0.143494531
JNK S183/185	EGFR y1045	0.392857143	0.147466655
RUNX1	LCK y505	0.389285714	0.151511937
EGFR y1148	AcetylCoA	0.385714286	0.155630795
eNos	Cleaved Caspase 3	0.382142857	0.15982363
Ras GFR s91	Bax	0.382142857	0.15982363
LCK y505	Cleaved Caspase 7	0.375	0.16843275
RUNX1	Beclin 1	0.364285714	0.181910259
LCK y505	Cleaved Caspase 3	0.357142857	0.191274763
TNFR1	Ras GFR s91	0.35	0.200945351
Ras GFR s91	RAGE	0.342857143	0.210923793
RUNX1	AKT	0.342857143	0.210923793
MDM2	EGFR y1148	0.335714286	0.221211538
RUNX1	Bax	0.335714286	0.221211538
Ras GFR s91	EGFR y1045	0.325	0.237225438
p53 Ser15	Cleaved Caspase 3	0.317857143	0.248290566
RUNX1	AMPKB s108	0.314285714	0.253940016
RUNX1	Cleaved Caspase 7	0.307142857	0.265472686
LCK y505	AcetylCoA	0.285714286	0.301936351
eNos	EGFR y1045	0.282142857	0.308284457
VEGFR y117	p53 Ser15	0.25	0.368846292
RUNX1	Ras GFR s91	0.246428571	0.375950516
RUNX1	MMP9	0.242857143	0.383128342
RUNX1	mTor	0.232142857	0.405098741
MMP9	AcetylCoA	0.228571429	0.41256617
RUNX1	RAGE	0.228571429	0.41256617
TNFR1	RUNX1	0.221428571	0.427713719
Ras GFR s91	Cleaved Caspase 7	0.214285714	0.443140935
Ras GFR s91	Cleaved Caspase 3	0.210714286	0.450957865
MDM2	Cleaved Caspase 3	0.207142857	0.458842805
p53 Ser15	LCK y505	0.189285714	0.499263033
MDM2	Cleaved Caspase 7	0.153571429	0.584764095
RUNX1	PP2A	0.15	0.593630203
p53 Ser15	AcetylCoA	0.128571429	0.647916329
p53 Ser15	E-Cadherin	0.121428571	0.666401114
Ras GFR s91	p53 Ser15	0.114285714	0.685065763
p53 Ser15	Bcl-2 Ser70	0.092857143	0.74204501
RUNX1	p53 Ser15	0.092857143	0.74204501
RAGE	p53 Ser15	0.089285714	0.751672517
RUNX1	E-Cadherin	0.085714286	0.761334126
RUNX1	EGFR y1045	0.082142857	0.771028565
p53 Ser15	AMPKB s108	0.071428571	0.800295987
p53 Ser15	LC3B	0.064285714	0.819947965
RUNX1	MDM2	0.064285714	0.819947965

RUNX1	AcetylCoA	0.035714286	0.899446993
p53 Ser15	MDM2	0.021428571	0.939577904
p53 Ser15	AKT	0.003571429	0.989921407
PP2A	p53 Ser15	-0.014285714	0.959699765
p53 Ser15	Beclin 1	-0.017857143	0.949635304
PI3K	p53 Ser15	-0.039285714	0.88944593
p53 Ser15	MMP9	-0.042857143	0.879460313
p53 Ser15	JNK S183/185	-0.05	0.859540943
p53 Ser15	eNos	-0.064285714	0.819947965
TNFR1	p53 Ser15	-0.071428571	0.800295987
p53 Ser15	EGFR y1148	-0.078571429	0.780754552
p53 Ser15	mTor	-0.085714286	0.761334126
p53 Ser15	Cleaved Caspase 7	-0.1	0.722897325
p53 Ser15	Bax	-0.15	0.593630203

The Spearman rank correlation coefficient, ρ, was calculated for each protein pair in the RPMA quantitative expression profiles of the Epithelial cells in all TRIM28 patients (n= 14) in the fresh-frozen cohort, $\rho \geq 0.75$ with $P \leq 0.01$ was considered significant.

Supplementary Table 5: Spearman's Rho correlation analysis results in the Stromal cells of the TRIM28 High Ratio Patients (n=8), using RPMA data

Source	Target	Spearman Rho	Prob>|Rho|
Cleaved Caspase 3	AcetylCoA	0.976190476	3.3144E-05
mTor	LC3B	0.976190476	3.3144E-05
PI3K	LC3B	0.976190476	3.3144E-05
PP2A	Cleaved Caspase 3	0.976190476	3.3144E-05
PP2A	EGFR y1148	0.976190476	3.3144E-05
PP2A	MDM2	0.976190476	3.3144E-05
EGFR y1148	Cleaved Caspase 3	0.952380952	0.0002604
MDM2	Cleaved Caspase 3	0.952380952	0.0002604
MDM2	EGFR y1148	0.952380952	0.0002604
mTor	Beclin 1	0.952380952	0.0002604
PI3K	Beclin 1	0.952380952	0.0002604
PI3K	mTor	0.952380952	0.0002604
TNFR1	Beclin 1	0.952380952	0.0002604
TNFR1	PI3K	0.952380952	0.0002604
VEGFR y117	JNK S183/185	0.952380952	0.0002604
E-Cadherin	AMPKB s108	0.928571429	0.000862968
LC3B	Beclin 1	0.928571429	0.000862968
LCK y505	Cleaved Caspase 7	0.928571429	0.000862968
PP2A	AcetylCoA	0.928571429	0.000862968
PP2A	AKT	0.928571429	0.000862968
RAGE	Bcl-2 Ser70	0.928571429	0.000862968

RAGE	EGFR y1148	0.928571429	0.000862968
Ras GFR s91	eNos	0.928571429	0.000862968
TNFR1	mTor	0.928571429	0.000862968
Beclin 1	Bax	0.904761905	0.002008276
E-Cadherin	Bcl-2 Ser70	0.904761905	0.002008276
EGFR y1148	AcetylCoA	0.904761905	0.002008276
EGFR y1148	AKT	0.904761905	0.002008276
JNK S183/185	Cleaved Caspase 3	0.904761905	0.002008276
LC3B	Cleaved Caspase 3	0.904761905	0.002008276
LCK y505	AMPKB s108	0.904761905	0.002008276
MMP9	EGFR y1045	0.904761905	0.002008276
MDM2	AcetylCoA	0.904761905	0.002008276
MDM2	JNK S183/185	0.904761905	0.002008276
mTor	AKT	0.904761905	0.002008276
mTor	Bax	0.904761905	0.002008276
PI3K	Bax	0.904761905	0.002008276
RAGE	Cleaved Caspase 3	0.904761905	0.002008276
RAGE	MDM2	0.904761905	0.002008276
Ras GFR s91	EGFR y1045	0.904761905	0.002008276
TNFR1	Bax	0.904761905	0.002008276
TNFR1	LC3B	0.904761905	0.002008276
VEGFR y117	Bcl-2 Ser70	0.904761905	0.002008276
Cleaved Caspase 3	AKT	0.880952381	0.00385032
eNos	AMPKB s108	0.880952381	0.00385032
JNK S183/185	AMPKB s108	0.880952381	0.00385032
JNK S183/185	Bcl-2 Ser70	0.880952381	0.00385032
LC3B	AcetylCoA	0.880952381	0.00385032
LC3B	AKT	0.880952381	0.00385032
LC3B	Bax	0.880952381	0.00385032
LC3B	EGFR y1148	0.880952381	0.00385032
LCK y505	E-Cadherin	0.880952381	0.00385032
MDM2	Bcl-2 Ser70	0.880952381	0.00385032
PP2A	JNK S183/185	0.880952381	0.00385032
RAGE	AcetylCoA	0.880952381	0.00385032
RAGE	PP2A	0.880952381	0.00385032
VEGFR y117	AMPKB s108	0.880952381	0.00385032
VEGFR y117	MDM2	0.880952381	0.00385032
EGFR y1045	E-Cadherin	0.857142857	0.006530017
EGFR y1148	Bcl-2 Ser70	0.857142857	0.006530017
JNK S183/185	EGFR y1148	0.857142857	0.006530017
JNK S183/185	eNos	0.857142857	0.006530017
LC3B	JNK S183/185	0.857142857	0.006530017
MDM2	AKT	0.857142857	0.006530017
PI3K	Cleaved Caspase 3	0.857142857	0.006530017
PI3K	EGFR y1148	0.857142857	0.006530017
PP2A	LC3B	0.857142857	0.006530017
RAGE	JNK S183/185	0.857142857	0.006530017
RAGE	PI3K	0.857142857	0.006530017

VEGFR y117	Cleaved Caspase 3	0.857142857	0.006530017
VEGFR y117	E-Cadherin	0.857142857	0.006530017
VEGFR y117	RAGE	0.857142857	0.006530017
Bcl-2 Ser70	AMPKB s108	0.833333333	0.01017554
Beclin 1	AKT	0.833333333	0.01017554
Cleaved Caspase 3	Bcl-2 Ser70	0.833333333	0.01017554
JNK S183/185	AcetylCoA	0.833333333	0.01017554
JNK S183/185	AKT	0.833333333	0.01017554
mTor	Cleaved Caspase 3	0.833333333	0.01017554
mTor	EGFR y1148	0.833333333	0.01017554
PI3K	AcetylCoA	0.833333333	0.01017554
PI3K	AKT	0.833333333	0.01017554
RAGE	LC3B	0.833333333	0.01017554
TNFR1	AKT	0.833333333	0.01017554
VEGFR y117	AcetylCoA	0.833333333	0.01017554
VEGFR y117	LCK y505	0.833333333	0.01017554
AKT	AcetylCoA	0.80952381	0.014902668
eNos	EGFR y1045	0.80952381	0.014902668
mTor	AcetylCoA	0.80952381	0.014902668
PI3K	JNK S183/185	0.80952381	0.014902668
PP2A	Bcl-2 Ser70	0.80952381	0.014902668
PP2A	mTor	0.80952381	0.014902668
PP2A	PI3K	0.80952381	0.014902668
RAGE	LCK y505	0.80952381	0.014902668
Ras GFR s91	MMP9	0.80952381	0.014902668
VEGFR y117	EGFR y1045	0.80952381	0.014902668
VEGFR y117	PP2A	0.80952381	0.014902668
Bcl-2 Ser70	AcetylCoA	0.785714286	0.020815127
EGFR y1045	AMPKB s108	0.785714286	0.020815127
JNK S183/185	Beclin 1	0.785714286	0.020815127
JNK S183/185	E-Cadherin	0.785714286	0.020815127
LCK y505	Bcl-2 Ser70	0.785714286	0.020815127
LCK y505	JNK S183/185	0.785714286	0.020815127
MDM2	AMPKB s108	0.785714286	0.020815127
MDM2	Cleaved Caspase 7	0.785714286	0.020815127
MDM2	E-Cadherin	0.785714286	0.020815127
MDM2	LC3B	0.785714286	0.020815127
mTor	JNK S183/185	0.785714286	0.020815127
RAGE	E-Cadherin	0.785714286	0.020815127
VEGFR y117	EGFR y1148	0.785714286	0.020815127
Cleaved Caspase 7	AMPKB s108	0.761904762	0.028004939
E-Cadherin	Cleaved Caspase 7	0.761904762	0.028004939
EGFR y1045	Bcl-2 Ser70	0.761904762	0.028004939
EGFR y1148	Beclin 1	0.761904762	0.028004939
eNos	E-Cadherin	0.761904762	0.028004939
MDM2	LCK y505	0.761904762	0.028004939
RAGE	AMPKB s108	0.761904762	0.028004939
RAGE	Cleaved Caspase 7	0.761904762	0.028004939

Ras GFR s91	AMPKB s108	0.761904762	0.028004939
Ras GFR s91	E-Cadherin	0.761904762	0.028004939
TNFR1	Cleaved Caspase 3	0.761904762	0.028004939
TNFR1	EGFR y1148	0.761904762	0.028004939
VEGFR y117	Cleaved Caspase 7	0.761904762	0.028004939
VEGFR y117	eNos	0.761904762	0.028004939
VEGFR y117	LC3B	0.761904762	0.028004939
Bax	AcetylCoA	0.738095238	0.036552761
Beclin 1	AMPKB s108	0.738095238	0.036552761
Cleaved Caspase 3	Beclin 1	0.738095238	0.036552761
EGFR y1148	AMPKB s108	0.738095238	0.036552761
JNK S183/185	Cleaved Caspase 7	0.738095238	0.036552761
JNK S183/185	EGFR y1045	0.738095238	0.036552761
LC3B	Bcl-2 Ser70	0.738095238	0.036552761
PI3K	MDM2	0.738095238	0.036552761
RAGE	AKT	0.738095238	0.036552761
RAGE	Beclin 1	0.738095238	0.036552761
RAGE	mTor	0.738095238	0.036552761
Ras GFR s91	JNK S183/185	0.738095238	0.036552761
TNFR1	AcetylCoA	0.738095238	0.036552761
TNFR1	PP2A	0.738095238	0.036552761
TNFR1	RAGE	0.738095238	0.036552761
AMPKB s108	AKT	0.714285714	0.046528232
Cleaved Caspase 7	Bcl-2 Ser70	0.714285714	0.046528232
EGFR y1148	E-Cadherin	0.714285714	0.046528232
eNos	AKT	0.714285714	0.046528232
eNos	Bcl-2 Ser70	0.714285714	0.046528232
MMP9	E-Cadherin	0.714285714	0.046528232
MDM2	EGFR y1045	0.714285714	0.046528232
MDM2	eNos	0.714285714	0.046528232
mTor	MDM2	0.714285714	0.046528232
PI3K	Bcl-2 Ser70	0.714285714	0.046528232
PP2A	AMPKB s108	0.714285714	0.046528232
PP2A	Beclin 1	0.714285714	0.046528232
Ras GFR s91	Bcl-2 Ser70	0.714285714	0.046528232
TNFR1	JNK S183/185	0.714285714	0.046528232
VEGFR y117	PI3K	0.714285714	0.046528232
Bax	AKT	0.69047619	0.057990318
Beclin 1	AcetylCoA	0.69047619	0.057990318
Cleaved Caspase 3	AMPKB s108	0.69047619	0.057990318
Cleaved Caspase 3	Bax	0.69047619	0.057990318
EGFR y1045	Cleaved Caspase 7	0.69047619	0.057990318
LC3B	AMPKB s108	0.69047619	0.057990318
LCK y505	EGFR y1045	0.69047619	0.057990318
LCK y505	EGFR y1148	0.69047619	0.057990318
LCK y505	eNos	0.69047619	0.057990318
MMP9	eNos	0.69047619	0.057990318
PP2A	Cleaved Caspase 7	0.69047619	0.057990318

RAGE	Bax	0.69047619	0.057990318
VEGFR y117	AKT	0.69047619	0.057990318
VEGFR y117	Ras GFR s91	0.69047619	0.057990318
EGFR y1148	Bax	0.666666667	0.070987654
EGFR y1148	Cleaved Caspase 7	0.666666667	0.070987654
MDM2	MMP9	0.666666667	0.070987654
mTor	AMPKB s108	0.666666667	0.070987654
PI3K	AMPKB s108	0.666666667	0.070987654
PP2A	E-Cadherin	0.666666667	0.070987654
PP2A	eNos	0.666666667	0.070987654
PP2A	LCK y505	0.666666667	0.070987654
Ras GFR s91	p53 Ser15	0.666666667	0.070987654
VEGFR y117	Beclin 1	0.666666667	0.070987654
VEGFR y117	mTor	0.666666667	0.070987654
Bcl-2 Ser70	AKT	0.642857143	0.085558891
Cleaved Caspase 7	Cleaved Caspase 3	0.642857143	0.085558891
E-Cadherin	Cleaved Caspase 3	0.642857143	0.085558891
eNos	Cleaved Caspase 7	0.642857143	0.085558891
eNos	EGFR y1148	0.642857143	0.085558891
JNK S183/185	Bax	0.642857143	0.085558891
LCK y505	Beclin 1	0.642857143	0.085558891
LCK y505	Cleaved Caspase 3	0.642857143	0.085558891
MDM2	Beclin 1	0.642857143	0.085558891
Ras GFR s91	MDM2	0.642857143	0.085558891
TNFR1	MDM2	0.642857143	0.085558891
AMPKB s108	AcetylCoA	0.619047619	0.101733037
Beclin 1	Bcl-2 Ser70	0.619047619	0.101733037
eNos	Beclin 1	0.619047619	0.101733037
eNos	Cleaved Caspase 3	0.619047619	0.101733037
MMP9	AMPKB s108	0.619047619	0.101733037
mTor	Bcl-2 Ser70	0.619047619	0.101733037
PI3K	LCK y505	0.619047619	0.101733037
PP2A	Bax	0.619047619	0.101733037
VEGFR y117	Bax	0.619047619	0.101733037
Bax	AMPKB s108	0.595238095	0.119529806
E-Cadherin	AcetylCoA	0.595238095	0.119529806
LC3B	eNos	0.595238095	0.119529806
LCK y505	AcetylCoA	0.595238095	0.119529806
LCK y505	AKT	0.595238095	0.119529806
MMP9	Cleaved Caspase 7	0.595238095	0.119529806
p53 Ser15	EGFR y1045	0.595238095	0.119529806
TNFR1	AMPKB s108	0.595238095	0.119529806
TNFR1	LCK y505	0.595238095	0.119529806
VEGFR y117	MMP9	0.595238095	0.119529806
VEGFR y117	TNFR1	0.595238095	0.119529806
Cleaved Caspase 7	AcetylCoA	0.571428571	0.138959957
Cleaved Caspase 7	AKT	0.571428571	0.138959957
LCK y505	LC3B	0.571428571	0.138959957

MMP9	Bcl-2 Ser70	0.571428571	0.138959957
mTor	eNos	0.571428571	0.138959957
PP2A	EGFR y1045	0.571428571	0.138959957
RAGE	eNos	0.571428571	0.138959957
Ras GFR s91	Cleaved Caspase 7	0.571428571	0.138959957
Ras GFR s91	LCK y505	0.571428571	0.138959957
RUNX1	AcetylCoA	0.571428571	0.138959957
RUNX1	Bax	0.571428571	0.138959957
E-Cadherin	AKT	0.547619048	0.160025643
EGFR y1045	Cleaved Caspase 3	0.547619048	0.160025643
LC3B	E-Cadherin	0.547619048	0.160025643
LCK y505	Bax	0.547619048	0.160025643
MMP9	JNK S183/185	0.547619048	0.160025643
MDM2	Bax	0.547619048	0.160025643
PP2A	MMP9	0.547619048	0.160025643
RAGE	EGFR y1045	0.547619048	0.160025643
Ras GFR s91	PP2A	0.547619048	0.160025643
Bcl-2 Ser70	Bax	0.523809524	0.182720751
E-Cadherin	Beclin 1	0.523809524	0.182720751
EGFR y1148	EGFR y1045	0.523809524	0.182720751
MMP9	LCK y505	0.523809524	0.182720751
mTor	LCK y505	0.523809524	0.182720751
PI3K	E-Cadherin	0.523809524	0.182720751
PI3K	eNos	0.523809524	0.182720751
Ras GFR s91	EGFR y1148	0.523809524	0.182720751
TNFR1	Bcl-2 Ser70	0.523809524	0.182720751
TNFR1	RUNX1	0.523809524	0.182720751
p53 Ser15	eNos	0.5	0.20703125
PI3K	Cleaved Caspase 7	0.5	0.20703125
Ras GFR s91	AKT	0.5	0.20703125
Ras GFR s91	Cleaved Caspase 3	0.5	0.20703125
TNFR1	Cleaved Caspase 7	0.5	0.20703125
Cleaved Caspase 7	Beclin 1	0.476190476	0.232935535
EGFR y1045	AcetylCoA	0.476190476	0.232935535
eNos	AcetylCoA	0.476190476	0.232935535
MMP9	EGFR y1148	0.476190476	0.232935535
mTor	E-Cadherin	0.476190476	0.232935535
Ras GFR s91	RAGE	0.476190476	0.232935535
RUNX1	PI3K	0.476190476	0.232935535
LC3B	Cleaved Caspase 7	0.452380952	0.260404767
MMP9	Cleaved Caspase 3	0.452380952	0.260404767
p53 Ser15	MMP9	0.452380952	0.260404767
RUNX1	Cleaved Caspase 3	0.452380952	0.260404767
RUNX1	LC3B	0.452380952	0.260404767
TNFR1	eNos	0.452380952	0.260404767
E-Cadherin	Bax	0.428571429	0.289403225
EGFR y1045	AKT	0.428571429	0.289403225
MMP9	AKT	0.428571429	0.289403225

RUNX1	mTor	0.404761905	0.319888641
MMP9	AcetylCoA	0.380952381	0.351812553
mTor	Cleaved Caspase 7	0.380952381	0.351812553
RAGE	MMP9	0.380952381	0.351812553
Ras GFR s91	LC3B	0.380952381	0.351812553
TNFR1	E-Cadherin	0.380952381	0.351812553
Ras GFR s91	AcetylCoA	0.357142857	0.385120644
Cleaved Caspase 7	Bax	0.333333333	0.419753086
eNos	Bax	0.333333333	0.419753086
LC3B	EGFR y1045	0.333333333	0.419753086
Ras GFR s91	Beclin 1	0.333333333	0.419753086
RUNX1	Beclin 1	0.333333333	0.419753086
RUNX1	RAGE	0.333333333	0.419753086
Ras GFR s91	mTor	0.30952381	0.455644891
RUNX1	PP2A	0.30952381	0.455644891
VEGFR y117	RUNX1	0.30952381	0.455644891
Ras GFR s91	PI3K	0.285714286	0.492726245
VEGFR y117	p53 Ser15	0.285714286	0.492726245
p53 Ser15	JNK S183/185	0.261904762	0.530922862
RUNX1	JNK S183/185	0.261904762	0.530922862
EGFR y1045	Beclin 1	0.238095238	0.570156321
mTor	EGFR y1045	0.238095238	0.570156321
p53 Ser15	AMPKB s108	0.238095238	0.570156321
p53 Ser15	E-Cadherin	0.238095238	0.570156321
PI3K	EGFR y1045	0.238095238	0.570156321
RUNX1	AKT	0.238095238	0.570156321
RUNX1	EGFR y1148	0.238095238	0.570156321
RUNX1	MDM2	0.238095238	0.570156321
p53 Ser15	Bcl-2 Ser70	0.19047619	0.651401496
MMP9	LC3B	0.166666667	0.693238812
TNFR1	Ras GFR s91	0.142857143	0.73576486
mTor	MMP9	0.119047619	0.778885726
RUNX1	Cleaved Caspase 7	0.119047619	0.778885726
EGFR y1045	Bax	0.095238095	0.82250543
RUNX1	Bcl-2 Ser70	0.095238095	0.82250543
RUNX1	LCK y505	0.095238095	0.82250543
TNFR1	EGFR y1045	0.095238095	0.82250543
MMP9	Beclin 1	0.047619048	0.910849169
PI3K	MMP9	0.047619048	0.910849169
Ras GFR s91	Bax	0.047619048	0.910849169
p53 Ser15	MDM2	0.023809524	0.955374012
p53 Ser15	Cleaved Caspase 3	-0.023809524	0.955374012
p53 Ser15	LCK y505	-0.023809524	0.955374012
p53 Ser15	Cleaved Caspase 7	-0.047619048	0.910849169
RUNX1	AMPKB s108	-0.047619048	0.910849169
TNFR1	MMP9	-0.047619048	0.910849169
p53 Ser15	LC3B	-0.071428571	0.866526271
PP2A	p53 Ser15	-0.071428571	0.866526271

MMP9	Bax	-0.095238095	0.82250543
p53 Ser15	AcetylCoA	-0.095238095	0.82250543
p53 Ser15	AKT	-0.095238095	0.82250543
p53 Ser15	Beclin 1	-0.142857143	0.73576486
p53 Ser15	EGFR y1148	-0.142857143	0.73576486
p53 Ser15	mTor	-0.142857143	0.73576486
RAGE	p53 Ser15	-0.142857143	0.73576486
RUNX1	E-Cadherin	-0.142857143	0.73576486
RUNX1	EGFR y1045	-0.19047619	0.651401496
PI3K	p53 Ser15	-0.214285714	0.610344416
RUNX1	eNos	-0.214285714	0.610344416
p53 Ser15	Bax	-0.285714286	0.492726245
RUNX1	p53 Ser15	-0.30952381	0.455644891
RUNX1	MMP9	-0.333333333	0.419753086
TNFR1	p53 Ser15	-0.357142857	0.385120644
RUNX1	Ras GFR s91	-0.380952381	0.351812553

The Spearman rank correlation coefficient, ρ, was calculated for each protein pair in the RPMA quantitative expression profiles of the Stromal cells in the TRIM28 High Ratio patients (n= 8) in the fresh-frozen cohort, $\rho \geq 0.75$ with $P \leq 0.01$ was considered significant.

Supplementary Table 6: Spearman's Rho correlation analysis results in the Stromal cells of the TRIM28 Low Ratio Patients (n=6), using RPMA data

Source	Target	Spearman Rho	Prob>|Rho|
EGFR y1045	Bcl-2 Ser70	1	0
EGFR y1148	Bcl-2 Ser70	1	0
EGFR y1148	EGFR y1045	1	0
LC3B	Bax	1	0
PP2A	AMPKB s108	1	0
Ras GFR s91	eNos	1	0
TNFR1	AcetylCoA	1	0
VEGFR y117	AMPKB s108	1	0
VEGFR y117	PP2A	1	0
AMPKB s108	AcetylCoA	0.942857143	0.004804665
Bax	AKT	0.942857143	0.004804665
Beclin 1	Bax	0.942857143	0.004804665
JNK S183/185	AKT	0.942857143	0.004804665
LC3B	AKT	0.942857143	0.004804665
LC3B	Beclin 1	0.942857143	0.004804665
MMP9	AKT	0.942857143	0.004804665
MMP9	AMPKB s108	0.942857143	0.004804665
MDM2	AcetylCoA	0.942857143	0.004804665
MDM2	eNos	0.942857143	0.004804665
mTor	AKT	0.942857143	0.004804665
mTor	AMPKB s108	0.942857143	0.004804665
mTor	Beclin 1	0.942857143	0.004804665
PI3K	AMPKB s108	0.942857143	0.004804665
PI3K	Beclin 1	0.942857143	0.004804665
PP2A	AcetylCoA	0.942857143	0.004804665
PP2A	MMP9	0.942857143	0.004804665
PP2A	mTor	0.942857143	0.004804665
PP2A	PI3K	0.942857143	0.004804665
RAGE	Cleaved Caspase 3	0.942857143	0.004804665
RAGE	PI3K	0.942857143	0.004804665
Ras GFR s91	MDM2	0.942857143	0.004804665
TNFR1	AMPKB s108	0.942857143	0.004804665
TNFR1	MDM2	0.942857143	0.004804665
TNFR1	PP2A	0.942857143	0.004804665
VEGFR y117	AcetylCoA	0.942857143	0.004804665
VEGFR y117	MMP9	0.942857143	0.004804665
VEGFR y117	mTor	0.942857143	0.004804665
VEGFR y117	PI3K	0.942857143	0.004804665
VEGFR y117	TNFR1	0.942857143	0.004804665
AMPKB s108	AKT	0.885714286	0.018845481
Beclin 1	AKT	0.885714286	0.018845481

Beclin 1	AMPKB s108	0.885714286	0.018845481
JNK S183/185	eNos	0.885714286	0.018845481
MMP9	Bax	0.885714286	0.018845481
MMP9	Bcl-2 Ser70	0.885714286	0.018845481
MMP9	EGFR y1045	0.885714286	0.018845481
MMP9	EGFR y1148	0.885714286	0.018845481
MMP9	JNK S183/185	0.885714286	0.018845481
MMP9	LC3B	0.885714286	0.018845481
mTor	AcetylCoA	0.885714286	0.018845481
mTor	Bax	0.885714286	0.018845481
mTor	LC3B	0.885714286	0.018845481
mTor	MMP9	0.885714286	0.018845481
PI3K	Bax	0.885714286	0.018845481
PI3K	Cleaved Caspase 3	0.885714286	0.018845481
PI3K	LC3B	0.885714286	0.018845481
PI3K	MMP9	0.885714286	0.018845481
PI3K	mTor	0.885714286	0.018845481
PP2A	AKT	0.885714286	0.018845481
PP2A	Beclin 1	0.885714286	0.018845481
RAGE	Beclin 1	0.885714286	0.018845481
Ras GFR s91	JNK S183/185	0.885714286	0.018845481
TNFR1	mTor	0.885714286	0.018845481
VEGFR y117	AKT	0.885714286	0.018845481
VEGFR y117	Beclin 1	0.885714286	0.018845481
Bax	AMPKB s108	0.828571429	0.041562682
Bcl-2 Ser70	Bax	0.828571429	0.041562682
EGFR y1045	Bax	0.828571429	0.041562682
EGFR y1148	Bax	0.828571429	0.041562682
eNos	AcetylCoA	0.828571429	0.041562682
JNK S183/185	Bax	0.828571429	0.041562682
LC3B	AMPKB s108	0.828571429	0.041562682
LC3B	Bcl-2 Ser70	0.828571429	0.041562682
LC3B	EGFR y1045	0.828571429	0.041562682
LC3B	EGFR y1148	0.828571429	0.041562682
LC3B	JNK S183/185	0.828571429	0.041562682
LCK y505	AMPKB s108	0.828571429	0.041562682
MMP9	AcetylCoA	0.828571429	0.041562682
MMP9	Beclin 1	0.828571429	0.041562682
MMP9	eNos	0.828571429	0.041562682
MDM2	AMPKB s108	0.828571429	0.041562682
mTor	JNK S183/185	0.828571429	0.041562682
PI3K	AcetylCoA	0.828571429	0.041562682
PI3K	AKT	0.828571429	0.041562682
PI3K	Bcl-2 Ser70	0.828571429	0.041562682
PI3K	EGFR y1045	0.828571429	0.041562682

PI3K	EGFR y1148	0.828571429	0.041562682
PP2A	Bax	0.828571429	0.041562682
PP2A	LC3B	0.828571429	0.041562682
PP2A	LCK y505	0.828571429	0.041562682
PP2A	MDM2	0.828571429	0.041562682
RAGE	AMPKB s108	0.828571429	0.041562682
RAGE	PP2A	0.828571429	0.041562682
Ras GFR s91	AcetylCoA	0.828571429	0.041562682
Ras GFR s91	MMP9	0.828571429	0.041562682
RUNX1	Bax	0.828571429	0.041562682
RUNX1	LC3B	0.828571429	0.041562682
TNFR1	eNos	0.828571429	0.041562682
TNFR1	MMP9	0.828571429	0.041562682
TNFR1	PI3K	0.828571429	0.041562682
TNFR1	Ras GFR s91	0.828571429	0.041562682
VEGFR y117	Bax	0.828571429	0.041562682
VEGFR y117	LC3B	0.828571429	0.041562682
VEGFR y117	LCK y505	0.828571429	0.041562682
VEGFR y117	MDM2	0.828571429	0.041562682
VEGFR y117	RAGE	0.828571429	0.041562682
AKT	AcetylCoA	0.771428571	0.072396501
Bcl-2 Ser70	AKT	0.771428571	0.072396501
Bcl-2 Ser70	AMPKB s108	0.771428571	0.072396501
Beclin 1	AcetylCoA	0.771428571	0.072396501
Cleaved Caspase 3	AMPKB s108	0.771428571	0.072396501
Cleaved Caspase 3	Beclin 1	0.771428571	0.072396501
EGFR y1045	AKT	0.771428571	0.072396501
EGFR y1045	AMPKB s108	0.771428571	0.072396501
EGFR y1148	AKT	0.771428571	0.072396501
EGFR y1148	AMPKB s108	0.771428571	0.072396501
eNos	AKT	0.771428571	0.072396501
eNos	AMPKB s108	0.771428571	0.072396501
JNK S183/185	AMPKB s108	0.771428571	0.072396501
LCK y505	Bcl-2 Ser70	0.771428571	0.072396501
LCK y505	EGFR y1045	0.771428571	0.072396501
LCK y505	EGFR y1148	0.771428571	0.072396501
MMP9	LCK y505	0.771428571	0.072396501
MDM2	JNK S183/185	0.771428571	0.072396501
MDM2	MMP9	0.771428571	0.072396501
mTor	MDM2	0.771428571	0.072396501
PI3K	LCK y505	0.771428571	0.072396501
PP2A	Bcl-2 Ser70	0.771428571	0.072396501
PP2A	Cleaved Caspase 3	0.771428571	0.072396501
PP2A	EGFR y1045	0.771428571	0.072396501
PP2A	EGFR y1148	0.771428571	0.072396501

PP2A	eNos	0.771428571	0.072396501
PP2A	JNK S183/185	0.771428571	0.072396501
RAGE	AcetylCoA	0.771428571	0.072396501
RAGE	Bax	0.771428571	0.072396501
RAGE	LC3B	0.771428571	0.072396501
RAGE	mTor	0.771428571	0.072396501
Ras GFR s91	AKT	0.771428571	0.072396501
Ras GFR s91	AMPKB s108	0.771428571	0.072396501
Ras GFR s91	PP2A	0.771428571	0.072396501
RUNX1	Beclin 1	0.771428571	0.072396501
RUNX1	RAGE	0.771428571	0.072396501
TNFR1	AKT	0.771428571	0.072396501
TNFR1	Beclin 1	0.771428571	0.072396501
TNFR1	RAGE	0.771428571	0.072396501
VEGFR y117	Bcl-2 Ser70	0.771428571	0.072396501
VEGFR y117	Cleaved Caspase 3	0.771428571	0.072396501
VEGFR y117	EGFR y1045	0.771428571	0.072396501
VEGFR y117	EGFR y1148	0.771428571	0.072396501
VEGFR y117	eNos	0.771428571	0.072396501
VEGFR y117	JNK S183/185	0.771428571	0.072396501
VEGFR y117	Ras GFR s91	0.771428571	0.072396501
Beclin 1	Bcl-2 Ser70	0.714285714	0.110787172
Cleaved Caspase 3	AcetylCoA	0.714285714	0.110787172
E-Cadherin	Cleaved Caspase 7	0.714285714	0.110787172
EGFR y1045	Beclin 1	0.714285714	0.110787172
EGFR y1148	Beclin 1	0.714285714	0.110787172
JNK S183/185	AcetylCoA	0.714285714	0.110787172
JNK S183/185	Beclin 1	0.714285714	0.110787172
LCK y505	AcetylCoA	0.714285714	0.110787172
LCK y505	Cleaved Caspase 3	0.714285714	0.110787172
MDM2	AKT	0.714285714	0.110787172
mTor	eNos	0.714285714	0.110787172
p53 Ser15	LCK y505	0.714285714	0.110787172
RAGE	MMP9	0.714285714	0.110787172
Ras GFR s91	mTor	0.714285714	0.110787172
RUNX1	PI3K	0.714285714	0.110787172
TNFR1	Cleaved Caspase 3	0.714285714	0.110787172
TNFR1	JNK S183/185	0.714285714	0.110787172
TNFR1	LCK y505	0.714285714	0.110787172
Bax	AcetylCoA	0.657142857	0.156174927
JNK S183/185	Bcl-2 Ser70	0.657142857	0.156174927
JNK S183/185	EGFR y1045	0.657142857	0.156174927
JNK S183/185	EGFR y1148	0.657142857	0.156174927
LC3B	AcetylCoA	0.657142857	0.156174927
mTor	Bcl-2 Ser70	0.657142857	0.156174927

mTor	Cleaved Caspase 3	0.657142857	0.156174927
mTor	EGFR y1045	0.657142857	0.156174927
mTor	EGFR y1148	0.657142857	0.156174927
mTor	LCK y505	0.657142857	0.156174927
p53 Ser15	Bcl-2 Ser70	0.657142857	0.156174927
p53 Ser15	EGFR y1045	0.657142857	0.156174927
p53 Ser15	EGFR y1148	0.657142857	0.156174927
PI3K	JNK S183/185	0.657142857	0.156174927
PI3K	MDM2	0.657142857	0.156174927
RAGE	AKT	0.657142857	0.156174927
RAGE	Bcl-2 Ser70	0.657142857	0.156174927
RAGE	EGFR y1045	0.657142857	0.156174927
RAGE	EGFR y1148	0.657142857	0.156174927
RUNX1	AKT	0.657142857	0.156174927
TNFR1	Bax	0.657142857	0.156174927
TNFR1	LC3B	0.657142857	0.156174927
Cleaved Caspase 3	Bax	0.6	0.208
Cleaved Caspase 3	Bcl-2 Ser70	0.6	0.208
EGFR y1045	Cleaved Caspase 3	0.6	0.208
EGFR y1148	Cleaved Caspase 3	0.6	0.208
eNos	Bax	0.6	0.208
LC3B	Cleaved Caspase 3	0.6	0.208
LC3B	eNos	0.6	0.208
LCK y505	AKT	0.6	0.208
LCK y505	Beclin 1	0.6	0.208
MMP9	Cleaved Caspase 3	0.6	0.208
MDM2	Beclin 1	0.6	0.208
p53 Ser15	Cleaved Caspase 7	0.6	0.208
PI3K	eNos	0.6	0.208
RAGE	LCK y505	0.6	0.208
RAGE	MDM2	0.6	0.208
Ras GFR s91	Bax	0.6	0.208
Ras GFR s91	LC3B	0.6	0.208
Ras GFR s91	PI3K	0.6	0.208
RUNX1	Bcl-2 Ser70	0.6	0.208
RUNX1	EGFR y1045	0.6	0.208
RUNX1	EGFR y1148	0.6	0.208
RUNX1	JNK S183/185	0.6	0.208
RUNX1	MMP9	0.6	0.208
RUNX1	mTor	0.6	0.208
Bcl-2 Ser70	AcetylCoA	0.542857143	0.265702624
EGFR y1045	AcetylCoA	0.542857143	0.265702624
EGFR y1148	AcetylCoA	0.542857143	0.265702624
eNos	Bcl-2 Ser70	0.542857143	0.265702624
eNos	Beclin 1	0.542857143	0.265702624

eNos	EGFR y1045	0.542857143	0.265702624
eNos	EGFR y1148	0.542857143	0.265702624
LCK y505	Bax	0.542857143	0.265702624
LCK y505	Cleaved Caspase 7	0.542857143	0.265702624
LCK y505	LC3B	0.542857143	0.265702624
MDM2	Bax	0.542857143	0.265702624
MDM2	LC3B	0.542857143	0.265702624
MDM2	LCK y505	0.542857143	0.265702624
Ras GFR s91	Bcl-2 Ser70	0.542857143	0.265702624
Ras GFR s91	Beclin 1	0.542857143	0.265702624
Ras GFR s91	EGFR y1045	0.542857143	0.265702624
Ras GFR s91	EGFR y1148	0.542857143	0.265702624
RUNX1	AMPKB s108	0.542857143	0.265702624
RUNX1	Cleaved Caspase 3	0.542857143	0.265702624
RUNX1	PP2A	0.542857143	0.265702624
TNFR1	Bcl-2 Ser70	0.542857143	0.265702624
TNFR1	EGFR y1045	0.542857143	0.265702624
TNFR1	EGFR y1148	0.542857143	0.265702624
VEGFR y117	RUNX1	0.542857143	0.265702624
Cleaved Caspase 3	AKT	0.485714286	0.328723032
Cleaved Caspase 7	Cleaved Caspase 3	0.485714286	0.328723032
LCK y505	eNos	0.485714286	0.328723032
MDM2	Cleaved Caspase 3	0.485714286	0.328723032
RAGE	eNos	0.485714286	0.328723032
RAGE	JNK S183/185	0.485714286	0.328723032
Ras GFR s91	LCK y505	0.485714286	0.328723032
Ras GFR s91	RAGE	0.485714286	0.328723032
LCK y505	JNK S183/185	0.428571429	0.396501458
MDM2	Bcl-2 Ser70	0.428571429	0.396501458
MDM2	EGFR y1045	0.428571429	0.396501458
MDM2	EGFR y1148	0.428571429	0.396501458
p53 Ser15	Cleaved Caspase 3	0.428571429	0.396501458
RUNX1	AcetylCoA	0.428571429	0.396501458
RUNX1	eNos	0.428571429	0.396501458
RUNX1	Ras GFR s91	0.428571429	0.396501458
TNFR1	RUNX1	0.428571429	0.396501458
Cleaved Caspase 7	AcetylCoA	0.371428571	0.468478134
p53 Ser15	MMP9	0.371428571	0.468478134
PI3K	p53 Ser15	0.371428571	0.468478134
RUNX1	MDM2	0.371428571	0.468478134
TNFR1	Cleaved Caspase 7	0.371428571	0.468478134
eNos	Cleaved Caspase 3	0.314285714	0.544093294
MDM2	Cleaved Caspase 7	0.314285714	0.544093294
p53 Ser15	AMPKB s108	0.314285714	0.544093294
PP2A	p53 Ser15	0.314285714	0.544093294

Ras GFR s91	Cleaved Caspase 3	0.314285714	0.544093294
VEGFR y117	p53 Ser15	0.314285714	0.544093294
Cleaved Caspase 7	AMPKB s108	0.257142857	0.622787172
JNK S183/185	Cleaved Caspase 3	0.257142857	0.622787172
PP2A	Cleaved Caspase 7	0.257142857	0.622787172
RAGE	Cleaved Caspase 7	0.257142857	0.622787172
RAGE	p53 Ser15	0.257142857	0.622787172
VEGFR y117	Cleaved Caspase 7	0.257142857	0.622787172
p53 Ser15	E-Cadherin	0.2	0.704
PI3K	Cleaved Caspase 7	0.2	0.704
eNos	Cleaved Caspase 7	0.142857143	0.787172012
MDM2	E-Cadherin	0.142857143	0.787172012
p53 Ser15	AcetylCoA	0.142857143	0.787172012
p53 Ser15	Bax	0.142857143	0.787172012
p53 Ser15	LC3B	0.142857143	0.787172012
Ras GFR s91	Cleaved Caspase 7	0.142857143	0.787172012
RUNX1	LCK y505	0.142857143	0.787172012
TNFR1	p53 Ser15	0.142857143	0.787172012
Cleaved Caspase 7	Bcl-2 Ser70	0.085714286	0.87174344
EGFR y1045	Cleaved Caspase 7	0.085714286	0.87174344
EGFR y1148	Cleaved Caspase 7	0.085714286	0.87174344
eNos	E-Cadherin	0.085714286	0.87174344
MMP9	Cleaved Caspase 7	0.085714286	0.87174344
p53 Ser15	AKT	0.085714286	0.87174344
p53 Ser15	Beclin 1	0.085714286	0.87174344
p53 Ser15	eNos	0.085714286	0.87174344
Ras GFR s91	E-Cadherin	0.085714286	0.87174344
Ras GFR s91	p53 Ser15	0.085714286	0.87174344
p53 Ser15	MDM2	0.028571429	0.957154519
p53 Ser15	mTor	0.028571429	0.957154519
E-Cadherin	AcetylCoA	-0.028571429	0.957154519
mTor	Cleaved Caspase 7	-0.028571429	0.957154519
p53 Ser15	JNK S183/185	-0.028571429	0.957154519
RUNX1	p53 Ser15	-0.028571429	0.957154519
TNFR1	E-Cadherin	-0.028571429	0.957154519
Cleaved Caspase 7	Beclin 1	-0.085714286	0.87174344
LCK y505	E-Cadherin	-0.085714286	0.87174344
E-Cadherin	Cleaved Caspase 3	-0.142857143	0.787172012
Cleaved Caspase 7	AKT	-0.2	0.704
Cleaved Caspase 7	Bax	-0.257142857	0.622787172
E-Cadherin	AMPKB s108	-0.257142857	0.622787172
JNK S183/185	Cleaved Caspase 7	-0.257142857	0.622787172
LC3B	Cleaved Caspase 7	-0.257142857	0.622787172
PP2A	E-Cadherin	-0.257142857	0.622787172
RAGE	E-Cadherin	-0.257142857	0.622787172

VEGFR y117	E-Cadherin	-0.257142857	0.622787172
MMP9	E-Cadherin	-0.314285714	0.544093294
RUNX1	Cleaved Caspase 7	-0.314285714	0.544093294
E-Cadherin	Bcl-2 Ser70	-0.371428571	0.468478134
EGFR y1045	E-Cadherin	-0.371428571	0.468478134
EGFR y1148	E-Cadherin	-0.371428571	0.468478134
JNK S183/185	E-Cadherin	-0.371428571	0.468478134
PI3K	E-Cadherin	-0.371428571	0.468478134
mTor	E-Cadherin	-0.485714286	0.328723032
RUNX1	E-Cadherin	-0.485714286	0.328723032
E-Cadherin	AKT	-0.542857143	0.265702624
E-Cadherin	Beclin 1	-0.6	0.208
E-Cadherin	Bax	-0.657142857	0.156174927
LC3B	E-Cadherin	-0.657142857	0.156174927

The Spearman rank correlation coefficient, ρ, was calculated for each protein pair in the RPMA quantitative expression profiles of the Stromal cells of the TRIM28 Low ratio patients (n= 6) in the fresh-frozen cohort, $\rho \geq 0.75$ with $P \leq 0.01$ was considered significant.